Sperm Induced Signalling Events in the Cells of the Female Reproductive Tract

by

James Richards

A thesis submitted to
The University of Birmingham
For the Degree of
DOCTOR OF PHILOSOPHY



Centre for Human Reproductive Science
Institute of Metabolism and Systems Research
College of Medical and Dental Sciences
University of Birmingham
March 2022

UNIVERSITY OF
BIRMINGHAM

University of Birmingham Research Archive

e-theses repository

This unpublished thesis/dissertation is copyright of the author and/or third parties. The intellectual property rights of the author or third parties in respect of this work are as defined by The Copyright Designs and Patents Act 1988 or as modified by any successor legislation.

Any use made of information contained in this thesis/dissertation must be in accordance with that legislation and must be properly acknowledged. Further distribution or reproduction in any format is prohibited without the permission of the copyright holder.

Abstract

Female reproductive tract regulation of the function of spermatozoa is relatively well characterised, but little is known about the influence which human sperm cells may have upon the cells of the female reproductive tract. Animal models suggest that signalling factors from the male ejaculate can prime the maternal immune response tolerance of the semi-allogeneic conceptus and elicit alterations in gene expression and the secretory proteome of the oviduct. The purpose of this study was to utilise Ca^{2+} imaging to identify signalling events that occur in response to factors from the male ejaculate in female reproductive tract cells. Cell line models of granulosa cells, endometrial epithelial cells and oviductal epithelial cells were utilised to establish that oviductal epithelial cells are significantly responsive to a range of semen sample preparations.

A novel series of semen preparation pathways were developed to identify the source of the signalling factor within the male ejaculate. These preparations revealed that the factor was likely to be a protein or peptide derived from the seminal plasma that loosely associated with the surface of spermatozoa and was transported into the upper regions of the female reproductive tract by motile sperm cells where it could elicit $[Ca^{2+}]_i$ oscillations in the oviductal epithelial cells via the release of intracellular Ca^{2+} stores through mechanisms independent of toll-like receptor 4 activation. Proteomic analysis of sperm conditioned media containing the signalling factor was undertaken and candidate peptides from semenogelin-1 and semenogelin-2 were synthesised, however, these peptides failed to elicit Ca^{2+} signalling. Further investigation is therefore necessary to elucidate the identity of the signalling factor.

Dedication

To my parents Alison & Glyn Richards, my grandparents Lorna & James Richards and Kenneth & Susan Ewart, who have raised and motivated me to achieve my goals.

Acknowledgements

First and foremost, I would like to thank Dr Jackson Kirkman-Brown and Dr Steve Publicover for seeing my potential and accepting me as a PhD student. Thank you for your constant guidance, mentorship, and advice throughout the entire process. There were many tough decisions to make regarding the path that this research took and you were always very patient in helping me navigate through everything.

I am very grateful to all the other members of our research team for your support and friendship throughout my studies, Dr Sarah Conner, Dr Claudia Román Montañana, Dr Jevan Medlock, Dr Meurig Gallagher and Professor David Smith.

Thank you to Professor Richard Lea, Professor David Gardner and Professor Gary England at the University of Nottingham for the very interesting days out in the field with the various canines and for giving me a fascinating insight into your research.

Thanks to Professor Daniel A. Tennant and Vikki Harrison for welcoming me as part of the Medical Research Council Doctoral Training Programme and for all their help over the years with external training programmes and trips.

I would like to gratefully acknowledge Dr Joao Correia for teaching me so much about the complex world of microscopy and fluorescent imaging techniques, as well as for the many times that he helped me troubleshoot my equipment and got everything working again. Also, Dr Peter Hewett for allowing me to use his lab equipment and teaching me about various assays and techniques.

A special thank you to my partner Sinead Doyle for always being there for me and being the best friend that I could ask for.

Table of Contents

Chapter 1 1

Introduction 1

1.1- The prevalence and causes of infertility 2

1.2- The Human Sperm Cell 3

1.2.1- The anatomy of spermatozoa 3

1.2.2- The Human Sperm Cell Head 6

1.2.3- The Human Sperm Midpiece 8

1.2.4- The Human Sperm Tail 9

1.2.5- Sperm cell production and storage 10

1.2.6- The Male Ejaculate 11

1.2.7- Capacitation and acquisition of hyperactivated motility 16

1.3- The Female Reproductive tract 21

1.3.1- Anatomy of the Female Reproductive Tract 21

1.3.2- The Vagina 23

1.3.3- The Cervix 23

1.3.4- The Uterus 24

1.3.5- The Oviducts 25

1.3.6- The Epithelium 29

1.3.7- The Menstrual Cycle 30

1.4- The Sperm Cell Journey through the FRT 33

1.5- Sperm cell modification of the female reproductive tract 37

1.6- The importance of Ca^{2+} in cellular signalling 43

1.6.1- Mechanisms of Ca^{2+} signalling 43

1.6.2- Spatial and temporal aspects of Ca^{2+} signalling 47

1.6.3- Ca^{2+} signalling in the cells of the female reproductive tract 50

1.7- Hypothesis, Aims and Objectives 53

Chapter 2 56

An Investigation of Ejaculate Induced Intracellular Calcium Signalling in Female Reproductive Tract Cells 56

2.1- Introduction 57

2.2- Materials & Methods 64

2.2.1- Materials 64
2.2.2- Culture of human female reproductive tract cell lines and human foreskin fibroblasts 64
2.2.2.1- Granulosa cell line (COV434) 65
2.2.2.2- Endometrial epithelial cell line (HEC-1B) 66
2.2.2.3- Oviductal epithelial cell line (OE-E6/E7) 66
2.2.2.4- Human foreskin fibroblasts cell line (HFF) 66
2.2.3- Preparation of human female reproductive tract cell lines for perfusion chambers 67
2.2.4- Recruitment of human sperm donors 67
2.2.5- Preparation of human sperm samples for perfusion as stimuli during initial Ca^{2+} imaging experiments 68
2.2.5.1- Density gradient centrifugation (DGC) prepared sperm cells 68
2.2.5.2- Swimup prepared sperm cells 69
2.2.5.3- Preparation of filtered and centrifuged seminal plasma 69
2.2.6- Setting up Ca^{2+} imaging apparatus 70
2.2.7- Staining of cells for Ca^{2+} imaging experiments 72
2.2.8- Ca^{2+} imaging of human reproductive tract cell lines with perfusion of human sperm cell preparations 73
2.2.9- Statistical analysis of Ca^{2+} imaging timelapse data 74
2.2.10- experimental plan for studying sperm cell and seminal plasma induced $[Ca^{2+}]_i$ signalling in female reproductive tract cells 79
2.3- Results 80
2.3.1- Culture of female reproductive tract cell lines and human foreskin fibroblasts 80
2.3.2- Staining of cell lines with Calcium Green-1 AM 82
2.3.3- Validation of Ca^{2+} imaging timelapse experimental protocol 84
2.3.4- Comparison of cells exposed to sEBSS with cells exposed to 100 µM ATP solution 86
2.3.5- Ca2+ imaging experiments with human foreskin fibroblast (HFF) cell line 87
2.3.6- HEC-1-B cell Ca^{2+} imaging experiments with stimulus perfusion 93
2.3.7- OE-E6/E7 Ca^{2+} imaging experiments with stimulus perfusion 99
..... 105
2.3.8- COV434 cell Ca^{2+} imaging experiments with stimulus perfusion ... 105

2.3.9- Initial Ca^{2+} imaging experiments summary 111
2.4- Discussion 115
Chapter 3 123
The Source of Semen Signalling Factors Eliciting a $[Ca^{2+}]_i$ Response in Oviductal Epithelial Cells 123
3.1- Introduction 124
3.2- Materials & Methods 128
3.2.1- Materials 128
3.2.2- Semen sample preparation pathway 129
3.2.2.1- Non-conditioned media: negative control condition 130
3.2.2.2- Time zero post-swimup sperm cells 131
3.2.2.3- Swimup capacitated sperm cells 131
3.2.2.4- Sperm conditioned media 132
3.2.2.5- Clean DGC sperm cells 132
3.2.2.6- "Contaminated" DGC sperm cells 132
3.2.3- Preparation of OE-E6/E7 cells for $[Ca^{2+}]_i$ imaging 133
3.2.4- Ca^{2+} imaging of OE-E6/E7 cells whilst perfusing with semen sample preparations 133
3.2.5- Statistical analysis of Ca^{2+} imaging timelapse data 133
3.3 Results 134
3.3.1- Variation in the kinetics of the OE-E6/E7 cell $[Ca^{2+}]_i$ response to stimuli 134
3.3.2- Perfusion of OE-E6/E7 cells with non-conditioned media 136
..... 138
3.3.3- Perfusion of OE-E6/E7 cells with time zero post-swimup sperm cells 138
3.3.4- Perfusion of OE-E6/E7 cells with swimup capacitated sperm cells 140
3.3.5- Perfusion of OE-E6/E7 cells with Sperm Conditioned Media 143
3.3.6- Perfusion of OE-E6/E7 cells with Clean DGC sperm cells 146
3.3.7- Perfusion of OE-E6/E7 cells with "Contaminated" DGC sperm cells 149
3.3.8- Comparison of OE-E6/E7 cells response to Semen sample preparations 152
3.4- Discussion 156
Chapter 4 164

Fractionation and proteomic analysis of sperm conditioned media 164
4.1- Introduction..... 165
4.2- Materials & Methods..... 169
4.2.1- Materials 169
4.2.2- Fractionation of sperm conditioned media..... 171
4.2.3- Ca^{2+} imaging of OE-E6/E7 cells with sperm conditioned media fractions..... 172
4.2.4- Precipitation of proteins from sperm conditioned media fractions 172
4.2.5- BCA assay of precipitated sperm conditioned media fractions 173
4.2.6- Proteomic analysis of sperm conditioned media fractions..... 173
4.2.7- Analysis of proteomic data 175
4.3- Results 176
4.3.1- Initial test of pooled sperm conditioned media reactivity in OE-E6/E7 cells 176
4.3.2- Assessment of post precipitation protein pellet for signalling efficacy..... 179
4.3.3- Proteomic analysis results from sperm conditioned media fractions 180
4.3.4- Investigation and analysis of semenogelin-1 & semenoglein-2 peptides 183
4.4- Discussion 193
Chapter 5..... 201
Semenogelin peptide synthesis and investigation into Oviductal Epithelial Cell $[Ca^{2+}]_i$ signalling mechanism of action..... 201
5.1- Introduction..... 202
5.1.1- Semenogelin peptide experiments..... 202
5.1.2- Elucidation of the mechanisms of action in the signalling pathway 204
5.2- Materials & Methods..... 208
5.2.1- Materials 208
5.2.2- Synthesis of semenogelin peptides..... 209
5.2.3- Ca^{2+} imaging experiments with semenogelin peptides 210
5.2.4- Ca^{2+} imaging experiments with TLR4 inhibitor 210
5.2.5- Ca^{2+} imaging experiments with Ca^{2+} free sEBSS 211

5.2.6- Ca^{2+} imaging experiments with <2 kDa dialysed sperm conditioned media 211
5.2.7- Ca^{2+} imaging experiments with thapsigargin 212
5.3- Results 213
5.3.1- Ca^{2+} imaging experiments with semenogelin peptides 213
5.3.2- Ca^{2+} imaging experiment with TLR4-IN-C34 217
5.3.3- Ca^{2+} imaging experiments with Ca^{2+} free media 219
5.3.4- Ca^{2+} imaging experiment with Thapsigargin 221
5.3.5- Ca^{2+} imaging experiment with dialysed sperm conditioned media 223
5.4- Discussion 225
5.4.1- Experiments with synthesised Semenogelin peptides 225
5.4.2- Experiments to elucidate the signalling mechanism of action 226
Chapter 6 231
General Discussion 231
6.1- Semen factors induce signalling in human female reproductive tract cells 232
6.2- The semen derived signalling molecules are carried by sperm cells 235
6.3- Proteomic analysis of sperm conditioned media 240
6.4- Signalling relies on the release of Ca^{2+} from intracellular stores 243
6.5- Conclusions and considerations for future research 251
Appendices 256
Appendix I 257
Supplemented Earle's balanced salt solution (sEBSS) 257
Appendix II 258
Validation of of Ca^{2+} imaging timelapse experimental protocol 258
Appendix III 264
Cell response summaries during initial Ca^{2+} imaging experiments 264
Appendix IV 275
OE-E6/E7 Cell response summaries during Ca^{2+} imaging experiments .. 275
Appendix V 283
BCA protein quantification assay results 283
Appendix VI 284
>50 kDa fraction of sperm conditioned media proteomic analysis data .. 284
Appendix VII 299

OE-E6/E7 cell responses to semenogelin peptide perfusion 299
OE-E6/E7 cell response to sperm conditioned media with TLR-IN-C34 ... 303
OE-E6/E7 cell response to sperm conditioned media in Ca^{2+} free sEBSS304
OE-E6/E7 cell response to thapsigargin and sperm conditioned media .. 305
OE-E6/E7 cell response to sperm conditioned media and <2kDa dialysed sperm conditioned media 306
Appendix VIII 307
Attempts to develop canine oviductal epithelial cell cultures 307
The effect of diet of canine semen sample quality and DNA damage 309
References 312

List of Figures

Figure 1.1- The morphological characteristics and dimensions of an 'ideal' mature human sperm cells, according to the Tygerberg Strict Criteria……5

Figure 1.2- The origins of the male ejaculate and the organs which contribute to the seminal plasma……14

Figure 1.3- The anatomy of the female reproductive tract in humans and mice……22

Figure 1.4- An illustration of the human oviduct, displaying the longitudinal folds in cross-section at the a) Infundibulum, b) ampulla and c) isthmus……28

Figure 1.5- A diagram of the various phases of the human menstrual cycle……..32

Figure 1.6- common mechanisms of Ca^{2+} signalling……46

Figure 2.1- A diagram of the imaging perfusion chambers utilised to simultaneously image cells grown onto 22x32 mm coverslips whilst various media preparations could be gently perfused across their surface…….71

Figure 2.2- An example graph of the expected average fluorescence intensity for a single cell throughout a timelapse Ca^{2+} imaging experiment.……..78

Figure 2.3- Bright field images of each of the female reproductive tract cell lines and the human foreskin fibroblasts……81

Figure 2.4- Images of each of the cultured cell lines, captured at spectral wavelengths of 488/535 nm captured using Metamorph imaging software after the cells have been loaded with 10 µM Calcium Green-1 AM solution as described in section 2.2.7.……83

Figure 2.5- Validation of Ca^{2+} imaging timelapse experimental protocol and statistical method of identifying $[Ca^{2+}]_i$ signalling…….84

Figure 2.6- Pseudocolour images from a Ca^{2+}imaging timelapse of HEC-1-B cells superfused with (A) sEBSS and (B) 100 µM ATP solution……86

Figure 2.7- Example average fluorescence intensity plot for HFF cells perfused with swimup sperm cells……..87

Figure 2.8- experiments to determine whether gentle perfusion of sEBSS can elicit a $[Ca^{2+}]_i$ response in HFF cells……..89

Figure 2.9- Experiment to determine whether increasing strengths of sEBSS perfusion can elicit a $[Ca^{2+}]_i$ response in HFF cells……...91

Figure 2.10- The effect of DGC sperm cell perfusion on $[Ca^{2+}]_i$ in HEC-1B cells……93

Figure 2.11- The effect of swimup sperm cell perfusion on $[Ca^{2+}]_i$ in HEC-1B cells……95

Figure 2.12- The effect of seminal plasma perfusion on $[Ca^{2+}]_i$ in HEC-1B cells……97

Figure 2.13- The effect of DGC sperm cell perfusion on $[Ca^{2+}]_i$ in OE-E6/E7 cells……99

Figure 2.14- The effect of swimup sperm cell perfusion on $[Ca^{2+}]_i$ in OE-E6/E7 cells……..101

Figure 2.15- The effect of seminal plasma perfusion on $[Ca^{2+}]_i$ in OE-E6/E7 cells……..103

Figure 2.16- The effect of DGC sperm cell perfusion on $[Ca^{2+}]_i$ in COV434 cells……..105

Figure 2.17- The effect of swimup sperm cell perfusion on $[Ca^{2+}]_i$ in COV434 cells……..107

Figure 2.18- The effect of seminal plasma perfusion on $[Ca^{2+}]_i$ in COV434 cells……..109

Figure 2.19- Bar chart of average rates at which cells were identified as showing an increase in $[Ca^{2+}]_i$ during the initial period of stimulus perfusion (±SE (Median)) for each of the three cell lines and stimuli investigated ……..111

Figure 2.20- Bar chart of median maximum peak height during stimulus perfusion as a percentage of maximum peak height during positive control perfusion (±SE (Median)) for each of the three cell lines and stimuli investigated……..……..……..…..113

Figure 3.1: Schematic of the various semen sample preparation methods that were designed to isolate specific proteins and signalling factors within the male ejaculate in order to identify the ligand responsible for the observed $[Ca^{2+}]_i$ signalling in OE-E6/E7 cells…….……129

Figure 3.2: Fluorescence intensity time plots for 4 individual OE-E6/E7 cells imaged in a single experiment with sperm conditioned media perfused across their surface, highlighting the variation in the kinetics of the observed $[Ca^{2+}]_i$ signalling……..……..……...134

Figure 3.3: The effect of non-conditioned media perfusion on OE-E6/E7 cells……..136

Figure 3.4: The effect of time zero post-swimup sperm cells perfusion on OE-E6/E7 cells…….……...138

Figure 3.5: The effect of swimup capacitated sperm cells perfusion on OE-E6/E7 cells…….……140

Figure 3.6: The effect of sperm conditioned media perfusion on OE-E6/E7 cells…….....143

Figure 3.7: The effect of clean DGC sperm cells perfusion on OE-E6/E7 cells……..146

Figure 3.8: The effect of "contaminated" DGC sperm cells perfusion on OE-E6/E7 cells……..……..……..149

Figure 3.9: Bar chart displaying the median number of OE-E6/E7 cells identified as increasing in $[Ca^{2+}]_i$ (±SE (median)) in response to each of the

semen sample preparations used as stimuli in this series of Ca^{2+} imaging experiments…….....152

Figure 3.10: Bar chart displaying the average maximum peak height in fluorescence intensity that was observed during stimulus perfusion as a percentage (±SE (median)) of the maximum peak height observed during ATP positive control stimulus perfusion……...154

Figure 4.1- A flowchart schematic of the fractionation process……..……..172

Figure 4.2- An Rtot plot of the timelapse Ca^{2+} imaging experiment carried out on 108 OE-E6/E7 cells using the pooled sperm conditioned media as a stimulus, before washing it off the surface of the cells with sEBSS and finally adding 100 µM ATP solution used as a positive control stimulus…….....176

Figure 4.3- Rtot plots for the timelapse Ca^{2+} imaging experiments carried out using each of the three fractions of sperm conditioned media, as well as the initial pooled conditioned media overlayed on the same line graph for comparison……177

Figure 4.4- Rtot plot for the timelapse Ca^{2+} imaging experiment carried out using the post-precipitation, resuspended protein pellet from the <3kDa fraction of sperm conditioned media as stimulus……..……179

Figure 4.5- The alignment of the sequence of amino acids within semenogelin-1 against semenogelin-2…….186

Figure 4.6- Semenogelin-1 peptides consistently identified in all three fractions of the pooled sperm conditioned media, as well as their alignment within the protein……..……..187

Figure 4.7- Semenogelin-2 peptides consistently identified in all three fractions of the pooled sperm conditioned media, as well as their alignment within the protein……188

Figure 4.8- The alignment of each peptide identified in the <3kDa fraction of pooled sperm conditioned media, with red lines indicated the predicted sites of trypsin cleavage……...189

Figure 4.9- The alignment of each peptide identified in the <3kDa fraction of pooled sperm conditioned media, with red lines indicated the predicted sites of trypsin cleavage……..……190

Figure 4.10- Predicted 3D structure of semenogelin-1, created using DNASTAR Protean 3D modelling software……..……..191

Figure 4.11- Predicted 3D structure of semenogelin-2, created using DNASTAR Protean 3D modelling software……..……..192

Figure 5.1- Rtot average fluorescence timelapse plots from experiments in which OE-E6/E7 cells were perfused with the three synthesized semenogelin peptides……..……213

Figure 5.2- Rtot average fluorescence timelapse plots from experiments in which OE-E6/E7 cells were perfused with the three synthesized semenogelin peptides and sperm conditioned media for comparison of response…..……215

Figure 5.3- Rtot average fluorescence timelapse plot from an experiment in which OE-E6/E7 cells which had been co-incubated with TLR4-IN-C34 were perfused with sperm conditioned media……..……..……217

Figure 5.4- Rtot average fluorescence timelapse plot from an experiment in which OE-E6/E7 cells were only exposed to Ca^{2+} free sEBSS and sperm conditioned media……219

Figure 5.5- Rtot average fluorescence timelapse plot from an experiment in which OE-E6/E7 cells were treated with 10 µM thapsigargin before assessing the effect of sperm conditioned media……..221

Figure 5.6- Rtot average fluorescence timelapse plots from experiments in which <2 kDa dialysed sperm conditioned media was compared to sperm conditioned media perfusion across OE-E6/E7 cells……..……..223

Figure 6.1- An overview of the proposed signalling mechanism through which protein/peptide factors present in the male ejaculate elicit Ca^{2+} signalling in the oviductal epithelial cells……....246

Figure 6.2- The reversible adherence of the protein/peptide signalling factors onto the surface of spermatozoa from the seminal plasma…….247

Figure 6.3- The transit of the signalling factors, adhered to the surface of motile sperm cells, through the cervical mucus and into the upper regions of the female reproductive tract……...248

Figure 6.4- The release of the male ejaculate signalling factors into the fluid within the lumen of the oviduct……..……..249

Figure 6.5- The proposed signalling mechanism by which the protein/peptide factors from the male ejaculate elicit Ca^{2+} signalling in the oviductal epithelial cells…….……250

List of Tables

Table 4.1- Results from the proteomic analysis of the <3 kDa fraction of the pooled sperm conditioned media……..……180

Table 4.2- Results from the proteomic analysis of the 3-50 kDa fraction of the pooled sperm conditioned media……..……181

Table 4.3- Peptides identified from semenogelin-1 and semenogelin-2 in the <3 kDa fraction of pooled sperm conditioned media……..……183

Table 4.4- Peptides identified from semenogelin-1 and semenogelin-2 in the digested 3-50 kDa fraction of pooled sperm conditioned media……....184

Table 4.5- Peptides identified from semenogelin-1 and semenogelin-2 in the >50 kDa fraction of pooled sperm conditioned media……185

Table 6.1- A summary of the semen sample preparations described in section 3.2.2 and their intended proteomic content…….……235

List of Abbreviations

ACE	Angiotensin converting enzyme
AR	Acrosome reaction
ATP	Adenosine triphosphate
BSA	Bovine serum albumin
Ca^{2+}	Calcium
$[Ca^{2+}]_i$	Intracellular calcium
cADPR	Cyclic ADP ribose
CAM	Calmodulin
CaMKII	Calmodulin dependent protein kinase II
cAMP	Cyclic adenosine monophosphate
CASA	Computer assisted semen analysis
CICR	Ca^{2+} induced Ca^{2+} release
Cl^-	Chloride
DGC	Density gradient centrifugation
DMEM	Dulbecco's modified Eagle's medium
DNA	Deoxyribonucleic acid
DTT	Dithiothreitol
E_2	Oestrogen
ELISA	Enzyme-linked immunosorbent assay
FBS	Foetal bovine serum
FRT	Female reproductive tract
FSH	Follicle stimulating hormone
Gd-S	Glycodelin S
H_2O_2	Hydrogen peroxide
HCO_3^-	Bicarbonate

HFF	Human foreskin fibroblast
IMDM	Iscove's modified Dublecco's medium
IP_3	Inositol 1,4,5-trisphosphate
IP_3R	Inositol-1,4,5-trisphosphate receptor
K^+	Potassium
LH	Luteinising hormone
MAPK	
miRNAs	MicroRNAs
mRNAs	Messenger RNAs
MWCO	Molecular weight-cut off
NFAT	Nuclear factor of activated T-cells
NF-κB	Nuclear factor kappa-light-chain-enhancer of activated B cell
NO	Nitric oxide
O_2^-	Superoxide anion
P_4	Progesterone
PAS	Postacrosomal sheath
PAWP	Post-acrosomal sheath WW domain-binding protein
PBS	Phosphate-buffered saline
PenStrep	Penicillin-Streptomycin
PKA	Protein kinase A
PLCζ	Phospholipase C-zeta
PSA	Prostate-specific antigen
PSAP	Prostatic-specific acid phosphatase
PT	Perinuclear theca
RYR	Ryanodine receptor
sAC	Soluble isoform of adenylyl cyclase
sEBSS,	Supplemented Earle's balanced salt solution

SL	Subacrosomal layer
SPMI	Seminal plasma motility inhibitor
SPPS	Solid-phase peptide synthesis
TGFB	Transforming growth factor-beta1
TLR4	Toll-like receptor 4
TRP	Transient receptor potential
TRPC	Transient receptor potential canonical
TUNEL	Terminal deoxynucleotidyl transferase dUTP nick end labelling
UPLC	Ultra-high performance liquid chromatography
Zn^{2+}	Zinc

COVID-19 Impact Statement

The COVID-19 pandemic has brought unprecedented challenges to the world, including the academic research community. As I embarked on my PhD journey, I envisioned a trajectory that would be characterized by a seamless flow of research activities, collaborations, and data collection. However, as the pandemic unfolded, it became apparent that this vision was unlikely to become a reality. The restrictions on physical interactions, travel, and laboratory access imposed to curb the spread of the virus forced me to adapt and modify my research plans.

One significant impact of the pandemic on my work was the hindrance of my collaboration with Professors Richard Lea and David Gardner, with whom I intended to develop cultures of porcine and canine oviductal epithelial cells to use in my experiments. The pandemic prevented us from carrying out this work, and as a result, I had to explore alternative models to study the effect of my treatments on oviductal cells. Another significant impact of the pandemic on my work was the inability to enter the hospital to acquire primary tissue samples from hysterectomy patients, which would have provided the basis for experiments on primary human cells in conjunction with the secondary cell lines used in my study. I was also unable to access the research laboratory for a long portion of my studies, which limited my ability to perform experimental work. However, this limitation also led to a unique opportunity to explore computational methods and software to carry out proteomics research. Through this experience, I gained new skills in data analysis and interpretation, which complemented my experimental work. Overall, the COVID-19 pandemic has significantly impacted my PhD journey, but it has also provided opportunities for personal and academic growth.

Chapter 1

Introduction

1.1- The prevalence and causes of infertility

Reproduction is essential for the propagation and survival of all vertebrate species. The first step of mammalian reproduction is the interaction between a sperm cell and an oocyte to form a zygote, however, the origins of the reproductive process begin much earlier with the development of the germ cell line in the embryo (Matzuk and Lamb 2008). Between the development of the germ cell line and the meeting of sperm cell and oocyte in the ampulla region of the oviduct (Avilés, Coy et al. 2015), the functionality of a wide range of genes, proteins, RNAs and cellular processes are required. Disruptions in any of these steps along the path to reproduction can lead to reproductive failure.

Infertility is defined as the failure to achieve a pregnancy after 12 months or more of regular unprotected sexual intercourse during the fertile phase of the menstrual cycles (Health and Excellence 2017). It is estimated that 8-12% of couples of reproductive age are affected by infertility (Ombelet, Cooke et al. 2008). 9% is the commonly cited figure for the global average prevalence of infertility (Boivin, Bunting et al. 2007), with rates reaching as high as 30% in some populations within developing countries (Nachtigall 2006). Infertility is thought to affect approximately 1 in 7 couples in the United Kingdom (NHS 2022).

Approximately 50% of cases of infertility are caused by solely female factors, whilst purely male factors account for between 20 and 30% of the infertile population. The remaining 20-30% of cases of infertility are due to a combination of the two (Sharlip, Jarow et al. 2002). The magnitude of male factor infertility is believed to be widely underestimated due to a range of stigmas associated with infertility due to religious and cultural beliefs worldwide, which has led to a distinct historical lack of research

into the causes and prevalence of the condition (Agarwal, Mulgund et al. 2015). Up to 30% of cases of infertility are unexplained (Abdallah, Hunt et al. 2020), meaning that they cannot be attributed to poor sperm quality, tubal pathology, anovulation or any other known cause of infertility (Mol, Tjon-Kon-Fat et al. 2018). The lack of research into the causes of male factor infertility and the prevalence of unexplained infertility highlight the necessity for further experimentation in human models of reproduction to elucidate currently unrecognised biological mechanisms that are necessary for successful fertilisation.

1.2- The Human Sperm Cell

1.2.1- The anatomy of spermatozoa

The mature human sperm cell is a specialised, differentiated cell which consists of a tail, midpiece and head region which are all bound by a singular plasma membrane (Mortimer 2018). The classification of assessment of spermatozoa morphology is conventionally assessed according to the Tygerberg Strict Criteria (Menkveld, Stander et al. 1990). These criteria for 'ideal' sperm morphology were developed on the basis of sperm cells that were recovered from post-coital cervical mucus (Mortimer and Menkveld 2001) and observations of spermatozoa which were bound to *in vitro* zona pellucida (Liu and Baker 1992). Although humans typically have a very low percentage of 'normal' spermatozoa within their ejaculate, according to these criteria, it has been demonstrated that abnormal sperm morphology is a significant negative predictor of biological function (Björndahl, Mortimer et al. 2010).

A 'normal' human spermatozoa should have an oval shaped head which is 4-5 μm in length and 2-3 μm in width (Mortimer 2018). The head section contains a clearly visible acrosome, which is an organelle with a cap-like structure derived from the

Golgi apparatus which covers 40-60% of the anterior section of the spermatozoa head and contains digestive enzymes and a range of other proteins (Khawar, Gao et al. 2019). The midpiece section of the human sperm cell connects the head to the tail section, this piece of the cell is typically around 1 μm in width and is no more than 150% the length of the head. The tail section should be approximately 45-50 μm in length without any sharp bends (Björndahl, Mortimer et al. 2010).

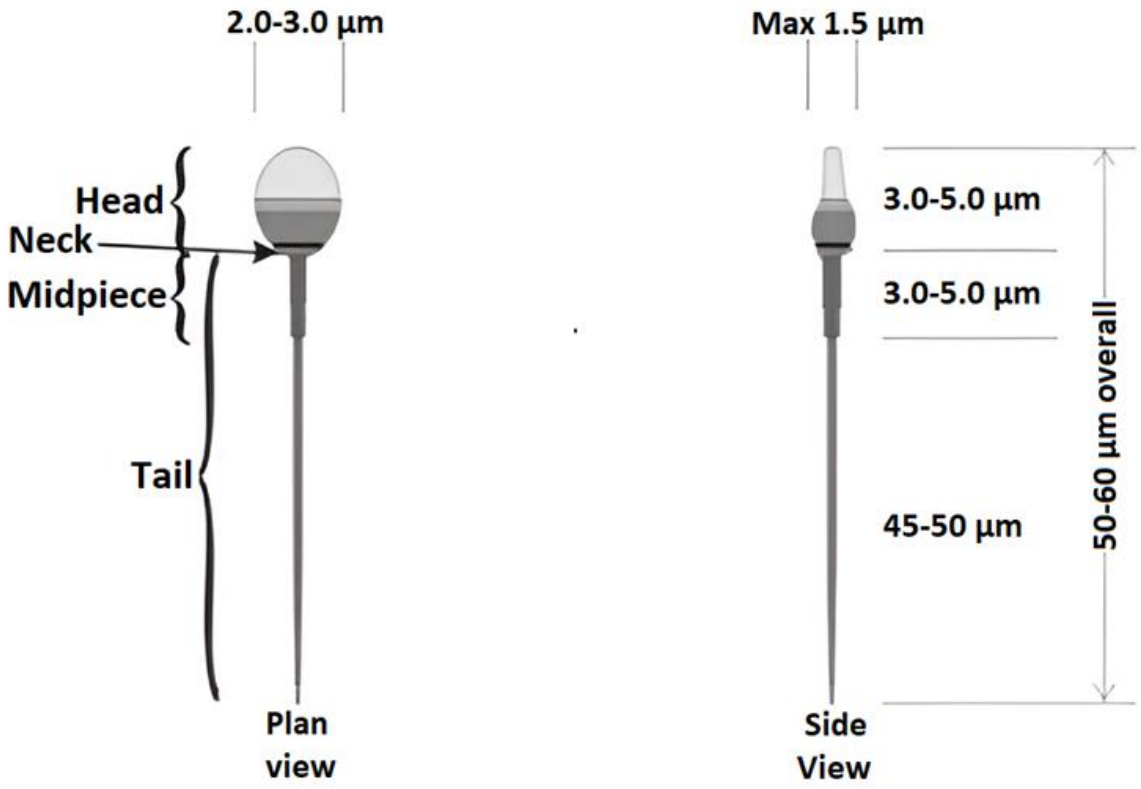


Figure 1.1- Adapted and modified from (Mortimer and Menkveld 2001). A diagram representing the morphological characteristics and dimensions of an 'ideal' mature human sperm cells, according to the Tygerberg Strict Criteria.

1.2.2- The Human Sperm Cell Head

The head of the human sperm cell contains the nucleus, which differs from the nuclei of somatic cells in that it contains half of the amount of DNA but in less than 40-fold the volume of an average somatic cell nucleus (Wyrobek, Meistrich et al. 1976). This is due to the structure of mammalian sperm chromatin, which is highly condensed and has protamines in the conventional place of histones, which form disulphide covalent bonds that provide stability and protection against DNA damage (Barratt, Aitken et al. 2010). This semi-crystalline structure also has zinc bound to it, which originates from the seminal plasma in the ejaculate and provides additional protection to the free sulphydryl groups as well as facilitating the process of unpacking the sperm chromatin once it has left the nuclear envelope into the oocyte cytoplasm during fertilisation (Kvist, Björndahl et al. 1987).

The nuclear envelope within the human sperm cell significantly differs from its somatic counterparts in that it is mostly lacking in nuclear pores apart from a very specific, thicker region of the envelope between the basal plate and the posterior ring, which is where the midpiece of the cell connects to the head (Mortimer 1994). The pores within the nuclear envelope are not necessary in spermatozoa due to the tight compaction and lack of activity within the chromatin and their absence provides an additional layer of protection for the genetic material (Mortimer and Menkveld 2001).

The acrosome forms a cap structure on the head of the human spermatozoa, forming a close association with the nuclear envelope and lying directly beneath the plasma membrane in the anterior head region. In order to acquire the ability to fertilise an oocyte, human spermatozoa must first undergo a calcium ion (Ca^{2+})-dependent exocytotic process known as the acrosome reaction (AR), which involves

the fusion of the outer acrosomal membrane with the sperm plasma membrane in various locations to allow for the release of the acrosomal contents from the sperm cell (Yanagimachi 2011). The rear section of the human sperm acrosome is referred to as the equatorial segment, this is the part of the acrosome that remains intact after the AR and is the site where the sperm cell fuses with the oocyte (Wolkowicz, Digilio et al. 2008). Phospholipase C-zeta (PLCζ) is the sperm cell derived factor that is thought to be responsible for 'oocyte activation' by eliciting the initiation of Ca^{2+} oscillations within the oocyte during fertilisation (Swann, Windsor et al. 2012, Swann 2018). This protein is reported to be localised within the equatorial segment of human sperm cells (Grasa, Coward et al. 2008).

The majority of the cytoplasm within the head of mammalian spermatozoa is condensed within the structure of the perinuclear theca (PT), which can be further subdivided into the subacrosomal layer (SL) and the postacrosomal sheath (PAS) (Oko, Aul et al. 2001). The PAS is a structure that is wrapped around the posterior section of the sperm cell head and forms the initial binding site between the spermatozoa and zona pellucida (Wu, Sutovsky et al. 2007). This region of spermatozoa has been demonstrated to contain a protein called post-acrosomal sheath WW domain-binding protein (PAWP), which is also reported to elicit Ca^{2+} oscillations upon entry into the oocyte (Aarabi, Balakier et al. 2014). The identity of the true human 'oocyte activation' factor is a topic of great debate, but the majority of the evidence suggests that PLCζ causes the specific Ca^{2+} oscillations that are essential for the successful fertilisation of the oocyte (Nomikos, Sanders et al. 2015).

1.2.3- The Human Sperm Midpiece

The human sperm midpiece is the section of the cell that connects the tail to the basal side of the sperm nuclear envelope (Fawcett 1970). The midpiece contains a distal and a proximal centriole, with the distal centriole attached to the base of the axoneme and the proximal centriole located close to the base of the sperm head (Avidor-Reiss, Mazur et al. 2019). Centrioles are cylinders formed by nine triplet microtubules that are arranged into a barrel like structure and they are essential cellular components for the processes of fertilisation and cell development (Nigg and Raff 2009). The human sperm cell distal centriole has an atypical structure, with splayed microtubules and dense outer fibres that form an inverted cone shape extending towards the proximal centriole (Fishman, Jo et al. 2018). It is theorised that upon the entry of a human spermatozoa into the oocyte cytoplasm during fertilisation, the proximal centriole is inherited by the zygote (Sathananthan, Kola et al. 1991) and duplicates to form the microtubule-organising centre that carries out the initial cellular cleavage in the embryo (Schatten and Sun 2011). There is evidence that the distal centriole is also inherited by the human zygote to form a daughter centriole that is localised to the spindle pole during the first mitotic division of the embryo (Fishman, Jo et al. 2018).

The human sperm midpiece also contains the anterior sections of the sperm cell flagellum or tail (Mortimer 2018). It is approximated that there are 24 to 26 mitochondria within the typical human sperm midpiece, however, these mitochondria differ from their somatic counterparts due to key biochemical differences in the presence of specific enzyme isoforms (Piomboni, Focarelli et al. 2012). The mitochondria within the sperm midpiece are arranged in a helix of approximately thirteen gyres, with two mitochondria per gyrus surrounding the axoneme. These

organelles are responsible for the production of energy in the form of adenosine triphosphate (ATP) which is essential for the maintenance of sperm motility (Rajender, Rahul et al. 2010). Mitochondria also play a role in the modulation of intracellular Ca^{2+} homoeostasis within spermatozoa as they are able to function as intracellular Ca^{2+} stores (Costello, Michelangeli et al. 2009). Ca^{2+} signalling is essential within sperm cells for the regulation of cellular processes such as capacitation, chemotaxis, hyperactivation and the aforementioned AR (Publicover, Harper et al. 2007). Ca^{2+} is taken into the sperm mitochondria by the mitochondrial Ca^{2+} uniporter that is localised on the inner membrane of the organelle (Kirichok, Krapivinsky et al. 2004).

1.2.4- The Human Sperm Tail

The human sperm cell tail section is made of the same microtubule structure as other cilia and flagella seen in somatic cells, however, the sperm cell flagella is different due to the presence of an additional set of dense outer set of fibres along its length up to the terminal segment which returns to the standard 9 + 2 microtubule structure commonly seen in flagella (Linck, Chemes et al. 2016). The additional dense fibres in the human sperm cell tail function as elastic elements that serve the purpose of increasing the generation of power when the tail is beating by elastically bouncing back after each wave (Fawcett 1975).

The principal piece of the sperm cell tail is surrounded by a fibrous sheath, which is assembled during spermiogenesis by the spindle-shaped body (Zamboni 1991). In the mature spermatozoa, this fibrous sheath functions as a mediator of the proximal plane of flagellar beating and regulates the level of flexibility within the tail, having a significant impact on the flagellar wave (Chemes, Brugo et al. 1987). The wave pattern produced by the sperm cell flagellum forms the basis of sperm motility and

the production of the wave is dependent upon the level of intracellular Ca^{2+} ($[Ca^{2+}]_i$) (Olson, Fauci et al. 2011). The expression of the sperm-specific calcium ion channel CatSper1 has been observed along the length of the plasma membrane above the fibrous sheath, organised into 4 rows of Ca^{2+} signalling domains in which signalling molecules such as calcineurin and CaMKII are included (Chung, Shim et al. 2014).

1.2.5- Sperm cell production and storage

Spermatogenesis occurs in the seminiferous tubules within the male testes, it is a multi-step process that begins with the proliferation of spermatogonia which then differentiate into spermatocytes, which undergo meiotic division to produce spermatids, upon maturation, spermatozoa are then released into the testicular tubule lumen (Neto, Bach et al. 2016). The process of spermatogenesis is approximated to take 80 days in total to produce mature spermatozoa (Heller and Clermont 1963), with between 150 and 275 million cells produced on a daily basis (Amann 2008).

Spermatozoa acquire their fertilisation capacity and motility during their transport through the epididymis (Jones and Lopez 2013). The epididymis is a long tubule connecting the male testes to the vas deferens and it is comprised of four distinct regions- the initial segment, caput, corpus and cauda (Plant and Zeleznik 2014). Each anatomical region of the epididymis has a unique luminal environment, with different fluids, ions, antioxidants and exosomes which contribute to the maturation of spermatozoa as they pass through each section (Nixon, De Iuliis et al. 2019, Trigg, Eamens et al. 2019). Aside from being the site of maturation of spermatozoa, the epididymis also protects the gametes from damage by factors in the external environment (Hinton, Palladino et al. 1996). Antioxidant enzymes are excreted from the epididymal epithelial cells in order to prevent damage to sperm DNA by the

reactive oxygen species that are produced by their own high levels of metabolic activity (O'Flaherty 2019). A blood-epididymis barrier is also present, which protects the spermatozoa from the immune system and any harmful substances within the bloodstream (Plant and Zeleznik 2014). The cauda epididymis is the location where functionally mature spermatozoa are stored and kept in a quiescent state by the secretions of the cauda epithelial cells until the point of ejaculation (James, Carrell et al. 2020).

1.2.6- The Male Ejaculate

The process of male ejaculation is commonly viewed as a singular event, however, it is actually two different processes referred to as emission and ejaculation (Master and Turek 2001). Ejaculation is a physiological process that is largely controlled by the autonomic nervous system (Alwaal, Breyer et al. 2015) and the process involves the function of a range of organs including the epididymis, vas deferens, seminal vesicle, prostate, prostatic urethra and the bladder neck (Giuliano and Clément 2005). The emission phase involves the ejection of spermatozoa into the prostatic urethra, where they are mixed with fluids that are secreted by the accessory sexual glands by smooth muscle fibre contractions in the epididymis, ductus deferens, seminal vesicles, and prostate. The expulsion phase is the ejection of semen from the urethra facilitated by involuntary contractions of the striated perineal muscles (Puppo and Puppo 2016).

Human seminal fluid is a complex mixture of various substances, including cytokines, growth factors, prostaglandins, hormones, and minerals, that play a crucial role in male fertility and reproductive function. Some of the key substances present in human seminal fluid are:

1. Cytokines: Interleukin-1α, Interleukin-1β, Interleukin-6, Interleukin-8, Tumor necrosis factor-alpha (TNF-α), and Granulocyte-macrophage colony-stimulating factor (GM-CSF) are some of the cytokines found in human seminal fluid (Loveland, Klein et al. 2017).

2. Growth factors: Several growth factors, including Epidermal growth factor (EGF), Insulin-like growth factor 1 (IGF-1), Transforming growth factor-beta (TGF-β), and Vascular endothelial growth factor (VEGF), have been identified in human seminal fluid (Ghasemian Nafchi, Azizi et al. 2022).

3. Prostaglandins: Prostaglandins are a group of lipid compounds that are involved in several physiological processes, including inflammation, pain, and blood clotting. Human seminal fluid contains various prostaglandins, including Prostaglandin E2 (PGE2), Prostaglandin F2α (PGF2α), and Prostaglandin D2 (PGD2) (Bygdeman, Bendvold et al. 1985).

4. Hormones: Several hormones are present in human seminal fluid, including Testosterone, Luteinizing hormone (LH), and Follicle-stimulating hormone (FSH) (Ney 1986).

5. Minerals: Human seminal fluid contains several minerals, including Zinc, Magnesium, Calcium, and Selenium (Saaranen, Suistomaa et al. 1987, Slivkova, Popelkova et al. 2009).

These substances play a critical role in various aspects of male reproductive function, including sperm motility, capacitation, and fertilization. Dysregulation of these substances in seminal fluid has been linked to several male fertility disorders, such as oligozoospermia and asthenozoospermia (Wang, Yang et al. 2020). For

example, the concentration of ATP per millilitre of ejaculate is significantly correlated with sperm concentration, motility and *in vitro* potential to penetrate zona-free hamster ova, with significantly lower concentrations of ATP present in the seminal plasma of infertile males compared to matched fertile donors (Comhaire, Vermeulen et al. 1983). This is likely due to the regulation of sperm cell mitochondrial metabolism by extracellular ATP in the seminal plasma to control sperm cells motility (Guo, Chang et al. 2019).

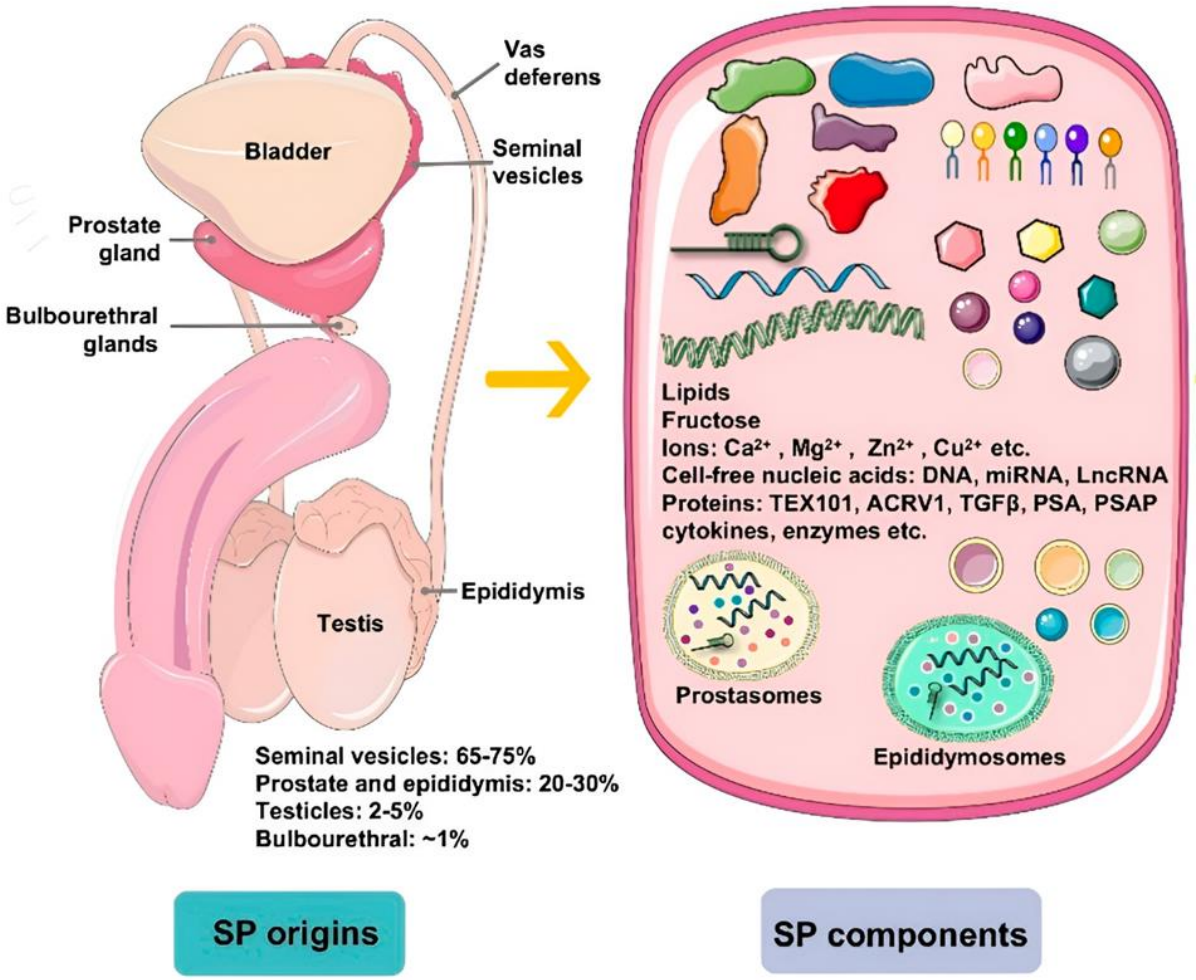


Figure 1.2- Adapted and modified from (Wang, Yang et al. 2020). The origins of the male ejaculate, the organs which contribute to the seminal plasma and a diagram detailing some of its primary components.

The seminal plasma is the fluid component of the ejaculate, which functions as a vehicle to carry spermatozoa throughout the male and female reproductive tract (FRT) during ejaculation (Wang, Yang et al. 2020). Due to the incomplete mixing of its components during the smooth muscle contractions in the male tract, the male ejaculate is not a homogenous mixture, and it is ejaculated in distinct portions. The first portion consists mostly of secretions from the bulbourethral glands, whilst the second portion is mostly derived from the secretions of the prostate gland followed by contributions from the epididymis and finally from the seminal vesicles, which

contribute the majority of the ejaculate volume (Owen and Katz 2005). The testicular secretions containing spermatozoa only account for approximately 2-5% of semen, whilst the seminal plasma makes up the remaining 95%. The secretions from the seminal vesicles account for approximately 65-75% of the volume of seminal plasma, whilst the prostate gland and epididymis contribute approximately 20-30% of the volume. The bulbourethral glands generate a small proportion, amounting to ~1% of the total volume of the male ejaculate (Robert and Gagnon 1994).

The molecular contents of the seminal plasma are a heterogenous mixture of proteins, sugars, lipids, DNA, microRNA, metabolites and ions (Wang, Yang et al. 2020). The predominant molecular components of seminal plasma are a diverse range of proteins and peptides that can directly bind to spermatozoa and contribute to the cells' maturation, function and ability to interact with the FRT (Manjunath, Bergeron et al. 2007). The overall protein concentration of seminal plasma is approximately 40 to 60 mg/mL (Drabovich, Saraon et al. 2014), with many of the proteins derived from prostasomes and epididysomes that are protein filled vesicles secreted by the prostate gland and the epididymal epithelium, respectively (Utleg, Yi et al. 2003, Thimon, Frenette et al. 2008). The most abundant proteins in the male ejaculate are semenogelin-1 and semenogelin-2, followed by laminin and various enzymes such as prostate-specific antigen (PSA), prostatic-specific acid phosphatase (PSAP) and creatine kinase (Edwards, Tollaksen et al. 1981). Differential expression within the seminal plasma proteome has a significant impact of male fertility. One example of this is a study which demonstrated that oligoasthenozoospermic patients have 22 upregulated and 20 downregulated proteins within their seminal plasma proteome of 734 proteins in comparison to normozoospermic males (Liu, Wang et al. 2018).

Post translational modification of the seminal plasma proteome is also an important aspect of sperm cell function. Glycosylation is the most abundant and complex protein modification that can have a significant impact on the structure and function of a protein (Clerc, Reiding et al. 2016). Glycosylation of proteins leads to the production of glycoproteins which are proteins that have a compound containing a carbohydrate (or glycan) covalently linked to them. Glycoproteins attached to the cell surface are commonly responsible for the mediation of cell-cell and cell-protein interactions (Yagi, Yanaka et al. 2018).

1.2.7- Capacitation and acquisition of hyperactivated motility

Freshly ejaculated spermatozoa must undergo a series of physiological changes in order to acquire the ability to penetrate the oocyte and achieve fertilisation (Austin 1952). This phenomenon of mammalian spermatozoa was first described in rat and rabbit models, with the observation that the spermatozoa must be present within the FRT for a period to acquire their fertilising capacity (Austin 1951, Chang 1951). Whilst *in vivo* capacitation of mammalian spermaotozoa takes place within the FRT, *in vitro* capacitation can be achieved by using media containing specific capacitation inducing compounds at a particular pH (Chang 1951). Only capacitated spermatozoa can undergo the AR and fertilise an oocyte, with processes leading to the initiation of the AR occurring within the sperm cell head and processes leading to the acquisition of hyperactivated motility occurring in the sperm tail (Jin and Yang 2017).

The parallel and sequential processes that lead to sperm cell capacitation have recently been divided into slow and fast events (Salicioni, Platt et al. 2007). The fast events such as the activation of asymmetric, vigorous beating of the sperm cell flagellum take place when spermatozoa first leave the epididymis, whilst the slow events such as gaining the ability to undergo the AR and the switch to

hyperactivated motility occur later on, facilitated by cell signalling cascades within the FRT (Salicioni, Platt et al. 2007). Capacitation is regulated by a complex range of factors and despite the first report of mammalian sperm cell capacitation over 70 years ago, the molecular basis of the process is still not completely understood.

One of the first events in human sperm cell capacitation is the albumin mediated removal of cholesterol from the plasma membrane, leading to a more fluid and permeable membrane and an altered lipid distribution that promotes capacitation (Petrounkina, Harrison et al. 2000, Cross 2004). This cholesterol efflux allows for phospholipid scrambling and reorganization of plasma membrane lipid microdomains to promote sperm binding to the zona pellucida and the AR, as well as supporting protein tyrosine phosphorylation (Boerke, Tsai et al. 2008).

Ejaculated spermatozoa are immediately introduced to high concentrations of bicarbonate (HCO_3^-) within the seminal fluid, which has an essential role in the capacitation of spermatozoa (Okamura, Tajima et al. 1986). HCO_3^- regulates the motility and metabolism of sperm cells through the stimulation of increased cyclic adenosine monophosphate (cAMP) concentration within the cells (Tajima, Okamura et al. 1987). The elevation in intracellular cAMP is induced by the stimulation of the sperm specific soluble isoform of adenylyl cyclase (sAC) (Litvin, Kamenetsky et al. 2003) which is responsible for the conversion of ATP to cAMP (Hess, Jones et al. 2005). The subsequent rise in intracellular cAMP leads to the activation of protein kinase A (PKA) (otherwise known as the cAMP-dependent kinase) by the removal of the regulatory subunits from the catalytic subunits (Baker 2016). The activation of PKA causes the upregulation of tyrosine phosphorylation of subsets of sperm proteins, which has been identified as a critical factor for the regulation of sperm cell capacitation, AR and various other physiological processes (Visconti, Bailey et al.

1995). Interestingly, the AR and acquisition of fertilising capacity has been achieved in murine sperm cells with brief exposure to the Ca^{2+} ionophore A23187 which elevates $[Ca^{2+}]_{i.}$ Subsequent fertilisation of oocytes with these spermatozoa led to the development of normal offspring, suggesting that a short elevation of $[Ca^{2+}]_i$ can overcome signalling pathways such as tyrosine phosphorylation in rendering sperm cells fertile (Tateno, Krapf et al. 2013).

Ca^{2+} is a key regulator of sperm cell capacitation, motility and hyperactivation. Variations in intracellular concentrations of Ca^{2+} within sperm cells initiate significant alterations in their functional behaviour that are essential for navigation of the FRT and the eventual fertilisation of the oocyte (Alasmari, Costello et al. 2013). $[Ca^{2+}]_i$ within sperm cells is increased via either the release of Ca^{2+} from intracellular stores (Scott, Ramirez-Reveco et al. 2016) or by the influx of Ca^{2+} through ion channels in the plasma membrane such as the sperm specific Ca^{2+} channels referred to as CatSper (Alasmari, Costello et al. 2013). The influx of extracellular Ca^{2+} into sperm cells is mediated by a range of permeable channel proteins (Kirichok, Navarro et al. 2006, Lishko and Kirichok 2010) that are regulated by factors such as ligands, pressure, voltage or the depletion of the intracellular Ca^{2+} stores (Jin and Yang 2017).

The AR is triggered by a sharp increase in $[Ca^{2+}]_i$ and intracellular pH that is initiated when spermatozoa come into contact with the cumulus oophorus or when binding with the glycoproteins that form the zona pellucida (Arnoult, Zeng et al. 1996, Ren and Xia 2010). $[Ca^{2+}]_i$ has also been shown to be responsible for the asymmetrical, rapid beating of the flagella that characterises hyperactivated motility (Ho and Suarez 2001). Throughout capacitation $[Ca^{2+}]_i$ and cAMP levels rise significantly in a time dependent manner until a threshold is met and hyperactivated motility on the

spermatozoa is initiated (Sánchez-Cárdenas, Montoya et al. 2018). It has been demonstrated that $[Ca^{2+}]_i$ is the key mediator of hyperactivation with cAMP acting as a secondary messenger (Suarez 2008). This has been made evident by the addition of Ca^{2+} to demembranated spermatozoa, which led to the induction of hyperactivated motility, showing that Ca^{2+} is capable of acting directly on cytoskeletal elements to promote the high amplitude, asymmetrical beating of the flagella (Ho, Granish et al. 2002).

Aside from ionic stimulation of sperm cell capacitation, there is also evidence that steroid hormones within the oviductal or follicular fluids are involved in the process. Progesterone and oestrogen are both demonstrated inducers of sperm cell capacitation (Meizel and Turner 1983, Ded, Sebkova et al. 2013). Progesterone is produced mostly by the cumulus and granulosa cells during ovulation, followed by production from the corpus luteum after ovulation has taken place (López-Torres and Chirinos 2017). The presence of a receptor for progesterone on the human sperm cell plasma membrane has been reviewed extensively (Aquila and De Amicis 2014). Exposure of human spermatozoa to progesterone induces immediate Ca^{2+} influx into the cells promoting motility and tyrosine phosphorylation and eventually causes the induction of the AR within minutes (Blackmore, Neulen et al. 1991). The progesterone induced Ca^{2+} influx is thought to be at least partially mediated by the activation of the sperm cell specific Ca^{2+} ion channel CatSper (Strünker, Goodwin et al. 2011). Oestrogen has also been reported to elicit extracellular Ca^{2+} influx to promote tyrosine phosphorylation within human sperm cells by stimulation of oestrogen receptor alpha and beta (Guido, Perrotta et al. 2011).

Other FRT derived molecules that have been shown to promote the process of sperm cell capacitation include the superoxide anion (O_2^-) (de Lamirande and

Gagnon 1995), hydrogen peroxide (H_2O_2) (Griveau, Renard et al. 1994) and nitric oxide (NO) (Herrero, de Lamirande et al. 1999). A wide range of molecular pathways and models have been elucidated as being involved in the process of sperm cell capacitation, with many of them crossing over each other and forming a complex network of processes that are still not completely understood.

1.3- The Female Reproductive tract

1.3.1- Anatomy of the Female Reproductive Tract

The FRT is responsible for the regulation of healthy oocyte maturation, the provision of a protective environment for sperm cells to fertilise the oocyte and the subsequent implantation of the embryo, as well as providing nutrition for sustained foetal growth (Chumduri and Turco 2021). The FRT consists of the ovaries, which are the site of oocyte maturation before they are released into the oviducts, or fallopian tubes, which act as the site of fertilisation in the ampulla region and are also responsible the early development of the embryo and its transport into the uterus (Pérez-Cerezales, Ramos-Ibeas et al. 2018). The uterus is the site of embryo implantation and foetal development throughout the pregnancy. The cervix acts is the passage which connects the uterus to the vagina, it acts as a barrier to protect the upper FRT from pathogens and selectively allows the passage of motile spermatozoa from the upper vagina which is the site of semen deposition during intercourse (Lacroix, Gouyer et al. 2020).

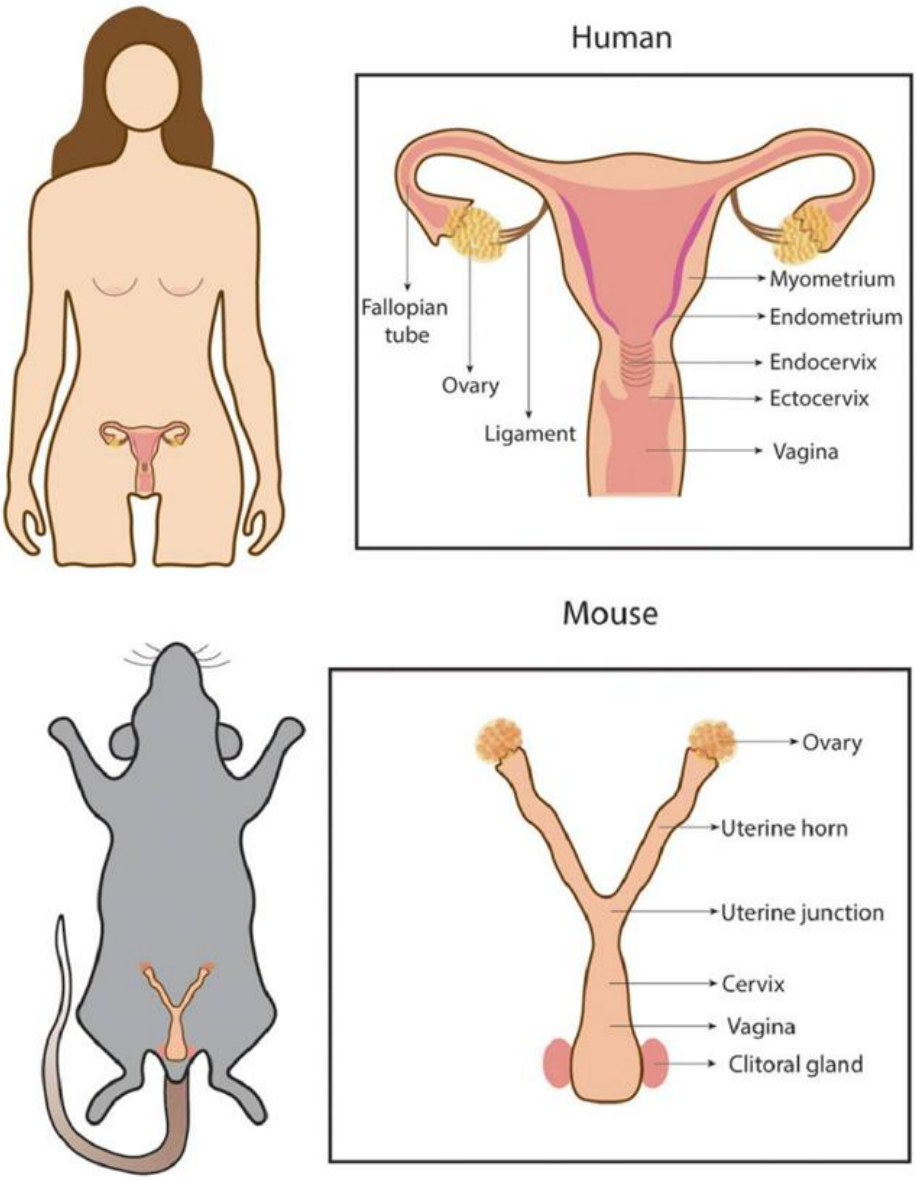


Figure 1.3- Adapted from (Chumduri and Turco 2021). The anatomy of the female reproductive tract in humans and mice.

The anatomy of the FRT is varied across mammalian species, with human FRT containing ovaries and pronounced oviducts, a uterus consisting of myometrium and endometrium and a cervix with a well define endocervix and ectocervix. In contrast, mice have a bicornuate uterus with uterine horns, the oviducts are much smaller in proportion to the rest of the murine FRT and the cervix does not form a clear barrier between the vagina and uterine junction, which leads to key differences in the

process of fertilisation and the journey that spermatozoa must undertake to reach the oocyte between species (Cunha, Sinclair et al. 2019).

1.3.2- The Vagina

The vagina is a distensible tube that extends from the vulva to the cervix and is covered with mucosal folds. One of the functions of the vagina is to prevent invasive organisms from reaching the uterus, thus providing a layer of protection to the site of embryo development (White, Creedon et al. 2011). The vagina has a complex microbiome, containing colonies of bacteria such as *Lactobacillus acidophilus* which contribute to the protection against harmful microorganisms by producing and secreting lactic acid and help to maintain an acidic environment within the vagina of approximately pH 3.5-4.9 (Boskey, Cone et al. 2001).

1.3.3- The Cervix

The cervix is a cylindrical structure that forms the passage linking the upper region of the vagina to the cavity of the uterus, acting as a physical barrier between the two. The cervix functions to facilitate the passage of motile spermatozoa from the site of semen deposition into the upper regions of the FRT and to add an additional layer of protection for the uterus from potentially invasive microorganisms from external sources (Nott, Bonney et al. 2016). The cervix consists of two distinct regions, the ectocervix which projects into the vagina and contains the external os of the cervical canal, and the endocervix which is located at the side of the cervix in contact with the uterus and contains the internal os of the narrow endocervical canal which connects the two regions (Singer and Jordan 2006).

The epithelial lining of the endocervical canal consists of a folded layer of mucus-secreting columnar epithelium that extends to the squamous epithelial lining of the vagina (Beckmann 1995). Rather than glands, the folds within the columnar

epithelium of the cervix form crypt-like structures and are the sites of mucus secretion and have been reported to acts as temporary storage sites for spermatozoa after they are deposited during intercourse (Fluhmann 1957). Much like other parts of the FRT, the cervix undergoes significant changes in physiology and function throughout the menstrual cycle, such as cyclical changes in the diameter of the internal cervical os (McCarthy, Tauber et al. 1986) and alterations to the consistency of the cervical mucus to allow for more optimal passage of spermatozoa during the fertile period following ovulation (Martyn, McAuliffe et al. 2014).

1.3.4- The Uterus

The uterus consists of a thick smooth muscle layer known as the myometrium and an inner mucosal layer known as the endometrium, together they function as a protective environment in which the embryo is implanted and undergoes development (Ochoa-Bernal and Fazleabas 2020). The myometrium has contractile properties that are utilised to push a developed baby through the cervical canal during childbirth and also undergoes contractions to guide an embryo before it implants (Bulletti, de Ziegler et al. 2000). The endometrium is a dynamic, regenerative tissue that exhibits significant alterations to its morphology and biochemical characteristics through the different stages of the menstrual cycle (Noyes, Hertig et al. 1975).

The endometrium is lined with a luminal epithelium that contains both ciliated and secretory cells (Ferenczy 1977) with an underlying stromal layer containing mesenchymal cells that are also subject to dramatic changes in their structure and function during the menstrual cycle (McCluggage, Sumathi et al. 2001). The endometrium receives its blood supply from spiral arteries which have essential roles

in supplementing nutrients to the developing foetus and the periodic breakdown of the endometrial lining during menstruation (Brosens, Robertson et al. 1967).

During the proliferative phase of the menstrual cycle, the functional layer of the endometrium responds to rising oestrogen concentrations by regenerating and thickening (Ludwig and Spornitz 1991). Following ovulation and the formation of the corpus luteum, during the progesterone dominant secretory phase of the menstrual cycle the process of decidualisation is triggered which differentiates the endometrial stromal cells and glands in preparation for pregnancy (Conrad, Rabaglino et al. 2017). If a pregnancy does not occur by the late secretory phrase, as the corpus luteum regresses and the withdrawal of progesterone production begins then menstruation ensues (Corner and Allen 1929). During menstruation the functional layer of the endometrium is broken down and shed, ready to be regenerated during the next menstrual cycle.

1.3.5- The Oviducts

The oviducts are a pair of structures which connect the ovaries to the upper part of the uterus, they contain the site of fertilisation and are the passage through which ovulated oocytes travel to the site of embryo implantation (Chumduri and Turco 2021). The human oviduct can be divided into four distinct subsections: the isthmus, the ampulla, the infundibulum and the interstitial portion within the wall of the uterus (Pauerstein and Eddy 1979). The transitional zone between the uterine cavity and the beginning of the mucous membrane lining the fallopian tube, referred to as the endosalpinx, is characterised by the expression of morphologically different secretory cells and an increase in the number of ciliated cells in the epithelium (Fadel, Berns et al. 1976). This interstitial section of the oviduct contains a ciliated mucosa that is differs from both the endometrial mucosa and that observed in the

rest of the oviduct, forming an intermediate between the two. This section contains a layer of longitudinal muscle immediately beneath the epithelium which forms a layer of circular muscle arranged in a spiral, thought to function as a sphincter that regulates the passage of gametes between the uterus and the oviduct (Pauerstein and Eddy 1979). The intermediate muscular layer of the oviduct is referred to as the myosalpinx.

The isthmus of the oviduct is the section located proximally to the uterus, extending from the ampulla to the uterotubal junction with a length of approximately 3 cm. This is the most muscular portion of the oviduct containing a circular layer of muscle fibers as well as inner and outer longitudinal musculature. This section of the oviduct has the most narrow lumen, with less ciliated cells and a mucosa arranged into four folds, functioning as a passage for spermatozoa to reach the site of fertilisation in the ampulla region, as well as embryos travelling towards the uterus in the opposite direction (Pauerstein and Eddy 1979).

The ampulla is the longest section of the oviduct up to 8 cm in length, the lumen of the ampulla is much more narrow at the end attached to the isthmus, approximately 1 mm in diameter, however it becomes gradually wider as the ampulla extends towards the distal end where the lumen can be over 1 cm in diameter (Patek, Nilsson et al. 1972). This is the site of fertilisation and early development of the embryo as it travels towards the site of implantation within the uterus (Besenfelder, Havlicek et al. 2012). At the distal end of the ampulla lies the infundibulum, which is a funnel shaped section of the oviduct that contains finger like projections which extend towards the ovaries. The function of the infundibulum is to collect ovulated oocytes from the ovaries into the oviduct, which it achieves due to its highly ciliated, folded

epithelial layer with a ciliary beat directed towards the uterus (Patek, Nilsson et al. 1972).

The lumen of the oviducts are filled with oviductal fluid which is mostly composed by the oviductal epithelial cells and consists of components that are either produced and secreted from the oviductal epithelial cells themselves, or transported over the barrier of the epithelium from the interstitial tissue or circulating blood (Leese, Tay et al. 2001). The fluid is a complex mixture of hormones, lipids, proteins, metabolites, and glycoproteins with a wide range of molecular weights. The specific contents and consistency of the oviductal secretions are under direct regulation by various factors such as ovulation, insemination, metabolic stress, and hormones from both exogenous and endogenous sources (Saint-Dizier, Schoen et al. 2019). Aside from metabolic components such as lactate, glucose, pyruvate and a range of amino acids (Gardner, Lane et al. 1996), the oviductal secretions also contain a large number of proteins that have a direct influence on the various biological processes that take place within them (Buhi, Alvarez et al. 2000). Investigation of the functions of oviductal fluid have revealed that is plays essential roles in gamete maturation, sperm cell capacitation and selection as well as the promotion of healthy early embryo development (Avilés, Gutiérrez-Adán et al. 2010).

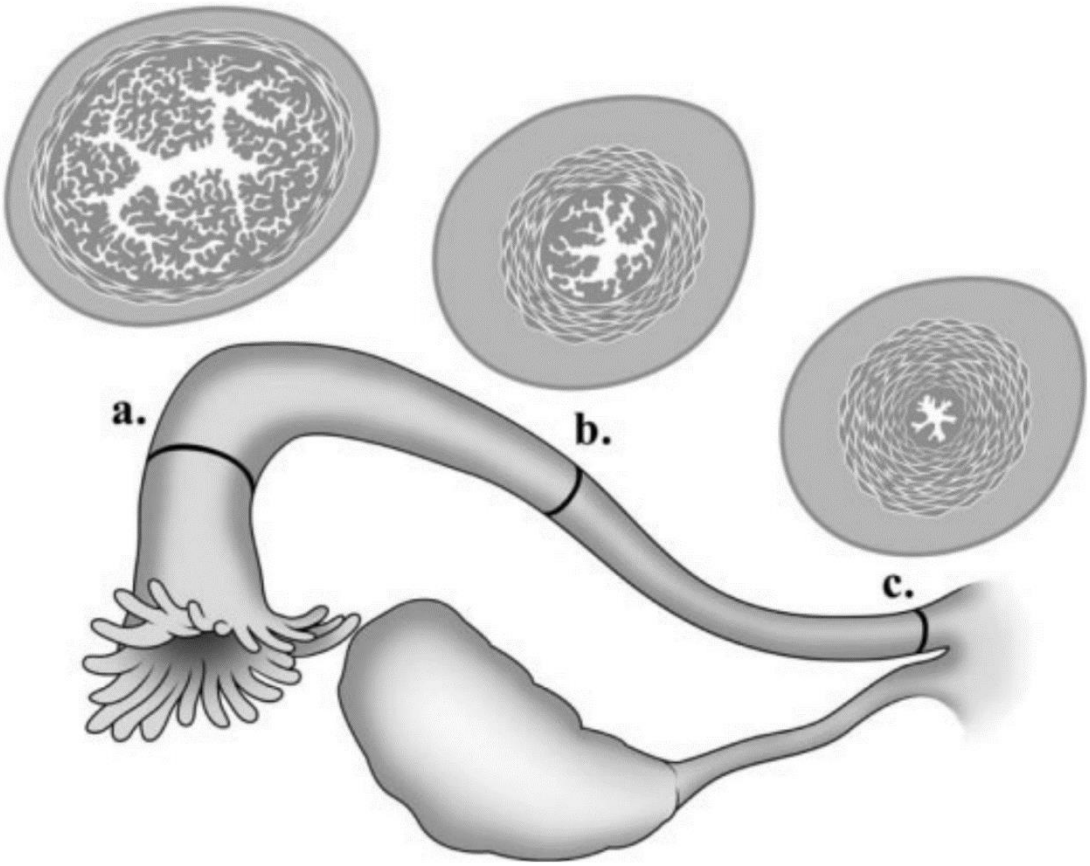


Figure 1.4- Reproduced from (Lyons, Saridogan et al. 2006). An illustration of the human oviduct, displaying the longitudinal folds in cross-section at the a) Infundibulum, b) ampulla and c) isthmus.

1.3.6- The Epithelium

The epithelium of the FRT is composed of several cell populations that are involved in the process of reproduction. The vagina and cervix are lined with specialised epithelial cells with unique functions in reproduction and protection against infection. The vaginal canal is lined with stratified squamous cells that are responsible for the maintenance of a healthy pH balance and the production of mucus which lubricates the vaginal canal and provides a barrier against infectio0n (Anderson, Marathe et al. 2014). The epithelial layer of the vaginal canal undergoes cyclical changes in response to fluctuations in oestrogen throughout the menstrual cycle (Attia 1998).

The epithelial cells of the cervix are composed primarily of squamous and columnar epithelial cells, with the squamous cells forming the outermost layer of the cervix, whilst the columnar cells line the cervical canal (Deng, Mondal et al. 2019). The primary function of the cervical epithelial cells is the secretion of cervical mucus which facilitates the passage of sperm cells through the cervical canal and acts as a barrier against infection. The cervical mucus also undergoes cyclic changes in response to the menstrual cycle, becoming less viscous and more permeable during the ovulatory phase (Martyn, McAuliffe et al. 2014).

The epithelial cells of the endometrium are specialised for secretion, they have essential roles in the processes of embryo implantation and early embryonic development. The luminal and glandular epithelial cells are the two primary types present within the endometrium (Schmidhauser, Ulbrich et al. 2022). Luminal epithelial cells line the uterine cavity and secrete glycogen, mucus and other substances that provide a protective and nourishing environment for the developing embryo such as growth factors, adhesion molecules and various cytokines which regulate implantation and development (Ye 2020). The glandular epithelial cells

within the endometrium are located deeper within the stromal layer, where they secrete cytokines, glycoproteins and enzymes which influence the regulation of the menstrual cycle, promote implantation and provide further support for embryo development (Hempstock, Cindrova-Davies et al. 2004).

The epithelial cells of the oviduct can be divided into two main types: ciliated and secretory. The ciliated epithelial cells are responsible for the movement of the oocyte and the early embryo through the oviduct. They achieve this by beating the cilia on their apical surface in a coordinated manner to generate a directional flow of fluid and create a microenvironment that is conducive to fertilisation and embryonic development (Koyama, Shi et al. 2019). This ciliary beating has been shown to be regulated by a range of hormones, growth factors and neurotransmitters. The secretory epithelial cells within the oviduct secrete a mixture of mucins, glycoproteins, lipids and enzymes to provide nutrition, protection and transport for the oocyte and early embryo (Abe 1996).

1.3.7- The Menstrual Cycle

The functionality of the human FRT is maintained by a complex cyclical system of hormonal regulation known as the menstrual cycle (Reed and Carr 2000). The hormones that influence the menstrual cycle are derived from the hypothalamus, pituitary and ovaries, with the entire 25-30 day cycle being divided into the secretory and proliferative phases (Vollman 1977). During the proliferative phase of the menstrual cycle, follicle stimulating hormone (FSH) stimulates the growth and development of follicles within the ovaries (Holesh, Bass et al. 2022), resulting in an increase in the levels of oestrogen (E_2) produced by the follicles which promotes the proliferation and thickening of the endometrium (Noyes, Hertig et al. 1975). At the peak level of oestrogen synthesis during the middle of the menstrual cycle, a surge

of luteinising hormone (LH) is produced, resulting in the ovulation of the oocyte, signalling the beginning of the secretory phase (Robker, Hennebold et al. 2018).

During the secretory phase of the menstrual cycle, progesterone (P_4) production by the corpus luteum stimulates the decidualisation of the endometrium in preparation for embryo implantation. Decidualisation results in morphological and functional alterations to the cells within the endometrium, as well as the presence of decidual white blood cells and alterations to vascularity and the maternal arteries (Ramathal, Bagchi et al. 2010). If an embryo is not implanted into the endometrium during this phase of the menstrual cycle, the subsequent drop in progesterone concentration triggers menstruation, which is the shedding of the functional layer of the endometrium leading to the entire menstrual cycle restarting (Critchley, Maybin et al. 2020).

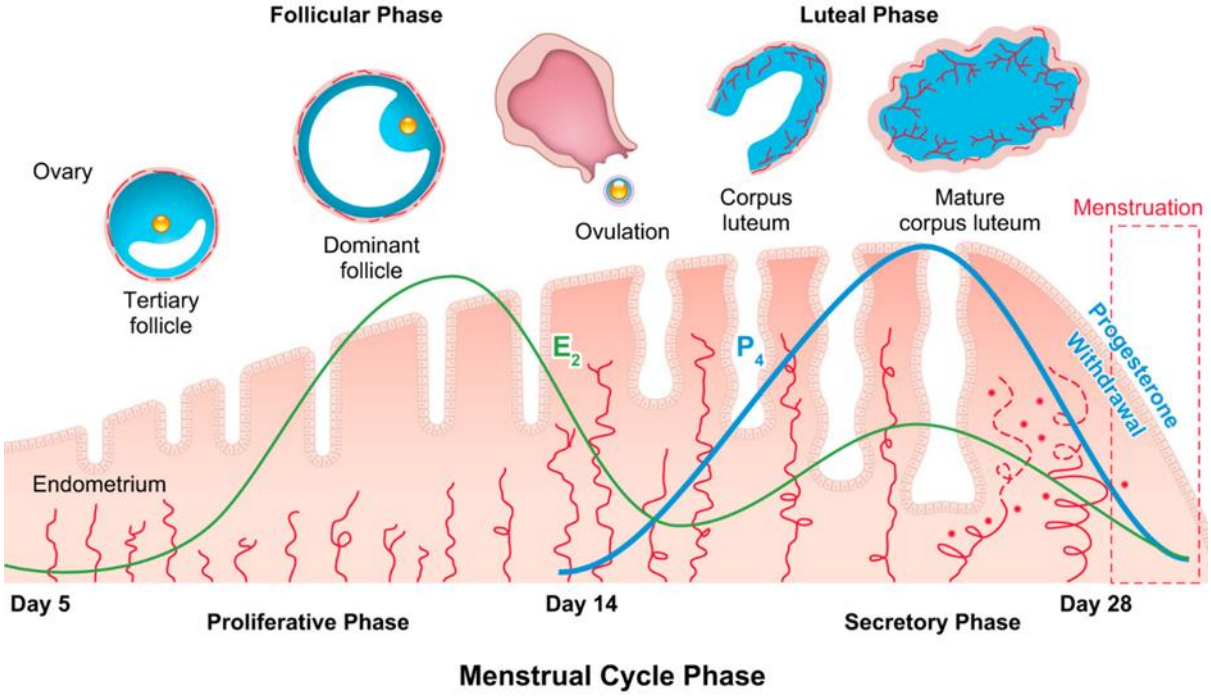


Figure 1.5- Adapted from (Critchley, Maybin et al. 2020). A diagram of the various phases of the human menstrual cycle. Oestrogen is the primary hormone which influences the menstrual cycle during the proliferative phase, stimulating endometrial proliferation. The secretory phase begins just after ovulation, during which the newly formed corpus luteum produces and secretes progesterone. This stimulates the decidualisation of the endometrium, but it's subsequent withdrawal in the absence of embryo implantation triggers menstruation and resets the menstrual cycle.

1.4- The Sperm Cell Journey through the FRT

Fertilisation of the human oocyte requires the penetration of just one sperm cell through the zona pellucida in the ampulla region of the oviduct, despite millions of sperm cells being deposited into the vagina during intercourse. These spermatozoa undergo a rigorous selection process through viscous fluids, hostile immune cells, potential dead ends and over extensively folded epithelium (Miller 2018). The site of human semen deposition is the anterior vagina, close to the cervical os (Suarez and Pacey 2005). Upon ejaculation, semen coagulates to form a loose gel due to the actions of semenogelin I and semenogelin II which are proteins produced in the seminal vesicles (Lilja 1985). This gel serves to protect spermatozoa from the acidic environment of the vagina and hold them at the cervical os (Lundwall, Giwercman et al. 2003) to allow motile spermatozoa to begin their journey into the upper regions of the FRT.

Motile spermatozoa that encounter the cervical mucus quickly enter the cervical canal. The oestrogen regulated consistency of the cervical mucus has a significant impact on the ability of spermatozoa to penetrate and swim through the cervical canal, with increased cervical mucus hydration synonymous with the time of ovulation shown to correlate with improved incidence of pregnancy (Bigelow, Dunson et al. 2004). The cervical mucus acts as a barrier to prevent immotile sperm cells or those exhibiting abnormal motility from reaching the upper regions of the FRT as they will be unable to penetrate the viscous fluid unless they are morphologically ‘normal’ and exhibit vigorous motility (Katz, Morales et al. 1990). The presence of semen stimulates an influx of leukocytes into the cervix and vagina, which appears to serve as a layer of protection against microbes rather than presenting a direct

barrier to the entry of motile spermatozoa (D'Cruz, Wang et al. 1992). It is thought that sperm cells are guided through the cervical canal by mucins, which are long, flexible glycoproteins within the cervical mucus which align with the secretory flow in mucosal grooves (Chrétien 2003) and act as a guide to allow motile sperm to swim in a straighter path than they usually exhibit in seminal plasma (Katz, Mills et al. 1978).

Upon entry into the uterine cavity, sperm cells can traverse through this relatively small space in less than 10 minutes at a speed of approximately 5 mm per minute (Mortimer and Swan 1995), although the actual speed of sperm travelling through the uterus is difficult to determine in humans due to experimental limitation (Suarez and Pacey 2006). The transport of sperm cells through the human uterus may be assisted by contractions of the myometrium directed towards the oviducts, which have been shown to increase in intensity in the late follicular phase of the menstrual cycle (Lyons, Taylor et al. 1991) and may also act to draw in the mixture of cervical mucus and sperm cells from the cervix into the uterus (Fukuda and Fukuda 1994). These contractions of the myometrium have been shown to be stimulated by components of the seminal fluid in a rat model (Crane and Martin 1991), suggesting that insemination directly initiates the movement of sperm cells from the cervix and through the uterus. This contraction assisted movement of sperm cells through the uterine cavity may enhance the survival of the gametes by minimising the amount of time that they can potentially come into contact with the leukocytes which invade the uterus upon insemination (Schjenken, Zhang et al. 2016), which have been observed to phagocytose sperm cells in animal models (Bedford 1965). The longer that sperm cells spend in the uterine cavity, the more likely it becomes that ‘normal’ spermatozoa will be attacked by the female immune system, due to their loss of

protection by their seminal plasma coating in a time dependent manner (Dostál, Veselský et al. 1997).

Upon reaching the uterotubal junction, sperm cells are met with a narrow, mucus filled lumen (Jansen 1980) that presents an additional barrier through which cells that exhibit progressive, linear motility are able to traverse more efficiently (Shalgi, Smith et al. 1992). The passage of sperm cells through the uterotubal junction appears to be mediated by the presence of specific chaperone proteins on the sperm cell surface, although the specific mechanism of this has not been elucidated, animal models have demonstrated that the presence of angiotensin converting enzyme (ACE) (Hagaman, Moyer et al. 1998), fertilin β (Cho, Bunch et al. 1998) and calmegin (Ikawa, Wada et al. 1997) are essential for sperm transport through the uterotubal junction and zona pellucida binding. This suggests that morphology and motility of sperm cells are not the only selection criteria for navigation through the upper FRT and that the sperm cell surface proteome also has a significant impact on their ability to pass through the uterotubal junction.

As motile sperm cells make their way through the uterotubal junction and reach the isthmus portion of the oviduct, there is conflicting evidence that this region acts as a sperm cell reservoir where the spermatozoa can be held in storage reservoirs until ovulation occurs (Yanagimachi and Chang 1963, Miller 2018), however, this type of sperm cell storage has never been demonstrated in a human model (Williams, Hill et al. 1993). Human sperm cells have been observed loosely and intermittently binding to the epithelial cells of the oviduct *in vitro*, however, the associations between the cells were not as strong or as rapid as those observed in other mammalian species (Pacey, Hill et al. 1995). Whilst this binding may not be strong enough to hold the human sperm cells in a reservoir within the oviduct, it could act in synchronicity with

the viscous mucus to slow their progress towards the site of fertilisation, prolonging the availability of viable sperm cells within the oviduct and preventing the likelihood of polyspermy due to multiple sperm penetrating the oocyte (Suarez and Pacey 2006).

The acquisition of hyperactivated motility by is likely to occur within the oviducts in response to signals derived from the secretory cells that line the oviductal epithelium or possibly from the oocyte cumulus complex itself (Alasmari, Costello et al. 2013). This initiation of hyperactivated motility, in conjunction with the activation of the AR and the modification of the proteins expressed on the sperm cell surface (De Jonge 2005) is essential for sperm cells to navigate through the viscoelastic mucus in the distal sections of the oviduct and eventually penetrate through the extracellular matrix of the cumulus oophorus and the zona pellucida (Stauss, Votta et al. 1995). Hyperactivated motility in sperm cells relies on the activation of the CatSper Ca^{2+} channels, as evidenced by the inability of sperm cells from CatSper1 and CatSper2 null mice to exhibit the rapid, asymmetrical flagellar waves that are associated with hyperactivation (Carlson, Westenbroek et al. 2003, Quill, Sugden et al. 2003).

The mechanism by which sperm cells navigate towards the oocyte is heavily debated. One theorised method of sperm taxis towards the oocyte through the oviduct is thermotaxis, as a rabbit model has demonstrated that there is a gradual rise in temperature along the oviduct with the isthmus being approximately 2°C colder than the ampulla region where fertilisation occurs. Rabbit sperm cells have also been observed to swim towards move in the direction of an increasing temperature gradient (Bahat, Tur-Kaspa et al. 2003), although there is a distinct lack of experimental evidence for this type of sperm taxis in a human model.

It has been proposed that the final stages of sperm taxis towards the oocyte in the oviductal ampulla could be chemotactic in nature (Babcock 2003), as mammalian sperm have been shown to travel towards an increasing concentration gradient of follicular fluid (Fabro, Rovasio et al. 2002) and the presence of sperm cell specific odorant receptors has been demonstrated on the human sperm cell flagellum (Spehr, Gisselmann et al. 2003). A specific odorant eliciting chemotaxis in human sperm cells has yet to be discovered. There are many unconfirmed and undiscovered aspects of sperm transport throughout the FRT, but further elucidation of the specific mechanisms involved could have a substantial impact on our understanding of infertility and our ability to diagnose and treat patients.

1.5- Sperm cell modification of the female reproductive tract

Whilst there is still far more to be discovered, our understanding of the regulation of sperm cell physiology by factors derived from the FRT is well established. Many aspects of this regulation have been discussed herein, such as the principal contribution of sperm cell capacitation being provided by the oviduct (Hunter and Rodriguez-Martinez 2004) due to the secretion of capacitation factors (Suarez 2008). There is evidence that ovulation can induce the upregulation of HCO_3^- secretion within the oviduct (Foley and Williams 1967), which could also have a role in the regulation of sperm motility and capacitation within the upper FRT to facilitate fertilisation (Tajima, Okamura et al. 1987, Zhou, Wang et al. 2005). Various other examples of the modulation of sperm cell physiology by the cells of the FRT are well documented, however, much less is known about any interactions between factors derived from the male ejaculate and their influence on the cells of the FRT.

The limited collection of evidence for the modulation of FRT cell function by sperm cells and other factors in the male ejaculate are almost entirely derived from animal models. It has been demonstrated that the presence of sperm cells can significantly alter the secretory proteome of oviductal epithelial cells (Georgiou, Sostaric et al. 2005). The co-culture of bovine oviductal epithelial cells with bull spermatozoa led to the discovery that de novo protein synthesis could be stimulated by co-incubation for just 24 hours, with significant alterations to the types and quantities of proteins secreted into the medium by the oviductal epithelial cells that were exposed to the male gametes (Ellington, Ignotz et al. 1993). A similar equine model demonstrated that the interaction of stallion sperm cells with equine oviductal epithelial cells resulted in significant alterations to the function of the cells. Quantitative and qualitative alterations were observed in the proteomic output of the equine oviductal epithelial cells after co-culture, with the downregulation of synthesis of 2 oviductal epithelial cell secretory proteins and the upregulation of synthesis of 6 proteins identified (Thomas, Ignotz et al. 1995).

Following on from these studies, a porcine model was developed using quantitative 2D gel electrophoresis, mass spectrometry and verification by Western blot analysis to identify the specific identities of proteins in the oviductal epithelial cell secretory proteome that were modulated by co-culture with boar spermatozoa (Georgiou, Sostaric et al. 2005). It was found that a total of 19 proteins were regulation exclusively by interactions with sperm cells, most of which were molecular chaperones, regulators of protein stability and folding or antioxidant and free radical scavenger proteins. The further use of bioinformatics allowed for the analysis of the functions of the upregulated proteins being secreted into the porcine oviductal environment. For example, the release of heath shock proteins in the oviduct was

upregulated in response to sperm, potentially to maintain the viability and function of spermatozoa within the oviduct (Guzhova, Kislyakova et al. 2001). Thioredoxin was also upregulated by sperm exposure (Georgiou, Sostaric et al. 2005), which is known to facilitate the protection of cells from oxidative stress (Nakamura, Matsuda et al. 1994), the stimulation of cell growth (Gasdaska, Berggren et al. 1995) and is thought to be involved in the maternal recognition of pregnancy and the prevention of embryo elimination (Clarke, Orozco et al. 1991). Many of the other proteins identified has functions involved in the protection and maintenance of both oocytes and sperm cells within the oviduct (Georgiou, Sostaric et al. 2005).

This porcine model was the first to demonstrate an oviduct specific proteomic response to sperm cell signalling factors (Georgiou, Sostaric et al. 2005), providing evidence that the proteomic environment of the upper FRT is not solely under the influence of maternal hormonal regulation, but could be modulated by sperm cells in preparation for the events of fertilisation and early pregnancy. Further experiments in other animal species such as *Drosophila melanogaster* have demonstrated sperm cell induced tissue remodelling of the oviduct, with biochemical and molecular alterations that allow for the development of the entire upper FRT into a mature, functional state in response to mating (Kapelnikov, Zelinger et al. 2008). The addition of sperm cells to cultured bovine oviductal epithelial cells has been shown to induce an upregulation of prostaglandin synthesis, which is known to regulate the contractile properties of the myometrium in the uterus and the oviductal myosalpinx, potentially demonstrating that sperm cell signalling to the oviductal epithelial cells can elicit contractions of the FRT to facilitate their passage towards the site of fertilisation (Kodithuwakku, Miyamoto et al. 2007).This concept of signalling factors within the

male ejaculate eliciting significant alterations to the FRT environment is an interesting subject and warrants further investigation in a human model.

The signalling between sperm cells and FRT cells does not appear to be limited to regulating alterations in oviductal function and proteomic output, but may also be implicated in the tolerance of the allogenic sperm cells by the innate and adaptive maternal immune defences (Georgiou, Snijders et al. 2007). A mouse model has demonstrated that exposure of the endometrial epithelial cells to seminal fluid induced toll-like receptor 4 (TLR4) regulated alterations to the expression of several hundred messenger RNAs (mRNAs) and noncoding microRNAs (miRNAs), many of which have roles in the maternal immune response such as the production of cytokines and chemokines (Schjenken, Glynn et al. 2015). These factors quickly recruit a range of immune cells into the endometrium (De, Choudhuri et al. 1991), where neutrophils and macrophages assist in the clearance of microbes introduced to the FRT during coitus, whilst dendritic cells traffic antigens from the seminal fluid to the lymph nodes (Moldenhauer, Diener et al. 2009). The presentation of these antigens promotes the generation of regulatory T cells, which migrate into the endometrium and promote embryo implantation by improving endometrial receptivity and providing an immunotolerant environment for the embryo which will express the same paternal antigens that were present in the seminal fluid (Guerin, Prins et al. 2009).

The presence of seminal plasma signalling factors in the FRT is not indispensable for a successful pregnancy to take place, as evidenced by the success of intrauterine insemination with washed or epididymal spermatozoa, as well as IVF followed by embryo transfer (Robertson and Sharkey 2016). However, animal models have indicated that a lack of seminal fluid factor signalling in the FRT can lead to impaired

fertility and foetal development, with miscarriage and foetal abnormalities significantly increased in rat and mouse models of embryo transfers to females mated with vasectomised males (Robertson 2005). An intricate experiment in which female mice mated with males with ablated seminal vesicles demonstrated that signalling factors specifically present in the seminal plasma did not only have a significant impact on fertilisation and embryo implantation, but also affected the ongoing health of the offspring (Bromfield, Schjenken et al. 2014). The pups born from females not exposed to seminal fluid exhibited altered growth trajectories and issues with metabolic function, such as obesity and hypertension (Bromfield 2014).

These findings may explain the observations of links between the duration of sexual cohabitation and reduced likelihood of pregnancy disorder such as foetal growth restriction and preeclampsia (Kho, McCowan et al. 2009). The outcomes of patients undergoing IVF treatment have also shown significant improvement in ongoing pregnancy and live birth rates when the women are exposed to seminal plasma around the time of oocyte collection or embryo transfer (Crawford, Ray et al. 2015).

Factors derived from the seminal plasma, such as transforming growth factor-beta1 (TGFB), have been shown to be capable of absorbing onto the sperm cell surface (Chu, Nocera et al. 1996). This suggests that the carriage of seminal plasma components into the upper FRT by motile spermatozoa in humans is a potential delivery mechanism of signalling agents to the cells of the endometrium and oviduct. Despite the primary evidence for the presence of seminal fluid and female tract cell signalling being derived from animal models such as mice, which have significantly different reproductive anatomies in terms of the extent of seminal fluid deposition into the endometrium compared to humans (Cunha, Sinclair et al. 2019), this delivery

mechanism demonstrates the relevance of studying components derived from the seminal plasma as candidate signalling factors in a human model.

1.6- The importance of Ca^{2+} in cellular signalling

1.6.1- Mechanisms of Ca^{2+} signalling

Ca^{2+} is a versatile, ubiquitous intracellular signal that is responsible for the regulation of a wide range of cellular processes (Berridge, Lipp et al. 2000). The signals encoded by changes in $[Ca^{2+}]_i$ show variation in their amplitude, speed and spatiotemporal patterning which allow for robust and precise regulation of diverse processes such as cell differentiation (Buonanno and Fields 1999) and proliferation (Berridge 1995), apoptosis (Szalai, Krishnamurthy et al. 1999) and gene expression (van Haasteren, Li et al. 1999). Ca^{2+} has distinct chemical properties which allow it to form low-affinity complexes with cellular components such as amino acids, ATP, phosphates and acid phospholipids, which is a quality of Ca^{2+} that is essential for its versatile function as a messenger (Carafoli, Santella et al. 2001). By forming such intracellular complexes, the concentration of unbound Ca^{2+} within the cytosol can be rapidly reduced which allows for the exploitation of Ca^{2+} sensitive sensor and effector proteins to transduce signals through a range of molecular pathways (Berridge, Lipp et al. 2000).

The first step of cellular Ca^{2+} signalling is the triggering of the mobilisation of Ca^{2+} signals by a stimulus. The generation of Ca^{2+} signals can originate from both the entry of Ca^{2+} through membrane channels from an extracellular sources or by the release of Ca^{2+} from the intracellular stores, which are usually within the endoplasmic reticulum or sarcoplasmic reticulum (Berridge, Lipp et al. 2000). The plasma membrane of cells contains Ca^{2+} permeable channels which allow for the influx of Ca^{2+} into the cytoplasm. The opening of these Ca^{2+} permeable channels can be regulated by changes in membrane potential for voltage operated channels in

excitable cells (Catterall 2011), whilst in other non-excitable cells the channels can be regulated by various factors such as ligand binding for receptor operated channels or the depletion of Ca^{2+} from intracellular stores for store-operated channels (Parekh and Putney 2005).

The function of the intracellular Ca^{2+} stores is regulated by receptors such as the inositol-1,4,5-trisphosphate receptor (IP_3R) (Berridge 1993) and ryanodine receptor (RYR) (Clapham 1995), which are both principally activated by the presence of Ca^{2+} itself in a process referred to as Ca^{2+} induced Ca^{2+} release (CICR) (Roderick, Berridge et al. 2003). These receptors rely on the binding of stimuli to cell surface receptors, which initiates the generation of second messengers such as inositol 1,4,5-trisphosphate (IP_3) in the case of the IP_3R (Taylor and Tovey 2010) or cyclic ADP ribose (cADPR) for RYR (Clapper, Walseth et al. 1987). These second messengers modulate the Ca^{2+} sensitivity of the channels on the intracellular Ca^{2+} stores and it is possible for more than one of these signalling pathways and receptors to be present in a single cell. The linking of so many Ca^{2+} mobilising messengers to different input signals attributes further to the versatility of cellular Ca^{2+} signalling networks and their downstream effects.

Once a Ca^{2+} signal has been generated within a cell it can be translated into a cellular response via Ca^{2+} binding proteins such as calmodulin (CAM). The binding of Ca^{2+} to CAM leads to a confirmational change in the protein that allows it to activate various downstream effectors. CAM activation by Ca^{2+} can regulate many processed such as ion channel modulation (Ben-Johny and Yue 2014), gene transcription (Kim, Chung et al. 2009) and smooth muscle contraction (Walsh 1994). There are numerous Ca^{2+} binding proteins with a wide range of functions and the possibility of

crosstalk between these signalling pathways (Bruce, Straub et al. 2003) further extends the versatility of Ca^{2+} signalling.

The sustained elevation of Ca^{2+} within the cytosol can lead to apoptosis and cell death (Jiang, Chow et al. 1994), therefore the presence of mechanisms for cytosolic Ca^{2+} clearance is an essential aspect of Ca^{2+} signalling. Ca^{2+} can be rapidly removed from the cytoplasm by a range of exchangers (Blaustein and Lederer 1999) and pumps (Pozzan, Rizzuto et al. 1994) that are present both on the surface of the intracellular Ca^{2+} stores and the cell plasma membrane. For example, the endoplasmic reticulum contains ATPase pumps which are responsible for the reuptake of Ca^{2+} from the cytoplasm to replenish the intracellular stores (Periasamy and Kalyanasundaram 2007), whilst plasma membrane has similar ATPase pumps which extrude Ca^{2+} into the extracellular environment in cooperation with the sodium calcium exchangers (Brini and Carafoli 2011). Mitochondria also play an important role in the clearance of cytosolic Ca^{2+}, as they rapidly sequester Ca^{2+} during the propagation of the Ca^{2+} signal before slowly releasing it back into the cytoplasm during the recovery phase of the signal (Budd and Nicholls 1996). Ca^{2+} uptake into the mitochondria is achieved through a low sensitivity uniporter (Fan, Zhang et al. 2020) which effectively collects Ca^{2+} in close proximity to Ca^{2+} releasing channels such as IP_3Rs and RYRs, forming feedback mechanisms between the intracellular Ca^{2+} stores and the mitochondria (Csordás, Thomas et al. 1999). The influence of mitochondrial Ca^{2+} sequestering and release can have a significant impact on the amplitude (Budd and Nicholls 1996) and spatiotemporal patterns of Ca^{2+} signals (Duchen 1999).

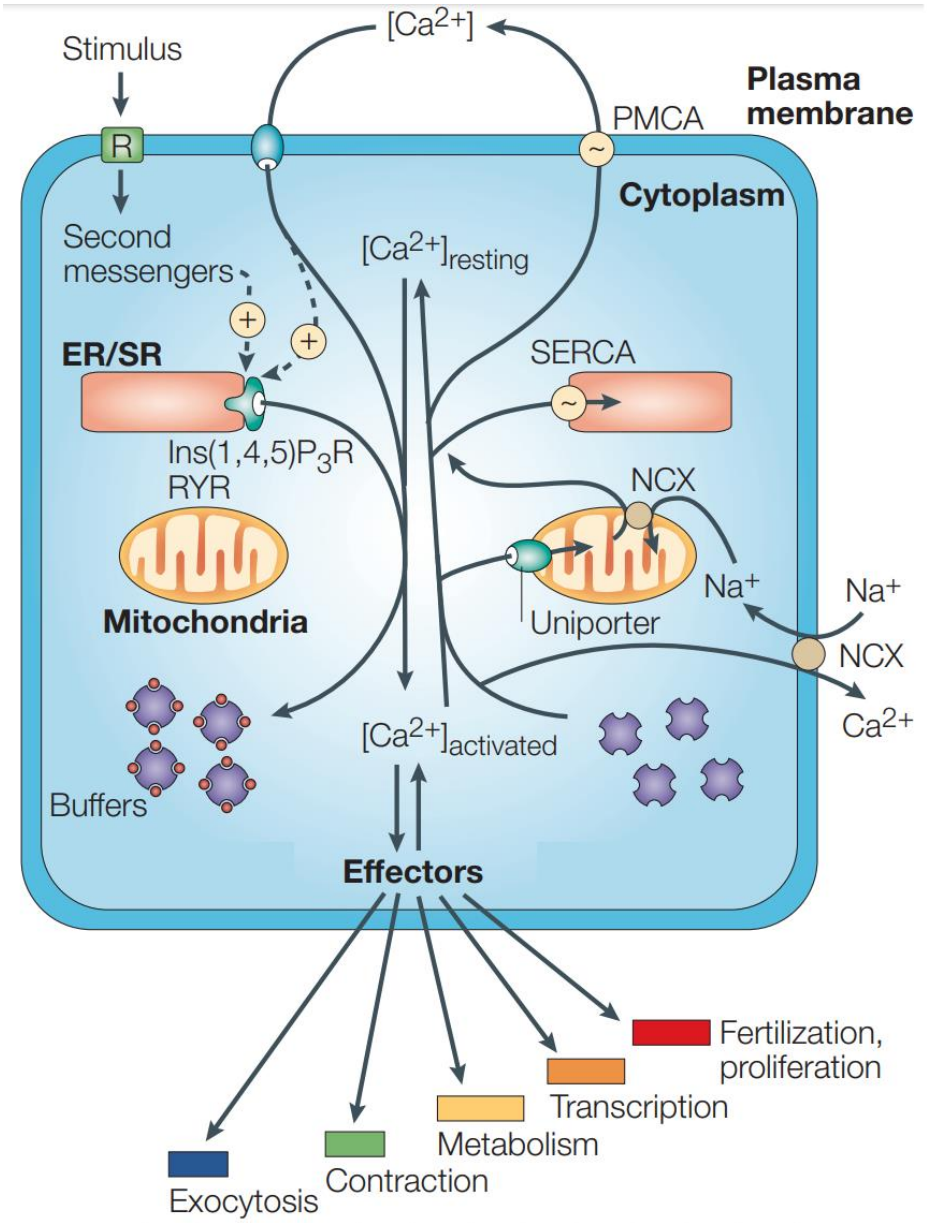


Figure 1.6- Adapted from (Berridge, Bootman et al. 2003). Ca^{2+} signalling can be induced by stimuli which can invoke the entry of external Ca^{2+} into the cell where second messengers can be formed to elicit the release of Ca^{2+} from intracellular stores in the endoplasmic/sarcoplasmic reticulum (ER/SR) via interaction with receptors such as the IP_3R or RyR. The majority of Ca^{2+} is bound to buffers, whilst the remaining free Ca^{2+} is able to bind to effectors within the cell that are capable of activating a wide range of cellular processes such as exocytosis, contraction, metabolism, transcription and proliferation. The removal of Ca^{2+} from the cytoplasm is achieved by various pumps and exchangers such as the plasma-membrane Ca^{2+}-ATPase (PMCA) and the Na^+/ Ca^{2+} exchanger (NCX), which both extrude Ca^{2+} to the extracellular environment. The intracellular Ca^{2+} stores are similarly replenished by the ER/SR Ca^{2+} ATPase (SERCA) pumps. In addition, mitochondria contribute to the recovery process by rapidly sequestering Ca^{2+} via a uniporter, before slowly releasing it back into the cytosol to be stored in the ER/SR or extruded by the PMCA.

The most common signalling pathway that increases cytoplasmic Ca^{2+} concentration is the phospholipase C pathway. There are a range of cell surface receptors, including receptor tyrosin kinases and G protein-coupled receptors that regulate the activation of phospholipase C (Bill and Vines 2020). For example, most cells types contain G protein coupled P2Y receptors which can be activated by extracellular ATP (Chang, Tzeng et al. 2008). The activated phospholipase C hydrolyses the membrane phospholipid phosphatidyl inositol-bisphosphate (PIP_2) to form IP_3 and diacylglycerol, both of which are potent second messengers. Diacylglycerol is a hydrophobic lipid which remains in the plasma membrane where it recruits protein kinase C from the cytosol (Carrasco and Mérida 2007), whilst IP_3 diffuses into the cytosol where it binds to the IP_3R Ca^{2+} channels on the endoplasmic reticulum, stimulating the release of Ca^{2+} from the intracellular stores (Mellor and Parker 1998, Bartok, Weaver et al. 2019).

1.6.2- Spatial and temporal aspects of Ca^{2+} signalling

The versatility of Ca^{2+} signalling is further extended by the variations in the spatial and temporal aspects of the Ca^{2+} signals propagated within the cells (Berridge 1997). The channels on the intracellular Ca^{2+} stores exhibit varying degrees of excitability which is dependent on the specific type and concentration of the messenger eliciting Ca^{2+} mobilisation. Small signalling events such as single RYR or IP_3R channels opening can cause a very small rise or “blip” in cytosolic Ca^{2+} concentrations (Bootman, Niggli et al. 1997), however, it is more common for small clusters of channels to open in a coordinated manner resulting in a “spark” of $[Ca^{2+}]_i$ (Cheng, Lederer et al. 1993). These small scall Ca^{2+} signalling events form the building blocks for the propagation of much larger $[Ca^{2+}]_i$ signals such as Ca^{2+} waves. These waves are initiated when RYR or IP_3R channels are opened after they have been

sufficiently sensitised to Ca^{2+} by interactions with second messengers, as discussed previously. This causes the propagation of Ca^{2+} signals to the other channels in proximity as the Ca^{2+} diffuses across and excites neighbouring receptors (Leybaert and Sanderson 2012). The passage of these signals through gap junctions between cells forms an intercellular Ca^{2+} wave which sweeps through to neighbouring cells and allows for the coordination of cellular activity (Lansley and Sanderson 1999). These signalling events can also be more localised to specific cellular domains, to trigger events such as exocytosis and vesicle release in secretory cells (Maturana, Casal et al. 1999).

The intricate concert of action between the various Ca^{2+} transporters within cells can lead to oscillations in the $[Ca^{2+}]_i$ with varying amplitude and frequency in a similar manner to a radio signal, which allow for the encoding and harmless transmission of signals throughout the cell (Smedler and Uhlén 2014). Cells are constantly exposed to extracellular stimuli and environmental cues such as temperature fluctuations and mechanical stress (Usoskin, Zilberter et al. 2010), all of which can lead to the production of Ca^{2+} signals that can exhibit an infinite number of patterns depending on the specific stimuli and their effects on the Ca^{2+} binding proteins, Ca^{2+} pumps and channels (Berridge, Lipp et al. 2000).

The Ca^{2+} oscillatory patterns produced can vary in frequency between the Hz and mHz range (Boulware and Marchant 2008) and the specific frequency is often dependent on the concentration of the stimulus that is eliciting the signal (Huang, Liu et al. 2013). Continuous oscillations in $[Ca^{2+}]_i$ are able to initiate alterations to gene expression more effectively than a steadily maintained concentration of $[Ca^{2+}]_i$ at the same concentration as the oscillatory peaks (Li, Llopis et al. 1998). Oscillatory Ca^{2+} signals are decoded by enzymes with multiple Ca^{2+} binding residues that can

diversely modify their total phosphorylation (Smedler and Uhlén 2014). To date, there have been several enzymes demonstrated to have Ca^{2+} oscillation frequency decoding properties including nuclear factor of activated T-cells (NFAT) (Dolmetsch, Xu et al. 1998), nuclear factor kappa-light-chain-enhancer of activated B cell (NF-κB) (Dolmetsch, Lewis et al. 1997), calmodulin dependent protein kinase II (CaMKII) (De Koninck and Schulman 1998), mitogen activated protein kinase (MAPK) (Kupzig, Walker et al. 2005) and the intracellular cysteine protease calpain (Tompa, Töth-Boconádi et al. 2001). All of these different frequency decoding molecules depend on varying frequencies and durations of Ca^{2+} oscillations, forming another layer of the diverse cellular Ca^{2+} signalling systems that enable different cell types to respond differently to the same type of stimuli (Smedler and Uhlén 2014).

1.6.3- Ca^{2+} signalling in the cells of the female reproductive tract

The lumen of the FRT is lined with epithelial cells, the functions of which have been demonstrated to be largely regulated by Ca^{2+} signalling mechanisms (Ghavideldarestani, Atkin et al. 2016). Volume regulation, secretion, absorption, and the cellular response to pathogens are all functions that are relevant to epithelial cells which have been demonstrated to be regulated by Ca^{2+} signalling (Petersen 1992, Zhang and O'Neil 1999). An example of this is the $[Ca^{2+}]_i$ mediated opening of secretory channels within epithelial cells through the activation of $[Ca^{2+}]_i$ sensitive basolateral K^+ channels and apical Cl^- channels that have been shown to be present in various cell types that are secretory in nature (Shuttleworth 1997).

Transient receptor potential (TRP) channels are a family of channel proteins which are known to regulate the cellular influx of Ca^{2+} (Song and Yuan 2010) and there are several types which have been identified within the cells in the epithelial lining of the FRT. For example, polycystin-2 and TRP4 have both been shown to be expressed in oviductal epithelial cells in a murine model, localised within the ciliary membrane (Teilmann, Byskov et al. 2005) where they are thought to function as mechanosensitive receptors for the detection of fluid movements and changes in fluid viscosity in the oviductal lumen (Andrade, Fernandes et al. 2005, Fernandes, Lorenzo et al. 2008). TRP channels 1, 2, 3, 4 and 6 are expressed in the bovine reproductive tract and their gene expression exhibits variation throughout the estrous cycle which leads to functional changes in Ca^{2+} mobilisation in bovine oviductal epithelial cells (Ghavideldarestani, Atkin et al. 2016).

The presence of a wide range of Ca^{2+} entry channels in the cells of the FRT may also be responsible for the regulation of alterations to gene expression and the proteomic profile alterations of the secretory cells that have previously been

observed in response to seminal fluid exposure in the porcine model (Georgiou, Sostaric et al. 2005). Many of the secretory cells that line the lumen of the oviduct have a ciliary membrane containing primary cilia which express Ca^{2+} entry channels such as polycystin-1 and polycystin-2 (Hagiwara, Ohwada et al. 2008). It has been demonstrated that increases in $[Ca^{2+}]_i$ can stimulate significantly faster cilia beat frequencies (Di Benedetto, Magnus et al. 1991, Evans and Sanderson 1999) which suggests that Ca^{2+} signalling plays a role in the transport of gametes and embryos within the upper FRT. Interestingly, the cilia beat frequency on human oviductal epithelial cell monolayers has been observed to significantly increase after the cells have been co-incubated *in vitro* with sperm cells (Morales, Palma et al. 1996).

The use of fluorescent Ca^{2+} indicators to record and analyse the levels of $[Ca^{2+}]_i$ within cells is a powerful tool for the investigation of cellular activity and signalling interactions (Russell 2011), however, there are relatively few studies which have adopted this technique to investigate Ca^{2+} signalling in the cells of the human FRT. The application of extracellular ATP to cultures of primary bovine oviductal epithelial cells induces a transient increase in $[Ca^{2+}]_I$ via release from intracellular stores in a dose dependent manner, this signalling is thought to mediate transepithelial ion movements to control the production of oviductal fluid (Cox and Leese 1995). Similar signalling mechanisms have been observed in primary human oviductal epithelial cell cultures. After investigating a wide range of agonists on $[Ca^{2+}]_i$ within the cells, the application of extracellular ATP exclusively induced changes in $[Ca^{2+}]_I$ that are dependent on the presence of both intracellular and extracellular Ca^{2+}, suggesting that Ca^{2+} signalling events also have a role in the regulation of human oviductal fluid formation (Dickens, Comer et al. 1996).

The exposure of cultured secretory and ciliated rabbit oviductal cells to the addition of dibutyryl cAMP induces two different types of $[Ca^{2+}]_I$ response, with some cells exhibiting a zero response and others having an increase in $[Ca^{2+}]_I$ that is dependent upon the presence of extracellular Ca^{2+}, highlighting the variations in response of different subtypes of epithelial cells to the same stimuli (Dickens, Cox et al. 1996). A study using cultured equine oviductal epithelial cell monolayers demonstrated that significant increases in $[Ca^{2+}]_i$ could be observed in response to the addition of sperm cells *in vitro* (Ellington, Varner et al. 1993), suggesting that sperm cell mediated Ca^{2+} signalling in the cells of the FRT could potentially be an upstream regulator of the various Ca^{2+} regulated cellular functions discussed herein. There is a distinct lack of experimental evidence for Ca^{2+} signalling in the cells of the FRT in a human model, especially in response to interactions with factors derived from the male ejaculate and this is a topic which warrants further investigation.

1.7- Hypothesis, Aims and Objectives

Signalling between sperm cells and the cells that they encounter as they travel through the FRT are well established across a range of mammalian species. Most of the evidence for this intercellular communication in humans is related to signalling factors produced by FRT cells which influence the behaviour and physiology of spermatozoa (Brewis and Gadella 2010), whilst the evidence for signalling factors derived from sperm cells which interact with the FRT cells to regulate the periconception environment are much more limited. Animal models have demonstrated that the exposure of FRT cells to seminal fluid can elicit significant alterations to the secretory proteome of the oviduct (Georgiou, Snijders et al. 2007), modulating the periconception environment to better facilitate the early stages of development for an embryo. It has also been demonstrated in a murine model that the presence of seminal fluid in the FRT can also have an impact on the immune system, creating a more immunotolerant environment for the resulting conceptus through a signalling pathway regulated by TLR4 (Schjenken, Glynn et al. 2015).

The occurrence of similar signalling mechanisms is evidenced in humans by the links between cohabitation with a sexual partner leading to reduced risk of preeclampsia and foetal growth restriction (Kho, McCowan et al. 2009), as well as outcomes for patients undergoing IVF treatment showing significant improvement in their live birth rates if they are also having regular, unprotected intercourse prior to treatment (Crawford, Ray et al. 2015). This suggests that signalling events similar to those observed in other mammalian species between seminal fluid derived factors and the cells of the FRT also occur in humans. This study aimed to establish the presence of

this type of signalling in human cell lines and to attempt to identify the factors responsible and their mechanism of action.

Hypothesis

This work is based on the following hypotheses:

- FRT cells respond to semen or sperm derived molecules.
- Specific components of the ejaculate are responsible for Ca^{2+} signalling in an oviductal cell line model.
- Soluble but stable protein factors, carried and released by sperm, are the mediators that induce oviductal signalling.
- The signalling mechanism of action involves TLR4 as in other animal models.

Aims and Objectives

The work presented in this thesis aimed to identify the presence of signalling events that occur in the cells of the FRT in response to exposure to spermatozoa. A range of cell lines derived from the FRT were cultured, each were cell types that would be encountered *in vivo* by sperm cells as they make their way towards the site of fertilisation in the ampulla region of the oviduct. Using fluorescence microscopy and staining of the cells with the labelled calcium indicator Calcium Green-1, AM, it was possible to produce timelapse recordings of the cultured FRT cells as they were superfused with preparations of human semen samples whilst monitoring the relative intracellular concentration of Ca^{2+}. Using this experimental setup, the aims of this thesis were as follows:

- To establish cultures of a range of cell lines derived from the FRT that sperm cells would be expected to encounter *in vivo*.

- To develop a reproducible staining method and experimental protocol for the measurement of intracellular Ca^{2+} within the cultured FRT cells as different stimuli are superfused across their surface.

- To assess the efficacy of human semen sample preparations in eliciting Ca^{2+} in each of the cultured cell lines.

- To identify a candidate cell line for further experiments to investigate the mechanism of action and the source of the signalling factor responsible for any observed Ca^{2+} signalling.

- To establish a semen sample preparation pathway that would isolate specific subgroups of proteins and signalling factors derived from components of the semen sample.

- To study the efficacy of a wide range of semen sample preparations in eliciting Ca^{2+} signalling in the candidate cell line to identify the specific source of the signalling factor responsible.

- To use a proteomics approach to attempt to identify the specific factor responsible for any observed signalling events.

- To synthesise and test the efficacy of any candidate signalling factors in eliciting the Ca^{2+} signalling in the candidate cell line.

- To further elucidate the mechanism of action of any observed Ca^{2+} signalling by utilising a range of inhibitors and experimental designs.

Chapter 2

An Investigation of Ejaculate Induced Intracellular Calcium Signalling in Female Reproductive Tract Cells

2.1- Introduction

The journey of a human sperm cell to reach the site of fertilisation in the ampulla region of the oviduct is characterised by interactions with a variety of cells and proteins throughout the FRT (Ikawa, Inoue et al. 2010). Throughout their journey the sperm cells are swimming in a viscous environment between relatively closely opposed surfaces (Gaffney, Gadêlha et al. 2011). Until recently, the uterine and oviductal environment was thought to simply be a passage through which sperm must navigate, providing a microenvironment in which the pH, temperature, osmolality and oxygen concentration were optimal for the process of fertilization and early embryo development (Pauerstein and Eddy 1979).

The epithelial lining of the FRT contains many cells which are secretory in nature, particularly within the oviductal region. We now know that these cells are responsible for releasing a wide range of proteins and molecules into the milieu of the female tract which, in some cases, have documented impacts on the motility and fertilising capacity of spermatozoa (Ghersevich, Massa et al. 2015). Though comparatively little has yet been investigated on how this environment may collectively modulate a sperm (Taiwo, Frettsome-Hook et al. 2021).

Even less is known about any interactions which take place in the cells of the FRT which are elicited by factors derived from the male ejaculate. There is now mounting evidence from a range of studies in mammalian species that the male ejaculate contains factors which modulate the peri-conception environment. For example, the co-culture of spermatozoa with oviductal cells has been shown to significantly alter the oviductal secretory proteome in a porcine and bovine model. (Ellington, Ignotz et al. 1993, Georgiou, Sostaric et al. 2005). Alterations in gene expression profiles in

response to male gamete exposure have also been reported in murine models (Fazeli, Affara et al. 2004) and *Drosophila melanogaster* (Mack, Kapelnikov et al. 2006). Particularly interesting data has arisen from the study of seminal plasma components and their impact on the periconception environment in mice (Bromfield 2014), suggesting that proteins or factors within the male ejaculate are not only key regulators of the female tract environment, but also have a significant impact on the ongoing health of future offspring (Robertson and Sharkey 2016).

Whilst experiments using mammalian species as a model for human fertility provide useful information regarding the potential molecular interactions between male gametes and the FRT, the data cannot be directly translated due to fundamental differences in the reproductive anatomy and gamete functionality between humans and other species (Suarez and Pacey 2005).

The purpose of this initial study is to establish the presence of any factors derived from the human male ejaculate which modulate and influence the cells of the FRT and could have a significant impact on both the periconception environment, the early development of an embryo and potentially its lifetime health. Once the presence of such factor(s) has been determined, attempts will be made to determine specific identity and the source within the male ejaculate from which it is/they are delivered - whether it is from seminal plasma or the sperm cell itself. In order to achieve this, a series of cell lines derived from the human FRT, which spermatozoa would naturally come into contact with along their journey towards the oocyte, will be cultured and assessed for any reactivity with various human sperm cell preparations.

The cell lines derived from the FRT which are intended for use in this study include:

A human endometrial epithelial cell line known as HEC-1B originally derived from a human endometrial carcenoma in 1968 which have been well established as a viable cell line for endometrial research. HEC-1-B cells exhibit a typical cobblestone-like morphology of epithelial cells and grow as adherent monolayers. This cell line has been widely used in endometrial cancer research and they have been shown to express markers of the endometrial epithelium, such as cytokeratin, progesterone receptors, oestrogen receptors and are responsive to hormonal stimulation in a similar manner to primary endometrial epithelial cells (Kurarmoto, Hamano et al. 2002).Endometrial epithelial cells are one of the first types of cell that human spermatozoa would come into direct contact with upon making their way through the cervical canal (Miller 2018), making them an ideal candidate cell line for this series of experiments.

The oviductal secretory epithelial cell line referred to as OE-E6/E7 cells, originally immortalized by treating human secretory oviductal epithelial cells with HPV 16 E6/E7 (Lee, Lee et al. 2001). These cells have been demonstrated to grow continuously and maintain an epithelial phenotype under the microscope. The OE-E6/E7 cells have also been demonstrated to express cytokeratin-19 in their cytoplasm, even after 50 passages which provides further evidence of their epithelial characteristics. In addition, the presence of an oviductal specific glycoprotein with roles in fertilization and embryo development, known as HuOGP has been shown to be present within this cell line, as well as the expression of its corresponding mRNA, suggesting that these cells also maintain their specific oviductal characteristics (Lee, Lee et al. 2001). During coculture with mouse embryos OE-E6/E7 cells elicited embryotrophic activity on in-vitro developing embryos, suggesting that they release embryotrophic factors in a similar fashion to primary oviductal epithelial secretory

cells (Liu, Chan et al. 1998), This cell line was kindly donated by Lee *et al.* at Hong Kong University.

A human foreskin fibroblast (HFF) cell line was intended for use as a negative control condition during these experiments, Due to the fact that cells derived from human foreskin would not be expected to elicit significant intracellular Ca^{2+} signalling in response to human sperm cells. These cells were also immortalised via the retrovirus-mediated gene transfer of the E6 and E7 genes of HPV 16 (Compton 1993).The HFF cells have been shown to be capable of proliferating indefinitely whilst retaining their distinct morphology characterised by their elongated spindle-like shape. (Compton 1993).

An immortalised human granulosa cell line referred to as COV434 cells was also cultured for use (Zhang, Vollmer et al. 2000). *In vivo* granulosa cells form a single, flattened layer around oocytes arrested in the prophase of their first meiotic division, which proliferate and form multiple layers as the oocyte matures into a secondary follicle (Speroff and Fritz 2005). A mature oocyte is surrounded by a layer of specialised granulosa cells, forming an oocyte cumulus complex with hyaluronic acid (Eppig 1991), which spermatozoa must break through in order to fertilise the oocyte (Kim, Yamashita et al. 2008). The COV434 cell line was originally derived from a 26 year old female who was suffering from a granulosa cell tumour (van den Berg-Bakker, Hagemeijer et al. 1993). The cell line that was established was similar to normal granulosa cells in that they were capable of synthesizing oestradiol in response to stimulation with FSH in culture. They were also shown to be capable of forming intercellular connections with clusters of cumulus cells containing an immature oocyte during *in vitro culture* and they were morphologically similar

according to both scanning electron microscopy and confocal light microscopy (Zhang, Vollmer et al. 2000).

The presence of any molecular interactions that occur between these FRT cells and factors within the male ejaculate would be determined by investigating their response to a range of semen sample preparation methods. One previous study in an equine model established that cultured primary oviductal epithelial cells responded to the presence of sperm cells by exhibiting significantly increased levels of intracellular calcium ions ($[Ca^{2+}]_i$) (Ellington, Varner et al. 1993). Previous experiments within our own lab have also demonstrated the present of $[Ca^{2+}]_i$ signalling events in primary human oviductal epithelial cells in response to capacitated spermatozoa (Connolly 2011). Fluctuations in $[Ca^{2+}]_i$ within cells in response to molecular interactions with ligands and environmental factors, are known to have upstream implications in a wide range of cellular activities (Bagur and Hajnóczky 2017). Significant increases of $[Ca^{2+}]_i$ have been associated with alterations in cellular gene regulation (van Haasteren, Li et al. 1999), immune response (Trebak and Kinet 2019), as well as fluid, electrolyte and protein secretion (Ambudkar 2012). This evidence suggests that an investigation into the $[Ca^{2+}]_i$ levels within female reproductive cells may prove to be an optimal method of determining the presence of cellular signalling in response to male ejaculate factors.

Potential signalling factors present within the male ejaculate could be derived from a range of sources. For example, they could be abundantly available in the seminal plasma which contains a wide range ions, proteins, cytokines and enzymes (Wang, Yang et al. 2020), some of which could be carried into the upper regions of the FRT by loosely adhering to the surface of motile spermatozoa (Schjenken and Robertson 2014, Tecle, Reynoso et al. 2019). Signalling agents could also be present on the

surface of the spermatozoa plasma membrane, such as the IZUMO1 protein found on the equatorial segment of acrosome-reacted sperm cells which is necessary for sperm binding to the oocyte and the subsequent fusion of the plasma membranes via the JUNO receptor (Aydin, Sultana et al. 2016). Additionally, the AR itself is known to elicit the release of a range of proteins and hydrolytic enzymes which could be responsible for molecular interaction with cells within the FRT as they are released by spermatozoa undergoing capacitation as they navigate towards the site of fertilisation (Breitbart and Spungin 1997). In order to ascertain the presence of signalling factors within the male ejaculate that interact with the cells of the human FRT it is essential to consider the heterogeneity of the proteome within the male ejaculate (Samanta, Parida et al. 2018) to design experiments which will lead to the identification of candidate signalling factors.

In this study we sought to establish whether cell lines derived from the human FRT were responsive to semen or sperm derived molecules. To achieve this, cultures of the HEC-1-B, OE-E6/E7, COV434 and HFF cells were established, all of which would be expected to come into contact with sperm cells *in vivo*. We aimed to develop a reproducible staining protocol with Calcium Green-1 AM to allow for the measurement of intracellular Ca^{2+} concentrations within each of these cell lines whilst they were superfused with a range of preparations derived from human semen samples. The three stimuli used in these initial experiments were sperm cells isolated by density gradient centrifugation (Malvezzi, Sharma et al. 2014), sperm cells isolated by the swimup method (Volpes, Sammartano et al. 2016) and filtered seminal plasma which did not contain any sperm cells. This experimental setup allowed us to ascertain the contribution of factors within the male ejaculate to the elicitation of intracellular Ca^{2+} signalling within each of these cell lines and to identify

if any of the cells were suitable candidates for further study into sperm induced signalling within the FRT.

2.2- Materials & Methods

2.2.1- Materials

0.2 µM PES syringe filters, (Corning). 100mm tissue-culture treated culture dishes, (Corning). 12mm round coverslips, (Warner instruments). 15 ml centrifuge tubes, (Falcon). 15 mL plastic disposable syringes, (ThermoFisher Scientific). 2 mm inner diameter translucent silicone tubing (Fisher Scientific). 22x32mm coverslips, (Appleton Woods). 25cm^2 tissue culture flasks, (Falcon). 5 mL Round Bottom High Clarity PP Test Tubes, (Falcon). 75cm^2 tissue culture flasks, (Falcon). Adenosine-5'-triphosphate (ATP), (Sigma). Calcium Green-1 AM, (Invitrogen). Dulbecco's modified Eagle's medium (DMEM), no phenol red, (Gibco™). DMEM/F12, no phenol red, (Gibco™). Iscove's modified Dublecco's medium (IMDM), no phenol red, (Gibco™). DMEM/F12, no phenol red, (Gibco™). Foetal bovine serum, (Sigma-Aldrich). PBS tablets, (ThermoFisher Scientific). Penicillin-Streptomycin (10,000 U/mL), (Gibco™). Pluronic F-127 10% in DMSO, (Sigma-Aldrich). PureSperm 40, (Nidacon). PureSperm 80 (Nidacon). Series 20 perfusion chambers, (Warner Instruments). Supplemented Modified Earle's balanced salt solution (sEBSS), (Lab Industries) (described in Appendix I). Trypsin-EDTA solution 10x, (Sigma-Aldrich).

2.2.2- Culture of human female reproductive tract cell lines and human foreskin fibroblasts

Immortalised cell lines derived from various sections of the human FRT were cultured in preparation for Ca^{2+} imaging experiments in which they would be exposed to various preparations of human sperm cells suspended in media, in order to assess the presence of any cellular signalling which may take place. An immortalised human foreskin fibroblast cell line was also cultured as an intended negative control for the proceeding Ca^{2+} imaging experiments.

2.2.2.1- Granulosa cell line (COV434)

An immortalised granulosa cell line (COV434) (Zhang, Vollmer et al. 2000) was utilised as a model cell line for initial experiments. These cells were retrieved from liquid nitrogen stores, thawed for approximately 60 seconds in a 37°C water bath before being resuspended in 10 ml of culture medium in a 15 ml Falcon tube. The culture medium for this cell line (DMEM culture media) consisted of DMEM (no phenol red) supplemented with 10% foetal bovine serum (FBS) and 0.3% Penicillin-Streptomycin (10,000 U/mL) (PenStrep). The Falcon tube was then centrifuged for 10 minutes at 300G before the supernatant was removed and the cell pellet was resuspended in DMEM culture media. The cell preparation was then seeded into 25cm^2 tissue culture flasks which were placed in a 37°C, 6% CO^2 incubator for approximately 5 days to reach 80-90% confluence. At this point, the media from the COV434 cell culture flasks was aspirated and replaced by 5 ml of PBS for approximately 60 seconds. The PBS was then aspirated and replaced by a preparation of PBS with 10% Trypsin and flasks were then returned to the incubator for 2 minutes to allow the cells to dissociate from the surface of the culture flasks. The cells suspended in trypsin PBS were aspirated and returned to 15 ml Falcon tubes before being centrifuged for 5 minutes at 300 g, after which the supernatant was aspirated and the cell pellet resuspended in the COV434 culture media described previously, before being split and subcultured in a 1:4 ratio in 75cm^2 tissue culture flasks in a 37°C, 6% CO^2 incubator. Upon reaching confluence in the 75cm^2 tissue culture flasks, cells would be trypsinised once again as described previously and subcultured in a 1:4 ratio.

2.2.2.2- Endometrial epithelial cell line (HEC-1B)

An endometrial epithelial cell line (HEC-1B) utilised as a model cell line in this study was the first to be initially derived from a human endometrial carcinoma (Kurarmoto, Hamano et al. 2002). This cell line was thawed, cultured, trypsinised and subcultured using the same media and methods as described in section 2.2.2.1.

2.2.2.3- Oviductal epithelial cell line (OE-E6/E7)

A human immortalised oviductal epithelial cell line (OE-E6/E7), originally donated by Lee *et al*. at Hong Kong University, were derived from the ampullary oviductal tissue taken from women during the follicular phase of their menstrual cycle (Lee, Lee et al. 2001). These cells were thawed as described in section 2.2.2.1, before being cultured in DMEM/F12 culture media, consisting of DMEM/F12 (no phenol red) supplemented with 10% FBS and 0.3% PenStrep. Upon reaching confluence these cells were trypsinised as described in section 2.2.2.1 before being subcultured in a 1:4 ratio in DMEM/F12 culture media.

2.2.2.4- Human foreskin fibroblasts cell line (HFF)

A human foreskin fibroblast cell line which was originally immortalised via retrovirus-mediated gene transfer of the E6 and E7 genes of human papillomavirus type 16 (Compton 1993) was intended for use as a negative control cell line. The HFF cells were thawed as described in section 2.2.2.1 before being cultured in IMDM culture media, consisting of IMDM (no phenol red) supplemented with 10% FBS and 0.3% PenStrep. Aside from the culture media used, HFF cells were cultured using the same methods as the FRT cell lines as described in section 2.2.2.1.

2.2.3- Preparation of human female reproductive tract cell lines for perfusion chambers

To prepare cell lines for use in Ca^{2+} imaging experiments they were cultured onto the surface of 22x32 mm coverslips so that they could be attached to the lower surface of the Series 20 imaging chambers. A 100 mm tissue culture dish was filled with pure ethanol and as many 22x32 mm coverslips as necessary (12 per culture flask) were placed into the ethanol and the 100 mm tissue culture dish was placed onto an orbital agitator for approximately 24 hours to sterilise the 22x32 mm coverslips. After 24 hours the 22x32 mm coverslips were removed from the ethanol and added to a new 100 mm tissue culture dish containing the respective culture media for the cell line which they were intended to be used to cultivate. This 100 mm tissue culture dish was then also be placed on an agitator for 1 hour to completely remove any remaining traces of ethanol and ensure that cells could adhere to their surface. The prepared 22x32 mm coverslips were then added to separate 100 mm tissue culture dishes before being seeded with cells which had undergone the trypsinising process described in section 2.2.2.1. These 100 mm tissue culture dishes were then returned to a 37°C, 6% CO^2 incubator to allow the cells to reach approximately 80% confluence on the surface of the 22x32 mm coverslips so that they could be used in Ca^{2+} imaging experiments.

2.2.4- Recruitment of human sperm donors

Human sperm donors were recruited at the Birmingham Women's Hospital (HFEA Centre 0119), in accordance with the Human Embryology Authority Code of Practice. Human sperm were obtained from healthy research donors by masturbation. All donors gave informed consent (LREC 2003/239). Donors were selected on the basis of assumed fertility, as they would preferentially have previously fathered children and consistently produced semen samples which would be considered healthy

according to the motility, concentration and volume parameters specified by the HFEA.

2.2.5- Preparation of human sperm samples for perfusion as stimuli during initial Ca^{2+} imaging experiments

Fresh semen samples supplied by human sperm donors were allowed to undergo liquefaction for approximately 30 minutes in a 37°C, 6% CO_2 incubator. Upon liquefaction the samples would be prepared using three different methods for the initial series of Ca^{2+} imaging experiments.

2.2.5.1- Density gradient centrifugation (DGC) prepared sperm cells

The first method of sperm sample preparation was density gradient centrifugation. A 1 ml layer of PureSperm 40 was added to a 15 ml Falcon tube, a 1 ml layer of Puresperm 80 was then carefully underlayed into the bottom of a 15 ml Falcon tube using a P1000 Gilson Pipette, ensuring that the two fractions did not mix and a clear divide was visible between the PureSperm 40 and PureSperm 80. 1 ml of the liquefied human semen sample was then aspirated and carefully added to the surface of the PureSperm fractions in the 15 ml Falcon tube. Additional density gradient centrifugation tubes were prepared, with 1 ml of the semen sample added to each tube until the entire sample provided was ready to be prepared. The Falcon tubes were then centrifuged at 300 g for 10 minutes, causing the motile spermatozoa with compact DNA structures to form a pellet at the bottom of the 15 ml Falcon tubes, underneath the two layers of PureSperm media. After centrifugation, the supernatant was aspirated, and the sperm cell pellets were resuspended in a new 15 ml Falcon tube containing supplemented Earle's balanced salt solution (sEBSS) (described in Appendix I). The 15 ml Falcon tubes were then centrifuged once more at 300 g for 5 minutes, acting as a wash step for the sperm cells to remove and

remaining PureSperm media, before the supernatant was aspirated and the sperm cell pellet resuspended in sEBSS. The sperm cells suspended in sEBSS were then placed in a 37°C, 6% CO^2 incubator for approximately 6 hours to allow the spermatozoa to undergo the process of capacitation. The concentration of sperm cells was determined using Hamilton Thorne computer assisted semen analysis (CASA) software and then diluted further with sEBSS to a concentration of 6 million cells per millilitre. This preparation method produced the semen sample preparation used as a stimulus in initial Ca^{2+} imaging, referred to as “DGC sperm cells”.

2.2.5.2- Swimup prepared sperm cells

Alternatively, sperm cells could be prepared by a conventional “swimup” method (E.V. Younglai et al., 2001). Briefly, upon liquefaction a 0.3 ml layer of semen sample was added to a series of 5 mL Round Bottom High Clarity PP Test Tubes. The semen was overlayered with 1 ml of sEBSS, the 5 mL Round Bottom High Clarity PP Test Tubes were then placed in a tube rack, inverted at a 45° angle and placed in a 37°C, 6% CO_2 incubator for one hour. After this incubation period, the top 0.5 ml layer of sEBSS was aspirated from each tube and combined in a 15 ml Falcon tube. The concentration of sperm cells was then determined using Hamilton Thorne computer assisted semen analysis (CASA) software and then diltuted further with sEBSS to a concentration of 6 million cells per millilitre. This sperm cell preparation method produced the initial Ca^{2+} imaging, referred to as “Swimup sperm cells”.

2.2.5.3- Preparation of filtered and centrifuged seminal plasma

The final stimulus to be produced from donor semen samples for use in the initial series of Ca^{2+} imaging experiments was a simple preparation of raw seminal plasma, without the presence of any sperm cells. To achieve this, liquefied semen sample was centrifuged in a 15 ml falcon tube at 300G for 10 minutes, after which the

supernatant (seminal plasma) was aspirated into a syringe. A disposable sterile filter (membrane pore size 0.2 μM) was then attached to the tip of the syringe and the semen pushed through the filter to ensure that any remaining spermatozoa after the centrifugation step were removed. This centrifuged and filtered semen was then diluted in sEBSS at a 1:100 volume to volume ratio to become the “Seminal plasma” stimulus condition in the initial Ca^{2+} imaging series of experiments.

2.2.6- Setting up Ca^{2+} imaging apparatus

To allow for the simultaneous imaging of cultured cells whilst gently perfusing different media preparations across their surface, perfusion chambers (Series 20, Warner Instruments) were used for this series of Ca^{2+} imaging experiments. Figure 2.1 depicts the setup of the perfusion chamber apparatus.

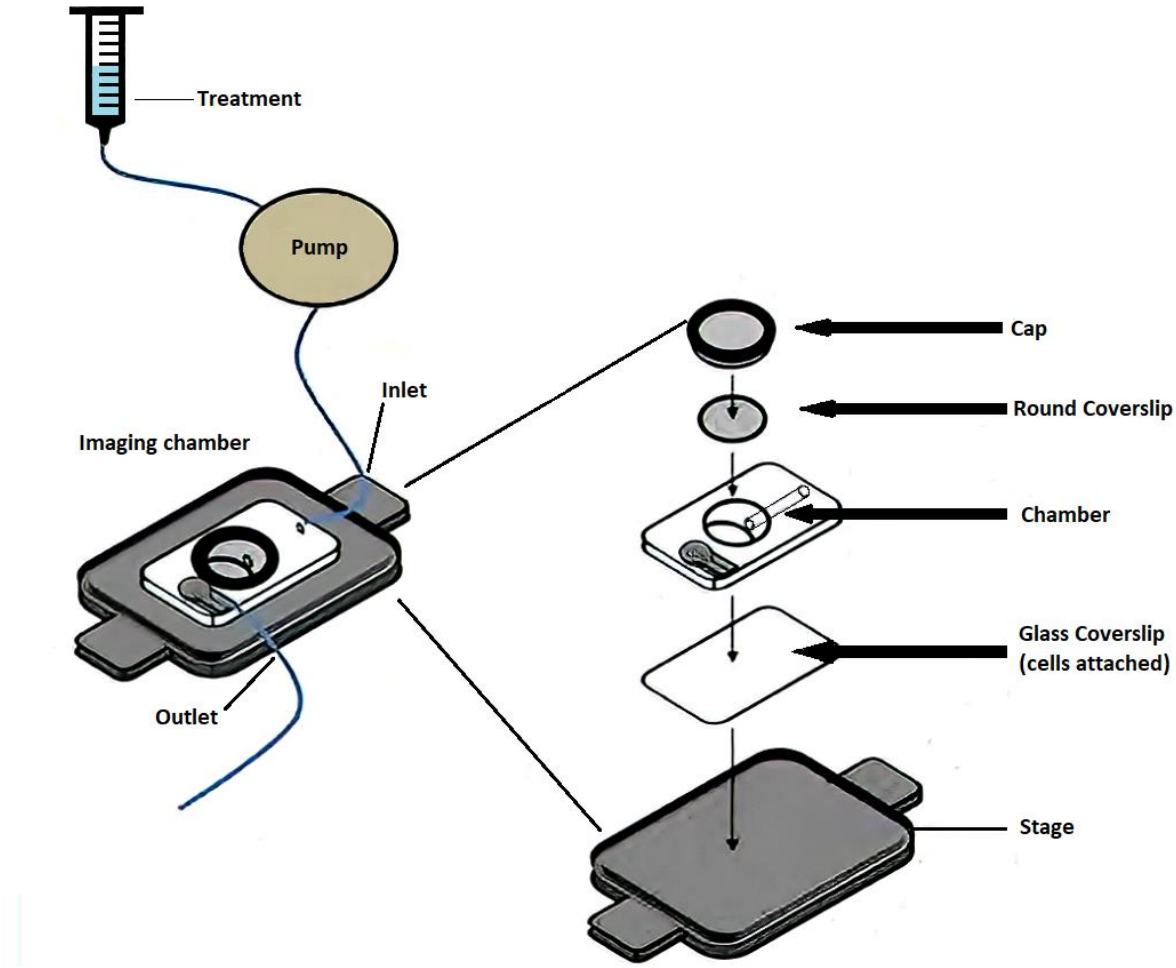


Figure 2.1- A diagram of the imaging perfusion chambers utilised to simultaneously image cells grown onto 22x32 mm coverslips whilst various media preparations could be gently perfused across their surface. Treatments added to the syringe could be gently pumped into the inlet of the imaging chamber, where it was perfused across the surface of the cells adhered to the glass coverslip within the sealed imaging chamber before being removed via the outlet. Adapted from (Connolly 2011)

22x32 mm coverslips with attached cells (grown as described in section 2.2.3) were removed from their culture dish and attached to the lower surface of a perfusion chamber using silicone grease (Warner Instruments) on their peripheral surface. A 12 mm round coverslip was then securely attached to the circular hole in the upper side of the perfusion chamber and a cap was inserted above the round coverslip, forming a water-tight seal. The perfusion chambers contained an inlet and outlet port on either side, allowing for the insertion of tubing attached to a peristaltic pump on

the inlet side and a vacuum pump leading to a waste bottle from the outlet port. Media preparations could be added to a 15ml syringe with tubing leading to a peristaltic pump, allowing for gentle, laminar perfusion of any stimuli in media across the upper surface of the cells within the perfusion chamber. The tubing and syringe were replaced after each experiment to ensure that there was no contamination from the perfusion of media from previous experiments. This apparatus provided an ideal environment for the assessment of stimuli effects on cells within the chamber, whilst allowing for the removal of previous treatments and introduction of new stimuli to create timelapse Ca^{2+} image files assessing cellular response to a range of consecutive media preparations.

2.2.7- Staining of cells for Ca^{2+} imaging experiments

Cell lines were grown on coverslips as described in section 2.2.3 until they reached approximately 80% confluence and were attached to the perfusion chamber as described in section 2.2.6. sEBSS was then pipetted into the inlet port of the perfusion chamber and aspirated from the outlet port, to wash any culture media from the surface of the cells as the FBS may interfere with the uptake of fluorescent staining in the cells. Calcium Green-1 AM was prepared by diluting to a concentration of 1 mM in Pluronic F-127 20% solution in DMSO. The solubilised Calcium Green-1 AM was then diluted to a working concentration of 10 µM in sEBSS. 125 µl of 10 µM Calcium Green-1 AM solution was added to each perfusion chamber and placed in a 37°C, 6% CO_2 incubator for 1 hour to allow for the uptake of the dye into the cells. Several replicate Ca^{2+} imaging experiments would be carried out on each day of experimentation; therefore, efforts were made to maintain consistency in the timings and concentrations of Calcium Green-1 AM staining in each perfusion chamber prepared.

2.2.8- Ca^{2+} imaging of human reproductive tract cell lines with perfusion of human sperm cell preparations

Cells stained with Calcium Green-1 AM were imaged with a Photometrics®Evolve camera attached to an Olympus IX81 inverted fluorescence microscope, with Metamorph imaging software. Images were captured every 3 seconds using illumination/emission wavelengths of 488/535 nm, correlating to the spectral characteristics of Calcium Green-1 AM. Before the start of timelapse imaging of each perfusion chamber preparation, the cells would be perfused with sEBSS for approximately 15 minutes, to ensure that any extracellular Calcium Green-1 AM within the perfusion chamber had been washed away. Timelapse videos for these initial Ca^{2+} imaging experiments were set up to record for a total of 12 minutes, with the initial 3 minutes consisting of sEBSS perfusion to establish a baseline level of fluorescence within the cells, followed by 3 minutes of stimulus perfusion, followed by a further 3 minutes of sEBSS perfusion to wash away the stimuli within the chamber and finally a 3-minute period of positive control stimulus perfusion (100 μM ATP in sEBSS).

2.2.9- Statistical analysis of Ca^{2+} imaging timelapse data

Statistical analysis of the Ca^{2+} imaging timelapse data acquired in this study was based upon methods previously used within our lab group in a range of previous studies (Kirkman-Brown, Bray et al. 2000, Kirkman-Brown, Lefièvre et al. 2002, Kirkman-Brown, Punt et al. 2002, Harper, Kirkman-Brown et al. 2003, Kirkman-Brown, Barratt et al. 2003, Kirkman-Brown, Barratt et al. 2004, Harper, Barratt et al. 2007). Data acquired from Ca^{2+} imaging timelapse experiments was analysed offline using MetaMorph Image Analysis Software. A region of interest was manually drawn around each clearly visible cell that demonstrated retention of Calcium Green-1 AM throughout the entirety of each timelapse video. Each image series was then reassessed to determine if any of the cells moved such that the drawn region of interest no longer contained the entire cell, in which case that cell was then excluded from further analysis. The average fluorescence intensity within each of the regions of interest, for each of the 3 second interval time points within a timelapse video were then extracted into a Microsoft Excel file. These raw intensity values were initially normalised to the baseline level of fluorescence using the following formula:

$$\mathbf{N= [(F-F_{baseline})/F_{baseline}] \times 100}$$

Where N is the normalised to baseline fluorescence intensity at a single time point for a single cell; F is the average fluorescence intensity within a region of interest at a single time point and $F_{baseline}$ was an average of 10 fluorescence intensity values for that specific region of interest spread throughout the initial baseline period of sEBSS perfusion (prior to the addition of any sperm cell/seminal plasma preparations as stimuli).

The normalised fluorescence intensity values for all cells in a timelapse were then used to calculate the overall average fluorescence intensity for each 3 second time point. The overall average fluorescence intensity across all the cells throughout a timelapse experiment were then compared (which, in what follows, we term R_{tot} plots).

A series of analyses were carried out on the normalised fluorescence intensity values for each cell to assess whether any changes in $[Ca^{2+}]_i$ occurred at different periods during each experiment. For each cell the mean and 95% confidence interval were calculated for: (1) 15 images during the first half of the initial control period of sEBSS perfusion ($\mu_{C1} \pm CI_{C1}$) (2) 15 images during the second half of the initial control period of sEBSS perfusion ($\mu_{C2} \pm CI_{C2}$) (3) 15 images during the first half of the stimulus perfusion period after the initial peak had occurred ($\mu_{R1} \pm CI_{R1}$) (4) 15 images during the second half of the stimulus perfusion period ($\mu_{R2} \pm CI_{R2}$) (5) 15 images during the first half of the sEBSS wash period ($\mu_{W1} \pm CI_{W1}$) (6) 15 images during the second half of the sEBSS wash period ($\mu_{W2} \pm CI_{W2}$) (7) 15 images during the first half of the positive control ATP solution perfusion period after the initial peak had occurred ($\mu_{A1} \pm CI_{A1}$) (8) 15 images during the second half of the positive control ATP solution perfusion period ($\mu_{A2} \pm CI_{A2}$).

By comparing the mean average ± 95% confidence intervals between these periods it was possible to identify which cells showed an increase, no change or a rise in $[Ca^{2+}]_i$ between each period during a timelapse perfusion experiment. For example, an individual cell was considered to have shown a rise in $[Ca^{2+}]_i$ to stimulus perfusion if ($\mu_{R1} - CI_{R1} > \mu_{C2} + CI_{C2}$). The effectiveness of the sEBSS wash period of each experiment in eliminating the observed signalling from the stimulus perfusion period

could be assessed for each cell by comparing the mean average ±95% confidence interval for the W1 period to the same values from the R2 period, for example, if ($\mu_{W1} - CI_{W1} < \mu_{R2} + CI_{R2}$)) then the sEBSS wash period was effective in reducing the changes in $[Ca^{2+}]_i$ elicited by the stimulus. If ($\mu_{W1} - CI_{W1} \geq \mu_{R2} + CI_{R2}$) then the changes in $[Ca^{2+}]_i$ elicited by the stimulus were sustained throughout the initial sEBSS wash period. The response to the positive control ATP solution perfusion period could be assessed by comparing the mean average ± 95% confidence intervals for each individual cell between the A1 and W2 periods, for example, if ($\mu_{A1} - CI_{A1} > \mu_{W2} + CI_{W2}$) then the cell exhibited a significant rise in $[Ca^{2+}]_i$ in response to ATP perfusion and the transience of this response could be assessed by comparing the A1 and A2 periods for each cell. From these comparisons, the mean average percentage of cells and the standard error of the mean could then be calculated for each experiment, to show how many cells showed a significant rise, decrease or no change between each of the periods assessed during a timelapse. An example of a standard timelapse perfusion experiment and the statistical analyses carried out on the resulting data are summarised within figure **2.2**.

In cases where the specific timings of the changes in stimuli perfusion in a Ca^{2+} imaging experiment were altered, or additional stimuli were added for experimental purposes, the periods of comparison were altered from this standard timelapse experimental framework (as discussed in each relevant case) to allow for the identification of the cellular $[Ca^{2+}]_i$ responses.

Comparison between groups of experiments to assess significant differences in the response rate to specific stimuli, or to compare the strength of signalling response between groups, were carried out using Mann-Whitney U tests with Dunns test of multiple comparisons. These statistical tests were chosen as the data acquired from

Ca^{2+} imaging experiments were non-normal, as confirmed by the Kolmogorov-Smirnov test, resulting in the need for non-parametric tests.

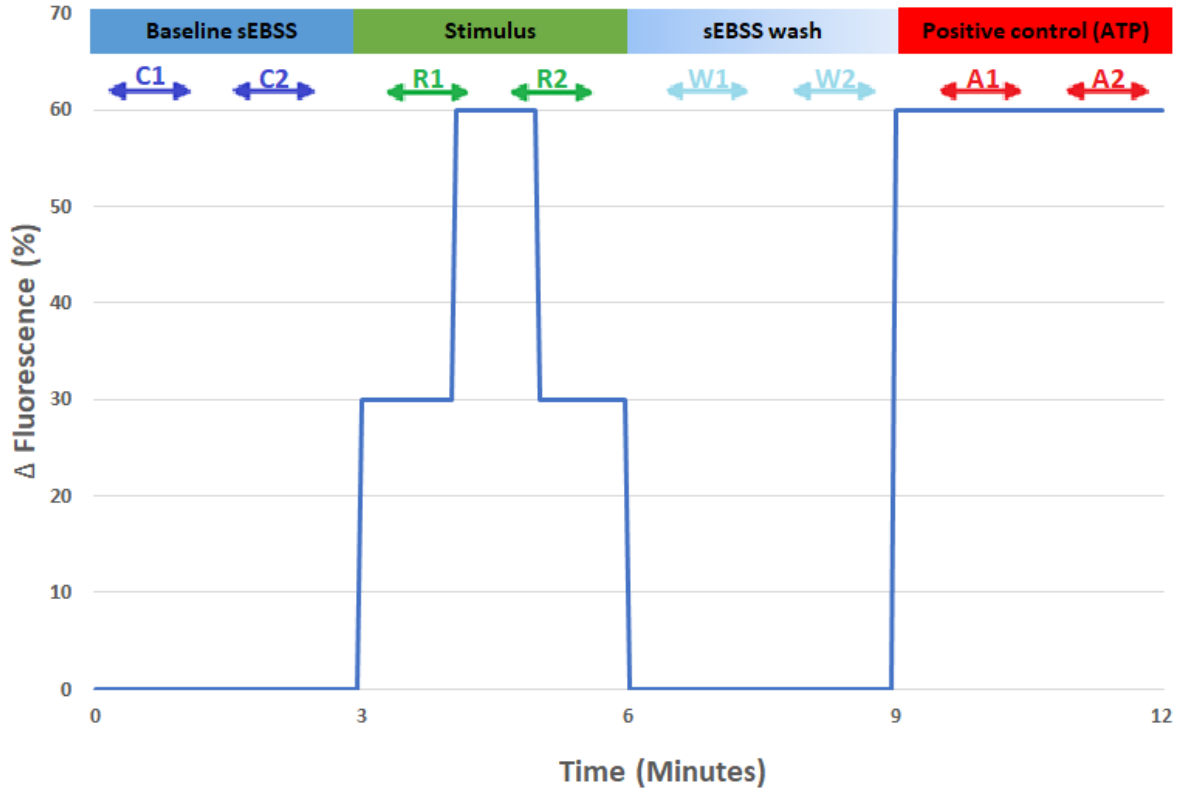


Figure 2.2- An example graph of the expected average fluorescence intensity for a single cell throughout a timelapse Ca^{2+} imaging experiment. The timeline across the top of the graph shows the type of media being perfused at that time point during the experiment. Each of the defined experimental periods used for statistical analyses are highlighted beneath the perfusion timeline: C1 represents the initial period of control sEBSS perfusion, C2 represents the second half of the control sEBSS perfusion, R1 is the first half of the stimulus perfusion period, R2 is the second half of stimulus perfusion, W1 is the first half of the sEBSS wash, W2 is the second half of the sEBSS wash, A1 is the first half of the ATP positive control perfusion and A2 is the second half of ATP positive control perfusion. Similar timelapse experimental layouts were used across all experiments, with some having slight deviations where necessary.

2.2.10- experimental plan for studying sperm cell and seminal plasma induced $[Ca^{2+}]_i$ signalling in female reproductive tract cells

The following initial Ca^{2+} imaging timelapse experiments set out to investigate the presence of any $[Ca^{2+}]_i$ signalling that could be induced by signalling factors derived from the sperm cell and semen preparations described in section 2.2.5, namely the DGC prepared sperm cells, swimup prepared sperm cells and seminal plasma stimulus conditions. Each of the stimuli would be gently perfused across the surface of the cell lines FRT cell lines described in section 2.2.2, with the HFF cells acting as a negative control cell line. Each stimulus condition would be assessed for its ability to elicit $[Ca^{2+}]_i$ signalling in the individual cell lines in separate prepared perfusion chambers (described in section 2.2.6) and each timelapse would also involve the perfusion of a 100 μM ATP solution which would act as a negative control due to its well documented capability of eliciting strong $[Ca^{2+}]_i$ responses in a wide variety of cells (Petersen and Verkhratsky 2016).

2.3- Results

2.3.1- Culture of female reproductive tract cell lines and human foreskin fibroblasts

Culture of all FRT cell lines and the HFF cells was successful and these cultures were maintained throughout the course of experimentation. Example images of each cell line used are shown in figure 2.3.

COV434 cells had a relatively small, circular morphology which grew together tightly and evenly. OE-E6/E7 cells had asymmetrical morphology between cells, but grew together tightly into “swirly” patterns. HEC-1B cells grew together in close-proximity clusters, whilst HFF cells had a more elongated shape and tended to overlap each other.

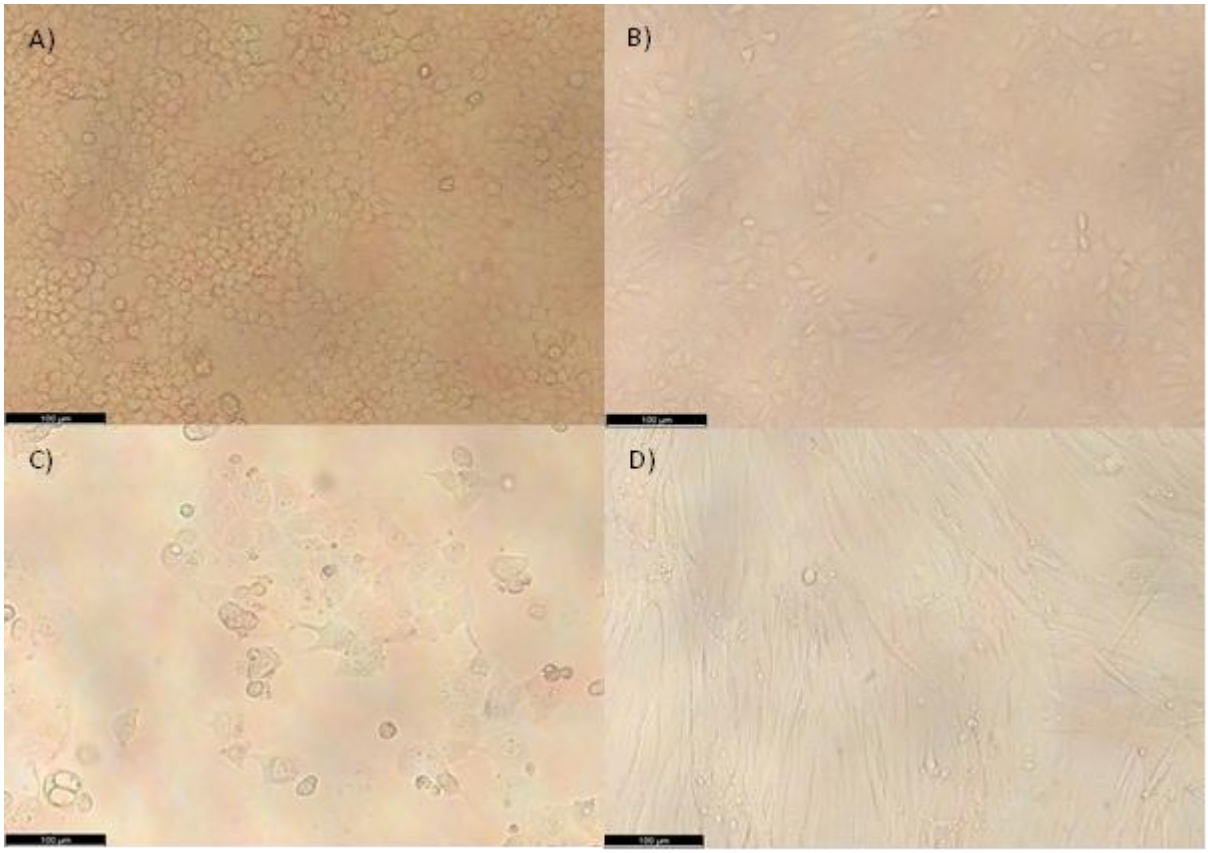


Figure 2.3- Bright field images of each of the female reproductive tract cell lines and the human foreskin fibroblasts. A) Granulosa cell line (COV434) B) Oviductal epithelial cell line (OE-E6/E7) C) Endometrial epithelial cell line (HEC-1B) D) Human foreskin fibroblasts cell line (HFF)

2.3.2- Staining of cell lines with Calcium Green-1 AM

Relatively even staining was observed throughout all of the FRT cell lines and human foreskin fibroblast cells, with some clusters of cells showing slight variation in their absorbance of the 10 μM Calcium Green-1 AM, without being oversaturated or too weakly stained for imaging to be successful.

Individual cells were easily distinguishable using this staining method and none of the cell lines were over saturated with fluorescence. COV434 cells showed some slight variation in overall fluorescence intensity between the cells. OE-E6/E7 cells showed fainter staining in the peripheral of the cells with much stronger absorbance of the Calcium Green-1 AM in the centre and nucleus of each cell. HEC-1B cells showed slight variation in staining throughout each cell, with clearly distinguishable boundaries between adjacent cells. HFF cells varied slightly in the intensity of the fluorescent staining absorbed between each cell, with a very strong absorbance around the nucleus of each cell.

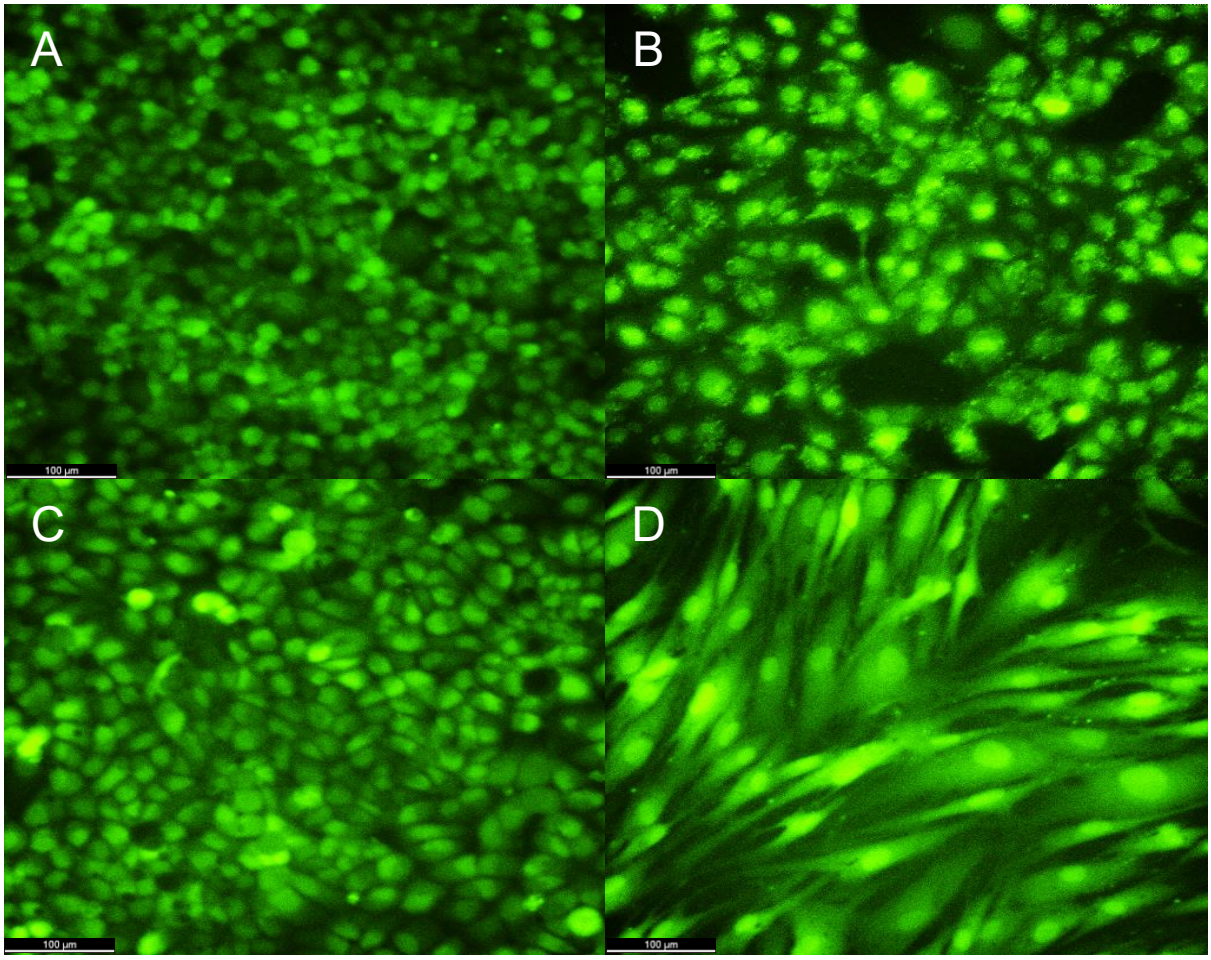


Figure 2.4- Images of each of the cultured cell lines, captured at spectral wavelengths of 488/535 nm captured using Metamorph imaging software after the cells have been loaded with 10 µM Calcium Green-1 AM solution as described in section 2.2.7. A) COV434 cells B) OE-E6/E7 cells C) HEC-1-B cells D) HFF cells.

2.3.3- Validation of Ca^{2+} imaging timelapse experimental protocol

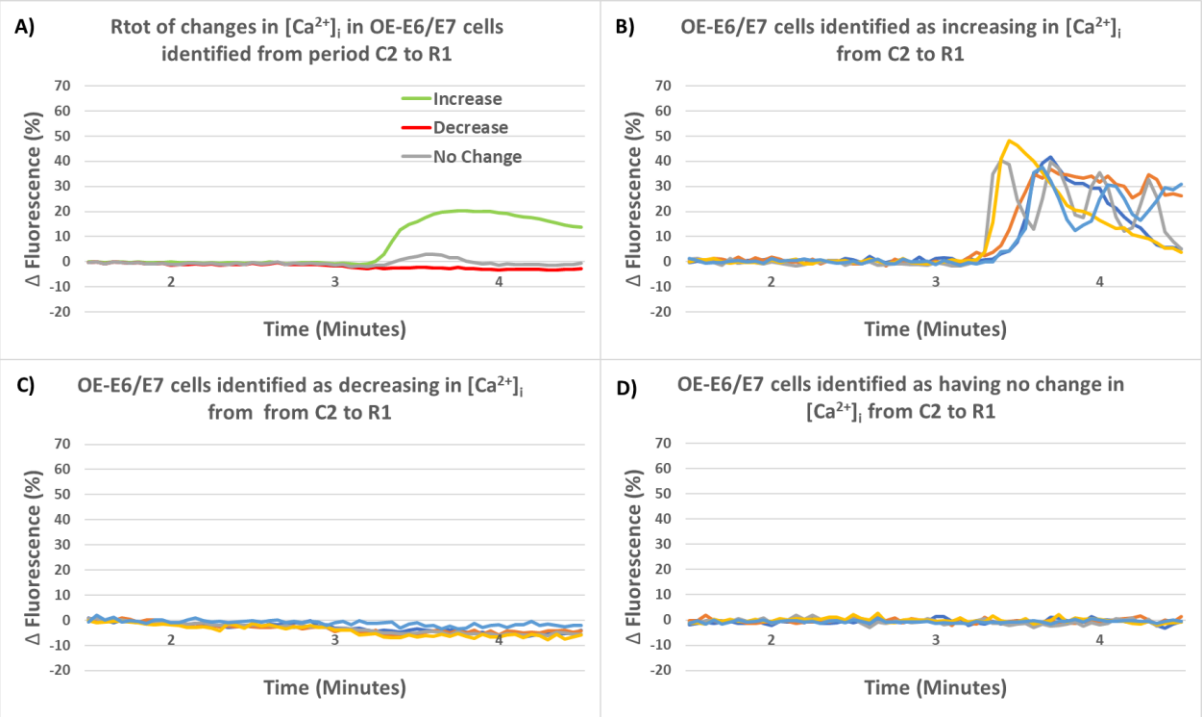


Figure 2.5- Validation of Ca^{2+} imaging timelapse experimental protocol and statistical method of identifying $[Ca^{2+}]_i$ signalling. A) The Rtot plots for a total of 666 cells recorded across 5 separate experiments in which OE-E6/E7 cells were were perfused with sEBSS for 3 minutes, followed by DGC sperm cells for 3 minutes, washed with sEBSS for 3 minutes and then exposed to ATP positive control solution for 3 minutes. Cells were grouped according to whether the statistical analysis described in section 2.2.9 identified them as having an increase, decrease or no change in $[Ca^{2+}]_i$ between the second half of the initial control period (C2) and the first half of the stimulus perfusion period (R1). B) a random selection of 5 fluorescence time plot for individual OE-E6/E7 cells identified as increasing in $[Ca^{2+}]_i$ between C2 and R1. C) a random selection of 5 fluorescence time plot for individual OE-E6/E7 cells identified as decreasing in $[Ca^{2+}]_i$ between C2 and R1. C) a random selection of 5 fluorescence time plot for individual OE-E6/E7 cells identified as showing no change in $[Ca^{2+}]_i$ between C2 and R1.

The experimental protocol for Ca^{2+} imaging timelapse experiments was effective in allowing for the recording and analysis of changes in the concentration of intracellular Ca^{2+} concentrations across the full range of cell lines used in this series of experiments. The statistical analysis described in section 2.2.9 allowed for the identification of cells which exhibited an increase, decrease of no change in their observed level of fluorescence during each period of timelapse experiments whilst

different stimuli and media were perfused across the surface of the cells through the perfusion chamber.

The Rtot plots shown in figure 2.5 demonstrate that increases in fluorescence that take place during the period of stimulus perfusion are accurately identified. Cells identified as showing no change during this period in some cases had small, transient increases in fluorescence but overall the method of identification was effective in isolating cells with negligible changes to $[Ca^{2+}]_i$ during these periods. The cells identified as exhibiting a decrease in fluorescence across these two periods appear to be cells which are non-responsive to the stimulus perfusion with a gradual, persistent decrease in fluorescence throughout these experimental periods.

Similar plots to those shown in figure 2.5 for the comparisons between each of the experimental periods outlined in section 2.2.9 are included in appendix II.

2.3.4- Comparison of cells exposed to sEBSS with cells exposed to 100 µM ATP solution

The 100 µM ATP solution positive control was reliable in eliciting Ca^{2+} signalling within the FRT cell lines and the Ca^{2+} imaging experimental setup was sufficient to record changes in intracellular Ca^{2+} concentration.

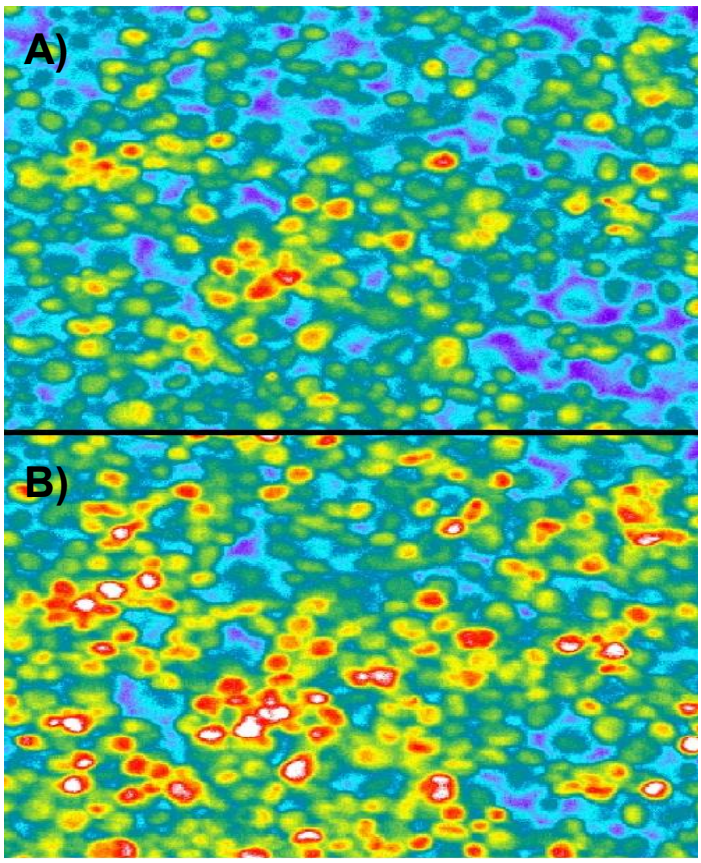


Figure 2.6- Pseudocolour images from a Ca^{2+}imaging timelapse of HEC-1-B cells superfused with (A) sEBSS and (B) 100 µM ATP solution. There is a clear rise in the concentration of intracellular Ca^{2+} when the cells are exposed to the positive control stimulus.

2.3.5- Ca2+ imaging experiments with human foreskin fibroblast (HFF) cell line

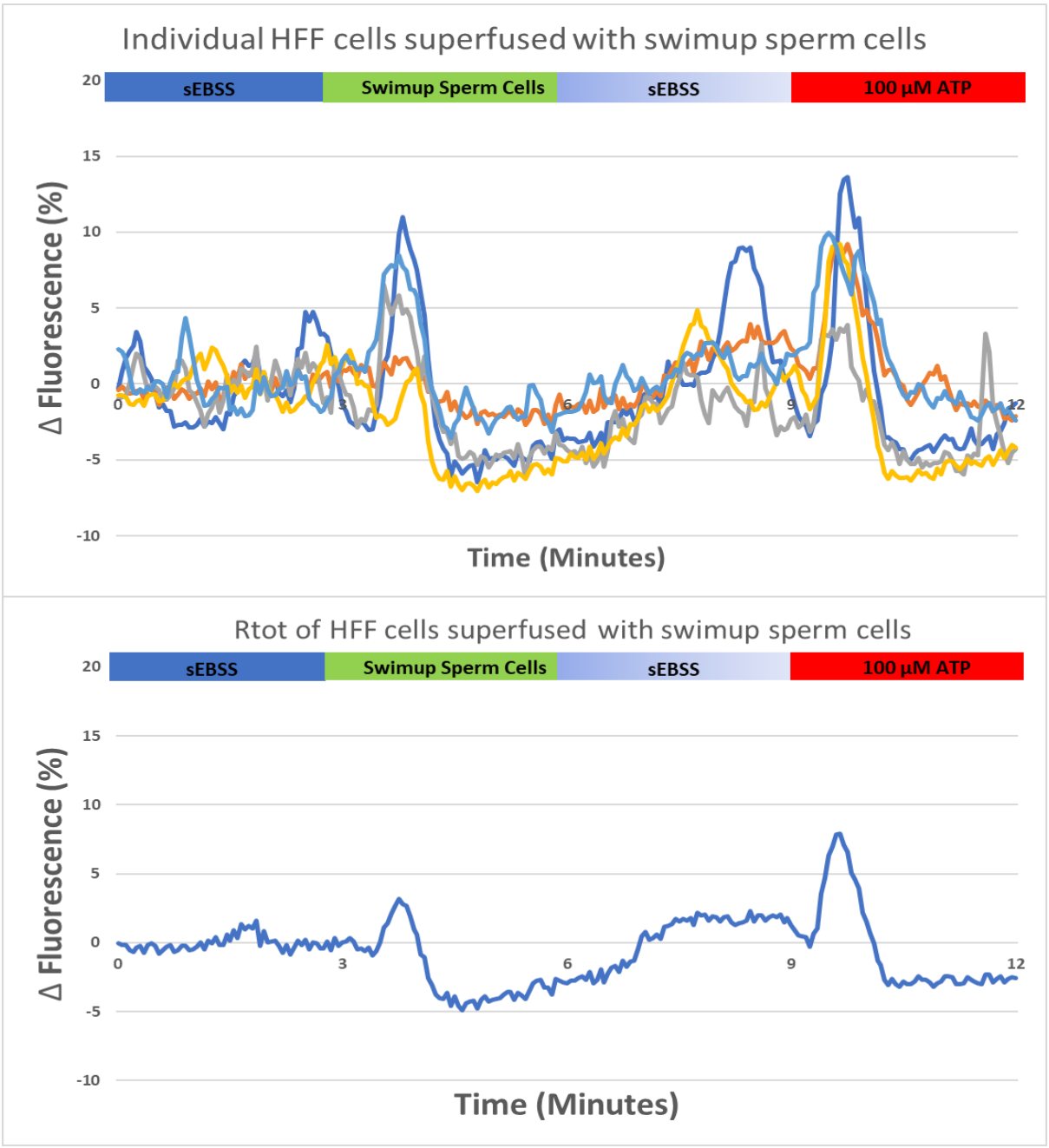


Figure 2.7- Example average fluorescence intensity plots for HFF cells perfused for 3 minutes with sEBSS followed by 3 minutes with swimup sperm cells before 3 minutes sEBSS wash period and then a 3-minute perfusion with the ATP positive control stimulus. (A) The fluorescence-time plot of 5 individual HFF cells from the experiment (B) The Rtot average fluorescence-time plot across all 49 HFF cells in the experiment.

These graphs show an example Ca^{2+} imaging experiment carried out on HFF cells.

A) The plot of average fluorescence intensity representing $[Ca^{2+}]_i$ within 5 individual

HFF cells throughout a perfusion timelapse video. The fluorescence intensity

fluctuates from the normalized baseline in each of the cells during initial period of gentle sEBSS perfusion, with a rise $[Ca^{2+}]_i$ being exhibited in response to the addition of both swimup sperm cells and the ATP positive control condition to the perfusion chamber. Rises in $[Ca^{2+}]_i$ were also observed during the sEBSS washoff period. B) Most of the cells in the the Rtot plot exhibit a slight peak and lots of variation in their $[Ca^{2+}]_i$ during the initial baseline sEBSS perfusion, followed by a small peak in response to swimup sperm cells which is quickly followed by a drop in $[Ca^{2+}]_i$ below the resting levels observed during the initial 3 minutes of sEBSS perfusion. The $[Ca^{2+}]_i$ then climbs back above baseline during the sEBSS washoff period and another peak is observed in response to the introduction of the ATP control condition.

To investigate if mechanosensitivity may contribute to the observed Ca^{2+} signalling in the HFF cells we set up an experiment in which the cells were exposed to sEBSS with no continuous flow across their surface, before turning on the peristaltic pump to begin the gentle laminar perfusion of sEBSS across their surface.

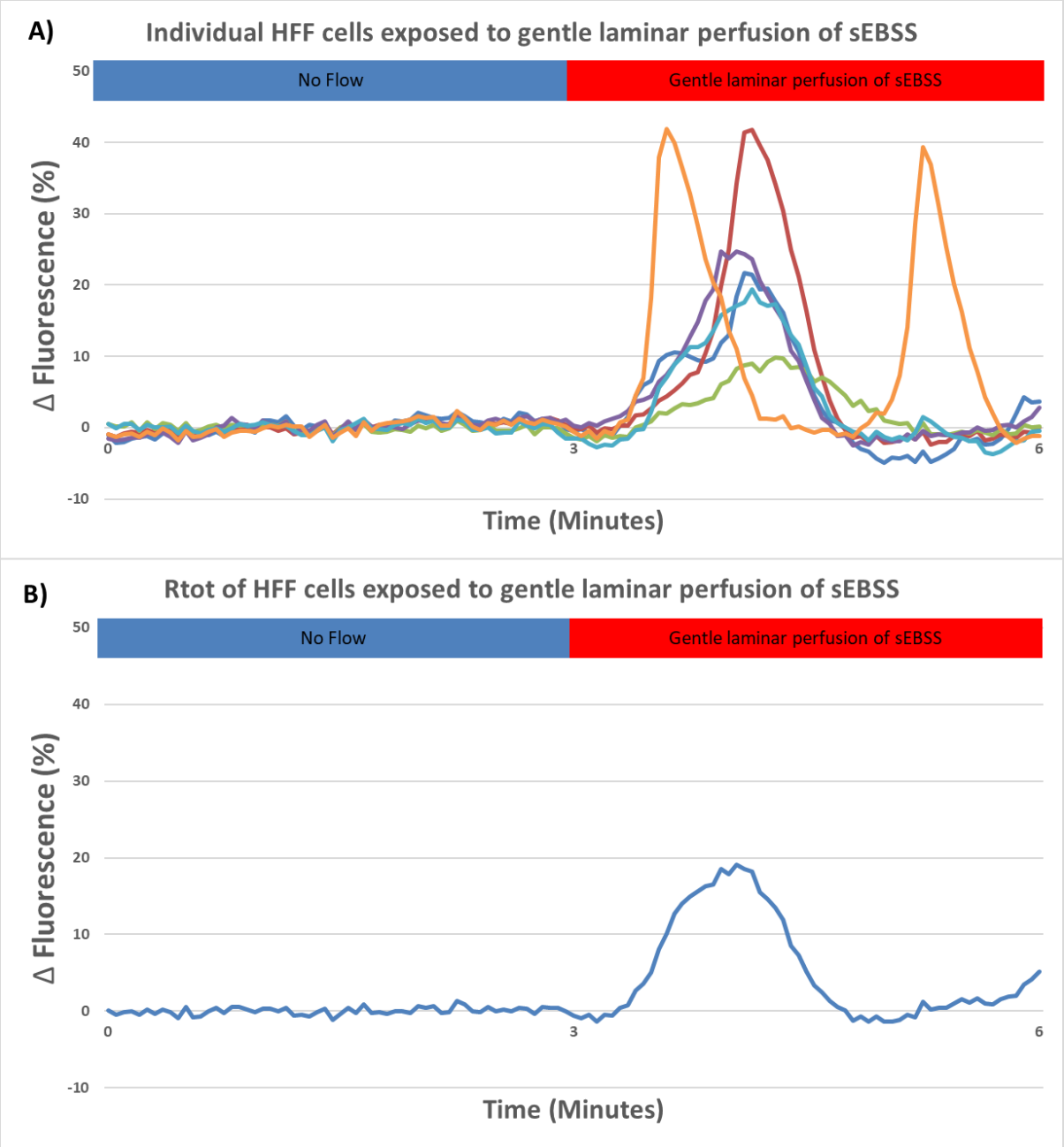


Figure 2.8- Experiments to determine whether gentle perfusion of sEBSS can elicit a $[Ca^{2+}]_i$ response in HFF cells in which cells were exposed to sEBSS with no flow through the chamber for 3 minutes followed by 3 minutes of gentle laminar perfusion of sEBSS across their surface. (A) fluorescence-time plots for 7 individual HFF cells in the experiment (B) Average fluorescence time plot for all 49 of the HFF cells imaged in this experiment.

To assess the influence of mechanosensitivity on observed changes in intracellular Ca^{2+} concentration within HFF cells they were imaged for an initial 3-minute period with the peristaltic pump attached to the inlet port of the perfusion chamber switched off so that the cells had sEBSS on their surface within the chamber but a lack of

laminar flow during this period. After 3 minutes the peristaltic pump was switched on and the laminar flow of sEBSS across the surface of the HFF cells began. A) These 7 individual HFF cells from this experiment exhibit a steady, baseline level of $[Ca^{2+}]_i$ during the initial 3 minute period with a lack of laminar flow. Once the sEBSS begins to flow through the chamber, the HFF cells exhibit strong peaks in $[Ca^{2+}]_i$, with some of the cells taking longer to response than others. B) The Rtot plot for this experiment shows a trend of the introduction of laminar flow eliciting a rise in $[Ca^{2+}]_i$ in the HFF cells.

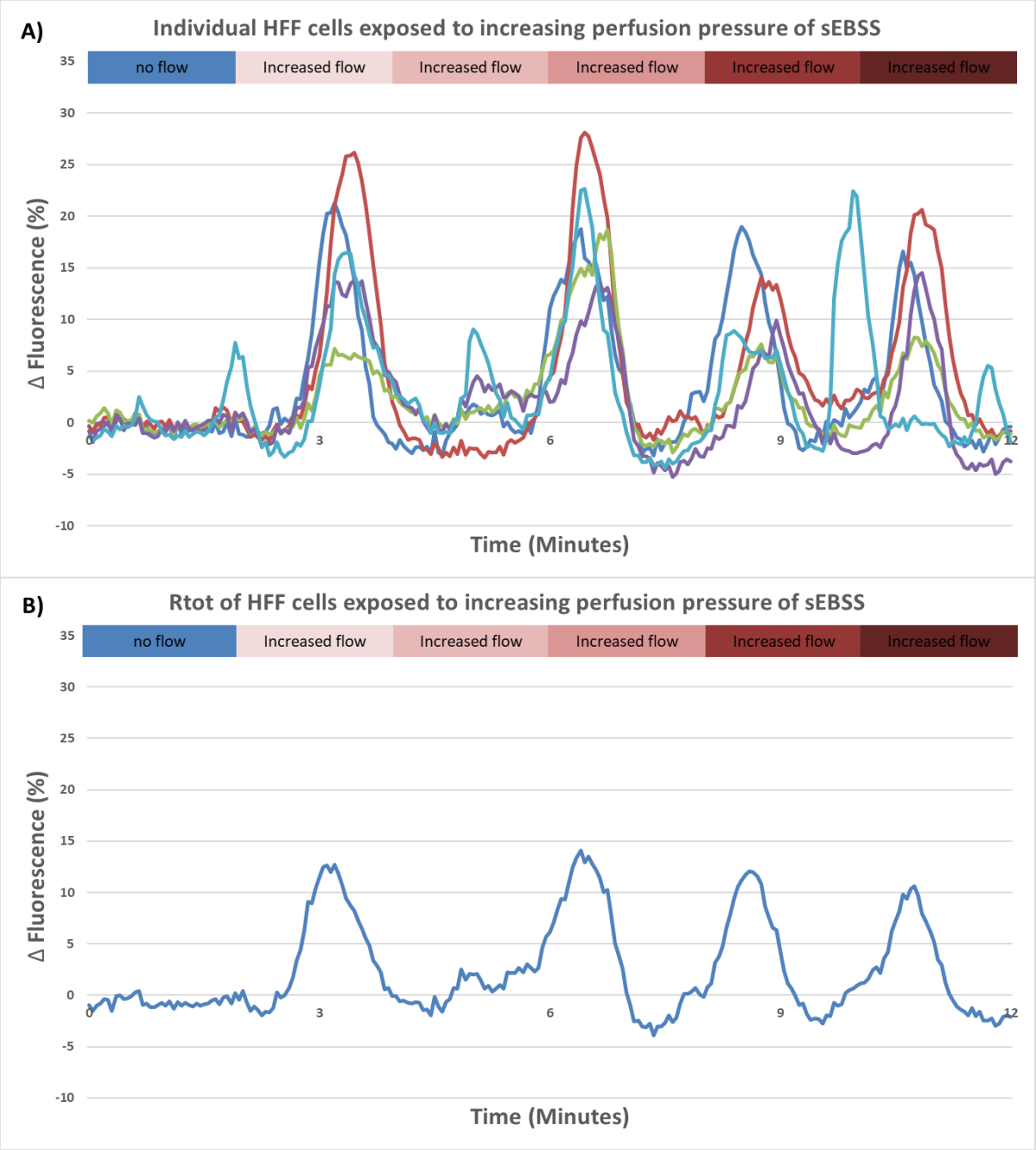


Figure 2.9- Experiment to determine whether increasing strengths of sEBSS perfusion can elicit a $[Ca^{2+}]_i$ response in HFF cells. (A) fluorescence-time plots for 5 individual HFF cells from a single experiment in which the cells were exposed to sEBSS at increasing perfusion pressure at 2 minute intervals. (B) The Rtot plot for all 46 HFF cells included in this experiment.

To assess the impact of perfusion pressure on the stimulation of Ca^{2+} signalling in the HFF cells we used increasing doses of perfusion pressure and measured the response. HFF cells were initially imaged in the perfusion chamber for 2 minutes with no laminar flow of sEBSS across their surface. After 2 minutes, the peristaltic pump

was turned on at a low setting to initiate laminar flow of sEBSS across the HFF cell surface. The strength of perfusion was increased by turning up the flow on the peristaltic pump at the beginning of every consecutive 2-minute period. A) The average fluorescence intensity time plot for 5 individual HFF cells in this experiment. The $[Ca^{2+}]_i$ levels stay close to baseline during the initial 2 minutes of no flow, but immediately upon the introduction of flow there is a large peak in $[Ca^{2+}]_i$. Further peaks are seen throughout the experiment; however, they do not seem to be initiated precisely at the point of increased flow beginning. B) The 46 individual cells represented in this Rtot plot show overall synchronicity between the $[Ca^{2+}]_i$ responses to the increasing of perfusion pressure of sEBSS across their surface. The $[Ca^{2+}]_i$ peaks that occur after the initial onset of flow in $[Ca^{2+}]_i$ are not occurring in coincidence with the increase of flow by the peristaltic pump.

2.3.6- HEC-1-B cell Ca^{2+} imaging experiments with stimulus perfusion

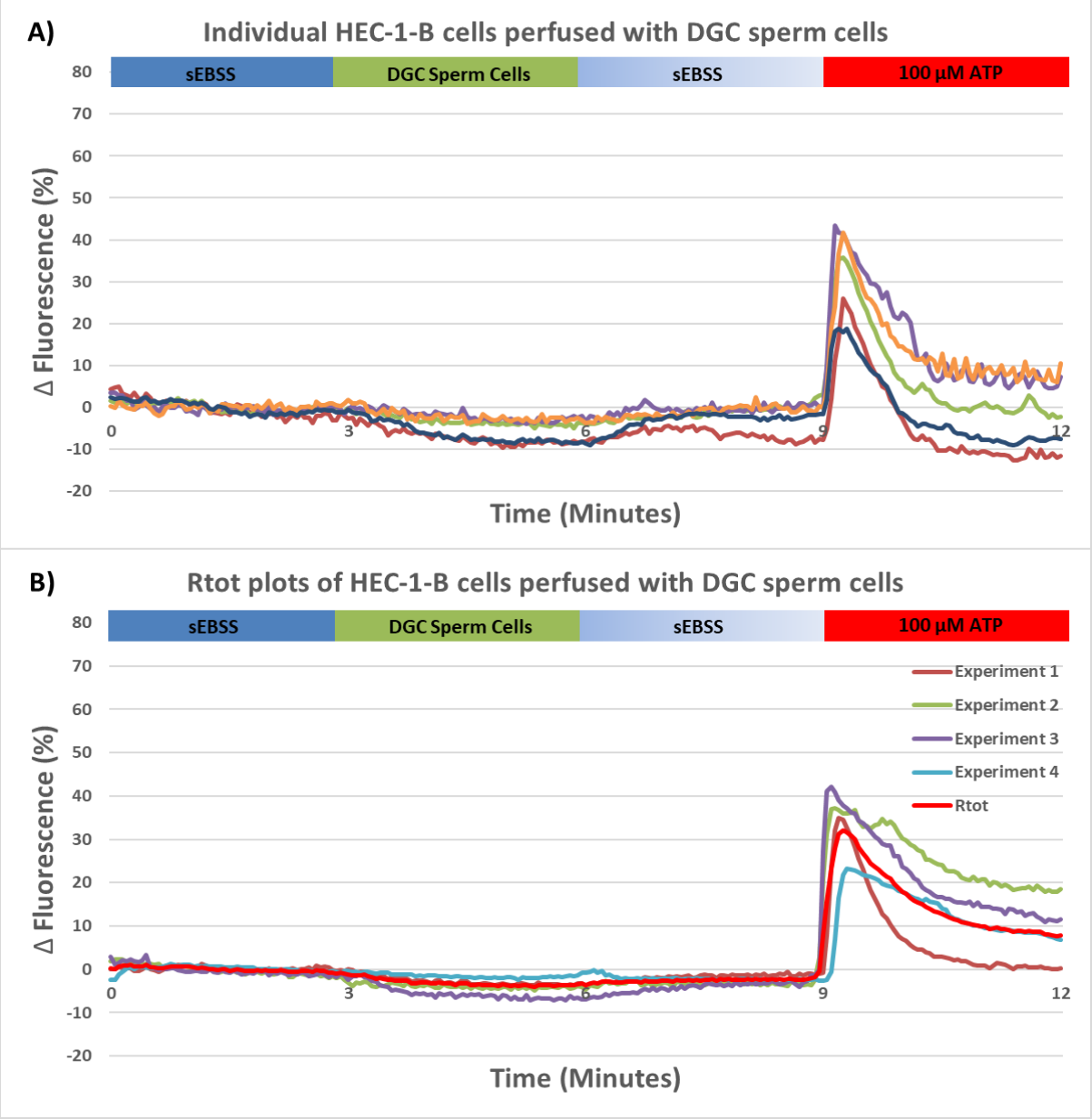


Figure 2.10- The effect of DGC sperm cell perfusion on $[Ca^{2+}]_i$ in HEC-1B cells. Cells were perfused with sEBSS for 3 minutes, then DGC sperm cells for 3 minutes, before a further 3 minutes sEBSS was period and finally 3 minutes of ATP positive control solution. (A) The fluorescence-time plot for 5 individual HEC-1B cells during a Ca^{2+} imaging timelapse experiment. (B) The Rtot plots for each of the 4 experiments carried out, with the overall Rtot plot for this series of experiments representing a total of 888 HEC-1-B cells highlighted in red.

A) Each of the 5 individual HEC-1-B cells in this plot exhibited a significant decrease in their fluorescence intensity upon the addition of DGC sperm cells to the perfusion

chamber in comparison to the fluorescence intensity observed during the initial 3 minute sEBSS perfusion control period. The observed fluorescence in each of the cells then increased as the sEBSS washoff period began before rising once again with a much larger peak upon the introduction of the ATP positive control stimulus to the chamber. B) The overall Rtot plot for this series of experiments shows that the response observed in the five individual HEC-1-B cells shown in figure 2.9A are largely representative of the total population of 888 cells tested under these conditions across 4 different experiments. An average of 93.97±3.6% of HEC-1-B cells showed a decrease in $[Ca^{2+}]_i$ in response to the addition of DGC sperm cells to the perfusion chamber, whilst only 0.8±0.64% of cells showed an increase during this period and 5.07±3.08% showed no change in their fluorescence. 66.59±24.55% of the cells then showed a rise in $[Ca^{2+}]_i$ at the beginning of the sEBSS washoff period and this was followed by 99.75±2.05% exhibiting a further rise in $[Ca^{2+}]_i$ in response to the ATP positive control stimulus. To assess the relative strength of the $[Ca^{2+}]_i$ response, the average maximum peak height observed during the period of DGC sperm cells perfusion in the HEC-1-B cells which were identified as exhibiting a rise in $[Ca^{2+}]_i$ during the initial period of stimulus perfusion was compared to the average maximum peak height observed during ATP positive control perfusion and expressed as a percentage. The average maximum stimulus peak height in this series of experiments was 12.9±2.9% of the average maximum peak height observed with exposure to the ATP solution. A full summary table of the responses observed during this series of experiments is displayed in appendix III.i.

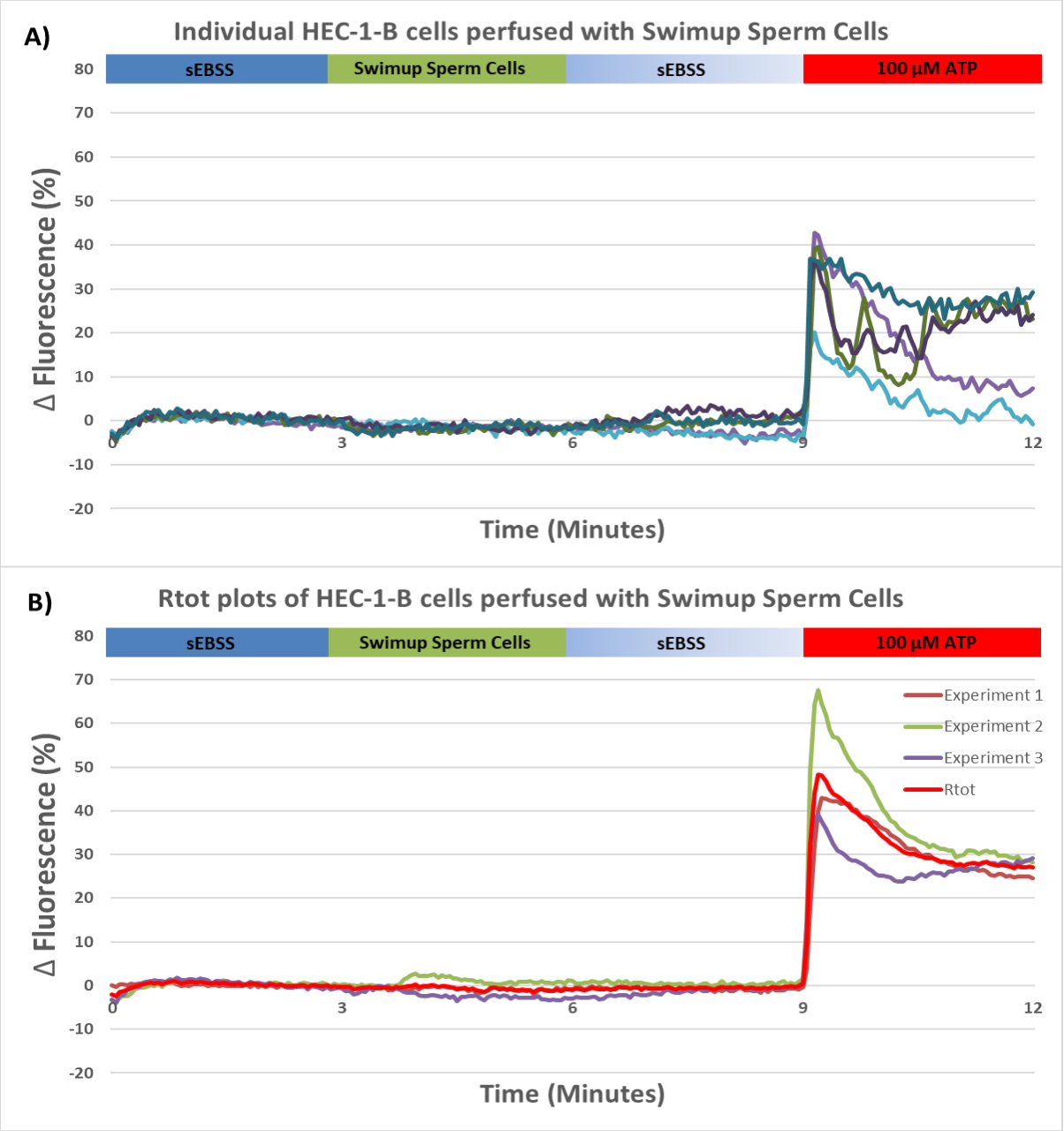


Figure 2.11- The effect of swimup sperm cell perfusion on $[Ca^{2+}]_i$ in HEC-1B cells. (A) The fluorescence-time plot for 5 individual HEC-1B cells during a Ca^{2+} imaging timelapse experiment in which they were perfused with sEBSS for 3 minutes, followed by swimup sperm cells for 3 minutes, washed with sEBSS for 3 minutes and then exposed to ATP positive control solution for 3 minutes. (B) The Rtot plots for each of the 3 separate experiments under these conditions with the overall Rtot plot for all 624 HEC-1-B cells highlighted in red.

A) The five individual HEC-1B cells shown as an example in the fluorescence-time plots from an experiment in which swimup sperm cells were perfused across their surface were not identified as showing any significant $[Ca^{2+}]_i$ response to the

perfusion of swimup sperm cells across their surfaces. They do however, all exhibit large peaks in $[Ca^{2+}]_i$ in response to the perfusion of the ATP positive control condition. B) The overall Rtot plot for 624 HEC-1B cells in Ca^{2+} imaging experiments with swimup sperm cell perfusion shows a clear trend of the cells not having a large response to swimup sperm cells, with 12.37±9.4% of cells exhibiting a rise in $[Ca^{2+}]_i$ during the initial period of stimulus perfusion, whilst 61.16±22% decreased and 26.86±13% showed no change. In contrast, 100-1.12% of the HEC-1-B cells were identified as having a rise in $[Ca^{2+}]_i$ when the ATP positive control solution was perfused across their surface. The average maximum stimulus peak height in HEC-1-B cells identified as responding to swimup sperm cell perfusion with an increase in $[Ca^{2+}]_i$ was 15.6±3.1% of the average maximum peak observed with ATP solution perfusion in the same cells. A full summary table of the responses observed during this series of experiments is displayed in appendix III.ii.

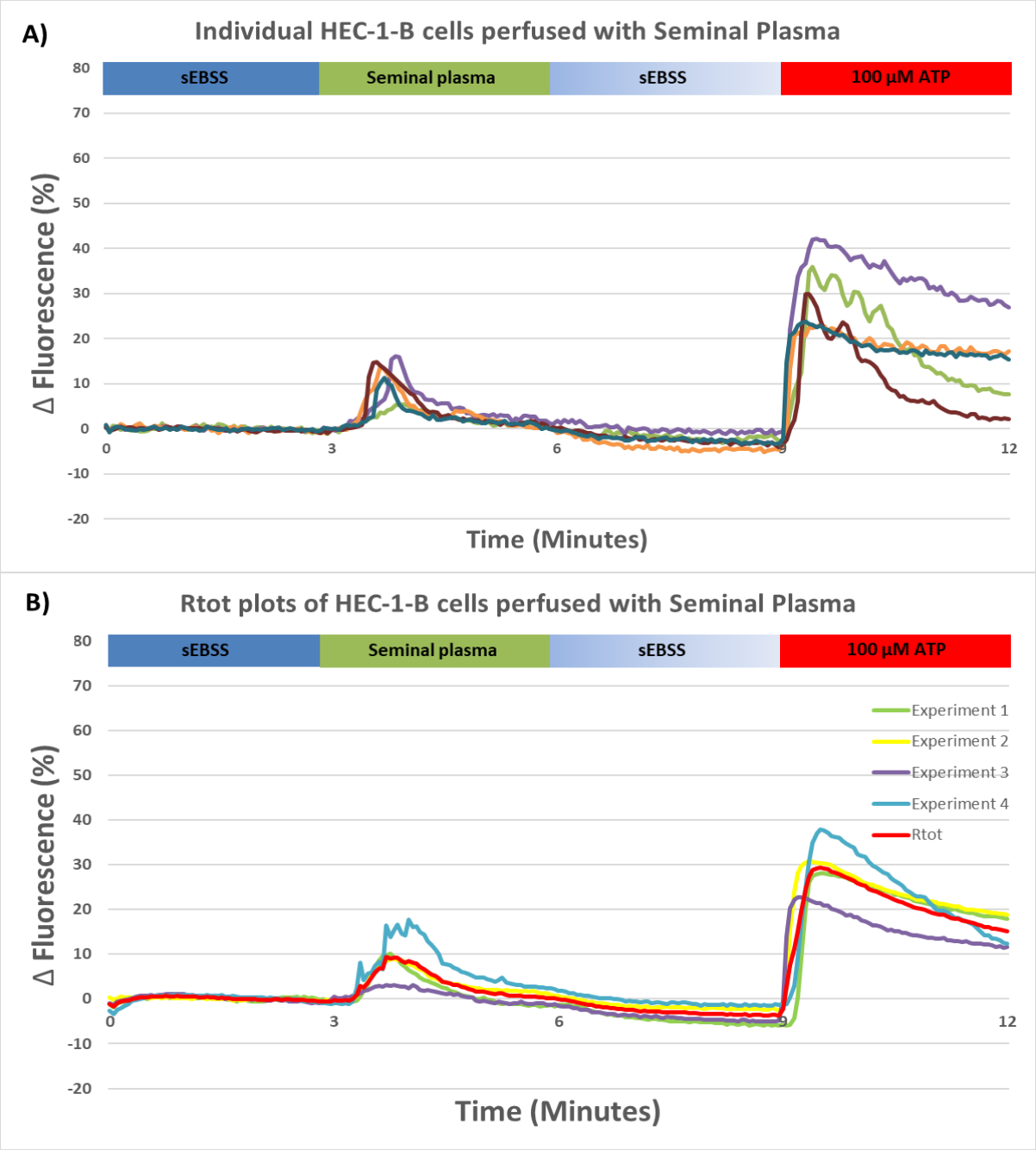


Figure 2.12- The effect of seminal plasma perfusion on $[Ca^{2+}]_i$ in HEC-1B cells. (A)The fluorescence-time plot for 5 individual HEC-1B cells during a Ca^{2+} imaging timelapse experiment in which they were perfused with sEBSS for 3 minutes, followed by seminal plasma for 3 minutes, washed with sEBSS for 3 minutes and then exposed to ATP positive control solution for 3 minutes. (B) The Rtot plots for each of the 4 separate experiments under these conditions with the overall Rtot plot for all 985 HEC-1-B cells highlighted in red.

Each of the five individual HEC-1B cells shown in the fluorescence intensity time plots shown in figure 2.11A were identified as exhibiting rises in $[Ca^{2+}]_i$ at the

beginning of the seminal plasma perfusion period. This rise forms a peak, after which the $[Ca^{2+}]_i$ decreases, but remains above the initial baseline levels, before being washed away during the proceeding period of sEBSS perfusion. Strong peaks are elicited by the ATP positive control condition in each of the cells. B) In all 4 of the experiments carried out with HEC-1B cells and semen perfusion, the Rtot plots clearly depict similar trends of significant rises in $[Ca^{2+}]_i$ in response to seminal perfusion. On average, 97.9±2.52% of the HEC-1-B cells were identified as having an increase in $[Ca^{2+}]_i$ in response to seminal plasma perfusion, with 0.2±0.29% showing a decrease and 1.61±2.37% showing no change in $[Ca^{2+}]_{i.}$ 99.8±0.29% of the cells then exhibited a decrease in $[Ca^{2+}]_{i.}$ as the sEBSS wash period began and 100% of the 985 cells assessed across this series of 4 experiments exhibited a rise in $[Ca^{2+}]_{i.}$ in response to the perfusion of the positive control ATP solution across their surface. The average maximum stimulus peak height in HEC-1-B cells identified as responding to seminal plasma perfusion with an increase in $[Ca^{2+}]_i$ was 39.8±2.4% of the average maximum peak observed with ATP solution perfusion in the same cells. A full summary table of the responses observed during this series of experiments is displayed in appendix III.iii.

2.3.7- OE-E6/E7 Ca^{2+} imaging experiments with stimulus perfusion

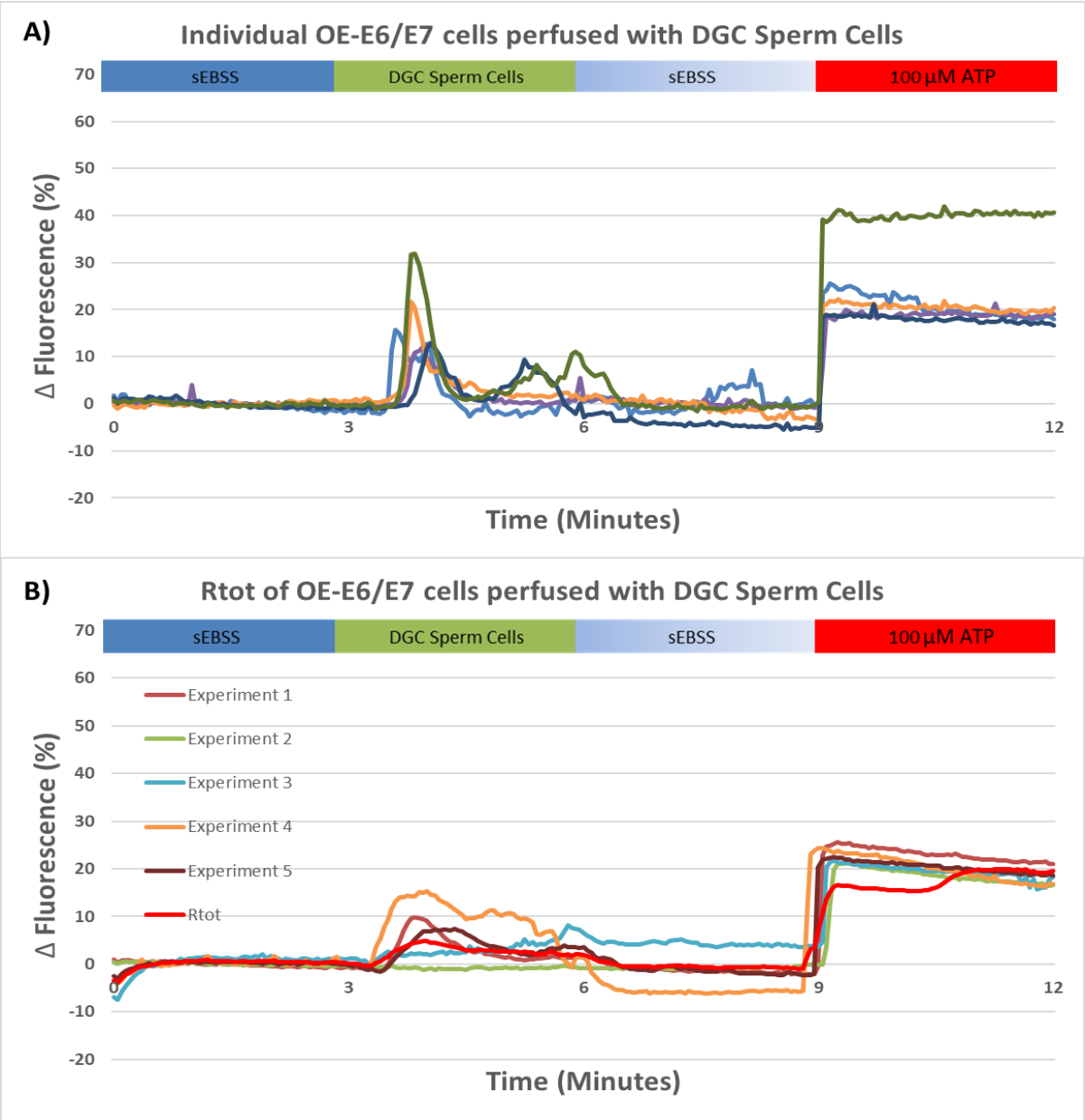


Figure 2.13- The effect of DGC sperm cell perfusion on $[Ca^{2+}]_i$ in OE-E6/E7 cells. (A)The fluorescence-time plot for 5 individual OE-E6/E7 cells during a Ca^{2+} imaging timelapse experiment in which they were perfused with sEBSS for 3 minutes, followed by DGC sperm cells for 3 minutes, washed with sEBSS for 3 minutes and then exposed to ATP positive control solution for 3 minutes. (B) The Rtot plots for each of the 5 separate experiments under these conditions with the overall Rtot plot for all 614 OE-E6/E7 cells highlighted in red.

A) The five individual OE-E6/E7 cells displayed in this timelapse plot were each identified as exhibiting a rise $[Ca^{2+}]_I$ in response to DGC sperm cell perfusion, with very strong $[Ca^{2+}]_i$ peaks as soon as stimulus perfusion begins. The initial peaks are

short lived, but in many cases are followed by weaker, secondary rises in $[Ca^{2+}]_i$. Most of the stimulus responses appear to be washed away during the perfusion of sEBSS, however, in some cases residual peaks are exhibited by cells even whilst DGC sperm cells are no longer being directly perfused across their surface. The OE-E6/E7 cells all exhibited very strong $[Ca^{2+}]_i$ responses to the ATP positive control perfusion. B) Across the 5 Rtot plots for the OE-E6/E7 experiments with DGC sperm cell perfusion, some variation in the types of $[Ca^{2+}]_i$ responses can be observed. Cell subsets in some experiments showed a stronger change in fluorescence in response to DGC sperm cell perfusion than others, with cells in experiment 2 appearing to show very little response to the stimulus. On average, 68.27±21.18% of the OE-E6/E7 cells in exhibited a rise in $[Ca^{2+}]_i$ in response to the perfusion of DGC sperm cells, whilst the fluorescence in 18.27±17.78% of the cells decreased and in 13.46±4.06% of cells there was no change. 100% of the OE-E6/E7 cells exhibited a rise in fluorescence in response to the ATP positive control condition. The average maximum stimulus peak height in OE-E6/E7 cells identified as responding to DGC sperm cell perfusion with an increase in $[Ca^{2+}]_i$ was 53.7±4.14% of the average maximum peak observed with ATP solution perfusion in the same cells. A full summary table of the responses observed during this series of experiments is displayed in appendix III.iv.

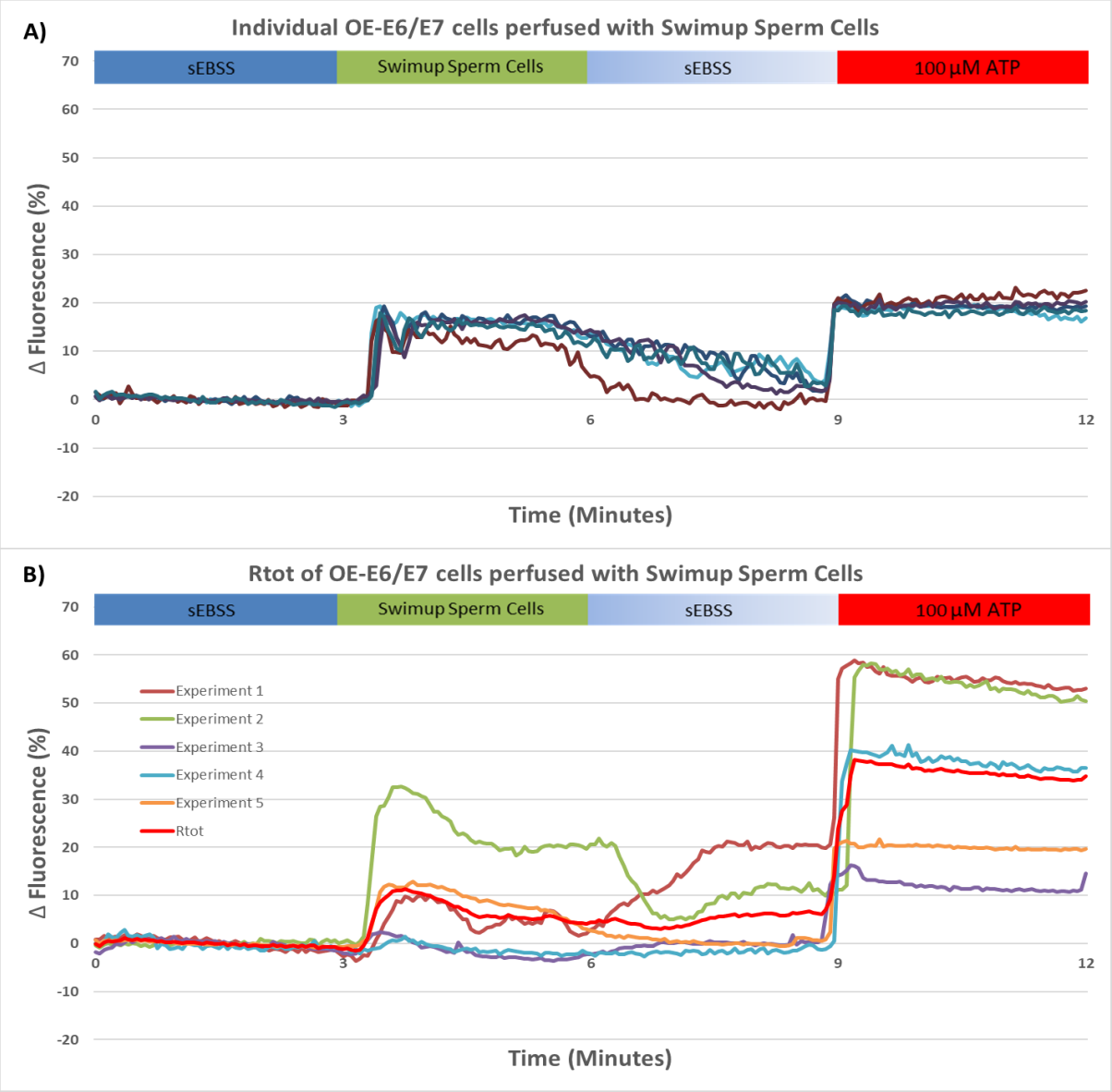


Figure 2.14- The effect of swimup sperm cell perfusion on $[Ca^{2+}]_i$ in OE-E6/E7 cells. (A)The fluorescence-time plot for 5 individual OE-E6/E7 cells during a Ca^{2+} imaging timelapse experiment in which they were perfused with sEBSS for 3 minutes, followed by swimup sperm cells for 3 minutes, washed with sEBSS for 3 minutes and then exposed to ATP positive control solution for 3 minutes. (B) The Rtot plots for each of the 5 separate experiments under these conditions with the overall Rtot plot for all 666 OE-E6/E7 cells highlighted in red.

A) Each of the five individual OE-E6/E7 cells shown in this average fluorescence intensity time plot exhibit a strong peak in $[Ca^{2+}]_i$ as soon as the perfusion of swimup sperm cells begins, the rise in $[Ca^{2+}]_i$ is sustained until the beginning of the sEBSS washoff period. During the washoff, $[Ca^{2+}]_i$ levels begin to decrease before the

addition of ATP positive control solution which causes a very strong, sustained peak in $[Ca^{2+}]_i$. B) The Rtot plots for each of the five experiments carried out on OE-E6/E7 cells with swimup sperm cell perfusion clearly demonstrate some level of response to swimup sperm cells in each of the experiments. Overall , 60.66±19.89% of the 666 OE-E6/E7 cells in this series of experiments were identified as showing a rise in $[Ca^{2+}]_i$ at the beginning of stimulus perfusion, whilst 26.23±12.87% decreased and 13.11±7.06% of them showed no change. An average of 100-0.71% of the cells exhibited a rise in $[Ca^{2+}]_i$ when the ATP positive control solution was perfused across their surface. The average maximum stimulus peak height in OE-E6/E7 cells identified as responding to swimup sperm cell perfusion with an increase in $[Ca^{2+}]_i$ was 57.5±3.05% of the average maximum peak observed with ATP solution perfusion in the same cells. A full summary table of the responses observed during this series of experiments is displayed in appendix III.v.

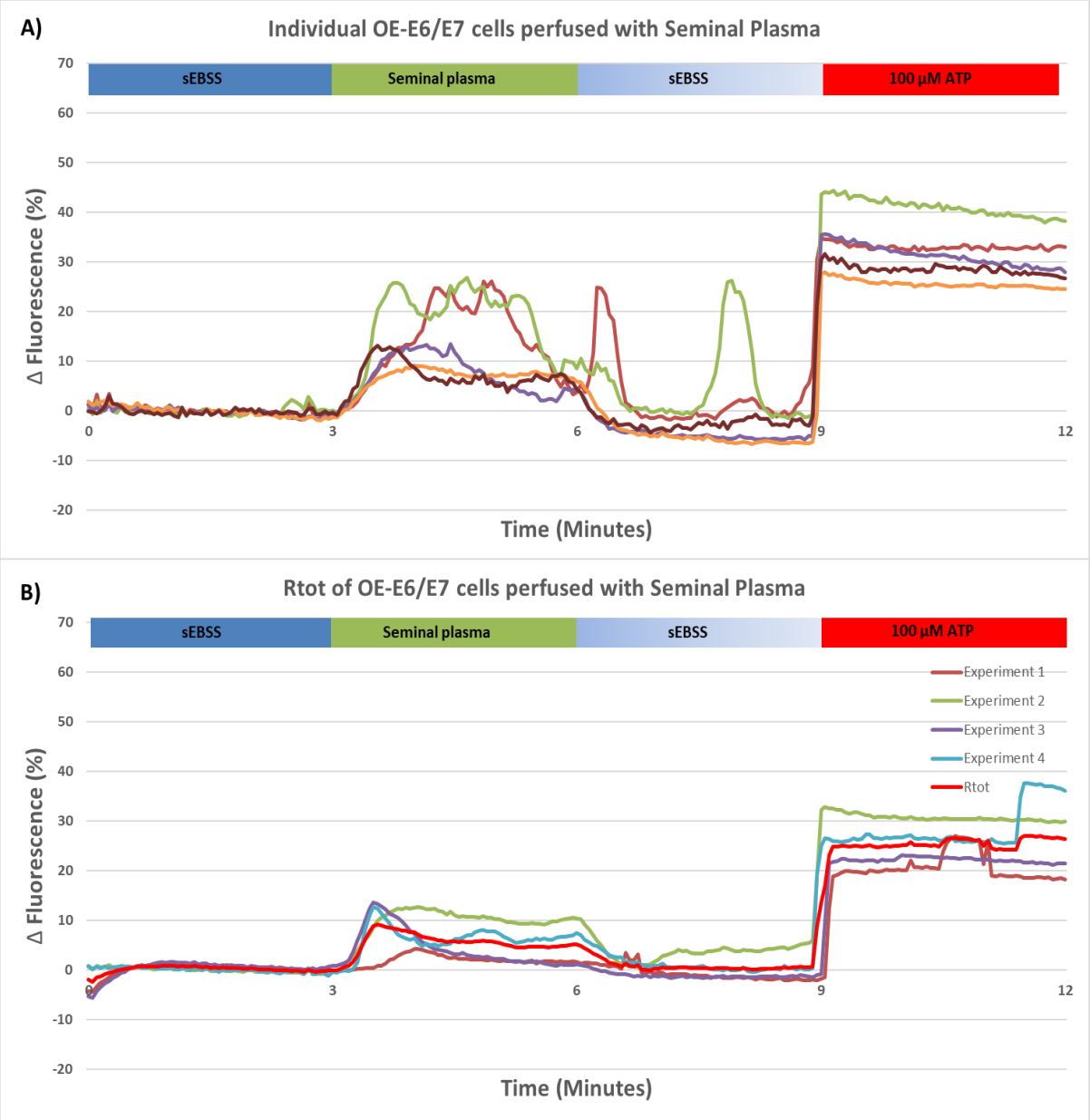


Figure 2.15- The effect of seminal plasma perfusion on $[Ca^{2+}]_i$ in OE-E6/E7 cells. (A)The fluorescence-time plot for 5 individual OE-E6/E7 cells during a Ca^{2+} imaging timelapse experiment in which they were perfused with sEBSS for 3 minutes, followed by seminal plasma for 3 minutes, washed with sEBSS for 3 minutes and then exposed to ATP positive control solution for 3 minutes. (B) The Rtot plots for each of the 4 separate experiments under these conditions with the overall Rtot plot for all 376 OE-E6/E7 cells highlighted in red.

A) Each of the 5 individual OE-E6/E7 cells in this timelapse plot show a clear rise in $[Ca^{2+}]_i$ at the beginning of seminal plasma perfusion across their surface. This initial peak was followed by secondary and tertiary peaks in some of the cells, whilst others exhibited a steady decline in $[Ca^{2+}]_i$ levels following their initial peak. The sEBSS

wash caused most cells to return to reduce in $[Ca^{2+}]_{i,}$ however, some cells exhibited additional peaks in $[Ca^{2+}]_i$ even whilst seminal plasma was no longer being directly perfused across their surface. All cells showed a rise in $[Ca^{2+}]_i$ in response to the ATP positive control condition. B) On average, 97.73±2.23% of the 376 OE-E6/E7 cells in this series of experiments were identified as exhibiting a rise in $[Ca^{2+}]_i$ in response to the addition of seminal plasma to the perfusion chamber, whilst 0±1.6% of the cells showed a decrease and 1.03±1.35% of cells showed no change. The perfusion of the ATP positive control stimulus was able to elicit a rise in $[Ca^{2+}]_i$ within 100% of the cells assessed in this series of experiments. The average maximum stimulus peak height in OE-E6/E7 cells identified as responding to seminal plasma perfusion with an increase in $[Ca^{2+}]_i$ was 50.6±3.73% of the average maximum peak observed with ATP solution perfusion in the same cells. A full summary table of the responses observed during this series of experiments is displayed in appendix III.vi.

2.3.8- COV434 cell Ca^{2+} imaging experiments with stimulus perfusion

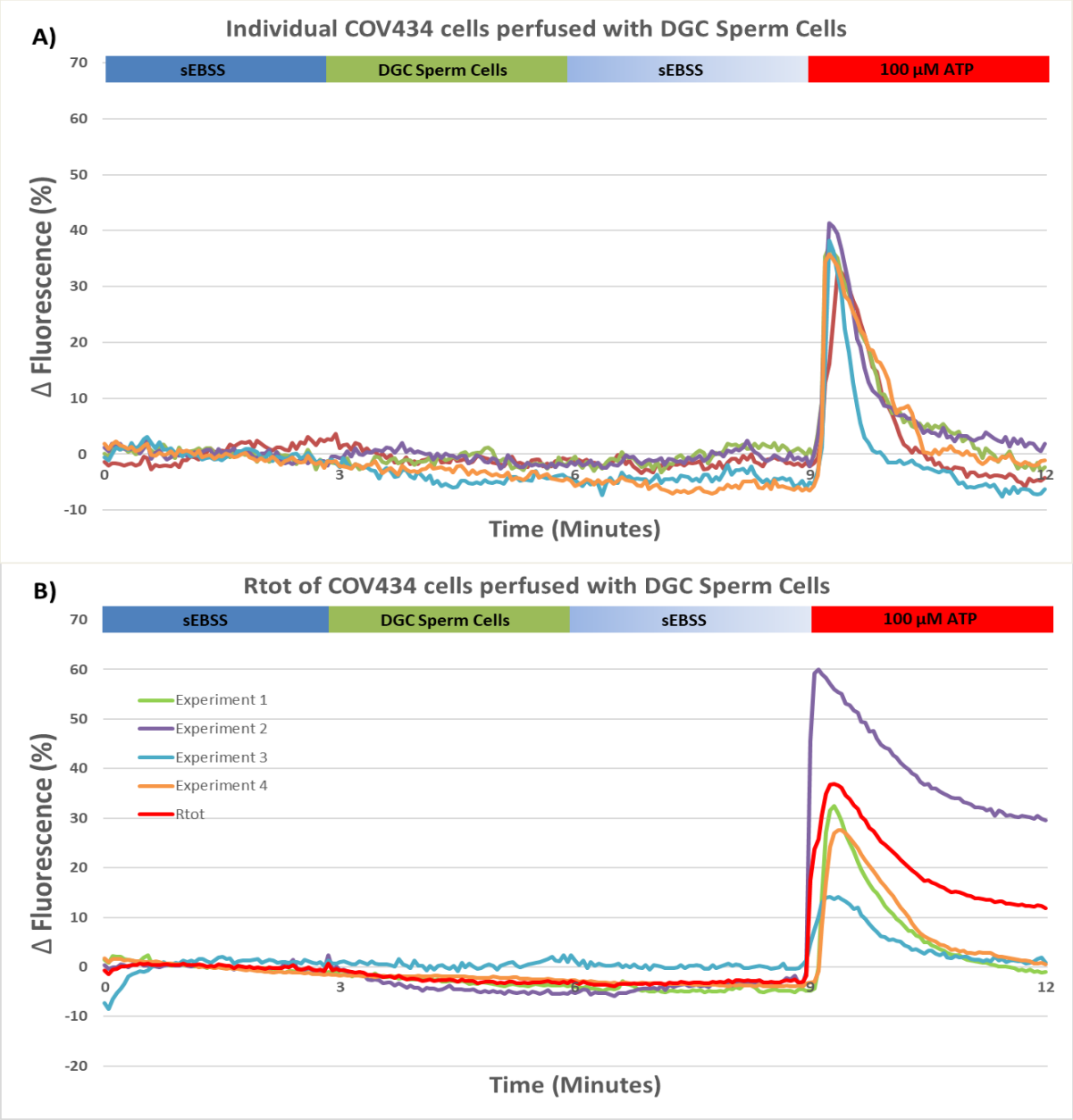


Figure 2.16- The effect of DGC sperm cell perfusion on $[Ca^{2+}]_i$ in COV434 cells. (A)The fluorescence-time plot for 5 individual COV434 cells during a Ca^{2+} imaging timelapse experiment in which they were perfused with sEBSS for 3 minutes, followed by DGC sperm cells for 3 minutes, washed with sEBSS for 3 minutes and then exposed to ATP positive control solution for 3 minutes. (B) The Rtot plots for each of the 4 separate experiments under these conditions with the overall Rtot plot for all 1372 COV434 cells highlighted in red.

To assess the impact of DGC sperm cells on intracellular Ca^{2+} signalling within COV434 cells, 4 perfusion timelapse experiments were carried out. A) Typical example responses of 5 individual COV434 cells within an experiment, in which none

of the cells exhibit a rise in $[Ca^{2+}]_i$ during DGC sperm cell perfusion, but all of them show a strong rise in $[Ca^{2+}]_i$ in response to ATP positive control perfusion. B) This graph shows the Rtot plots for the 4 separate experiments carried out under these conditions, as well as the overall Rtot plot. From the 1372 COV434 cells that were analysed in this series of experiments, 6.38±2.76% exhibited a rise in fluorescence when DGC sperm cells were perfused across their surface, whilst 78.55±16.18% showed a decrease and 15.07±13.71% exhibited no change during this period. The ATP positive control stimulus elicited a rise in $[Ca^{2+}]_i$ in 100±4.49% of the COV434 cells in these experiments. The average maximum stimulus peak height in COV434 cells identified as responding to DGC sperm cells perfusion with an increase in $[Ca^{2+}]_i$ was 20.2±14.4% of the average maximum peak observed with ATP solution perfusion in the same cells. A full summary table of the responses observed during this series of experiments is displayed in appendix III.vii.

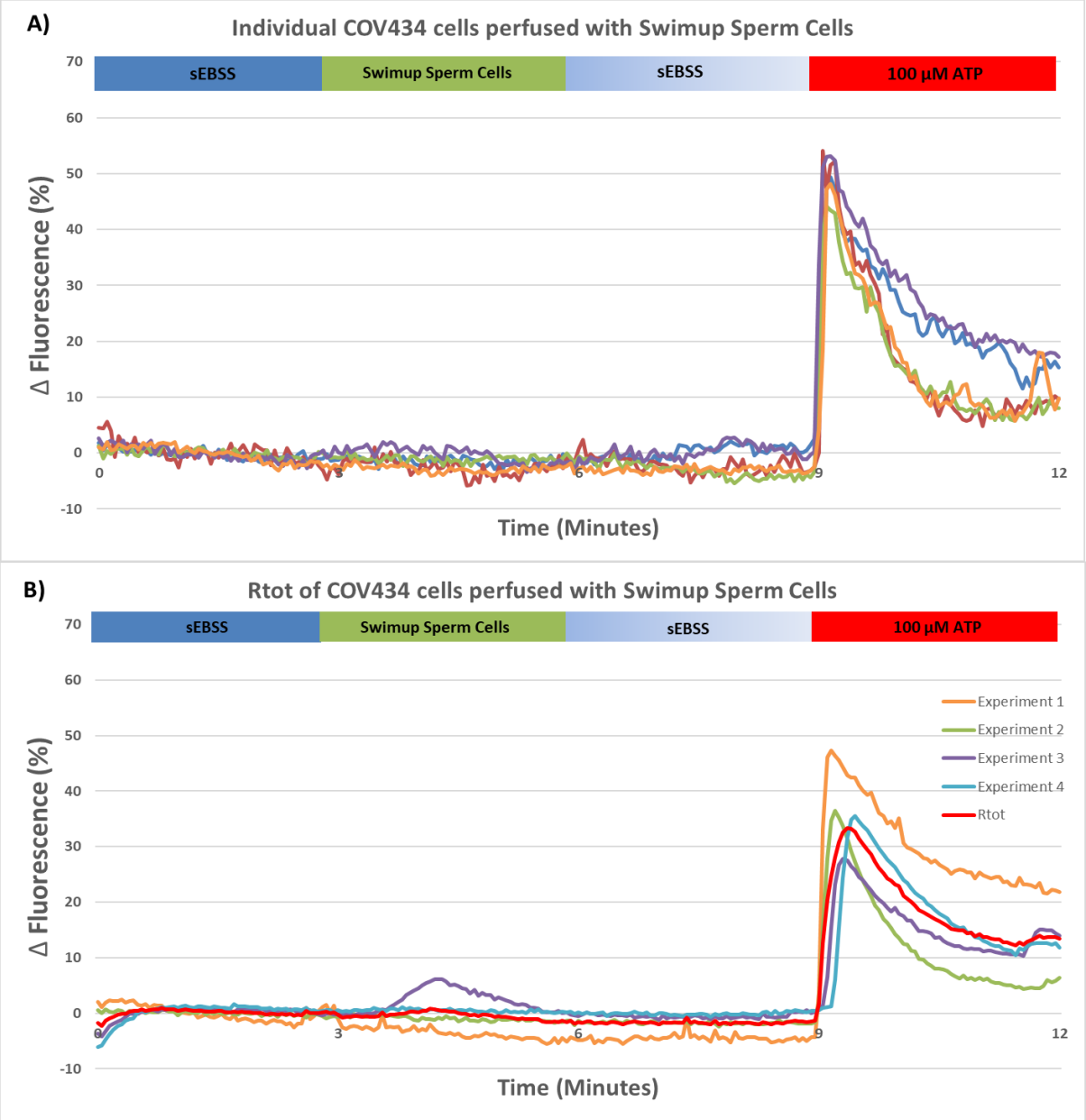


Figure 2.17- The effect of swimup sperm cell perfusion on $[Ca^{2+}]_i$ in COV434 cells. (A)The fluorescence-time plot for 5 individual COV434 cells during a Ca^{2+} imaging timelapse experiment in which they were perfused with sEBSS for 3 minutes, followed by swimup sperm cells for 3 minutes, washed with sEBSS for 3 minutes and then exposed to ATP positive control solution for 3 minutes. (B) The Rtot plots for each of the 4 separate experiments under these conditions with the overall Rtot plot for all 1213 COV434 cells highlighted in red.

The swimup sperm cell solution was assessed for its efficacy in eliciting $[Ca^{2+}]_I$ in COV434 cells, in total 1213 cells were analysed over a series of 4 experiments. A) Example $[Ca^{2+}]_i$ responses of 5 individual COV434 cells within an experiment, 3 of which were identified as showing no change in $[Ca^{2+}]_i$ in response to swimup sperm

cell perfusion, whilst 2 of them showed a slight decrease over the course of stimulus perfusion. Each of the cells exhibited a rise in $[Ca^{2+}]_i$ in response to ATP solution perfusion. B) The Rtot plots for the 4 separate experiments carried out under these conditions as well as the overall Rtot plot representing all COV434 cells in this series. An average of 25.91±14.48% of the cells in each experiment exhibited a rise in fluorescence upon the addition of swimup sperm cells to the perfusion chamber, whilst fluorescence in 40.72±18.35% of the cells decreased and 26.05±7.08% of the COV434 cells showed no change during this period. The perfusion of the ATP positive control stimulus elicited an increase in $[Ca^{2+}]_i$ in 100±0.24% of the cells in this series of experiments. The average maximum stimulus peak height in COV434 cells identified as responding to swimup sperm cells perfusion with an increase in $[Ca^{2+}]_i$ was 19.84±1.79% of the average maximum peak observed with ATP solution perfusion in the same cells. A full summary table of the responses observed during this series of experiments is displayed in appendix III.viii.

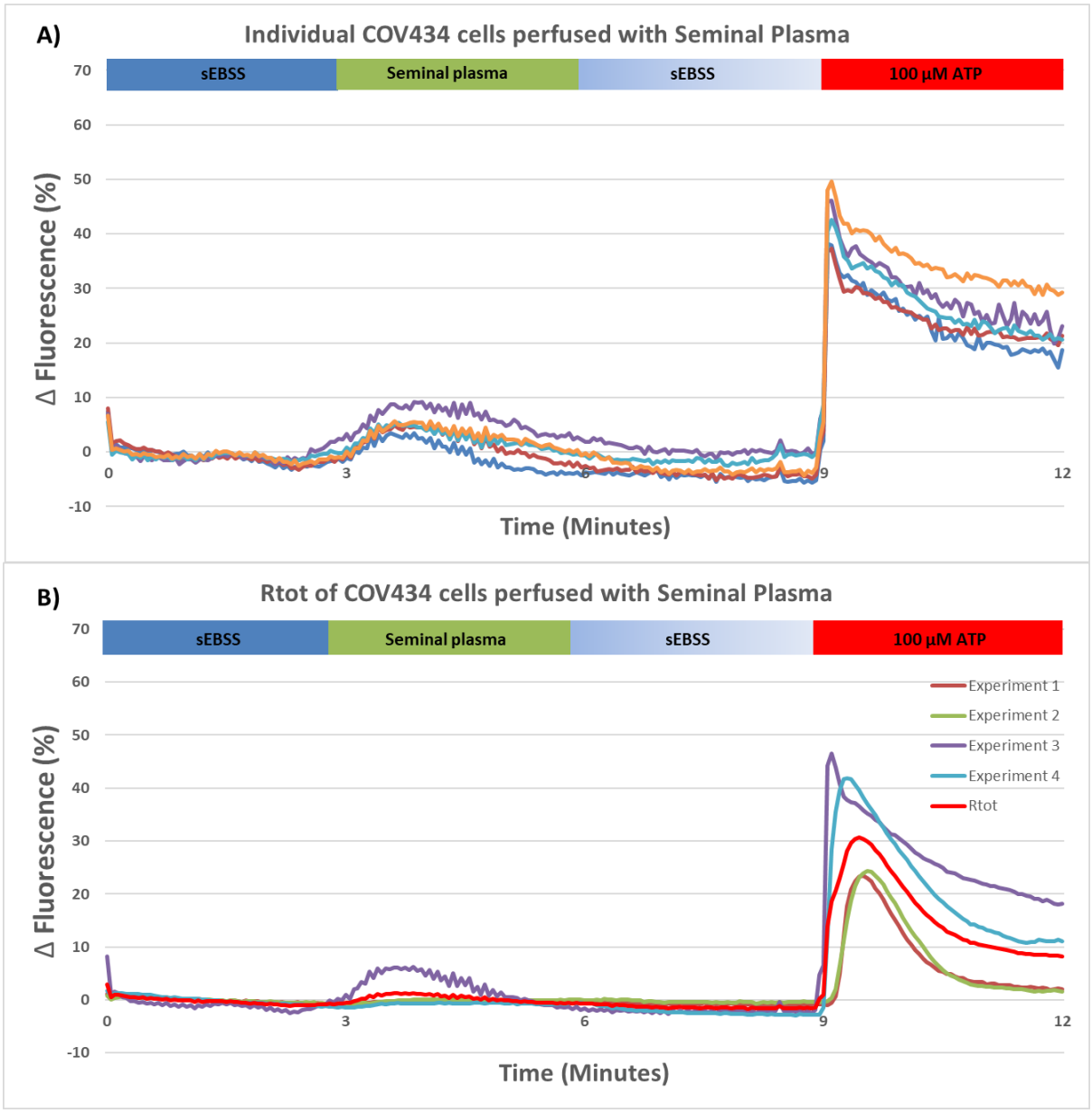


Figure 2.18- The effect of seminal plasma perfusion on $[Ca^{2+}]_i$ in COV434 cells. (A)The fluorescence-time plot for 5 individual COV434 cells during a Ca^{2+} imaging timelapse experiment in which they were perfused with sEBSS for 3 minutes, followed by seminal plasma for 3 minutes, washed with sEBSS for 3 minutes and then exposed to ATP positive control solution for 3 minutes. (B) The Rtot plots for each of the 4 separate experiments under these conditions with the overall Rtot plot for all 1261 COV434 cells highlighted in red.

To assess the presence of signalling factors within seminal plasma and their ability to elicit Ca^{2+} signalling in COV434 cells, a series of 4 perfusion timelapse experiments were carried out in which 1261 cells were individually analysed. A) The fluorescence intensity time plots for the 5 example individual COV434 cells in this

figure show each of them exhibit an increase in $[Ca^{2+}]_i$ in response to the beginning of seminal plasma perfusion across their surface. The rise in $[Ca^{2+}]_i$ is then decreased by the sEBSS was period, before the ATP positive control condition elicits a further rise in $[Ca^{2+}]_i$. B) It is clear from these plots at the COV434 cells $[Ca^{2+}]_i$ response rates to the perfusion of semen showed some inconsistency between experiments. In the overall Rtot plot for this series of experiments, there is a small rise in $[Ca^{2+}]_i$ observed at the beginning of semen perfusion, which is consequently washed away and followed by a much larger peak elicited by the ATP positive control. On average, 53.26±15.66% of cells exhibited an increase in fluorescence in response to seminal plasma perfusion, whilst 22.38±7.38% showed a decrease and there was no change observed in 24.37±8.35% of the cells during this period. 99.56±0.47% of cells in this series of experiments had a rise in $[Ca^{2+}]_i$ elicited by the ATP positive control stimulus. The average maximum stimulus peak height in COV434 cells identified as responding to seminal plasma perfusion with an increase in $[Ca^{2+}]_i$ was 10.03±5.8% of the average maximum peak observed with ATP solution perfusion in the same cells. A full summary table of the responses observed during this series of experiments is displayed in appendix III.ix.

2.3.9- Initial Ca^{2+} imaging experiments summary

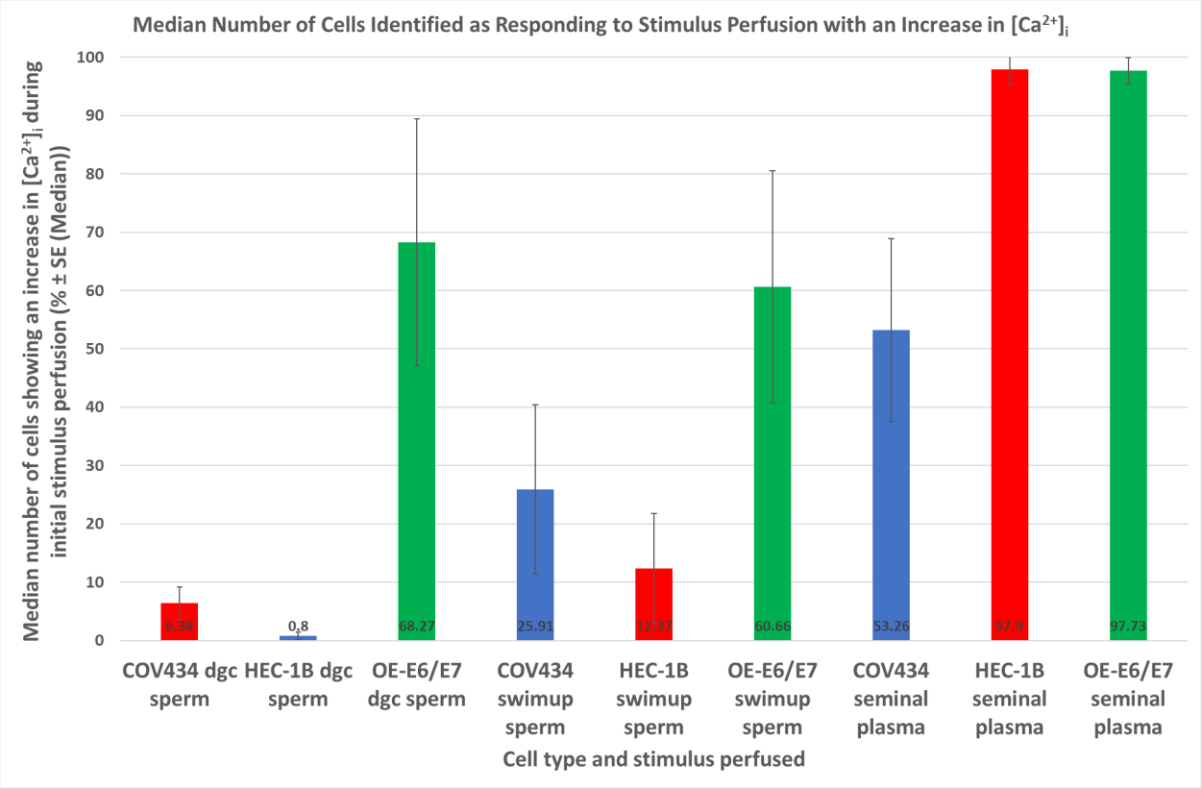


Figure 2.19- Bar chart of median average rates at which cells were identified as showing an increase in $[Ca^{2+}]_i$ during the initial period of stimulus perfusion (±SE (Median)) for each of the three cell lines and stimuli investigated.

To compare the relative rates of response to stimuli observed within each of the FRT cell lines investigated during this initial series of Ca^{2+} imaging experiments the median percentage of cells that were identified as showing an increase in Ca^{2+} during the initial period of stimulus perfusion were compared. Mann-Whitney U tests with Dunn's test as a correction for multiple comparisons were used to identify significant differences between the response rates. OE-E6/E7 cells responded at a significantly higher rate to the perfusion of DGC sperm cells than both COV434 cells ($P= 0.027$) and HEC-1B cells ($P= 0.014$), which both exhibited very low $[Ca^{2+}]_i$ response rates to this stimulus. The perfusion of swimup sperm cells elicited a rise in $[Ca^{2+}]_i$ within significantly higher numbers of OE-E6/E7 cells compared to HEC-1B

cells (P>0.002) but the difference between COV434 cells and the other cell lines was not significant with this stimulus (P=0.177). The perfusion of seminal plasma across the surface of the FRT cells elicited the strongest $[Ca^{2+}]_i$ response rates overall in all three cell lines, with no significant differences between any of the cell lines (P>0.05) The overall trend in the response rates to the three stimuli assessed appears to be DGC sperm cells eliciting the lowest $[Ca^{2+}]_i$ response rates, with swimup sperm cells eliciting more of a response in each cell line apart from OE-E6/E7 cells and seminal plasma perfusion causing the highest rates of $[Ca^{2+}]_i$ increase in all of the FRT cell lines assessed, respectively. The P values acquired from each comparison between cell lines and stimuli using Mann-Whitney U tests with Dunn's tests are included in appendix III.x.

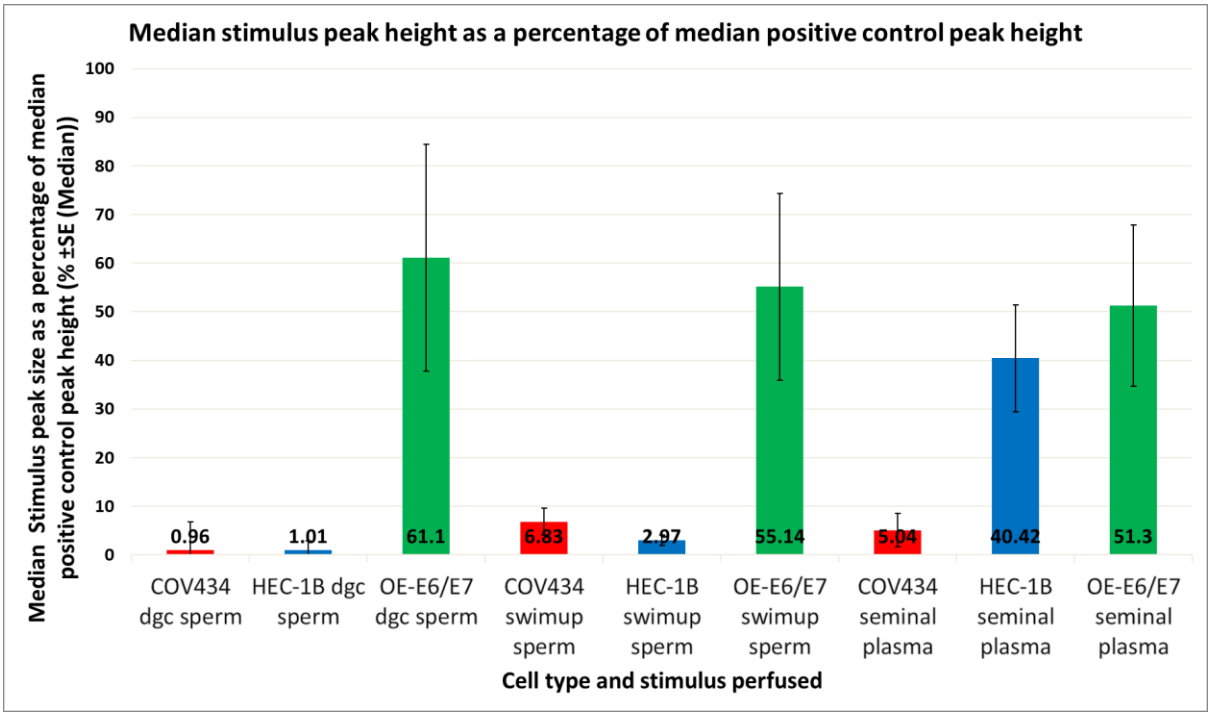


Figure 2.20- Bar chart of median maximum peak height during stimulus perfusion as a percentage of maximum peak height during positive control perfusion (±SE (Median)) for each of the three cell lines and stimuli investigated.

To compare the relative strength of the observed increased in $[Ca^{2+}]_i$ during the initial period of stimulus perfusion, peak heights were calculated by dividing the median maximum peak height observed during the initial period of stimulus perfusion across all of the cells in each Ca^{2+} imaging experiment, then dividing that by the median maximum peak height in the same cells that was observed during the perfusion of the ATP positive control condition and then multiplying the result by 100. This gave the maximum stimulus peak height as a percentage of the maximum positive control peak height, allowing for clear comparison of the relative strengths of the $[Ca^{2+}]_i$ responses that were observed across each of the FRT cell lines with each of the stimuli. Mann-Whitney U tests with Dunn's test as a correction for multiple comparisons were used to identify significant differences. Seminal plasma elicited a significantly stronger $[Ca^{2+}]_i$ response in OE-E6/E7 cells than COV434 cells (P=0.021) but the difference was not significantly different from the peak strength

observed in HEC-1B cells (P=0.773). HEC-1B cells which were perfused with seminal plasma a significantly stronger $[Ca^{2+}]_i$ response than any of the COV434 cell experiments (P=0.021). The differences between the three cell lines response strength to the DGC sperm cells and swimup sperm cell stimuli were not statistically significant (P>0.05). The P values acquired from each comparison between cell lines and stimuli using Mann-Whitney U tests with Dunn's tests are included in appendix III.xi.

2.4- Discussion

This series of Ca^{2+} imaging experiments set out to determine the presence of any $[Ca^{2+}]_i$ signalling events that could be elicited by three different semen sample preparations. The purpose of the different methods of preparation for the stimuli was to make an elementary attempt to determine the source of any candidate signalling factors within the male ejaculate.

- The seminal plasma condition, in which sperm cells were effectively filtered out from the media suspension, was designed to determine whether seminal fluid components were capable of eliciting signalling without the presence of spermatozoa (Bromfield 2014).
- The density gradient method of sperm cell preparation is a method of isolating motile, viable sperm cells from a sample by using centrifugal force to separate cells through a Percoll gradient, which has been demonstrated to significantly affect the spermatozoa proteome (Luppi, Martinelli et al. 2015).
- The swimup method of sperm cell isolation from a semen sample is a more gentle method of separation, in which motile spermatozoa swim freely into media, potentially carrying components of the seminal fluid loosely bound onto their surface membrane (Manjunath, Bergeron et al. 2007).

Each of the four cell lines cultured for this series of experiments adapted well to their culture media and were able to consistently reach confluence whilst maintaining their individual characteristics similar to those observed in the primary cells from which they were derived (Figure 2.3). Their adherence onto glass coverslips and subsequent staining with Calcium green-1 AM was successful and each of the cell lines exhibited staining which was sufficient for the measurement of $[Ca^{2+}]_i$ during the

course of experimentation, as none of them appeared to be oversaturated with fluorescence (figure 2.4).

Granulosa cells, from which the COV434 cell line is derived (Zhang, Vollmer et al. 2000), form a layer that surround the oocyte *in vivo* and play important roles in the process of fertilisation. The interactions between sperm cells and granulosa cells are complex and involve a wide range of cellular and molecular mechanisms. Granulosa cells are responsible for the production of hyaluronic acid (Salustri, Yanagishita et al. 1992), which attracts and binds to sperm cells via receptors on the plasma membrane in a process thought to play a role in sperm cell selection (West, Coomarasamy et al. 2022). The cells also produce factors such as progesterone, which facilitate the capacitation of sperm cells as they navigate their way towards the oocyte (Sumigama, Mansell et al. 2015). Sperm cells must pass through granulosa cells in the cumulus oophorus in order to reach the oocyte, which is achieved with hyperactivated sperm motility and the proteolytic action of hyaluronan-hydrolyzing enzymes derived from sperm cells (Kim, Yamashita et al. 2008), although the molecular mechanism by which sperm cells pass through these physical barriers has not been completely elucidated.

The COV434 cell line exhibited a significantly lower level of $[Ca^{2+}]_i$ response to the perfusion of DGC sperm cells across their surface than OE-E7/E7 cells, however, the rate at which COV434 cells were identified as exhibiting an increase in $[Ca^{2+}]_i$ in response to swimup sperm cells and seminal plasma was not significantly different from the other two FRT cell lines.cells. The absence of $[Ca^{2+}]_i$ signalling observed in the COV434 cells in response to DGC sperm cells suggests that the process of direct sperm cell contact with the granulosa cells is not an event which is upstream of $[Ca^{2+}]_i$ signalling events. The higher incidence of increases in $[Ca^{2+}]_i$ observed in

response to swimup sperm cells and seminal plasma perfusion suggests that signalling factors present in the seminal plasma, which could potentially be carried into the upper FRT by loosely adhering to sperm cells (Manjunath, Bergeron et al. 2007) are able to elicit $[Ca^{2+}]_i$ signalling in some of the COV434 cells. This is an interesting observation which has not currently been described in the literature, although the downstream effects of these interactions and their relevance to the process of fertilisation are not clear without further investigation.

HEC-1B cells are derived from endometrial epithelial cells (Kurarmoto, Hamano et al. 2002), which are known to undergo a range of interactions with sperm cells as they pass through the endometrium on their way to the site of fertilization (Ibrahim, Rizo et al. 2019). Murine models investigating the effect of sperm-endometrium interactions have demonstrated that factors present within the seminal plasma are capable of eliciting significant alterations to the endometrial receptivity pathway by upregulating the expression of genes such as LIF, VEGF, FGF2 (Ajdary, Zandieh et al. 2020).

The HEC-1B cells exhibited very low $[Ca^{2+}]_i$ response rates to the perfusion of DGC sperm cells and swimup sperm cells, which were both significantly lower than the rates observed in OE-E6/E7 cells. In one of the three experiments it does appear that a small subset of the cells exhibited a small rise in $[Ca^{2+}]_i$ during perfusion of the swimup sperm cells, potentially facilitated by contamination with seminal plasma, which elicited an increase in $[Ca^{2+}]_i$ in a significantly higher number of the HEC-1B cells than the other two stimuli. Due to the fact that fluctuations in $[Ca^{2+}]_i$ are known to be upstream regulators of alterations in gene expression (Puri 2020), the observed $[Ca^{2+}]_i$ signalling in the HEC-1B endometrial epithelial cell line in response to seminal plasma within this study is particularly interesting. It suggests that similar

mechanisms to those observed in animal models may be present in the human endometrium (Robertson 2007, Robertson and Sharkey 2016, Ajdary, Zandieh et al. 2020). It is important to note the key differences between murine and human FRT anatomy (Chumduri and Turco 2021) and the way in which the human cervix acts as a very effective barrier to prevent seminal plasma from reaching the upper FRT (Cunha, Sinclair et al. 2019), suggesting that factors derived from human seminal plasma would only interact with endometrial epithelial cells if they were carried by motile spermatozoa (Manjunath, Bergeron et al. 2007). The fact that swimup sperm cells were only able to elicit rises in $[Ca^{2+}]_i$ within a small number of HEC-1B cells suggests that the signalling factors present in the seminal plasma are unable to be effectively be transported by motile sperm cells in the majority of cases. Further investigation of the effects of seminal plasma mediated $[Ca^{2+}]_i$ signalling and its downstream effects on gene expression in human models would be interesting to see if similar mechanisms as those observed in murine models are preserved (Schjenken, Glynn et al. 2015).

The OE-E6/E7 cell line is derived from human secretory oviductal epithelial cells (Lee, Lee et al. 2001), which are known to play key functions in the regulation of the oviductal fluid proteome, the facilitation of fertilisation and the healthy early development of the embryo (Abe 1996). There is an abundance of evidence in the literature that male ejaculate derived factors interact with oviductal epithelial cells to significantly alter their function and secretory proteome in preparation for the arrival of an early embryo in the oviduct (Georgiou, Sostaric et al. 2005). The vast majority of studies describing these interactions are based on a range of animal models (Ellington, Ignotz et al. 1993, Thomas, Ignotz et al. 1995, Morales, Palma et al. 1996, Fazeli, Affara et al. 2004, Georgiou, Snijders et al. 2007, Kapelnikov, Zelinger et al.

2008, Bromfield, Schjenken et al. 2014, Ghersevich, Massa et al. 2015, Reshi, Viil et al. 2020) and of the three model FRT cell lines investigated in this study it is the oviductal epithelial cells for which the most evidence is available for the presence of direct interactions with sperm cell derived factors and the mechanisms of action underlying those interactions.

The OE-E6/E7 cell line to DGC sperm cells with an increase of $[Ca^{2+}]_i$ at a significantly higher rate than the other two cell lines tested. OE-E6/E7 cells also responded in significantly higher numbers to the perfusion of the swimup sperm cell stimulus than HEC-1B cells. Seminal plasma was capable of eliciting a similar response in the OE-E6/E7 cells to that observed in the other two cell lines. Whilst all of the cell lines responded in significant numbers to the perfusion of the seminal plasma stimulus and, to a lesser extent, the swimup sperm cells, the difference in response rates between the cells perfused with DGC sperm cells was statistically significantly higher OE-E6/E7 cells than the other two cell lines in which the response rate was negligible. This would suggest that the signalling factor responsible for eliciting $[Ca^{2+}]_i$ signalling in all of the FRT cell lines that were present in the seminal plasma and swimup sperm cell stimuli were different to the factors which were eliciting $[Ca^{2+}]_i$ signalling in the DGC sperm cell stimulus when OE-E6/E7 cells were exposed to it. This observation highlights the potential importance of utilising different methods of semen sample preparation in order to isolate specific proteomic subgroups and determine the specific source of any male ejaculate derived signalling factors.

The maximum peak height observed during the period of stimulus perfusion, when presented as a percentage of the maximum peak height observed during the perfusion of the ATP positive control condition was a useful parameter in determining

the overall strength of $[Ca^{2+}]_i$ responses across each of the cell types and stimuli. The results from this analysis show that the OE-E6/E7 cells had a higher strength of $[Ca^{2+}]_i$ response to each of the three stimuli tested in comparison to the COV434 and HEC-1B cells, although in the majority of cases these differences were not statistically significant. It was also clear that the use of 100 μM ATP solution in sEBSS was successful as a positive control condition, as it was capable of eliciting a very strong $[Ca^{2+}]_i$ response in the vast majority of all three of the FRT cell types and in each case the strength of response to the perfusion of the positive control condition across their surface was higher than any of the peaks in $[Ca^{2+}]_i$ stimulated by the semen sample preparations. In addition to ATP solution being an effective positive control in these experiments, it may also function as a measure of overall cell viability in experiments, as the ability of this molecule to elicit $[Ca^{2+}]_i$ signalling through the stimulation of the phospholipase C pathway to induce the release of Ca^{2+} from intracellular stores in the endoplasmic reticulum (Vanoverberghe, Mariot et al. 2003) is well documented.

The HFF cell line proved to unsuitable as a negative control for this series of Ca^{2+} imaging experiments. Initial results showed a tendency for the HFF cells to exhibit mechanosensitive properties as there were spontaneous $[Ca^{2+}]_i$ fluctuations in response to shear from the perfusion of any type of media across their surface. The mechanosensitivity of fibroblast cells is well established (Kim, Han et al. 2009), with some types of fibroblast even expressing mechanosensitive Ca^{2+} ion channel proteins such as Piezo1 (Stewart and Turner 2021), which would explain the observed signalling in these experiments. Due to this mechanosensitive response to the gentle perfusion of media across their surface, it was decided that the HFF cells

would no longer be used as a negative control cell line, however, these observations were interesting and may prove useful in future experiments.

These initial experiments made it clear that cell lines derived from the FRT are responsive to factors derived from the male ejaculate, as it has been clearly demonstrated that Ca^{2+} signalling can be elicited to varying extents in each of the three cell lines investigated. A key limitation of this study is the use of immortalised cell lines, although each of the cell lines used herein have been demonstrated to preserve many of the morphological and biochemical characteristics of the primary cells from which they were derived (Zhang, Vollmer et al. 2000, Lee, Lee et al. 2001, Kurarmoto, Hamano et al. 2002), it would be interesting to repeat these experiments using primary human cells. The benefits of using these cells lines in this instance are that they provide a pure population of cells, which is relatively easy to culture and bypasses many of the ethical concerns of acquiring primary human tissue from the FRT (Kaur and Dufour 2012).

The variation in response between the different types of semen sample preparations used as stimuli has highlighted the need for more intricate pathways of semen sample preparation to be developed in order to identify the specific source of this factor. The OE-E6/E7 cells were the only FRT cell line which exhibited substantial numbers of cells responding to the perfusion of DGC sperm cells being perfused across their surface. This suggests that signalling factors within the DGC sperm cell media is capable of exclusively eliciting $[Ca^{2+}]_i$ signals in the OE-E6/E7 cells and that this molecular mechanism is independent of the signalling observed in HEC-1B and COV434 cells with the seminal plasma and swimup sperm cell stimuli. For this reason, as well as the overall high response rates and strength of Ca^{2+} signalling

observed, the OE-E6/E7 cell line will be used as the primary candidate cell line for further experiments in the identification of signalling factors within the male ejaculate.

Chapter 3

The Source of Semen Signalling Factors Eliciting a $[Ca^{2+}]_i$ Response in Oviductal Epithelial Cells

3.1- Introduction

The previous chapter focused upon identifying the presence of $[Ca^{2+}]_i$ signalling in a range of cell lines derived from the FRT in response to various semen sample preparations. Although the cell lines exhibited varying levels of response to the stimuli, the oviductal epithelial cell line was robustly responsive to all three of the semen sample preparations tested. This suggested that this cell line was exquisitely sensitive and therefore an ideal candidate for further investigations into the identity of the male derived signalling factor that could potentially be interacting with the cells of the FRT. A more intricate pathway of semen sample preparation was designed to isolate individual sources of proteins and signalling factors within the male ejaculate, all of which were utilised as stimuli in further $[Ca^{2+}]_i$ imaging experiments on the oviductal epithelial cell line in order to narrow down the search for signalling factors.

The male ejaculate is a complex mixture, containing sperm cells suspended in secretions derived from the epididymis, testes, prostate gland and seminal vesicles (Brown 1956). The various components of human seminal fluid elicit protection and nourishment for spermatozoa as they are ejaculated and make their way throughout the FRT (Hopkins, Sepil et al. 2017). There are factors solubilised within seminal fluid that are bioactive and have been demonstrated to be capable of interacting with cells within the FRT (Robertson 2005), some of which have been shown to be carried on the surface of spermatozoa (Schjenken and Robertson 2014, Tecle, Reynoso et al. 2019). The majority of data regarding male ejaculate factors that interact with the cells of the FRT are derived from animal models, however, this data may not be directly translatable to human models due to key differences in both the

site of deposition and the composition of seminal fluid between species (Schjenken and Robertson 2020).

Whilst the molecular mechanisms of sperm cell and seminal fluid factor interactions with the cells of the human FRT are not clearly defined, clinical studies have demonstrated that seminal fluid exposure in human females has a direct impact on reproductive success (Robertson and Sharkey 2016). These effects on fecundity are apparent in studies on couples undergoing assisted reproductive therapies, in case where couples are lacking seminal fluid exposure there is a decreased rate of embryo implantation and successful pregnancies (Hart and Norman 2013, Crawford, Ray et al. 2015).

The site of semen deposition in humans is the ectocervix, in the anterior region of the vagina (Pudney, Quayle et al. 2005). The cervical mucus effectively acts as a filter, only allowing motile spermatozoa to leave the pool of seminal fluid and enter the cervical canal (Sobrero and Macleod 1962). From here, motile spermatozoa must travel through the uterus and into the oviduct to reach the site of fertilisation in the ampulla region (Coy, García-Vázquez et al. 2012). For a male ejaculate derived factor to be capable of directly interacting with epithelial cells in the oviduct, there are a limited selection of sources from which it could be derived. For example, it could be a protein that is present on the spermatozoa membrane surface proteome (Brewis and Gadella 2010), a component of the seminal fluid which is able to bind to the motile spermatozoa which make their way through the cervical canal (Tecle, Reynoso et al. 2019) or a signalling agent that is released as spermatozoa undergo capacitation and release the contents of the acrosome (Castillo, Bogle et al. 2019). The factor could originate from the extracellular vesicles present in seminal fluid, most of which are prostasomes (Aalberts, Stout et al. 2014) formed by the secretory

acinar cells in the prostate (Ronquist 2012), however, if this were the case then the contents of this vesicles would need to also be carried by motile spermatozoa into the oviduct.

The data presented in this study represent novel insights directly into the signalling mechanism by which spermatozoa communicate with the epithelial cells of female human reproductive tract. The observed $[Ca^{2+}]_i$ signalling in OE-E6/E7 cells show that a factor present in the male ejaculate is potentially capable of eliciting epigenetic changes in the human periconception environment, prior to the fertilisation of an oocyte (Puri 2020). This signalling and the factors responsible warrant further investigation to elucidate the specific mechanism of action, the identity of the factors responsible and the potential impact that this signalling may have on human fertility.

The next step in identifying the signalling factors responsible for the observed $[Ca^{2+}]_i$ oscillations was to investigate the efficacy of specific components of the male ejaculate by developing an intricate pathway of semen sample preparation methods to isolate different proteomic subgroups. Sperm cells could be isolated by the density gradient centrifugation method or alternatively by a gentler procedure of allowing the motile cells to swim up through viscous media, to more accurately simulate their passage through the cervical canal *in vivo* (Ivic 2002). Alterations could be made to the length of time that sperm cells were incubated in sEBSS to assess the effect of capacitation and the AR on the release of potential signalling factors (Castillo, Bogle et al. 2019). The removal of sperm cells from the media by filtration allowed for an investigation into the necessity of direct sperm cell binding to initiate the previously observed $[Ca^{2+}]_i$ oscillations. An intricate pathway of semen sample preparation methods was developed to identify the specific source of proteins or signalling factors from the male ejaculate in order to narrow down the list of candidate factors

that could then be identified with proteomic analysis. OE-E6/E7 cells had been selected as an ideal candidate cell line for further investigation using the same Ca^{2+} imaging experimental protocol described in the previous chapter. The efficacy of the various semen sample preparations in eliciting $[Ca^{2+}]_i$ oscillations within the OE-E7/E7 cells was assessed in order to identify a specific preparation method which effectively isolated signalling factors from the male ejaculate with the least amount of proteomic content to undergo proteomic analysis and develop a list of candidate factors to investigate.

3.2- Materials & Methods

3.2.1- Materials

0.2 µM PES syringe filters, (Corning). 100mm tissue-culture treated culture dishes, (Corning). 12mm round coverslips, (Warner instruments). 15 ml centrifuge tubes, (Falcon). 15 mL plastic disposable syringes, (ThermoFisher Scientific). 2 mm inner diameter translucent silicone tubing (Fisher Scientific). 22x32mm coverslips, (Appleton Woods). 25 cm^2 tissue culture flasks, (Falcon). 5 mL Round Bottom High Clarity PP Test Tubes, (Falcon). 7 5cm^2 tissue culture flasks, (Falcon). Adenosine-5'-triphosphate (ATP), (Sigma). Calcium Green-1 AM, (Invitrogen). Dulbecco's modified Eagle's medium (DMEM), no phenol red, (Gibco™). DMEM/F12, no phenol red, (Gibco™). Iscove's modified Dublecco's medium (IMDM), no phenol red, (Gibco™). DMEM/F12, no phenol red, (Gibco™). Foetal bovine serum, (Sigma-Aldrich). Methylcellulose, viscosity: 4000cP, (Sigma-Aldrich). PBS tablets, (ThermoFisher Scientific). Penicillin-Streptomycin (10,000 U/mL), (Gibco™). Pluronic F-127 10% in DMSO, (Sigma-Aldrich). PureSperm 40, (Nidacon). PureSperm 80 (Nidacon). Series 20 perfusion chambers, (Warner Instruments). Supplemented Modified Earle's balanced salt solution (sEBSS), (Lab Industries) (described in Appendix I). Trypsin-EDTA solution 10x, (Sigma-Aldrich.

3.2.2- Semen sample preparation pathway

Raw semen samples were acquired as described in section 2.2.4. An intricate pathway of semen sample preparation methods was developed in order to further isolate different sources of proteins and signalling factors within the male ejaculate. A total of 6 different stimuli for use in $[Ca^{2+}]_i$ imaging experiments could be produced from a single semen sample.

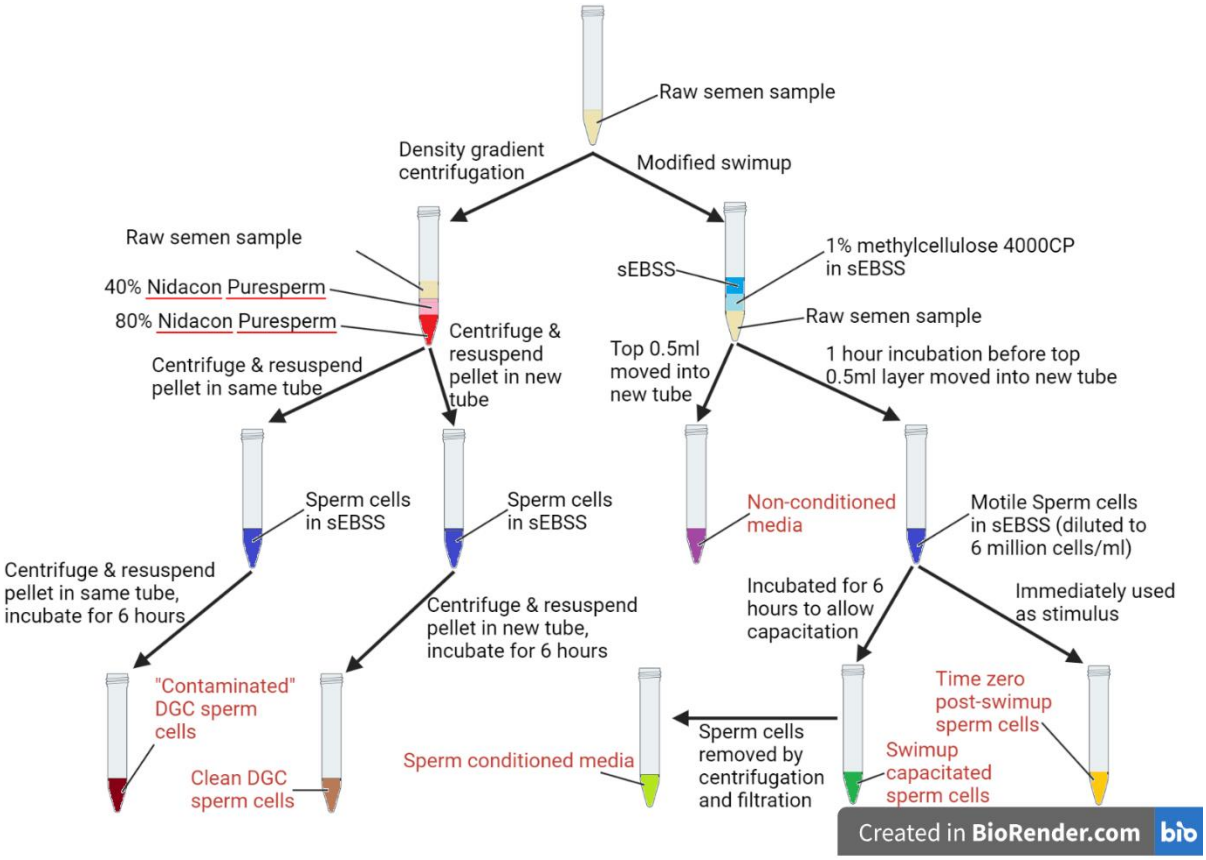


Figure 3.1- Schematic of the various semen sample preparation methods that were designed to isolate specific proteins and signalling factors within the male ejaculate in order to identify the ligand responsible for the observed $[Ca^{2+}]_i$ signalling in OE-E6/E7 cells.

3.2.2.1- Non-conditioned media: negative control condition

Non-conditioned media was the negative control condition designed for this series of experiments, the intention of this method of semen sample preparation was to show that the sEBSS solution itself was not capable of eliciting $[Ca^{2+}]_i$ signalling in the OE-E6/E7 cells, as well as ensuring that the other preparation methods used in these experiments did not cause unwanted contamination with seminal fluid or other potential signalling factors. Non-conditioned media was produced by carrying out a modified version of the swimup preparation method, in which raw semen sample was prepared as described in section 2.2.5, however an additional layer was added to the 5 mL Round Bottom High Clarity PP Test Tube in between the raw semen sample and the sEBSS. This additional layer consisted of 1% methylcellulose 4000CP which had been gently mixed into sEBSS in a cold room for at least 24 hours. This methylcellulose solution has previously been shown to be an effective and reproducible alternative to hyaluronic acid in sperm migration tests (Ivic 2002), therefore it was utilised as an additional layer in this modified swimup preparation for spermatozoa to swim through, as it would be a more accurate representation of a sperm cells journey *in vivo.* Rather than leaving the spermatozoa to migrate through the swimup tube over the course of an hour in a 37°C, 6% CO_2 incubator at a 45° angle, the top 0.5 ml layer of sEBSS was aspirated from the tube immediately upon the preparation of the modified swimup and this was the non-conditioned media. This was to ensure that no sperm cells were able to migrate through the methylcellulose solution into the non-conditioned media, meaning that this condition could act a negative control condition in $[Ca^{2+}]_i$ signalling experiments due to the fact it should not contain any male ejaculate derived proteins. This condition also acted as a control for seminal fluid contamination, as any response by the OE-E6/E7 cells to

this stimulus would suggest that the preparation of the modified swimup tube itself led to the presence of signalling factors within the non-conditioned media.

3.2.2.2- Time zero post-swimup sperm cells

The time zero post-swimup sperm cell stimulus was intended to contain signalling factors that spermatozoa would carry through the hyaluronic acid substitute (methylcellulose solution) via the modified swimup preparation method described in section 3.2.2.1. Rather than immediately removing the top 0.5 ml layer of sEBSS upon the preparation of the swimup tube, they were placed into a 37°C, 6% CO_2 incubator at a 45° angle for one hour to allow spermatozoa to migrate through the methylcellulose solution, carrying with them any signalling factors from the seminal fluid as they do *in vivo* (Suarez and Pacey 2005). Upon the completion of the one hour incubation period, the top 0.5 ml layer of sEBSS was aspirated into a new tube and immediately used as a stimulus in a $[Ca^{2+}]_i$ imaging experiment, before the spermatozoa were allowed enough time to undergo the process of capacitation and the AR, hence, this condition was referred to as the time zero post-swimup sperm cell stimulus.

3.2.2.3- Swimup capacitated sperm cells

The swimup capacitated sperm cells stimulus was prepared in the same way described in section 3.2.2.2, however, in this instance the time zero post-swimup sperm cell preparation was incubated for a further period of at least 6 hours in a 37°C, 6% CO_2 incubator in order to ensure the spermatozoa within the stimulus were able to undergo capacitation and the AR- releasing any signalling factors associated with this process into the media to form the swimup capacitated sperm cells stimulus.

3.2.2.4- Sperm conditioned media

The sperm conditioned media stimulus was prepared by removing any spermatozoa from the swimup capacitated sperm cell condition described in section 3.2.2.3. This was done by centrifuging an aliquot of the swimup capacitated sperm cell stimulus at 300 g for 10 minutes, the supernatant was then removed and then passed through a 0.22 µm syringe filter to ensure any spermatozoa were removed from the media. The resulting solution was the sperm conditioned media stimulus, consisting of any proteins, peptides and signalling factors that were present within the swimup capacitated sperm cell suspension, without any of the actual sperm cells or other cellular debris present.

3.2.2.5- Clean DGC sperm cells

The clean DGC sperm cells stimulus was produced by carrying out density gradient centrifugation on a raw semen sample, in the same way described in section 2.2.5.1. The sperm pellet formed after each centrifugation was apirated into a new falcon tube for each of the subsequent wash steps. This preparation method produced the stimulus referred to as clean DGC sperm cells, as the changing of Falcon tubes throughout the preparation ensured that no seminal plasma contamination was present in the final solution.

3.2.2.6- “Contaminated” DGC sperm cells

The “contaminated” DGC sperm cells stimulus was prepared in a similar fashion to the clean DGC sperm cells described in section 3.2.2.5, however, the same Falcon tube was used throughout each of the centrifugation steps. The purpose of this “contaminated” DGC sperm cell condition was to investigate the presence of seminal plasma contamination after the density gradient centrifugation method of semen sample preparation.

3.2.3- Preparation of OE-E6/E7 cells for $[Ca^{2+}]_i$ imaging

The oviductal epithelial cell line was cultured as described in section 2.2.2.3, the cells were then prepared for use in $[Ca^{2+}]_i$ imaging experiments as described in section 2.2.3, 2.2.4 and 2.2.7.

3.2.4- Ca^{2+} imaging of OE-E6/E7 cells whilst perfusing with semen sample preparations

The Ca^{2+} imaging experiments on OE-E6/E7 cells were carried out using the same methodology as described in section 2.2.7. For this series of experiments, the range of semen sample preparations described in section 3.2.2 were used as stimuli, whilst maintaining the 100 μM ATP in sEBSS solution as a positive control condition perfused across the surface of the OE-E6/E7 cells at the end of each experiment.

3.2.5- Statistical analysis of Ca^{2+} imaging timelapse data

The identification of cells exhibiting different types of $[Ca^{2+}]_i$ response to the perfusion of stimuli across their surface was carried out using the same statistical methods that were outlined in section 2.2.9.

3.3 Results

3.3.1- Variation in the kinetics of the OE-E6/E7 cell $[Ca^{2+}]_i$ response to stimuli

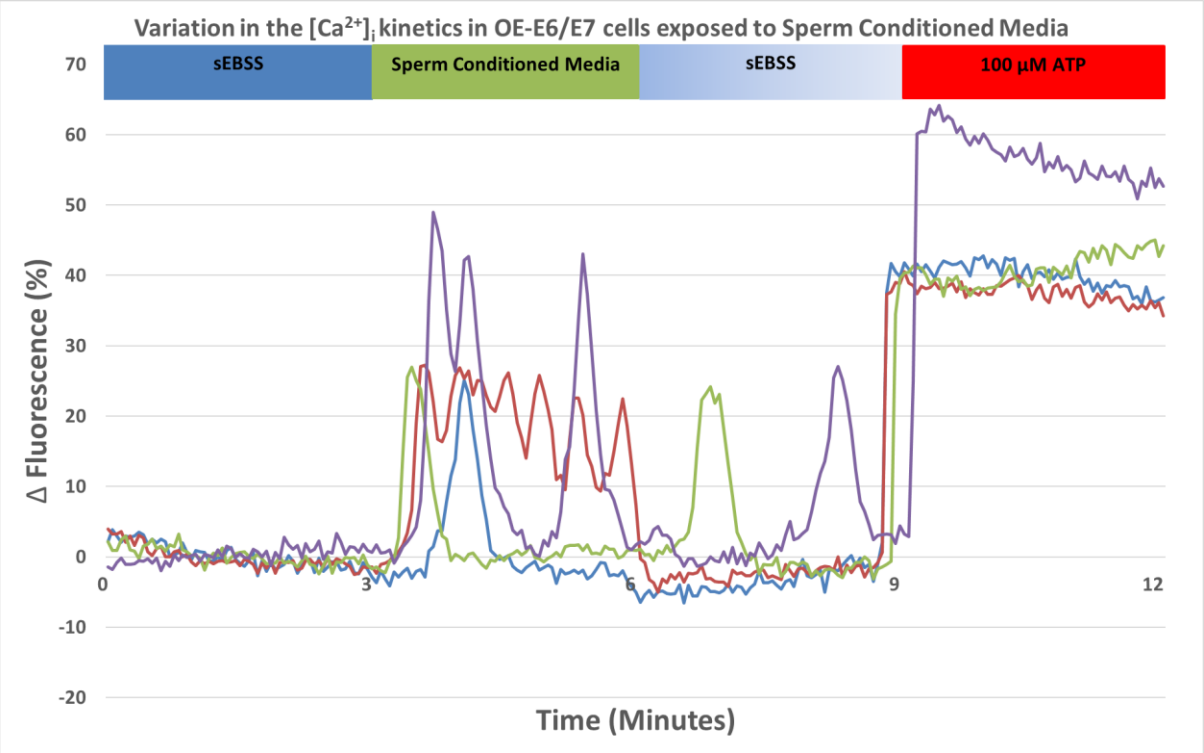


Figure 3.2- Fluorescence intensity time plots for 4 individual OE-E6/E7 cells imaged in a single experiment with sperm conditioned media perfused across their surface, highlighting the variation in the kinetics of the observed $[Ca^{2+}]_i$ signalling.

These four example plots for individual OE-E6/E7 cells over the course of a Ca^{2+} imaging experiment highlight the variation observed in the kinetics of the $[Ca^{2+}]_i$ signalling observed in response to exposure to sperm conditioned media. These fluorescence time plots are taken from an experiment in which the OE-E6/E7 were perfused with sEBSS for 3 minutes, then sperm conditioned media for 3 minutes, followed by a sEBSS washoff period and finally a 3-minute period of ATP positive control solution perfusion across their surface.

One of the cells by the red line plot in figure 3.2 exhibits an oscillating $[Ca^{2+}]_i$ response during the period of sperm conditioned media perfusion across its surface,

maintaining a raised level of observed fluorescence intensity throughout the period of stimulus perfusion. The cell represented by the blue line exhibits a single, sharp peak in $[Ca^{2+}]_i$ in response to the sperm conditioned media stimulus, whilst the cell represented by the green plot appears to have a transient initial peak in $[Ca^{2+}]_i$, before fading back to baseline levels of observed fluorescence and then exhibiting a secondary, short lived, sharp peak in $[Ca^{2+}]_i$ during the proceeding period of sEBSS wash perfusion. The cell represented in figure 3.2 by a purple line exhibited several separate $[Ca^{2+}]_i$ peaks in response to sperm conditioned media, one of which occurred during the consequent 3 minute sEBSS washoff period. It was typical throughout this series of experiments for individual cells to exhibit a wide range of $[Ca^{2+}]_i$ response kinetics, with no clear trend towards a specific type of peak being elicited by a particular stimulus.

3.3.2- Perfusion of OE-E6/E7 cells with non-conditioned media

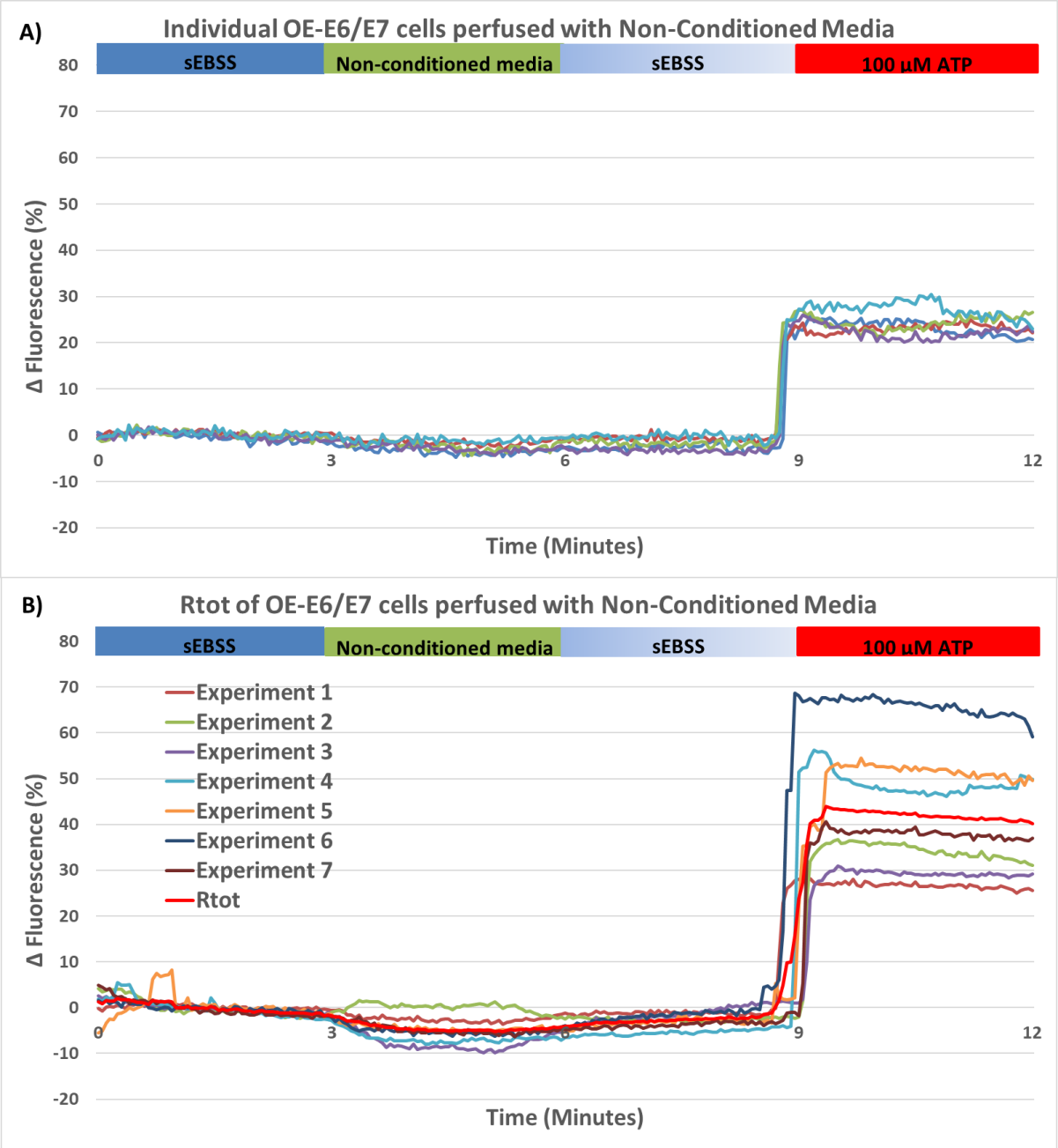


Figure 3.3- The effect of non-conditioned media perfusion on OE-E6/E7 cells. Cells were perfused with sEBSS for 3 minutes, then non-conditioned media for 3 minutes, before a further 3 minutes sEBSS wash period and finally 3 minutes of ATP positive control solution. (A) The fluorescence-time plot for 5 individual OE-E6/E7 cells during a Ca^{2+} imaging timelapse experiment. (B) The Rtot plots for each of the 7 experiments carried out, with the overall Rtot plot for this series of experiments representing a total of 1105 OE-E6/E7 cells highlighted in red.

To assess effectiveness of the modified swimup technique in preventing

contamination with seminal plasma, the efficacy of the non-conditioned media

negative control stimulus on the intracellular Ca^{2+} concentration within OE-E6/E7 cells, a series of 7 experiments were carried out. It is clear from the individual cell timelapse plots shown in figure 3.3A that the OE-E6/E7 cells were not responsive to the perfusion of non-conditioned media across their surface, however, they all exhibited strong, sustained rises in $[Ca^{2+}]_i$ as soon as the 100 μM ATP was introduced to the perfusion chamber. There is some variation in the responses observed to the negative control stimulus, as shown in figure 3.3B, with some of the experimental subsets of OE-E6/E7 CELLS exhibit small increases or decreases in $[Ca^{2+}]_i$ during the period of stimulus perfusion, however, these changes are small in comparison to the sharp rise in $[Ca^{2+}]_i$ in response to 100 μM ATP solution. On average, 1.64±13.77% of OE-E6/E7 cells were identified as exhibiting an increase in $[Ca^{2+}]_i$ during the initial period of non-conditioned media perfusion, whilst 96.17±15.92% decreased and 2.29±2.59% showed no change. In comparison, 100-0.41% of cells showed an increase in fluorescence in response to the introduction of the ATP solution to the perfusion chamber. The average maximum peak height in fluorescence during non-conditioned media perfusion was 2.72±2.29% of the peak height observed in the same cells during ATP solution perfusion. A full summary table of the responses observed during this series of experiments is displayed in appendix IV.i.

3.3.3- Perfusion of OE-E6/E7 cells with time zero post-swimup sperm cells

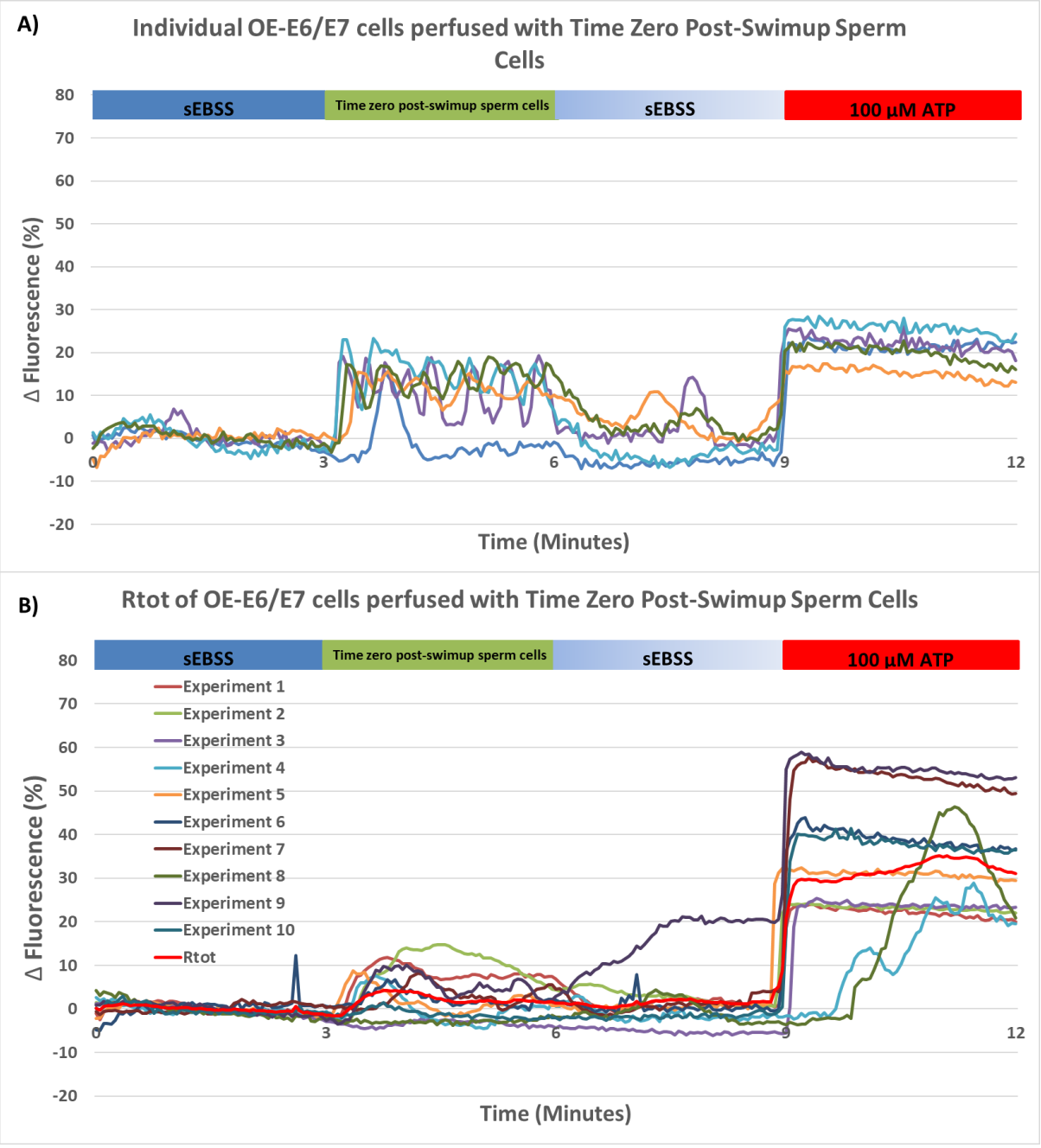


Figure 3.4- The effect of time zero post-swimup sperm cells perfusion on OE-E6/E7 cells. Cells were perfused with sEBSS for 3 minutes, then time zero post-swimup sperm cells for 3 minutes, before a further 3 minutes sEBSS wash period and finally 3 minutes of ATP positive control solution. (A) The fluorescence-time plot for 5 individual OE-E6/E7 cells during a Ca^{2+} imaging timelapse experiment. (B) The Rtot plots for each of the 10 experiments carried out, with the overall Rtot plot for this series of experiments representing a total of 1754 OE-E6/E7 cells highlighted in red.

To investigate the necessity of sperm cell capacitation on the presence of signalling factors, the efficacy of the time zero post-swimup sperm cells preparation in eliciting

Ca^{2+} in OE-E6/E7 cells was assessed across a series of 10 experiments. Timelapse plots for the individual OE-E6/E7 cells in figure 3.4A show a clear, strong rise in $[Ca^{2+}]_i$ levels upon the addition of time zero post-swimup cells to the perfusion chamber. In many cases, the $[Ca^{2+}]_i$ concentration appears to oscillate throughout the entire period of stimulus perfusion, although the kinetics of the response is not uniform across all 5 of the individual cells within this figure. For the most part, the increased levels of $[Ca^{2+}]_i$ begin to return to baseline levels as the period of sEBSS washoff begins. However, some of the cells still exhibit residual peaks in $[Ca^{2+}]_i$ throughout this period. A very sharp rise in $[Ca^{2+}]_i$ is observed across all of the cells upon perfusion of the 100 μM ATP positive control solution across their surface.

The introduction of time zero post-swimup sperm cells to the perfusion chamber elicited an increase in $[Ca^{2+}]_i$ in 36.23±12.65% of the OE-E6/E7 cells, whilst 27.32±10.99% decreased and 23.37±7.84 were identified as showing no change during this period, on average. 100-2.51% of the cells exhibited an increase in fluorescence upon the perfusion of the ATP solution across their surface. The average maximum peak height in fluorescence during time zero post-swimup sperm cells perfusion was 20.09±12.83% of the peak height observed in the same cells during ATP solution perfusion. A full summary table of the responses observed during this series of experiments is displayed in appendix IV.ii.

3.3.4- Perfusion of OE-E6/E7 cells with swimup capacitated sperm cells

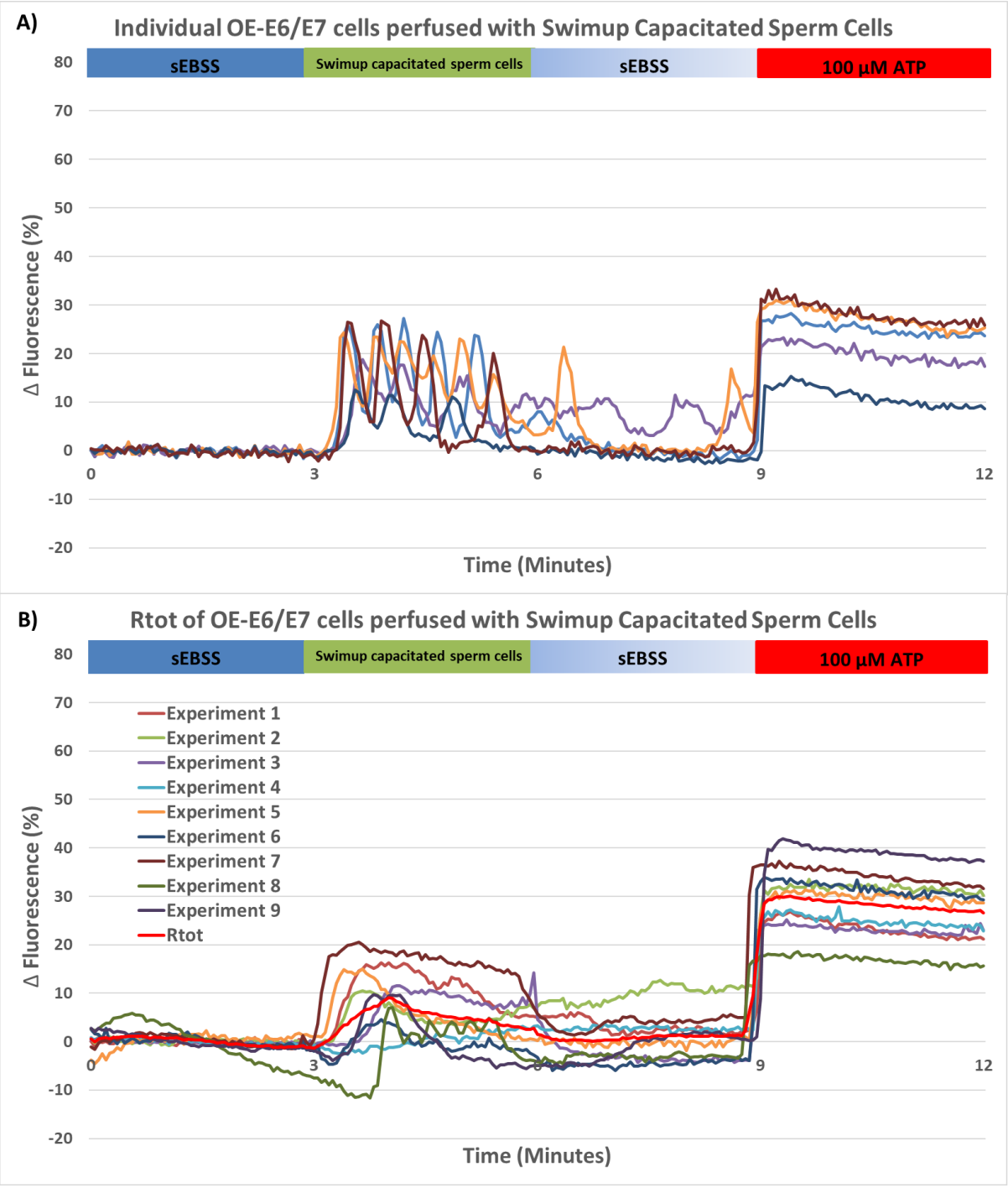


Figure 3.5- The effect of swimup capacitated sperm cells perfusion on OE-E6/E7 cells. Cells were perfused with sEBSS for 3 minutes, then swimup capacitated sperm cells for 3 minutes, before a further 3 minutes sEBSS wash period and finally 3 minutes of ATP positive control solution. (A) The fluorescence-time plot for 5 individual OE-E6/E7 cells during a Ca^{2+} imaging timelapse experiment. (B) The Rtot plots for each of the 9 experiments carried out, with the overall Rtot plot for this series of experiments representing a total of 1279 OE-E6/E7 cells highlighted in red.

To investigate the presence of signalling factors in media containing capacitated motile sperm cells which had swam through a viscous media in a modified version of the swimup preparation method a series of 9 experiments were carried out in which OE-E6/E7 cells were perfused with swimup capacitated sperm cells. The individual OE-E6/E7 cells represented in figure 3.5A each show a sharp rise in $[Ca^{2+}]_i$ upon the addition of swimup capacitated sperm cells to the perfusion chamber, which then oscillates throughout the period of stimulus perfusion at consistently higher $[Ca^{2+}]_i$ concentrations than were observed during the initial baseline period of sEBSS perfusion. This increased level of $[Ca^{2+}]_i$ was washed away by the subsequent period of sEBSS perfusion in most cases, however, some of the OE-E6/E7 cells exhibited further peaks in $[Ca^{2+}]_i$ despite the swimup capacitated sperm cells being gradually washed away. All of the cells showed a strong increase in $[Ca^{2+}]_i$ in response to the ATP positive control solution.

The Rtots for the different individual experiments in which OE-E6/E7 cells were perfused with swimup capacitated sperm cells displayed in figure 3.5B shows the variation between the strengths of the $[Ca^{2+}]_i$ response to the stimulus condition observed in the OE-E6/E7 cells. with some of the experimental subsets exhibiting much stronger, instantaneous peaks in $[Ca^{2+}]_i$ upon the introduction of the stimulus to the perfusion chamber, whilst others appear to have a slightly delayed or weaker $[Ca^{2+}]_i$ response. The variation is also apparent in the way in which the OE-E6/E7 cells respond to the sEBSS wash perfusion period following on from the stimulus, with some subsets of cells exhibiting a faster return to baseline levels of $[Ca^{2+}]_i$, whilst others appear to maintain their raised levels of $[Ca^{2+}]_i$ throughout this period. There is more uniformity however in the OE-E6/E7 cell response to the ATP positive control

stimulus, with which all of the experimental subsets of OE-E6/E7 cells exhibit a strong, sustained rise in $[Ca^{2+}]_i$ throughout this period of perfusion.

On average, 78.89±11.57% of the OE-E6/E7 cells were identified as showing a rise in fluorescence when swimup capacitated sperm cells were perfused across their surface, whilst 3.49±8.69% showed a decrease and 12.79±4.3% showed no change. 100-0.31% of the cells in this series of experiments responsed to exposure to the ATP solution with an increase in fluorescence. The average maximum peak height in fluorescence during swimup capacitated sperm cells perfusion was 37.46±11.5% of the peak height observed in the same cells during ATP solution perfusion. A full summary table of the responses observed during this series of experiments is displayed in appendix IV.iii.

3.3.5- Perfusion of OE-E6/E7 cells with Sperm Conditioned Media

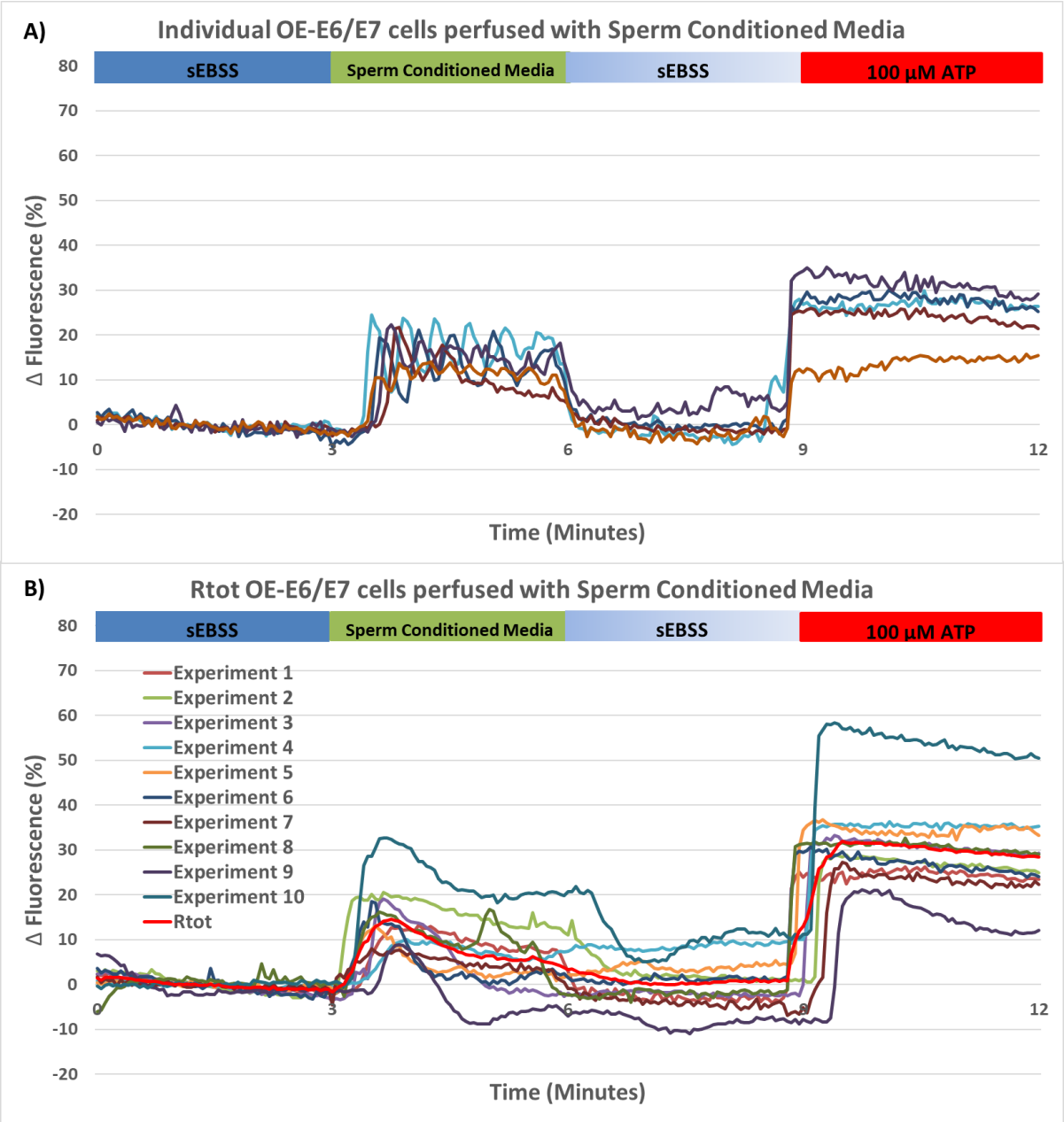


Figure 3.6- The effect of sperm conditioned media perfusion on OE-E6/E7 cells. Cells were perfused with sEBSS for 3 minutes, then sperm conditioned media for 3 minutes, before a further 3 minutes sEBSS wash period and finally 3 minutes of ATP positive control solution. (A) The fluorescence-time plot for 5 individual OE-E6/E7 cells during a Ca^{2+} imaging timelapse experiment. (B) The Rtot plots for each of the 9 experiments carried out, with the overall Rtot plot for this series of experiments representing a total of 1279 OE-E6/E7 cells highlighted in red.

To investigate whether the observed Ca^{2+} signalling relied upon direct contact with sperm cells or if the signalling factors responsible are solubilised in the media the

sperm conditioned media preparation was produced. A series of 10 Ca^{2+} imaging experiments were carried out in which OE-6/E7 cells were exposed to this stimulus. Each of the five average fluorescence intensity time plots for the individual OE-E6/E7 cells in figure 3.6A show that the cells have a steady level of baseline $[Ca^{2+}]_i$ during the initial 3 minutes of sEBSS perfusion, with each of them exhibiting a sharp rise in $[Ca^{2+}]_i$ upon the addition of sperm conditioned media to the perfusion chamber. The OE-E6/E7 cells tend to exhibit an oscillatory response to this stimulus, maintaining increased levels of $[Ca^{2+}]_i$ throughout the entire 3 minute period of stimulus perfusion, which is then very quickly washed away during the following 3 minutes of sEBSS perfusion. Most of the cells appear to return to baseline levels of $[Ca^{2+}]_i$ during this sEBSS wash period, with one of the five cells maintaining slightly elevated level of $[Ca^{2+}]_i$. All of the OE-E6/E7 cells represented in this plot had a strong, sustained $[Ca^{2+}]_i$ response to the ATP positive control solution.

The type of $[Ca^{2+}]_i$ responses observed in these individual cells appears to be mirrored in each of the 10 Rtot plots for each individual experiment in this subset shown in figure 3.6B. The OE-E6/E7 experimental subsets show a strong initial peak in response to sperm conditioned media perfusion, which then gradually tapers off as the $[Ca^{2+}]_i$ within the cells oscillate prior to the beginning of the sEBSS wash period of perfusion, in which most the cells appear to return to baseline levels of $[Ca^{2+}]_i$ in the majority of experiments. Some experimental subsets do appear to maintain $[Ca^{2+}]_i$ levels slightly above baseline levels during this sEBSS wash period, however, all of them show a strong response to the ATP positive control which is maintained throughout the rest of the perfusion timelapse. On average, 92.28±4.79% of the cells were identified as showing an increase in $[Ca^{2+}]_i$ in response to exposure to the sperm conditioned media, whilst 3.51±3.29% showed no change and 2.13±1.93%

showed a decrease in fluorescence. 100-0.22% of the OE-E6/E7 cells showed an increase in fluorescence in response to the ATP solution. The average maximum peak height in fluorescence during sperm conditioned media perfusion was 48.08±8.34% of the peak height observed in the same cells during ATP solution perfusion. A full summary table of the responses observed during this series of experiments is displayed in appendix IV.iv.

3.3.6- Perfusion of OE-E6/E7 cells with Clean DGC sperm cells

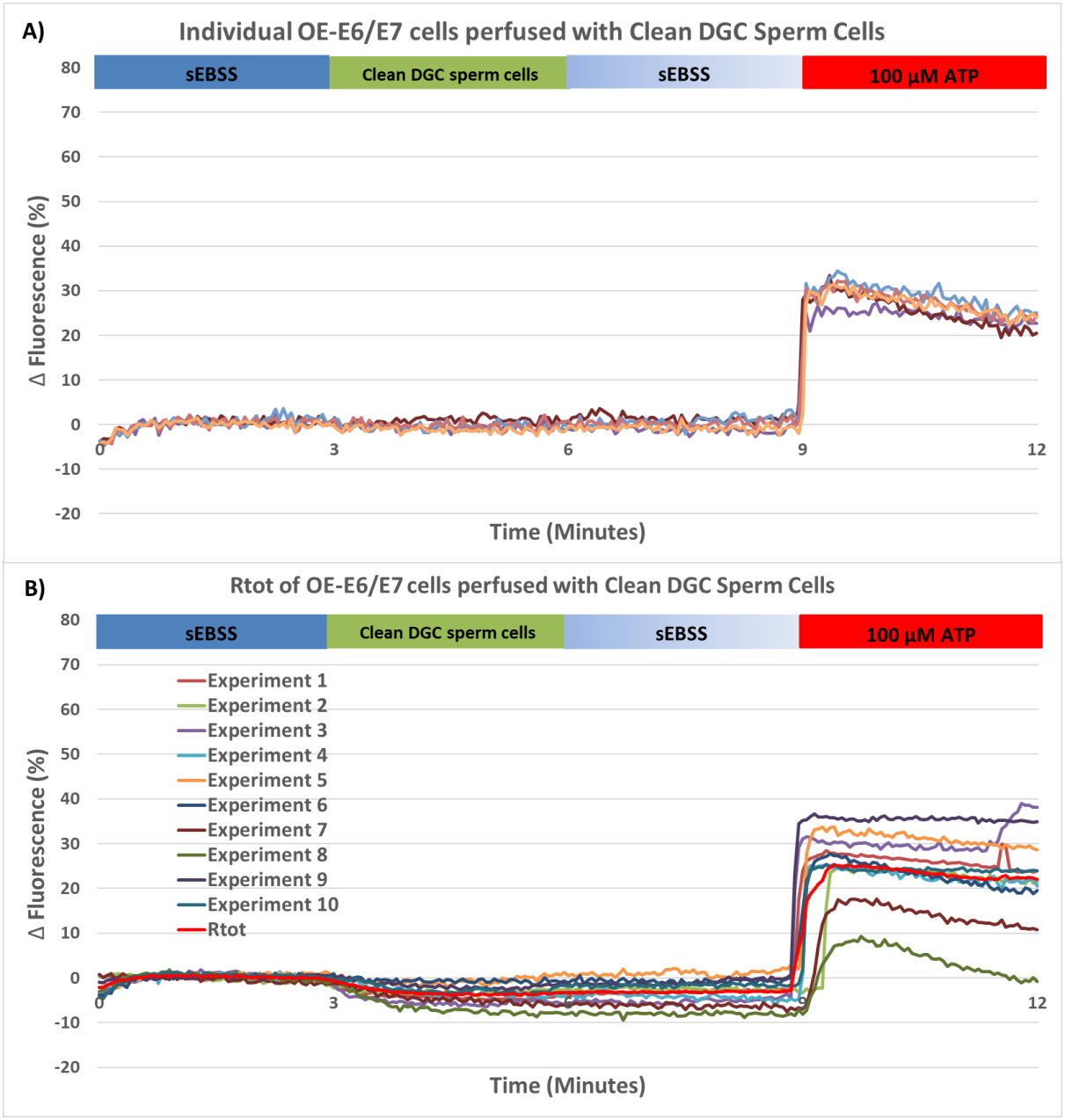


Figure 3.7- The effect of clean DGC sperm cells perfusion on OE-E6/E7 cells. Cells were perfused with sEBSS for 3 minutes, then clean DGC sperm cells for 3 minutes, before a further 3 minutes sEBSS wash period and finally 3 minutes of ATP positive control solution. (A) The fluorescence-time plot for 5 individual OE-E6/E7 cells during a Ca^{2+} imaging timelapse experiment. (B) The Rtot plots for each of the 10 experiments carried out, with the overall Rtot plot for this series of experiments representing a total of 1317 OE-E6/E7 cells highlighted in red.

To investigate the effect of using a clean tube between each step of the density gradient centrifugation preparation method in order to ensure that no seminal plasma

contamination is present, a series of 10 experiments were carried out in which OE-E6/E7 cells were perfused with clean DGC sperm cells. Each of the five fluorescence intensity timelapse plots for individual OE-E6/E7 cells perfused with Clean DGC sperm cells shown in figure 3.7A show a distinct lack of $[Ca^{2+}]_i$ response to the perfusion of this stimulus across the surface of the cells. The levels of $[Ca^{2+}]_i$ appear to be maintained at baseline levels in each of these individual cells throughout the initial sEBSS perfusion period, no change is observed when Clean DGC sperm cells are added to the perfusion chamber and the baseline level of fluorescence is then maintained throughout the following sEBSS wash period. Each of the cells then show a sharp, sustained rise in $[Ca^{2+}]_i$ immediately upon the perfusion of the ATP positive control condition across their surface.

The Rtot plots for each of the 10 individual experiments that were carried out with Clean DGC sperm cells perfusion over OE-E6/E7 cells displayed in figure 3.7B show the clear lack of increases in $[Ca^{2+}]_i$ throughout all of the experiments. In many cases a reduction in $[Ca^{2+}]_i$ is actually observed in response to the perfusion of this stimulus across the surface of the OE-E6/E7 cells, the strength of this drop in $[Ca^{2+}]_i$ shows varies throughout each experimental subset. This reduction in $[Ca^{2+}]_i$ or lack of response is maintained throughout the sEBSS wash period until the ATP positive control condition is introduced to the perfusion chamber after 9 minutes, at which point each of the experimental subsets of OE-E6/E7 cells appear to exhibit their characteristic sharp, maintained rise in $[Ca^{2+}]_i$ in response to this stimulus.

The perfusion of clean DGC sperm cells elicited an increase in $[Ca^{2+}]_i$ in 0.67±0.27% of the OE-E6/E7 cells on average, whilst the fluorescence in 96.36±3.82% of cells decreased and 3.3±3.63% showed no change. The ATP solution elicited an increase in fluorescence in 100-0.38% of the cells on average. The average maximum peak

height in fluorescence during clean DGC sperm cells perfusion was 2.92±2.5% of the peak height observed in the same cells during ATP solution perfusion. A full summary table of the responses observed during this series of experiments is displayed in appendix IV.v.

3.3.7- Perfusion of OE-E6/E7 cells with “Contaminated” DGC sperm cells

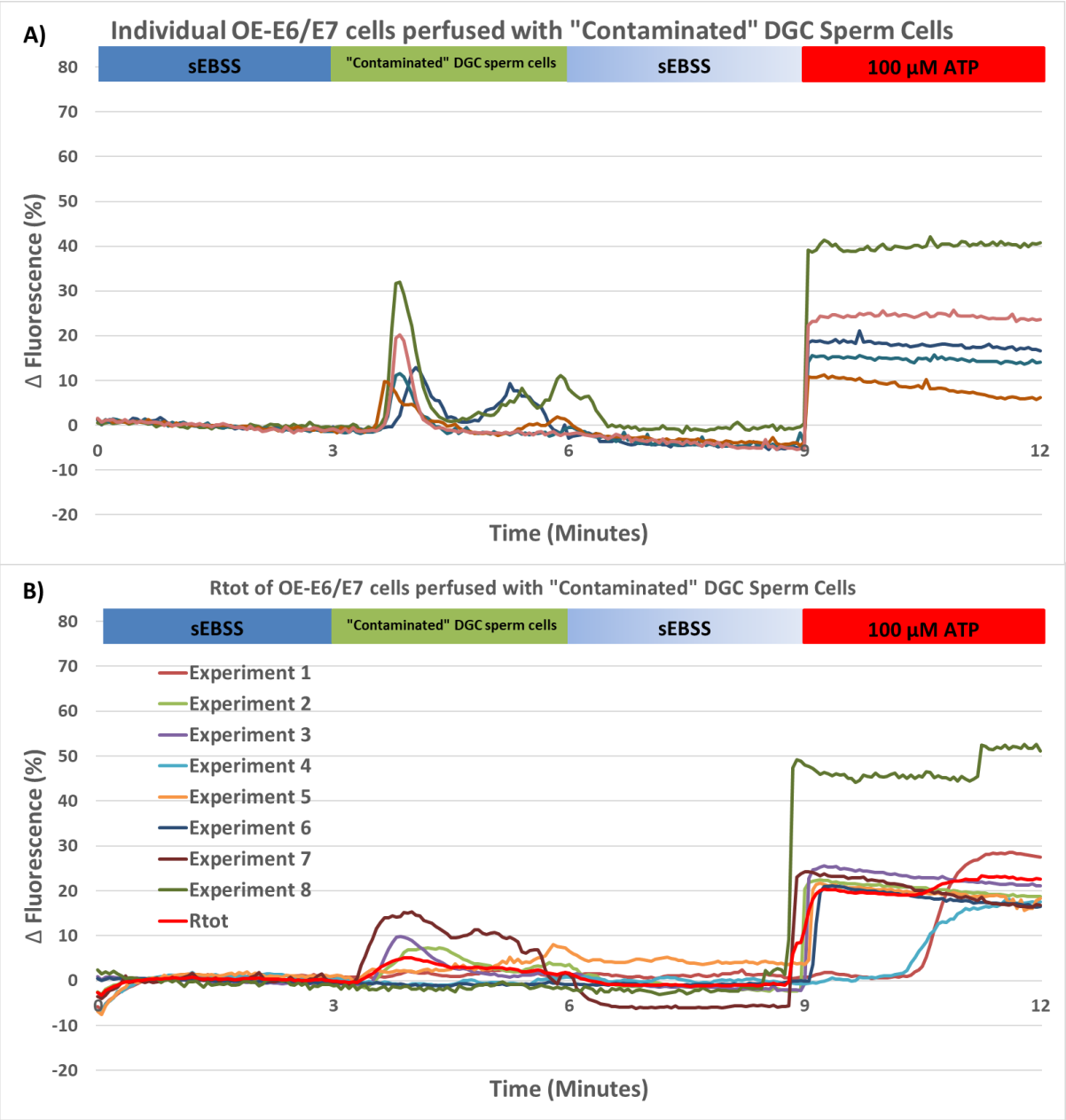


Figure 3.8- The effect of “contaminated” DGC sperm cells perfusion on OE-E6/E7 cells. Cells were perfused with sEBSS for 3 minutes, then “contaminated” DGC sperm cells for 3 minutes, before a further 3 minutes sEBSS wash period and finally 3 minutes of ATP positive control solution. (A) The fluorescence-time plot for 5 individual OE-E6/E7 cells during a Ca^{2+} imaging timelapse experiment. (B) The Rtot plots for each of the 8 experiments carried out, with the overall Rtot plot for this series of experiments representing a total of 799 OE-E6/E7 cells highlighted in red.

To investigate the effect of potential seminal plasma contamination present in the media after carrying out each step of the density gradient centrifugation preparation method in the same tube, 8 Ca^{2+} imaging experiments were carried out in which OE-

E6/E7 cells were perfused with “contaminated” DGC sperm cells. The five average fluorescence timelapse plots for individual OE-E6/E7 cells that were perfused with “Contaminated” DGC sperm cells across their surface in figure 3.8A each exhibit a sharp, strong peak in $[Ca^{2+}]_i$ immediately upon the addition of the stimulus to the perfusion chamber. After this initial peak, the cells appear to return almost to baseline levels of $[Ca^{2+}]_i$, with some of the cells exhibiting secondary $[Ca^{2+}]_i$ peaks during the 3 minute period of “Contaminated” DGC sperm cells stimulus perfusion. This response is mostly washed away by the following 3 minute period of sEBSS perfusion, before each cell exhibits a strong, sustained peak in $[Ca^{2+}]_i$ in response to the ATP positive control solution.

The Rtot plots for each of the 8 experimental subsets of OE-E6/E7 cells which were perfused with “Contaminated” DGC sperm cells in figure 3.8B show the variation in response between different experiments. 3 of the Rtot plots appear to show very little response to the “Contaminated” DGC sperm cells stimulus at all, whilst the others showing varying strengths of rises in $[Ca^{2+}]_i$ during stimulus perfusion. One of the experimental subsets of OE-E6/E7 cells appears to exhibit a more sustained elevation in $[Ca^{2+}]_i$ during stimulus perfusion, whilst others appear to exhibit a more short lived peak in $[Ca^{2+}]_i$ before returning to baseline levels of average fluorescence intensity. The sEBSS washoff period of perfusion appears to mostly eliminate any rises in $[Ca^{2+}]_i$ apart from in one of the experimental subsets, however, the OE-E6/E7 cells in each of the 8 experiments show a strong rise in $[Ca^{2+}]_i$ at some point during the perfusion of the 100 μM ATP solution.

On average, 37.96±17.19% of the OE-E6/E7 cells were identified as showing a rise in fluorescence when “contaminated” DGC sperm cells were perfused across their surface, whilst 42.71±15.33% showed a decrease and 15.87±3.27% showed no

change. 100-14.72% of the cells in this series of experiments responded to the ATP solution with an increase in fluorescence on average. The average maximum peak height in fluorescence during swimup capacitated sperm cells perfusion was 22.78±14.34% of the peak height observed in the same cells during ATP solution perfusion. A full summary table of the responses observed during this series of experiments is displayed in appendix IV.vi.

3.3.8- Comparison of OE-E6/E7 cells response to Semen sample preparations

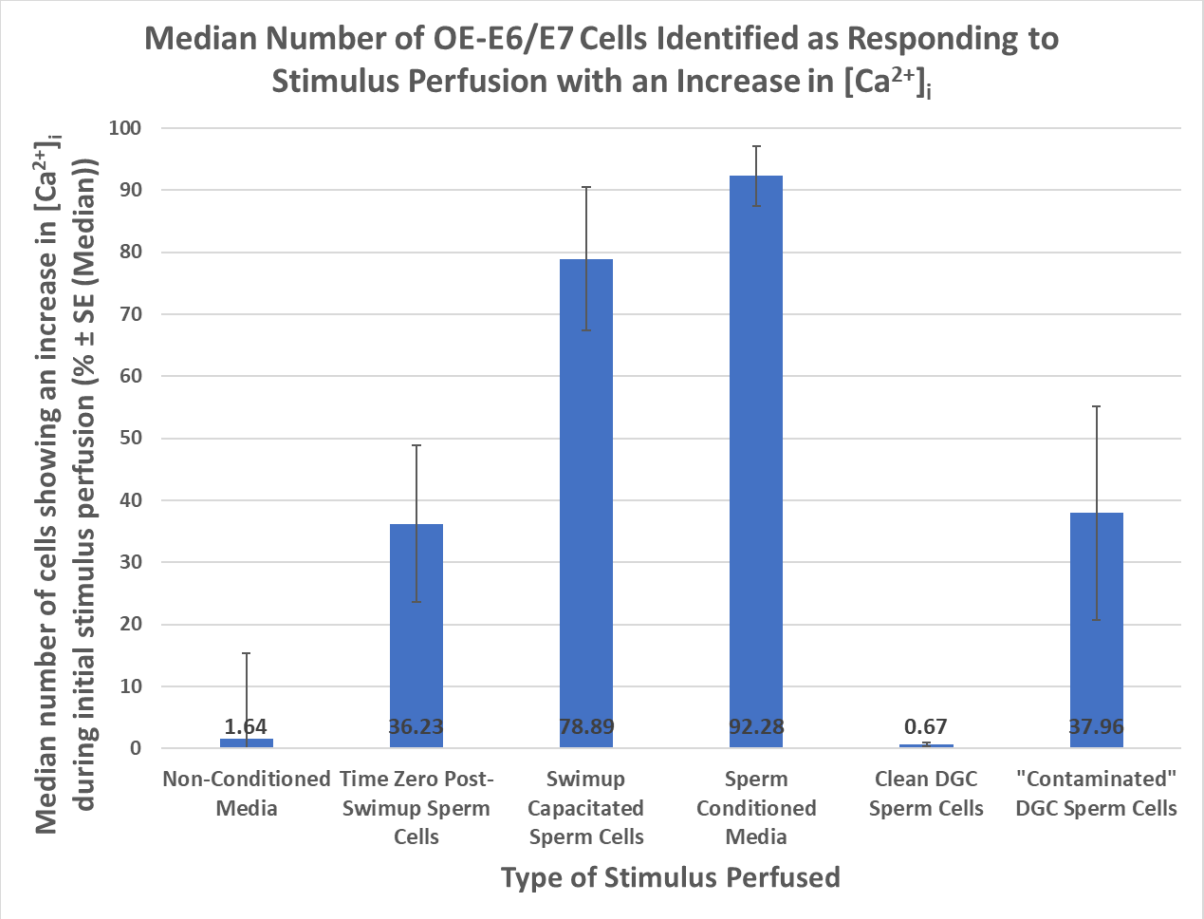


Figure 3.9- Bar chart displaying the median number of OE-E6/E7 cells identified as increasing in $[Ca^{2+}]_i$ (±SE (median)) in response to each of the semen sample preparations used as stimuli in this series of Ca^{2+} imaging experiments.

The median average percentage rate of cells which increased in $[Ca^{2+}]_i$ in response to stimulus perfusion across each experiment in which OE-E6/E7 cells were exposed to each of the semen sample preparations are visualised in figure 3.9. The non-conditioned media negative control stimulus elicited significantly lower response rates in OE-E6/E7 cells than the time zero post-swimup sperm cells (P=0.019), swimup capacitated sperm cells (P=0.004), sperm conditioned media (P=0.001) and "contaminated DGC sperm cells (P=0.028), however, the response rate was not significantly different from clean DGC sperm cells (P=0.205). The highest significant $[Ca^{2+}]_i$ response rate observed was elicited by sperm conditioned media, which was

not significantly higher than swimup capacitated sperm cells (P=0.221) but was higher than time zero post-swimup sperm cells (P=0.003) and “contaminated” DGC sperm cells (P=0.016). There was no significant difference in response rates between time zero post-swimup sperm cells and “contaminated” DGC sperm cells (P=0.859), however, these stimuli elicited significantly higher response rates than non-conditioned media and clean DGC sperm cells (P>0.05). The P values acquired from each comparison between cell lines and stimuli using Mann-Whitney U tests with Dunn’s tests are included in appendix IV.vii.

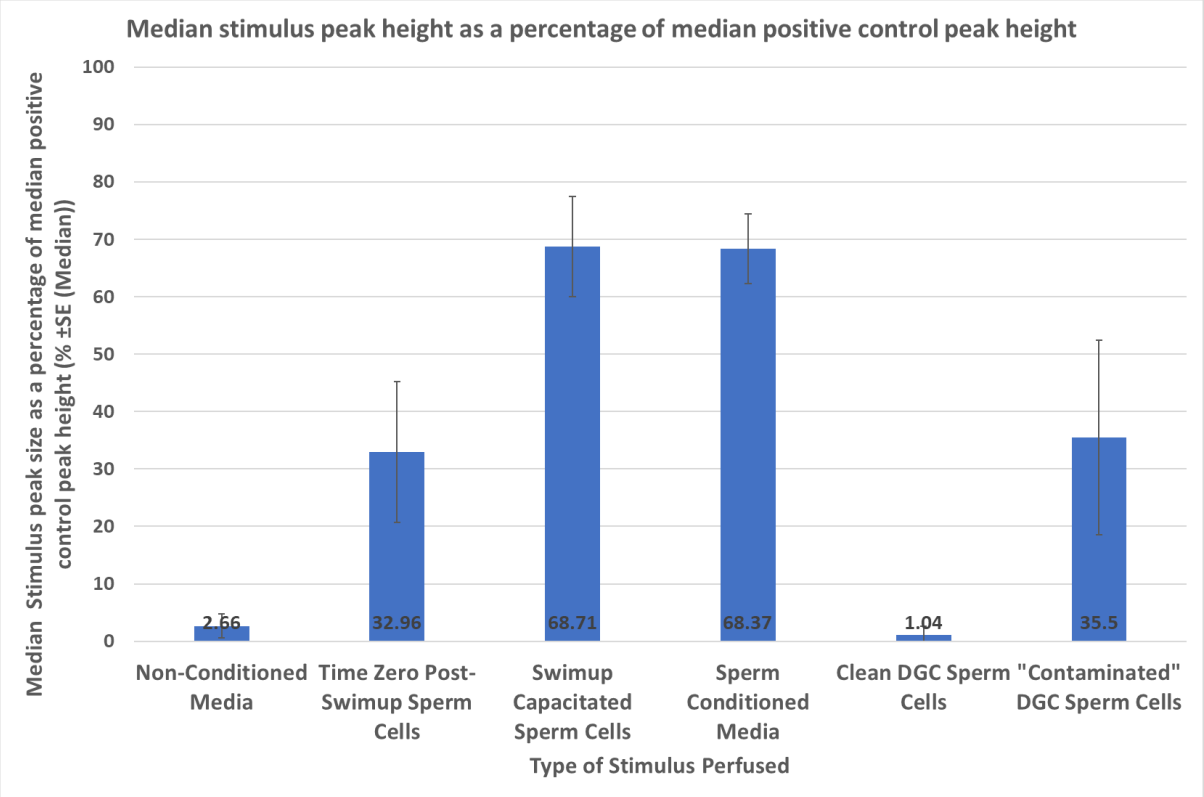


Figure 3.10- Bar chart displaying the average maximum peak height in fluorescence intensity that was observed during stimulus perfusion as a percentage (±SE (median)) of the maximum peak height observed during ATP positive control stimulus perfusion.

The results in figure 3.10 were calculated by dividing the average maximum peak height observed during the perfusion of the stimulus condition during each Ca^{2+} imaging experiment, then dividing that by the average maximum peak height in the same cells that was observed during the perfusion of the ATP positive control condition and then multiplying the result by 100. This gave the maximum stimulus peak height as a percentage of the maximum positive control peak height, allowing for clear comparison of the relative strengths of the $[Ca^{2+}]_i$ responses that were observed in the OE-E6/E7 cells whilst being perfused with each of the semen sample preparations. The non-conditioned media negative control stimulus and the clean DGC cells elicited the weakest $[Ca^{2+}]_i$ response in the OE-E6/E7 cells and they were not significantly different from each other ($P=0.77$). Both of these stimuli elicited significantly weaker $[Ca^{2+}]_i$ responses than all of the other stimuli tested ($P<0.05$)

apart from the difference between “contaminated” DGC sperm cells and non-conditioned media (P=0.105) and time zero post-swimup sperm cells (P=0.118). Sperm conditioned media elicited the strongest response in the OE-E6/E7 cells, however, this was not significantly higher than swimup capacitated sperm cells (P=0.87). Time zero post-swimup sperm cells and “contaminated” DGC sperm cells elicited $[Ca^{2+}]_i$ responses that were significantly weaker than sperm conditioned media ($P<0.05$), but not significantly different from those observed when swimup capacitated sperm cells were perfused across the surface of the OE-E6/E7 cells ($P>0.05$). The P values acquired from each comparison between cell lines and stimuli using Mann-Whitney U tests with Dunn’s tests are included in appendix IV.viii.

3.4- Discussion

The series of Ca^{2+} imaging experiments detailed in this chapter were intended to further investigate the source of the signalling factor within the male ejaculate, that has been established to elicit significant $[Ca^{2+}]_i$ signalling within OE-E6/E7 cells. To achieve this, intricate pathways of semen sample preparation were designed to isolate various groups of proteins and metabolites within the ejaculate, which could then be used as stimuli by gently perfusing them across the surface of OE-E6/E7 cells to assess their responsiveness. The intention was to narrow down the source of the male ejaculate signalling factors- whether they were present exclusively within the sperm cells (Oliva, De Mateo et al. 2009), the seminal plasma (Edwards, Tollaksen et al. 1981) or released by the process of capacitation and the AR (Castillo, Bogle et al. 2019), this would make the identification of the specific signalling factors more streamlined with a later proteomics approach by allowing us to search within a narrower range of candidate factors.

The negative control stimulus utilised in this series of experiments was referred to as non-conditioned media. This solution was prepared by assembling sperm swimup tubes but not allowing the cells any time to swim through the methylcellulose solution layer (Ivic 2002) into the sEBSS, meaning that this solution should have solely consisted of sEBSS with no seminal plasma contamination or any intact sperm cells. This stimulus acted a control measure to indicate the potential presence of any seminal plasma or sperm cell contamination that could arise due to human error during the preparation of the sperm swimup tubes (Mortimer, Swan et al. 1998)- as it has previously been demonstrated in section 2.3.6 that even small (1:100 dilution) traces of seminal plasma are able to elicit strong $[Ca^{2+}]_i$ signalling in the OE-E6/E7 cells. The non-conditioned media did not elicit significant rises in $[Ca^{2+}]_i$ in the vast

majority of OE-E6/E7 cells, with only 1.64±13.77% of the cells exhibiting an increase in fluorescence when exposed to this stimulus, with an average peak height of just 2.72±2.29% in comparison to the peak height observed in the same cells during ATP positive control stimulus perfusion. These results suggest that the preparation of the sperm swimup tubes was able to be carried out with minimal contamination of the upper layer of sEBSS with components of the semen sample, whilst also showing that the sEBSS solution itself was not able to elicit significant $[Ca^{2+}]_i$ responses in the OE-E6/E7 cells.

The purpose of the time zero post-swimup sperm cells stimulus was to examine the effect of sperm cell capacitation on the observed signalling in the OE-E6/E7 cells. In this condition, the spermatozoa were not allowed sufficient time to undergo capacitation (Ostermeier, Cardona et al. 2018) and release further potential signalling factors from their acrosome (Mayorga, Tomes et al. 2007). The perfusion of this time zero post-swimup sperm cell solution across the surface of OE-E6/E7 cells was able to elicit increases in $[Ca^{2+}]_i$ in an average of 36.23±12.65% of OE-E6/E7 cells per experiment, with an average peak height of 20.09±12.83% in comparison to the average peak height elicited by the ATP positive control solution in the same cells. This data suggests that signalling factors that can elicit the observed reactions within OE-E6/E7 cells that stimulate Ca^{2+} oscillations are present within this time zero post-swimup sperm cells stimulus, meaning that they must be derived from either the sperm cell surface (Panner Selvam, Agarwal et al. 2019) or components of the seminal plasma that are able to loosely adhere to spermatozoa (Manjunath, Bergeron et al. 2007) and be carried through viscous methylcellulose solution. It suggests that the male ejaculate derived signalling factors are not

exclusive components of the acrosomal sheath or factors otherwise released by the process of sperm capacitation (Baker, Nixon et al. 2012).

The swimup capacitated sperm cells stimulus was prepared in the same manner as the time zero post-swimup sperm cells, however, this stimulus was the spermatozoa in this preparation were allowed sufficient time to undergo capacitation (Ostermeier, Cardona et al. 2018). This meant that the swimup capacitated sperm cells stimulus also contained the solubilised potential signalling factors that are released as sperm cells undergo the exocytosis of the acrosome (Mayorga, Tomes et al. 2007), allowing us to assess their efficacy in eliciting $[Ca^{2+}]_i$ signalling in the OE-E6/E7 cells. The perfusion of swimup capacitated sperm cells across the surface of OE-E6/E7 cells elicited a rise in $[Ca^{2+}]_i$ within 78.89±11.57% in each experiment on average, with an average peak height of 37.46±11.5% in comparison to the peak elicited by the ATP positive control stimulus in the same cells. Whilst the response strength of response is not significantly higher than that observed with the perfusion of time zero post-swimup sperm cells, there was a significant difference in the number of cells that responded to swimup capacitated sperm cells. This could either suggest that additional signalling factors are released into the media throughout the process of capacitation and the AR (Breitbart and Spungin 1997), alternatively, it could simply suggest that more of the same signalling factors that are responsible for the signalling observed with time zero post-swimup sperm cells are able to be solubilised into the media due to the additional period of incubation (Kopf, Dörr et al. 2020).

The sperm conditioned media stimulus allowed for the assessment of any solubilised proteins, peptides or metabolites to be assessed for their efficacy in stimulating $[Ca^{2+}]_i$ signalling in the OE-E6/E7 cells, without the presence of actual spermatozoa or the proteins present on their surface membrane (Brewis and Gadella 2010). This

stimulus proved to be very effective in eliciting an oscillatory $[Ca^{2+}]_i$ response in the OE-E6/E7 cells, with 92.28±4.79% of the cells exhibiting an increase in $[Ca^{2+}]_i$ and an average strength of response of 48.08±8.34% in comparison to the ATP positive control stimulus in the same cells. This response rate was significantly higher than non-conditioned media, both clean and "contaminated" DGC sperm cells and time zero post-swimup sperm cells, whilst the relative strength of response was significantly higher than all conditions apart from swimup capacitated sperm cells. This result suggests that the signalling factors responsible for the observed signalling in the OE-E6/E7 cells are soluble, like many proteins present in the male ejaculate (Parrington, Lai et al. 2000, Hess, Jones et al. 2005, Johnston, Wooters et al. 2005). This data also shows the presence of spermatozoa in the media is not necessary for the signalling to occur, suggesting that direct sperm cell contact is not necessary and therefore the factors responsible can't one of the many transmembrane proteins present on the sperm cell surface (Rajeev and Reddy 2004).

The clean DGC sperm cells stimulus was intended to determine whether the relatively harsh process of density gradient centrifugation (Sun and Sethu 2018) was sufficient to remove or significantly reduce the presence of the signalling factor responsible for the observed $[Ca^{2+}]_i$ signalling in the OE-E6/E7 cells. It is clear from the results of this series of experiments that this is the case, as the clean DGC sperm cells were only able to elicit increases in $[Ca^{2+}]_i$ within 0.67±0.27% of the OE-E6/E7 cells on average, with an average peak height of just 2.92±2.5% compared to the ATP stimulus. Both the response rate and strength of response of the OE-E6/E7 cells to clean DGC sperm cells was significantly lower than all the other stimuli assessed in this series of experiments, apart from the negative control condition of non-conditioned media. The fact that clean DGC sperm cells caused a similar

response in the OE-E6/E7 cells as the negative control condition suggests that the process of density gradient centrifugation, followed by 2 separate wash steps is sufficient to remove the signalling factor from this solution in sufficient quantity to negate the observed signalling. This observation fits with the hypothesis that the signalling factors are soluble proteins or metabolites from the seminal plasma that can be loosely adhered to motile sperm cells (Manjunath, Bergeron et al. 2007) as it would be expected that transmembrane proteins are anchored within the lipid bilayer of the plasma membrane (Hickey and Buhr 2011) would be preserved in the density gradient centrifugation protocol used in this study.

The purpose of the “contaminated” DGC sperm cells stimulus was to assess the effect of seminal fluid contamination on the sides of the falcon tube which would remain from the initial density gradient centrifugation intended to separate the motile spermatozoa from the semen sample (Björndahl, Mohammadieh et al. 2005). These experiments confirmed that the small amount of seminal fluid contamination present on the inner surface of the falcon tube after density gradient centrifugation is sufficient to stimulate a rise in $[Ca^{2+}]_i$ within 37.96±17.19% of the OE-E6/E7 cells on average, with average elicited peak heights of 22.78±14.34% compared to the ATP stimulus. The responses observed with this stimulus were significantly higher than with clean DGC sperm cells and was comparable to the response observed with time zero post-swimup sperm cells. This data further suggests that the factors responsible are derived from the seminal plasma (Edwards, Tollaksen et al. 1981) rather than being endogenous to the sperm cells themselves (Panner Selvam, Agarwal et al. 2019).

Variations in the $[Ca^{2+}]_i$ peak kinetics were observed in the various cells imaged in each experiment, as shown in figure 3.2. The specific variations in peak kinetics and

frequency of $[Ca^{2+}]_i$ oscillations within cells has previously been shown to be interpreted by intracellular downstream effectors. (Parekh 2011) The $[Ca^{2+}]_i$ oscillations and the decoding of their specific frequencies represent a diverse signalling system within cells that can regulate a wide range of processes (Smedler and Uhlén 2014). This makes the variation in the peak kinetics observed in the OE-E6/E7 cells during these experiments particularly interesting, as it suggests that various downstream cellular responses could be initiated by the perfusion of these stimuli across their surface (Sanders, Pelloux et al. 2002). The variation in $[Ca^{2+}]_i$ kinetics also indicates that more than one signalling factor could be present within the male ejaculate (Antunes, Roque et al. 2016).

Overall, the observed variation in the $[Ca^{2+}]_i$ signalling elicited within OE-E6/E7 cells in this series of experiments has demonstrated the effectiveness of the semen sample preparation pathways that were devised to isolate specific proteomic subgroups from of the male ejaculate. The significantly higher response rates observed with “contaminated” DGC sperm cells in comparison to clean DGC sperm cells indicated that the male ejaculate signalling factors are derived from the seminal plasma rather than the spermatozoa themselves (Björndahl, Mohammadieh et al. 2005). Swimup capacitated sperm cells elicited significantly higher levels of $[Ca^{2+}]_i$ response in the OE-E6/E7 cells than the non-conditioned media negative control. Assuming that the modified swimup through viscous media technique used herein is an effective method of replicating the passage of motile spermatozoa through the viscous cervical mucus (Ivic 2002), carrying with them any potential signalling factors from the seminal plasma that they would be expected to carry *in vivo*, this shows that the signalling factors present within the seminal plasma could be carried into the upper regions of the FRT (Tecle, Reynoso et al. 2019).

The time zero post-swimup sperm cells elicited significantly lower rates of $[Ca^{2+}]_i$ signalling in the OE-E6/E7 cells than the swimup sperm cells stimulus. This could suggest that the factors exclusively released during the process of sperm capacitation or the AR (Breitbart and Spungin 1997) could either potentiate signalling or activate other independent pathways, however, the lack of signalling observed in response to clean DGC sperm cells, which also underwent capacitation, indicates that the increased period of incubation in the swimup sperm cell condition simply allowed for more of the same signalling factors to be shed into the media. The sperm conditioned media was able to elicit both the highest rate and strength of $[Ca^{2+}]_i$ response in the OE-E6/E7 cells, which further demonstrates that direct sperm cell contact is not necessary the signalling to occur.

In conclusion, this data shows that the male ejaculate derived signalling factors are able to loosely adhere to the surface of spermatozoa, as many proteins have previously shown to be capable of (Rodríguez-Martínez, Kvist et al. 2011). These factors can be carried through viscous media, intended to replicate human cervical mucus (Ivic 2002), and then solubilised into the sperm conditioned media in sufficient concentrations to elicit a strong $[Ca^{2+}]_i$ response in the OE-E6/E7 cells. This hypothesis of signalling factor transport into the upper FRT by their adherence to motile human spermatozoa shows that despite key differences in FRT anatomy and physiology (Chumduri and Turco 2021), the signalling observed herein could account for the seminal fluid derived signalling mechanisms between sperm cells and oviductal epithelial cells that have been studied extensively in a range of animal models (Ellington, Ignotz et al. 1993, Fazeli, Affara et al. 2004, Georgiou, Sostaric et al. 2005, Georgiou, Snijders et al. 2007, Kodithuwakku, Miyamoto et al. 2007,

Schjenken and Robertson 2014, Ghersevich, Massa et al. 2015, Schjenken, Glynn et al. 2015, Suarez 2016, Reshi, Viil et al. 2020, Schjenken and Robertson 2020).

On the basis of the data acquired from this series of experiments, it was established that the sperm conditioned media stimulus would be the ideal semen sample preparation to use for further proteomic analysis to elucidate the identity of the male ejaculate derived signalling factors. This conclusion was reached because this condition not only elicited the strongest rate and strength of response in the OE-E6/E7 cells, but also because it was deemed to contain the lowest level of proteomic "noise". All of the other stimuli tested that elicited significant $[Ca^{2+}]_i$ responses in the OE-E6/E7 cells also contained spermatozoa, which are known to contain a wide range of proteins and potential signalling factors (Agarwal, Panner Selvam et al. 2020) which have been demonstrated to not be necessary for the observed signalling in this series of experiments.

Chapter 4

Fractionation and proteomic analysis of sperm conditioned media

4.1- Introduction

Human sperm cells are widely accepted to be transcriptionally and translationally inactive (Casas and Vavouri 2014), as such they are dependent upon acquisition of proteins from their external environment to extend or modify their function. One example of this is the three isoforms of glycodelin, which are encountered by spermatozoa as they navigate their way to the site of fertilisation and modulate different aspects of sperm function (Yeung, Lee et al. 2007). A concept that has been given less consideration is whether proteins originating from sperm cells can modulate the FRT. In previous chapters I have discussed and demonstrated that sperm-released factors can initiate signalling in the cells of the FRT, so the next stage is to identify the specific factors involved.

The human proteome is estimated to be encoded by somewhere between 25000 and 30000 genes (Southan 2004). The purpose of this study is to identify signalling factors derived from the human male ejaculate that interact with FRT cells, which narrows down the range of candidate proteins. The male ejaculate contains a very large number of proteins (Gilany, Lakpour et al. 2011), though only a small proportion of these are able to be carried by spermatozoa and released within the FRT. Various sperm sample preparation methods were utilised in chapter 3 to further narrow down the range of proteins that would undergo analysis. From these preparations, sperm conditioned media was established as the ideal candidate semen sample preparation for proteomic analysis in order to identify its constituent proteins and peptides as potential signalling factors responsible for the observed $[Ca^{2+}]_i$ signalling in OE-E6/E7 cells.

The science of proteomics is the application technologies to identify and quantify the overall protein content of a cell, tissue, media or organism (Aslam, Basit et al. 2017). Purification of proteins for analysis is conventionally carried out by ion exchange, size exclusion or affinity chromatography (Otwinowski and Minor 1997, Voedisch and Thie 2010, Hildonen, Halvorsen et al. 2014). The analysis of specific selected proteins can be carried out using methods such as western blotting (Kurien and Scofield 2006) or enzyme-linked immunosorbent assay (ELISA) (Lequin 2005), however, in cases where complex mixtures of proteins need to be analysed it is essential to separate the proteins using electrophoresis techniques (Dunn 2014). Mass spectrometry can be used to identify these complex protein mixtures with extremely high sensitivity (Yates III 2011), but in order for the acquired data to be analysed the molecular weights of the peptides found and their mass spectra must be matched with sequences within an established database (Henzel, Billeci et al. 1993). Proteins within a sample must be digested, usually by enzymes, since endogenous proteolytic processing and post-translational modifications can alter the molecular weight of a protein to such an extent that matching it to the predicted molecular weight within a database becomes unreliable (Yates III 2011). These methods of identifying proteins within a mixture using mass spectrometry and sequence databases is referred to as “bottom up” or “shotgun” proteomics (Zhang, Fonslow et al. 2013).

Human sperm cells are good candidates for proteomic analysis because they can easily be isolated from seminal fluid and they are both translationally and transcriptionally quiescent (Baker, Nixon et al. 2012). The first study to qualitatively identify proteins from the human sperm cell proteome identified 1760 proteins (Johnston, Wooters et al. 2005), however, as proteomic technologies have improved

over the years since then, a more recent study demonstrated the presence of 4675 proteins within human spermatozoa (Wang, Guo et al. 2013). Proteomics studies have provided greater understanding of the molecular factors that are associated with the process of fertilisation, deepening our understanding of sperm biochemistry and providing information that could improve the reproductive outcomes of patients with infertility (Agarwal, Panner Selvam et al. 2020). The extensive study of the human sperm proteome has identified several biomarkers identified that are associated with male fertility (Panner Selvam, Agarwal et al. 2019).

The intention of these studies was to examine the proteome of the entire spermatozoa, however, there has been a recent shift in the focus of fertility-based proteomics research towards subcellular proteomics. By using techniques such as differential centrifugation it is possible to separate proteins localised in specific sections of sperm cell anatomy, in order to gain a better understanding of the proteins that are necessary to carry out specific cellular functions (Agarwal, Panner Selvam et al. 2020). For example, one study isolated the tails of spermatozoa from normozoospermic males by sonication, before carrying out liquid chromatography and tandem mass spectrometry on the isolated tail peptides (Amaral, Castillo et al. 2013). This analysis provided evidence that fatty acid oxidation was much more essential for sperm motility than previously thought, and a range of enzymes involved in lipid metabolism and mitochondrial beta-oxidation were identified (Amaral, Castillo et al. 2013). This concept of subcellular proteomic analysis has been adapted for this study to extend to proteomic analysis of sperm conditioned media, which does not actually contain any spermatozoa, however, it is intended to represent the milieu of peptides that motile spermatozoa would carry through the cervical mucus into the upper regions of the FRT.

The use of centrifugal filters to isolate peptides and proteins within media into separate fractions based on their size is an effective method of preparing samples for bottom-up type proteomic analysis (Wiśniewski 2018). The fractions produced by this process each contain separate weight groups of proteins, allowing them to be assessed in Ca^{2+} imaging experiments with OE-E6/E7 cells to see if the previously observed $[Ca^{2+}]_i$ signalling can be knocked out by removing proteins of a certain size from the media. These fractions can then be sent for proteomic analysis and the resulting list of proteins may then be analysed for potential candidate factors that warrant further investigation.

Based on the results from previous Ca^{2+} imaging experiments described in this study, it appears that soluble signalling factors, which are potentially protein factors that are loosely associated and released by sperm cells as they navigate through the FRT, are the mediators of the signalling that has been observed in the oviductal epithelial cell line (OE-E6/E7 cells). The sperm conditioned media preparation is the ideal candidate preparation for further proteomic analysis, due to the high level of $[Ca^{2+}]_i$ signalling observed when OE-E6/E7 cells are exposed to this stimulus, as well as the relatively low proteomic content of this preparation due to the removal of intact sperm cells, which would significantly contribute to a reduction in the number of different proteins present in the media (Oliva, De Mateo et al. 2009). The purpose of this chapter is to use a proteomics approach to identify potential signalling factors present within the sperm conditioned media, which can then be assessed for reactivity with the OE-E6/E7 cells in an attempt to identify the specific signalling factor responsible for the observed $[Ca^{2+}]_i$ signalling.

4.2- Materials & Methods

4.2.1- Materials

0.2 µM PES syringe filters, (Corning). 100mm tissue-culture treated culture dishes, (Corning). 12mm round coverslips, (Warner instruments). 15 ml centrifuge tubes, (Falcon). 15 mL plastic disposable syringes, (ThermoFisher Scientific). 2 mm inner diameter translucent silicone tubing (Fisher Scientific). 22x32mm coverslips, (Appleton Woods). 25cm^2 tissue culture flasks, (Falcon). 5 mL Round Bottom High Clarity PP Test Tubes, (Falcon). 75cm^2 tissue culture flasks, (Falcon). 80 Mohm water. Acclaim PepMap 100 C18, 5 um, 100A 300um i.d. x 5mm (Dionex, Sunnyvale, CA USA). Acetone ≥99.9%, (Merck). Adenosine-5'-triphosphate (ATP), (Sigma). Amicon® 50 kDa Ultra Centrifugal Filters, (Merck). Amicon® 3 kDa Ultra Centrifugal Filters, (Merck). Ammonium Bicarbonate, (Merck). Calcium Green-1 AM, (Invitrogen). Dulbecco's modified Eagle's medium (DMEM), no phenol red, (Gibco™). DMEM/F12, no phenol red, (Gibco™). Iscove's modified Dublecco's medium (IMDM), no phenol red, (Gibco™). DMEM/F12, no phenol red, (Gibco™). Foetal bovine serum, (Sigma-Aldrich). Nano Series™ Standard Columns 75 µm i.d. x 15 cm, packed with C18 PepMap100, 3 µm, 100Å (Dionex, Sunnyvale, CA USA). PBS tablets, (ThermoFisher Scientific). Penicillin-Streptomycin (10,000 U/mL), (Gibco™). Pierce™ 96–Well Plate, (Thermo Scientific). Pierce™ BCA Protein Assay Kit, (Thermo Scientific). Pluronic F-127 10% in DMSO, (Sigma-Aldrich). Protein Discovery 2.2 software, Sequest HT algorithm (Thermo Fisher). PureSperm 40, (Nidacon). PureSperm 80 (Nidacon). QExactive HF Orbitrap mass spectrometer (ThermoFisher Scientific). Series 20 perfusion chambers, (Warner Instruments). Supplemented Modified Earle's balanced salt solution (sEBSS), (Lab Industries) (described in Appendix I). Triversa Nanomate nanospray source (Advion

Biosciences, NY). Trypsin-EDTA solution 10x, (Sigma-Aldrich). Trypsin gold (Promega, Southampton, Hampshire, UK, 6 ng/µl). UltiMate® 3000 HPLC series (Dionex, Sunnyvale, CA USA).

4.2.2- Fractionation of sperm conditioned media

Samples of sperm conditioned media were pooled from various donors to increase the available volume as well as the concentration of proteins within the media for subsequent fractionation and proteomic analysis. The pooled sperm conditioned media was fractionated into 3 distinct fractions based on the weight of the proteins within the media, using Amicon® Ultra Centrifugal Filters. 15 ml of pooled sperm conditioned media was added to the filter device in the Amicon® 50 kDa Ultra Centrifugal Filter, the filter device was then inserted into the centrifuge tube and the cap was securely attached. The device was then centrifuged at 5000 g for 45 minutes. After centrifugation, the concentrated solute from the bottom of the filter device was aspirated into a 15 ml falcon tube. The ultrafiltrate in the bottom of the centrifuge tube was aspirated back into the filter device and the process was repeated two more times, to ensure that as much of the protein content was filtered as possible. After the third pass through the filter device, the filtrate was aspirated into the filter device of an Amicon® 3 kDa Ultra Centrifugal Filter. The same centrifugation process was then carried out at 5000 g for 45 minutes, before the concentrated solute and ultrafiltrate were both aspirated into separate, new 15 ml falcon tubes. The >50 kDa filtrate and the <3kDa filtrate were resuspended in a volume of sEBSS that was equal to the original volume of the pooled sperm conditioned media sample, to ensure that a similar concentration of the proteins within the filtrate were present. The 3 kDa< x <50kDa ultrafiltrate did not need to be diluted as it was approximately the same volume as the initial sperm conditioned media sample.

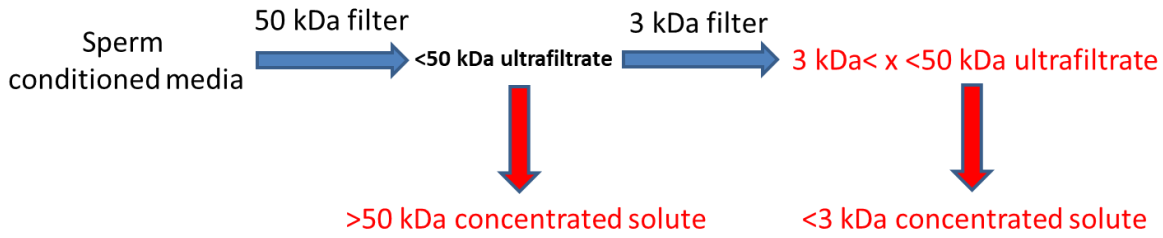


Figure 4.1- A flowchart schematic of the fractionation process. Sperm conditioned media was passed through the 50 kDa Amicon® Ultra Centrifugal Filter to isolate the >50 kDa concentrated solute fraction. The <50 kDa ultrafiltrate was then passed through the 3 kDa Amicon® Ultra Centrifugal Filter to produce the 3 kDa< x <50 kDa ultrafiltrate fraction and the <3kDa concentrated solute. Upon dilution of the two concentrated solutes there were three distinct fractions of the sperm conditioned media, separated by the kDa of the proteins within the media and of approximately equal protein concentrations as the initial sperm conditioned media sample.

4.2.3- Ca^{2+} imaging of OE-E6/E7 cells with sperm conditioned media fractions

All Ca^{2+} imaging experiments to assess the efficacy of the different sperm conditioned media fractions in eliciting $[Ca^{2+}]_i$ signalling were carried out using the same methodology as described in sections 2.2.6, 2.2.7 and 2.2.8.

4.2.4- Precipitation of proteins from sperm conditioned media fractions

Proteins and peptides from the sperm conditioned media fractions were extracted by acetone precipitation (Simpson and Beynon 2010). Acetone was aliquoted into polypropylene 15 ml Falcon tubes and then cooled to -20°C in a freezer. 3 mL of a sperm conditioned media fraction was placed into a polypropylene 15 ml Falcon tube and then 12 mL of the -20°C acetone was added to the tube. The mixture was then vortexed thoroughly and incubated for 60 minutes at -20°C before being centrifuged at 15000 g for 10 minutes. The supernatant was decanted to be disposed and the remaining acetone was allowed to evaporate from the tube by leaving it at room temperature without a cap for 30 minutes. The remaining pellet was then resuspended in 100 µL of ammonium bicarbonate solution (100 mM) in 80 Mohm water.

4.2.5- BCA assay of precipitated sperm conditioned media fractions

A BCA assay was used to quantify the protein content of the fractions and determine the necessary dilution factor before sending them for proteomic analysis. Working reagents were prepared according to the manufacturer's instructions and diluted bovine serum albumin (BSA) standards were prepared at concentrations of 2000, 1500, 1000, 750, 500, 250, 125, 25 and 0 µg/mL in the same ammonium bicarbonate solution (100 mM) in 80 Mohm water. 25 µL of each standard and precipitated sperm conditioned media fraction solution (with additional aliquots of 1:10, 1:100 and 1:1000 in ammonium bicarbonate solution) were added to separate wells in a Thermo Scientific™ Pierce™ 96–Well Plate, before 200 µL of working reagent was added to each. The plate was covered and incubated 37°C for 30 minutes. The plate was then cooled to room temperature and the absorbance was measured at 562 nm on a plate reader. The average absorbance from the blank standard replicates was subtracted from the measurements of all the other individual standard and sperm conditioned media fraction replicates. A standard curve was produced by plotting the absorbance of each BSA standard against its known protein concentration to determine the protein concentration of each of the sperm conditioned media fractions and their known dilutions. This was used to calculate the necessary dilution factor for the sperm conditioned media fractions to undergo proteomic analysis at the required concentration between 5-10 µg/mL.

4.2.6- Proteomic analysis of sperm conditioned media fractions

The Advanced Mass Spectrometry Facility in the School of Biosciences at the University of Birmingham undertook the proteomic analysis of the precipitated sperm conditioned media fractions. Duplicate samples of the resuspended pellet of >50kDa, 3-50kDa and <3kDa fractions of pooled sperm conditioned media in 100 µL of

ammonium bicarbonate solution (100 mM) in 80 Mohm water were sent for analysis, as well as two vials of the negative control 100 µL of ammonium bicarbonate solution (100 mM) in 80 Mohm water. Trypsin digestion was performed by addition of 10 mM dithiothreitol (DTT) and incubation of the samples at 56^{o}C for 30 minutes. Samples were then cooled to room temperature and cysteines alkylated by addition of 50mM iodoacetamide, mixed and incubated at room temperature in the dark for 30 minutes. Trypsin gold (Promega, Southampton, Hampshire, UK, 6 ng/µl) was subsequently added to the samples, which were then incubated at 37^{o}C overnight.

The liquid samples contained the mixture of peptides and were desalted using millipore C18 ZipTips. Tips were prepared by pre-wetting in 100% acetonitrile and rinsed in 2x10 µL 0.1% formic acid. Samples were repeat pipetted throughout the volume of the samples ten times. The tip was then washed with 3x10µl 0.1% formic acid to remove excess salts before elution of peptides with 10µL of 50% acetonitrile/water/0.1% formic acid. Samples were dried down to remove the acetonitrile, and then re-suspended in 0.1% formic acid solution in water.

UltiMate® 3000 HPLC series (Dionex, Sunnyvale, CA USA) was used for peptide concentration and separation. Samples were trapped on precolumn, Acclaim PepMap 100 C18, 5 um, 100A 300um i.d. x 5mm (Dionex, Sunnyvale, CA USA) and separated in Nano Series™ Standard Columns 75 µm i.d. x 15 cm, packed with C18 PepMap100, 3 µm, 100Å (Dionex, Sunnyvale, CA USA). The gradient used was from 3.2% to 44% solvent B (0.1% formic acid in acetonitrile) for 30 min. The column was then washed with 90 % mobile phase B before re-equilibrating at 3.2 % mobile phase B. Peptides were eluted directly (~ 350 nL min-1) via a Triversa Nanomate nanospray source (Advion Biosciences, NY) into a QExactive HF Orbitrap mass spectrometer (ThermoFisher Scientific). The spray voltage of QE HF was set to 1.7

kV through Triversa NanoMate and heated capillary at 275°C. The mass spectrometer performed a full FT-MS scan (m/z 360−1600) and subsequent HCD MS/MS scans of the 20 most abundant ions with dynamic exclusion setting 15S. Full scan mass spectra were recorded at a resolution of 120,000 at m/z 200 and ACG target of 3×106. Precursor ions were fragmented in HCD MS/MS with resolution set up at 15,000 and a normalized collision energy of 28. ACG target for HCD MS/MS was 1x105. The width of the precursor isolation window was 1.2 m/z and only multiply-charged precursor ions were selected for MS/MS. Spectra were acquired for 56 mins.

The MS and MS/MS scans were searched against Uniprot database using Protein Discovery 2.2 software, Sequest HT algorithm (Thermo Fisher). Variable modifications were deamidation (N and Q), oxidation (M), phosphorylation (S, T and Y) and acetylation (K). The precursor mass tolerance was 10 ppm and the MS/MS mass tolerance was 0.02Da. Two missed cleavage was allowed and data were filtered with a false discovery rate (FDR) of 0.01. Proteins with at least two high confidence peptides were accepted as a real hit.

4.2.7- Analysis of proteomic data

Peptides of interest from the proteomic analysis data were further analysed using DNASTAR LASERGENE Bioinformatics Software (Version 17.3.1). This software package allowed for sequence analysis and comparison of the peptides identified within the sperm conditioned media fractions, as well as pairwise sequence alignments and predicted 3D modelling of tertiary protein structure.

4.3- Results

4.3.1- Initial test of pooled sperm conditioned media reactivity in OE-E6/E7 cells

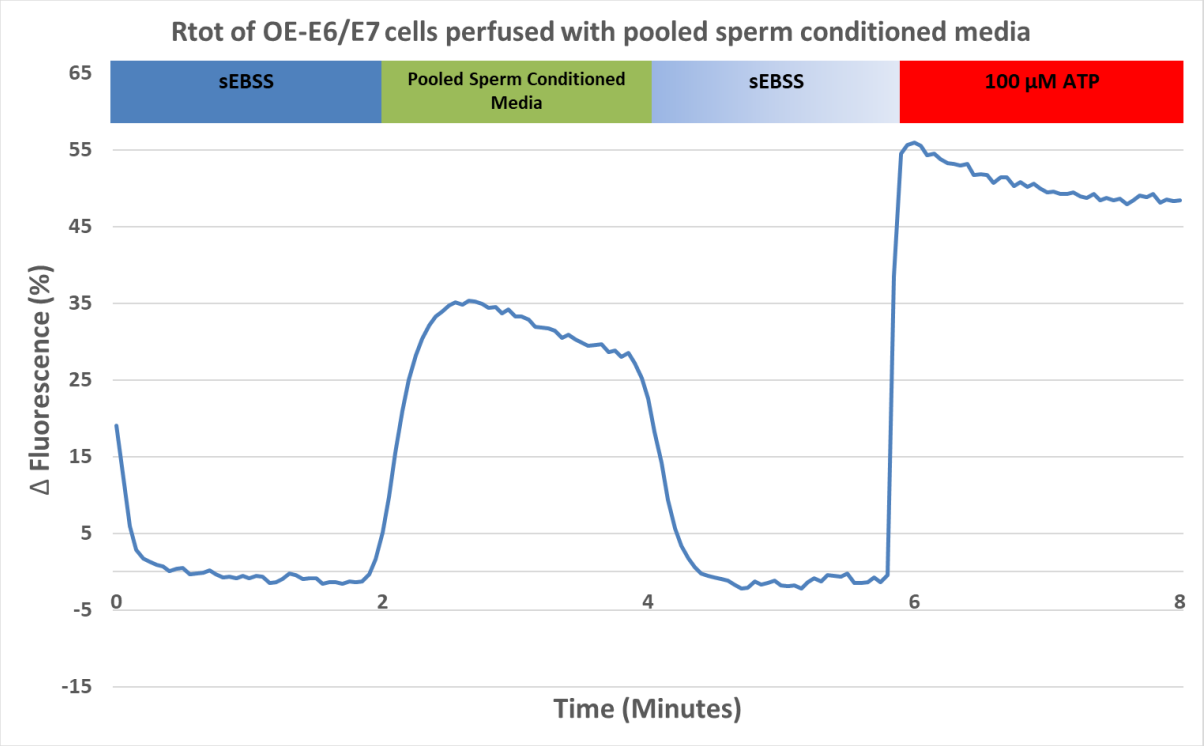


Figure 4.2- An Rtot plot of the timelapse Ca^{2+} imaging experiment carried out on 108 OE-E6/E7 cells using the pooled sperm conditioned media as a stimulus, before washing it off the surface of the cells with sEBSS and finally adding 100 µM ATP solution as a positive control stimulus.

Before beginning the process of fractionation of the sperm conditioned media to begin the proteomic analysis, it was necessary to make sure that the pooled sample of sperm conditioned media was able to elicit the previously observed $[Ca^{2+}]_i$ signalling in the OE-E6/E7 cells. It is clear from this experiment that the pooled sperm conditioned media was able to elicit a strong $[Ca^{2+}]_i$ response in the OE-E6/E7 cells in a similar fashion to what was observed in previous experiments, with 75.9% of the cells identified as exhibiting a rise in fluorescence. After confirming this, the pooled sperm conditioned media sample was fractionated as described in section 4.2.2.

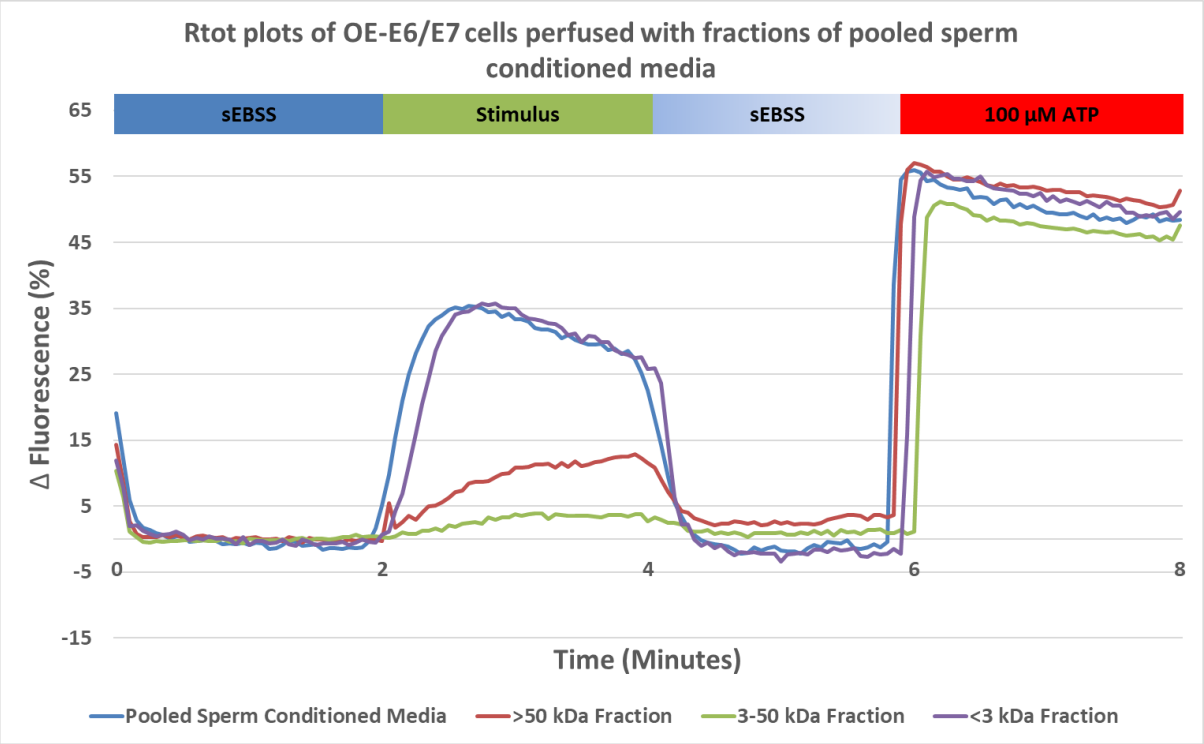


Figure 4.3- Rtot plots for the four individual timelapse Ca^{2+} imaging experiments carried out using each of the three fractions of sperm conditioned media, as well as the initial pooled conditioned media as stimuli, before washing it off the surface of the cells with sEBSS and finally adding 100 µM ATP solution as a positive control stimulus- overlayed on the same graph for comparison. A total of 96 OE-E6/E7 cells were recorded in the experiment with the >50kDa fraction, with 102 cells in the experiment with the 3-50kDa fraction and 88 cells in the <3kDa fraction experiment.

The three fractions of sperm conditioned media were capable of eliciting $[Ca^{2+}]_i$ signalling the OE-E6/E7 cells to varying extents. The 3-50 kDa fraction elicited the weakest rise in $[Ca^{2+}]_i$ with just 21.6% of the OE-E6/E7 cells exhibiting a rise in fluorescence when it was perfused across their surface. The >50 kDa fraction elicited a slightly stronger rise in fluorescence upon introduction to the perfusion chamber and with this stimulus 41.7% of the OE-E6/E7 cells exhibited a rise in $[Ca^{2+}]_i$. The <3kDa fraction elicited a very similar $[Ca^{2+}]_i$ response in the OE-E6/E7 cells to the initial pooled sperm conditioned media stimulus, with a sharp rise in $[Ca^{2+}]_i$ immediately upon entry to the perfusion chamber within 73.9% of the cells, this rise was sustained but faded slightly throughout the stimulus perfusion period before

being washed away to baseline levels of $[Ca^{2+}]_I$ fluorescence during the sEBSS wash period. The ATP positive control stimulus was able to elicit a strong, sustained peak in $[Ca^{2+}]_i$ throughout all of these experiments.

After that each of the sperm conditioned media fractions were able to elicit $[Ca^{2+}]_i$ signalling in the OE-E6/E7 cells to varying extents, the proteins were precipitated from the media as described in section 4.2.4. Once the protein pellet had been resuspended in 100 µL of ammonium bicarbonate solution (100 mM) in 80 Mohm water, a small 5 µL aliquot was aspirated and resuspended in 1995 µL of sEBSS to be used as stimuli in another Ca^{2+} imaging experiment to ensure that the ammonium bicarbonate solution was not able to elicit $[Ca^{2+}]_i$ signalling in the OE-E6/E7 cells alone, the initial 3 minute period of sEBSS perfusion was carried out using 5 µL of 100 mM ammonium bicarbonate solution mixed with 1995 µL of sEBSS.

4.3.2- Assessment of post precipitation protein pellet for signalling efficacy

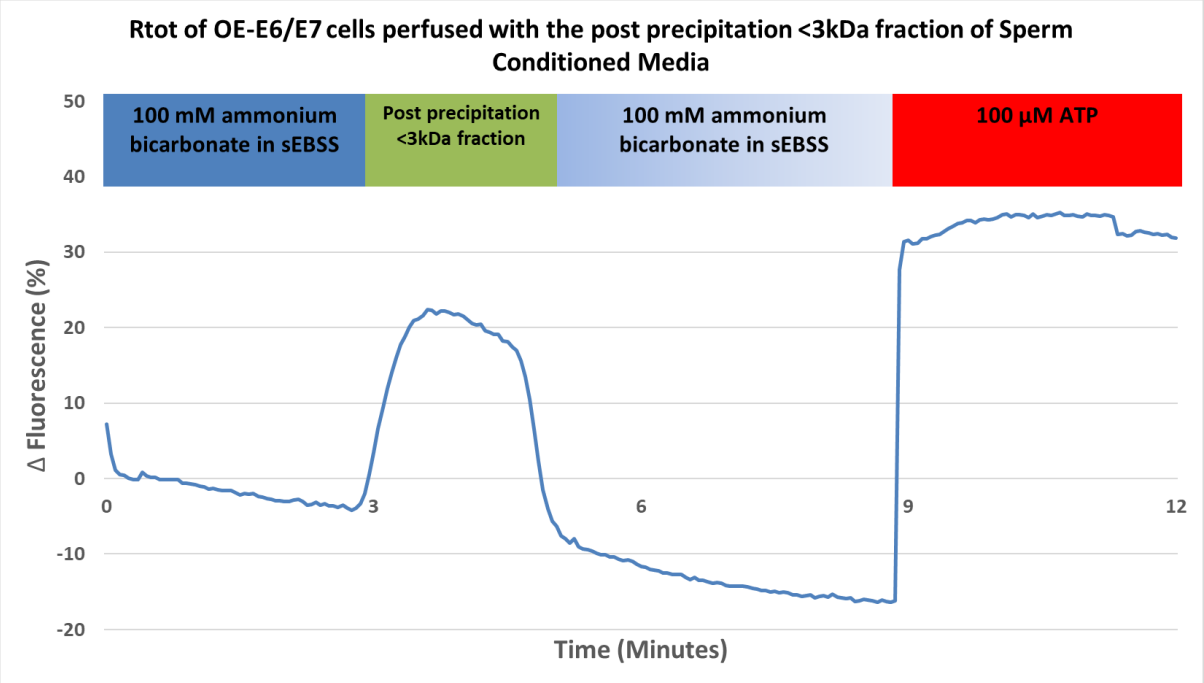


Figure 4.4- Rtot plot for the timelapse Ca^{2+} imaging experiment carried out using the post-precipitation, resuspended protein pellet from the <3kDa fraction of sperm conditioned media as stimulus on a total of 109 OE-E6/E7 cells.

The <3kDa fraction of the pooled conditioned media retained efficacy in eliciting $[Ca^{2+}]_i$ signalling in the OE-E6/E7 cells after undergoing acetone precipitation, stimulating increases in $[Ca^{2+}]_i$ fluorescence when perfused across the surface of the cells. The Initial 3 minute period of perfusion with 100 mM ammonium bicarbonate solution in sEBSS did not elicit a rise in $[Ca^{2+}]_i$ in any of the OE-E6/E7 cells, but the introduction of the post-precipitation sperm conditioned media <3kDa fraction caused a rise in $[Ca^{2+}]_i$ within 64.2% of the cells, which was consequently washed away by the proceeding period of sEBSS perfusion, before a strong sustained peak was caused by the ATP positive control stimulus.

A BCA assay was used to quantify the protein content of the three fractions of precipitated pooled sperm conditioned media (shown in Appendix V) before they were sent for proteomic analysis, as described in section 4.2.6.

4.3.3- Proteomic analysis results from sperm conditioned media fractions

Table 4.1- Results from the proteomic analysis of the <3 kDa fraction of the pooled sperm conditioned media. This table displays the name of each protein identified, the number of peptides identified, the number of the identified peptides which were unique, as well as the number of amino acids and molecular weight of the identified protein.

Description	# Peptides	# Unique Peptides	# AAs	MW [kDa]
Semenogelin-1	6	5	462	52.1
Semenogelin-2	8	1	582	65.4
Multiple C2 and transmembrane domain-containing protein 2	1	1	878	99.5
Neurensin-2	1	1	204	22
E3 ubiquitin-protein ligase RNF34	1	1	507	56.8
cDNA FLJ76879	1	1	1220	139.3

The <3 kDa fraction of the pooled sperm conditioned media contained a total of 6 identifiable proteins. 4 of these proteins only had a single peptide identified, whilst semenogelin-1 and semenogelin-2 had 6 and 8 peptides identified, respectively. Of the 6 peptides identified from semenogelin-1, 5 were demonstrated to be unique, whilst only 1 of the peptides identified in semenogelin-2 were unique.

Table 4.2- Results from the proteomic analysis of the 3-50 kDa fraction of the pooled sperm conditioned media.

Description	# Peptides	# Unique Peptides	# AAs	MW [kDa]
Semenogelin-1	28	22	462	52.1
Semenogelin-2	21	1	582	65.4
Semenogelin-1 (Fragment)	5	1	93	10.4
Prostate-specific antigen (Fragment)	5	5	262	28.6
AMP deaminase 3	1	1	767	88.8
Epididymis secretory protein Li 2	2	2	146	15.8
Fibronectin	2	2	2477	272.2
NPC intracellular cholesterol transporter 2 (Fragment)	2	2	221	23.7
Follistatin-related protein 1	2	2	308	35
39S ribosomal protein L16, mitochondrial	1	1	251	28.4
Prolactin-inducible protein	2	2	146	16.6
Antileukoproteinase	2	2	132	14.3
WAP four-disulfide core domain protein 2	1	1	124	13
Diazepam binding inhibitor, splice form 1D(2)	1	1	144	16.1
Cystatin-S	1	1	141	16.2
cDNA FLJ30597 fis, clone BRAWH2009261	1	1	177	20.4
CD59 glycoprotein	1	1	128	14.2
Testicular tissue protein Li 61	1	1	540	60.6

The proteomic analysis of the 3-50 kDa fraction of the pooled sperm conditioned media identified 18 proteins. Semenogelin-1 and semenogelin-2 were also found in this fraction of the sperm conditioned media, as they were in the <3 kDa fraction. In this fraction there were 28 peptides identified from semenogelin-1 and 21 peptides from semenogelin-2, with 22 of them being unique to semenogelin-1 and 1 being unique to semenogelin-2. 5 peptides from a fragment of PSA were also identified, whilst the rest of the proteins present within this sample only had either 1 or 2 peptides identified.

The >50 kDa fraction of the pooled conditioned media contained over 400 unique proteins (full table of results included in Appendix VI). Semenogelin-1 and semenogelin-2 were also present in this fraction, meaning that these two proteins were identified in each of the three fractions of pooled sperm conditioned media that were sent for proteomic analysis. In the >50 kDa fraction, 27 peptides from semenogelin-2 were identified, of which, 1 was unique. 28 peptides from

semenogelin-1 were identified, with 10 of them being unique. PSA was also identified in the >50 kDa fraction with 13 peptides found, of which, 12 were unique.

Due to the presence of semenogelin-1 and semenogelin-2 in each of the fractions of sperm conditioned media that underwent proteomic analysis, combined with the Ca^{2+} imaging data suggesting that each of the fractions were capable of eliciting $[Ca^{2+}]_i$ signalling within the OE-E6/E7 cells to varying extents, these proteins warranted further investigation as a potential signalling factor. A range of peptides from semenogelin-1 and semenogelin-2 were present in each of the fractions of pooled sperm conditioned media, so a search was carried out to establish which peptides were present in each fraction.

4.3.4- Investigation and analysis of semenogelin-1 & semenoglein-2 peptides

Table 4.3- Peptides identified from semenogelin-1 and semenogelin-2 in the digested <3 kDa fraction of pooled sperm conditioned media, the positions of the amino acids that make up each peptide in the parent protein are also displayed.

Semenogelin-1 OS=Homo sapiens	
Annotated Sequence	Positions in Protein
[K].GESGQSTNREQDLLSHEQK.[G]	[405-423]
[K].QITIPSQEQEHSQK.[A]	[329-342]
[K].QEPWHGENAKGESGQSTNR.[E]	[395-413]
[R].EQDLLSHEQK.[G]	[414-423]
[K].GHYQNVVEVR.[E]	[218-227]
[R].LWVHGLSK.[E]	[166-173]
Semenogelin-2 OS=Homo sapiens	
Annotated Sequence	Positions in Protein
[K].SGQSADSKQDLLSHEQK.[G]	[527-543]
[R].IPSQAQEYGHK.[E]	[392-402]
[K].SQNQVTIPSQDQEHGHKENK.[M]	[446-465]
[K].GSISIQTEEK.[I]	[312-321]; [432-441]
[K].GQLPSGSSQFPHGQK.[G]	[30-44]
[K].ISYPSSR.[T]	[286-292]
[R].LWVHGLSK.[E]	[166-173]
[K].SQNQVTIPSQDQEHGHK.[E]	[446-462]

A total of 6 peptides were identified from semenogelin-1 and 8 were found in semenogelin-2. The peptides identified in semenogelin-1 represent a percentage coverage of 13% of the whole protein, whilst those found from semenogelin-2 represent a 17% coverage.

Semenogelin-1 OS=Homo sapiens	
Annotated Sequence	Positions in Protein
[R].KQGGSQSSYVLQTEELVANK.[Q]	[186-205]
[K].GRLPSEFSQFPHGQK.[G]	[30-44]
[R].HLAQHLNNDRNPLFT.[-]	[448-462]
[K].QEPWHGENAKGESGQSTNREQDLLSHEQK.[G]	[395-423]
[K].GESGQSTNREQDLLSHEQK.[G]	[405-423]
[R].KQGGSQSSYVLQTEELVANKQQR.[E]	[186-208]
[R].KSQQYDLNALHK.[AT]	[81-92]
[K].DIFSTQDELLVYNKNQHQTK.[N]	[252-271]
[R].KQGGSQSSYVLQTEELVANK.[Q]	[186-205]
[K].QITIPSQEQEHSQK.[A]	[329-342]
[K].QGGSQSSYVLQTEELVANK.[Q]	[187-205]
[R].HLGGSQQLLHNKQEGR.[D]	[99-114]
[K].VQTSLCPAHQDK.[L]	[234-245]
[R].LPSEFSQFPHGQK.[G]	[32-44]
[K].QEPWHGENAKGESGQSTNREQDLLSHEQK.[G]	[395-423]
[R].EQDLLSHEQK.[G]	[414-423]
[R].LWVHGLSKEQTSVSGAQK.[G]	[166-183]
[K].SQIQAPNPK.[Q]	[386-394]
[K].LVAGKSQIQAPNPK.[Q]	[381-394]
[R].LWVHGLSKEQTSVSGAQK.[G]	[166-183]
[K].GHYQNVVEVR.[E]	[218-227]
[K].GISSQYSNTEER.[L]	[154-165]
[K].DVSQSSIYSQTEEK.[A]	[308-321]
[K].SQKQITIPSQEQEHSQK.[A]	[326-342]
[K].ISYQSSSTEER.[HR]	[286-296]; [346-356]
[R].LWVHGLSK.[E]	[166-173]
[R].GTQNPSQDQGNSPSGK.[G]	[138-153]
[R].HLAQHLNNDRNPLFT.[-]	[448-462]
Semenogelin-2 OS=Homo sapiens	
Annotated Sequence	Positions in Protein
[K].SQNQVTIPSQDQEHGHKENK.[M]	[446-465]
[R].KSQQYDLNALHK.[AT]	[81-92]
[K].DIFTTQDELLVYNKNQHQTK.[N]	[252-271]
[K].SGQSADSKQDLLSHEQK.[G]	[527-543]
[K].SQNQVTIPSQDQEHGHKENK.[M]	[446-465]
[K].GQLPSGSSQFPHGQK.[G]	[30-44]
[K].DVSQSSISFQIEK.[L]	[488-500]
[R].IPSQAQEYGHK.[E]	[392-402]
[K].SGQSADSKQDLLSHEQKGR.[Y]	[527-545]
[K].SQNQVTIPSQDQEHGHK.[E]	[446-462]
[K].GSISIQTEEQIHGK.[S]	[372-385]
[K].DIFTTQDELLVYNK.[N]	[252-265]
[K].RLWVHGLSK.[E]	[165-173]
[K].SQIQTPNPNQDQWSGQNAK.[G]	[506-524]
[K].GSISIQTEEK.[I]	[312-321]; [432-441]
[R].TQGGSQSSYVLQTEELVVNK.[Q]	[186-205]
[K].DVSKGSISIQTEEK.[I]	[308-321]
[K].QDLLSHEQK.[G]	[535-543]
[K].ISYQSSSTEER.[HR]	[346-356]; [406-416]
[R].LWVHGLSK.[E]	[166-173]
[K].GHYQNVVDVR.[E]	[218-227]

Table 4.4- Peptides identified from semenogelin-1 and semenogelin-2 in the digested 3-50 kDa fraction of pooled sperm conditioned media, along with the relative positions of the amino acids that constitute each peptide within the sequence of the parent protein.

A total of 28 peptides were identified from semenogelin-1 and 21 peptides were found from semenogelin-2. The coverage of these peptides represents 58% of the sequence of semenogelin-1, whilst the coverage for semenogelin-2 was 39%.

Semenogelin-1 OS=Homo sapiens	
Annotated Sequence	Positions in Protein
[K].DIFSTQDELLVYNKNQHQTK.[N]	[252-271]
[K].VQTSLCPAHQDKLQHGSK.[D]	[234-251]
[R].KSQQYDLNALHK.[AT]	[81-92]
[K].GRLPSEFSQFPHGQK.[G]	[30-44]
[K].QEPWHGENAKGESGQSTNR.[E]	[395-413]
[R].KQGGSQSSYVLQTEELVANK.[Q]	[186-205]
[K].GESGQSTNREQDLLSHEQK.[G]	[405-423]
[K].DIFSTQDELLVYNK.[N]	[252-265]
[R].HLAQHLNNDRNPLFT.[-]	[448-462]
[R].HQHGSHGGLDIVIIEQEDDSDR.[H]	[426-447]
[K].NSHQNKGHYQNVVEVR.[E]	[212-227]
[K].LVAGKSQIQAPNPK.[Q]	[381-394]
[K].VQTSLCPAHQDK.[L]	[234-245]
[K].GSFSIQYTYHVDANDHDQSRK.[S]	[61-81]
[R].KSQQYDLNALHK.[AT]	[81-92]
[K].QEPWHGENAKGESGQSTNR.[E]	[395-413]
[K].GISSQYSNTEER.[L]	[154-165]
[K].SQIQAPNPK.[Q]	[386-394]
[K].GHYQNVVEVR.[E]	[218-227]
[R].HLGGSQQLLHNK.[Q]	[99-110]
[K].ISYQSSSTEER.[HR]	[286-296]; [346-356]
[R].EQDLLSHEQK.[G]	[414-423]
[K].QGGSQSSYVLQTEELVANK.[Q]	[187-205]
[R].HLAQHLNNDRNPLFT.[-]	[448-462]
[R].LWVHGLSK.[E]	[166-173]
[R].RLHYGENGVQK.[D]	[297-307]; [357-367]
[K].DVSQSSIYSQTEEK.[A]	[308-321]
[R].LPSEFSQFPHGQK.[G]	[32-44]
Semenogelin-2 OS=Homo sapiens	
Annotated Sequence	Positions in Protein
[K].GSFSIQHTYHVDINDHDWTR.[K]	[61-80]
[K].GHFHMIVIHHK.[G]	[121-131]
[K].GGQAHHGTQNPSQDQGNSPSGK.[G]	[132-153]
[K].SQNQVTIPSQDQEHGHKENK.[M]	[446-465]
[K].DIFTTQDELLVYNK.[N]	[252-265]
[K].DIFTTQDELLVYNKNQHQTK.[N]	[252-271]
[R].KSQQYDLNALHK.[AT]	[81-92]
[K].GSISIQTEEQIHGK.[S]	[372-385]
[R].TQGGSQSSYVLQTEELVVNK.[Q]	[186-205]
[K].RLWVHGLSK.[E]	[165-173]
[R].YKQESSESHNIVITEHEVAQDDHLTQQYNEDRNPIST.[-]	[546-582]
[K].GQLPSGSSQFPHGQK.[G]	[30-44]
[K].DVSQSSISFQIEK.[L]	[488-500]
[K].SGQSADSKQDLLSHEQK.[G]	[527-543]
[K].GHFHMIVIHHK.[G]	[121-131]
[K].GHYQNVVDVR.[E]	[218-227]
[K].QHLGGSQQLLNYK.[Q]	[98-110]
[K].GSISIQTEEK.[I]	[312-321]; [432-441]
[K].ISYQSSSTEER.[HR]	[346-356]; [406-416]
[K].GLSSQCSNTEK.[R]	[154-164]
[R].IPSQAQEYGHK.[E]	[392-402]
[R].LWVHGLSK.[E]	[166-173]
[K].QDLLSHEQK.[G]	[535-543]
[K].SQIQTPNPNQDQWSGQNAK.[G]	[506-524]
[K].SQIQTPNPNQDQWSGQNAK.[G]	[506-524]
[K].NSHQNKGHYQNVVDVR.[E]	[212-227]
[K].DIFTTQDELLVYNK.[N]	[252-265]

Table 4.5- Peptides identified from semenogelin-1 and semenogelin-2 in the >50 kDa fraction of pooled sperm conditioned media, along with the relative positions of the amino acids which make up each peptide within their respective parent protein.

A total of 28 peptides were identified from semenogelin-1 and 27 peptides were found from semenogelin-2. The total coverage of these peptides from semenogelin-1 was 75% of the overall sequence of the protein, whilst the coverage for the peptides identified from semenogelin-2 was 59%.

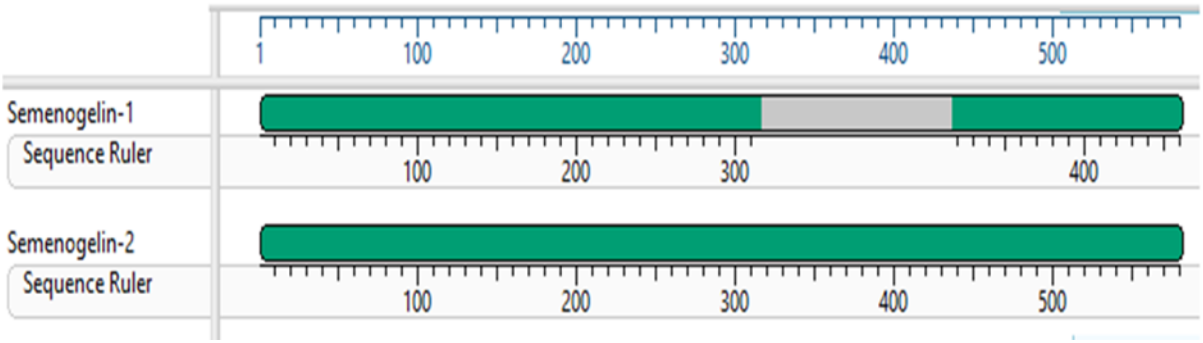


Figure 4.5- The alignment of the sequence of amino acids within semenogelin-1 against semenogelin-2.

The two sequence rulers in figure 4.5 show the alignment of semenogelin-1 in comparison to semenogelin-2. Semenogelin-1 has a total length of 462 amino acids with a 52.1 kDa, whilst semenogelin-2 is 582 amino acids in length with a 65.4 kDa. The similarities in the sequence of the two proteins are clear, with amino acid sequences showing alignment from the N terminus to amino acid 310 along the sequence ruler. At this point, semenogelin-2 contains an additional section, 120 amino acids in length. Sequence alignment between the two proteins then continues all the way to the C terminus.

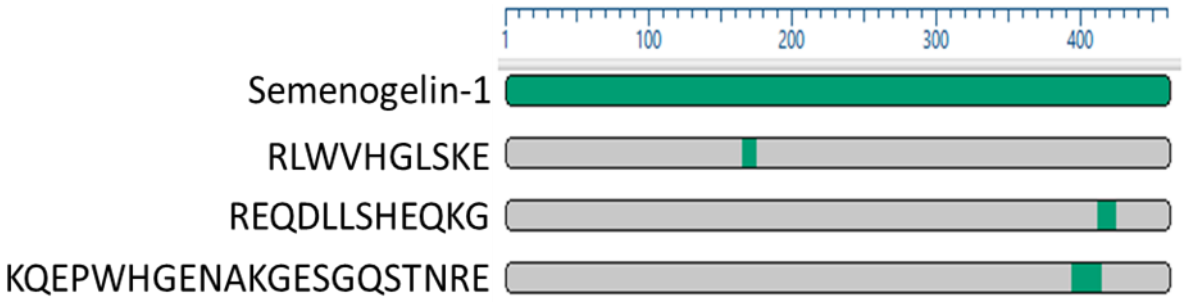


Figure 4.6- The only three semenogelin-1 peptides that were identified in each of the three fractions of pooled sperm conditioned media that underwent proteomic analysis. Their alignment within semenogelin-1 is represented by the green section of their respective sequence ruler.

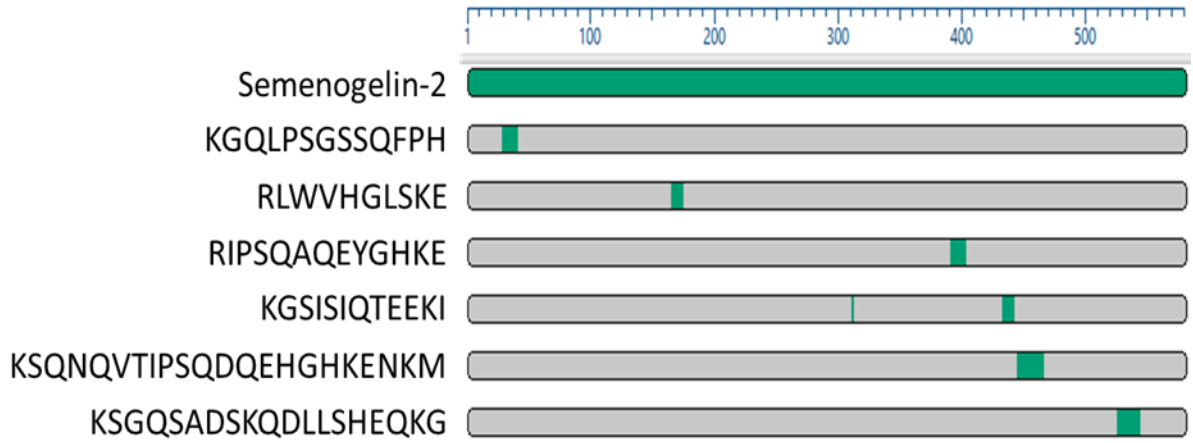


Figure 4.7- A total of six semenogelin-2 peptides that the proteomic analysis were identified in each of the three fractions of pooled sperm conditioned media sent for analysis. The alignment of each peptide within semenogelin-2 is represented by the green section of their sequence ruler.

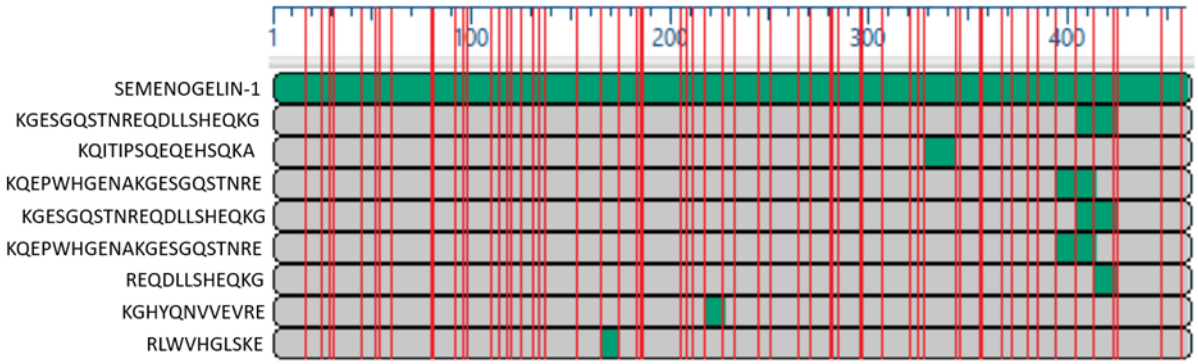


Figure 4.8- The alignment of each peptide identified in the <3kDa fraction of pooled sperm conditioned media, with red lines indicated the predicted sites of trypsin cleavage.

The fractions of pooled sperm conditioned media underwent digestion by the enzyme trypsin before the proteomic analysis was carried out. Predicted trypsin cleavage sites were derived from the DNASTAR structural analysis protein software. The sequence rulers shown in figure 4.8 for each of the peptides in the <3 kDa fraction contain red lines to indicate each of the predicted sites at which trypsin would cleave semenogelin-1. It is clear from this diagram that all the peptides identified could have been cleaved from a larger peptide by this trypsin digestion.

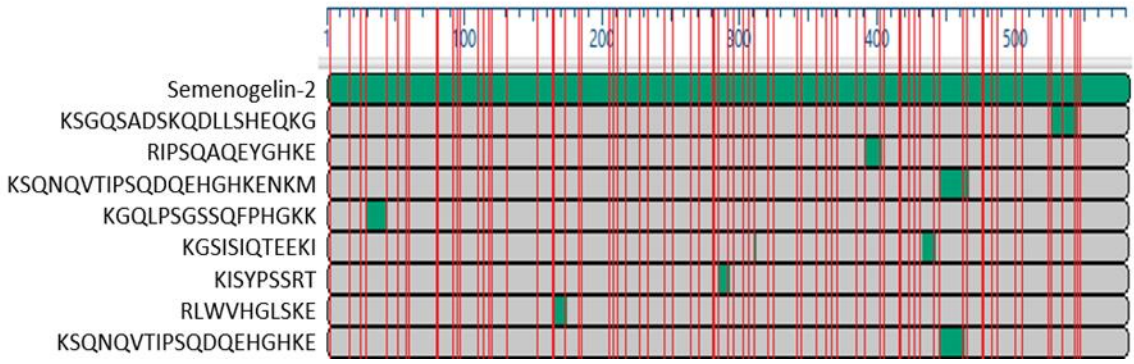


Figure 4.9- The alignment of each peptide identified in the <3kDa fraction of pooled sperm conditioned media, with red lines indicated the predicted sites of trypsin cleavage.

The semenogelin-2 peptides identified within the <3 kDa fraction are aligned with their parent protein in the collection of sequence rulers shown in figure 4.9. The red lines indicate predicted cleavage sites for the enzyme trypsin. The alignment of each identified peptide with the predicted trypsin cleavage sites suggests that the peptides were larger prior to digestion in preparation for proteomic analysis.

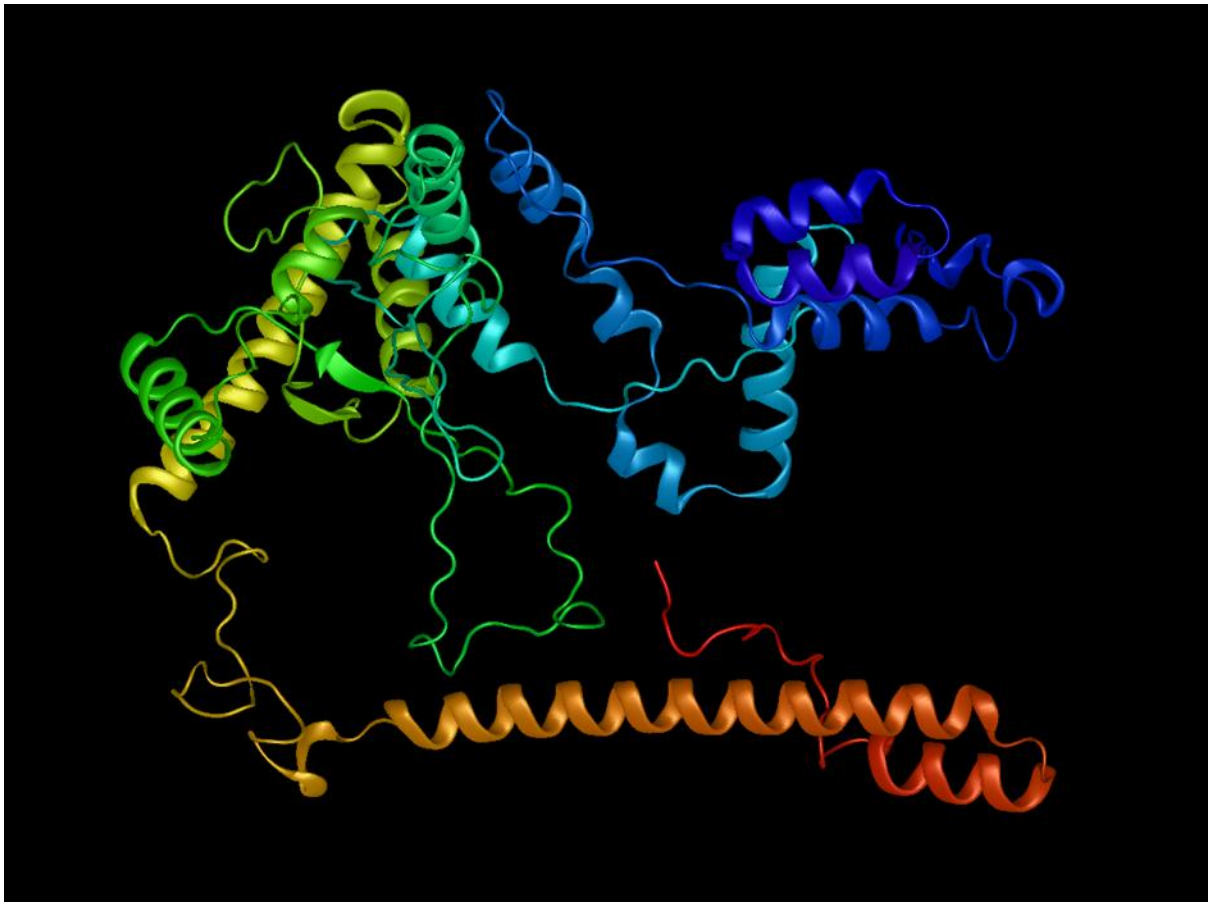


Figure 4.10- Predicted 3D structure of semenogelin-1, created using DNASTAR Protean 3D modelling software.

The colour scheme of this predicted 3D structure of semenogelin-1 indicates the order of the amino acid sequence, with blue indicating the N-terminal, gradually changing to red indicating the C-terminal. The predicted structure of this protein appears to contain 13 alpha helixes separated by varying lengths of amino acid chains.

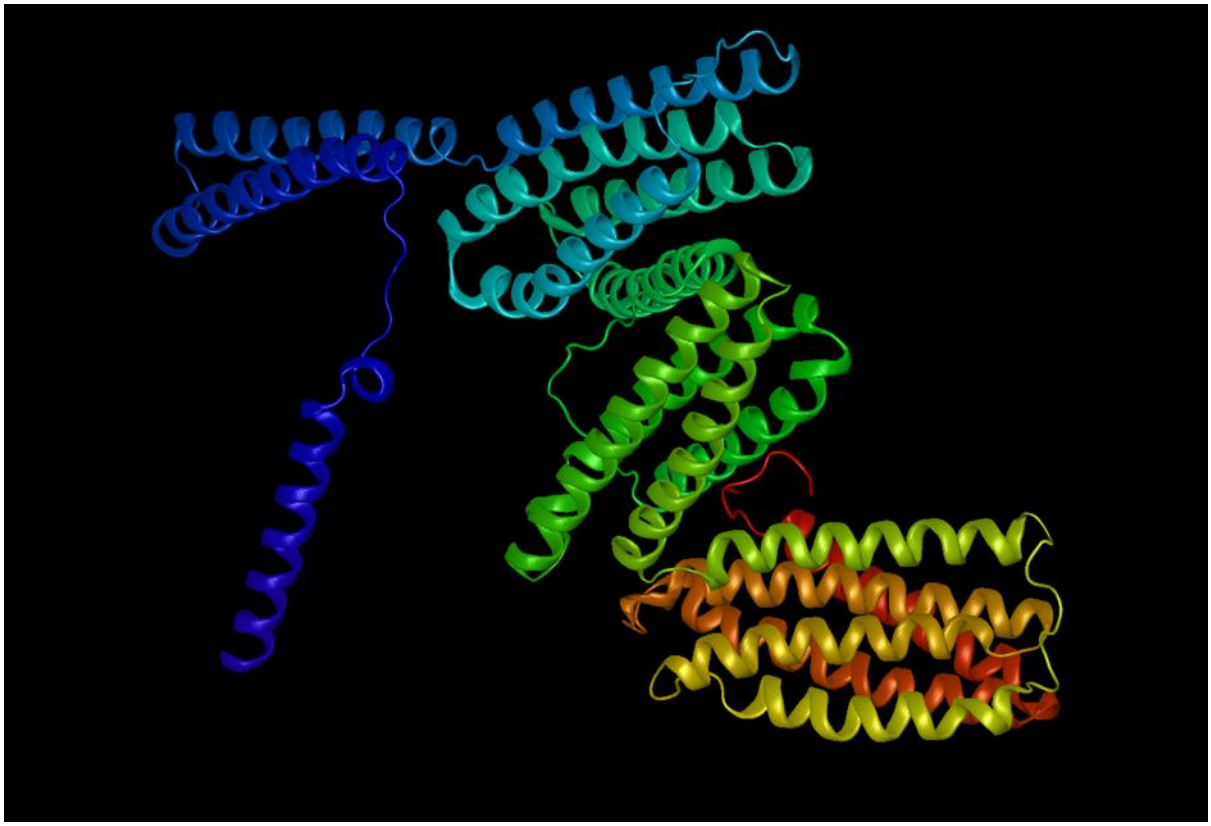


Figure 4.11- Predicted 3D structure of semenogelin-2, created using DNASTAR Protean 3D modelling software.

The colour scheme of this predicted 3D structure of semenogelin-2 indicates the order of the amino acid sequence, with blue indicating the N-terminal, gradually changing to red indicating the C-terminal. The predicted structure of this protein appears to contain 18 alpha helix domains separated by varying lengths of amino acid chains.

4.4- Discussion

The proteomic analysis of fractionated sperm conditioned media represents a novel approach to identifying male ejaculate derived factors that are potentially carried into the FRT beyond the cervical barrier. Previous studies have carried out proteomic analysis on spermatozoa and seminal fluid (Brewis and Gadella 2010, Jodar, Soler-Ventura et al. 2017, Agarwal, Panner Selvam et al. 2020), however, this is the first study that has attempted to simulate the passage of motile spermatozoa from seminal fluid, through a cervical mucus substitute and then attempted to identify any proteins which are carried by the spermatozoa and released into the FRT. This is also the first study to demonstrate that the factors carried into the FRT by loosely associating with spermatozoa are capable of eliciting $[Ca^{2+}]_i$ signalling within human FRT cells.

The fractionation of the sperm conditioned media using Amicon® Ultra Centrifugal Filters appeared to be successful in separating proteins within the media based on their size (kDa). The stated retention rate in the user manual for the filters at the volumes and concentrations of proteins used in this study were approximately 95%, which was a key limitation of this method of fractionation (Vergauwen, Dhondt et al. 2017) and for this reason the pooled sperm conditioned media was passed through each Amicon® Ultra Centrifugal Filter 3 times to ensure that the protein content of the media was sufficiently separated into distinct fractions. It would have been advantageous to utilise a method of fractionation with a higher yield such as high-resolution size exclusion chromatography, which is capable of separating proteins at similar molecular sizes with approximately 99.5% affinity (Stein, Heinen-Kreuzig et al. 2016).

All three of the fractions of sperm conditioned media were perfused across OE-E6/E7 cells in Ca^{2+} imaging experiments and it was clear that each of them were able to elicit the previously observed $[Ca^{2+}]_i$ signalling to varying extents, however, the >3 kDa was the most potent of the three fractions in this regard. Due to the efficacy of all three fractions eliciting $[Ca^{2+}]_i$ signalling in the OE-E6/E7 cells, all of them were sent for proteomic analysis. it was confirmed that the process of precipitation and resuspension of the protein content from each fraction in preparation for proteomic analysis did not lead to the removal of the signalling factors that we were searching for (Feist and Hummon 2015). This additional Ca^{2+} imaging experiment demonstrated that the preparation process for proteomic analysis allowed for the retention of sufficient concentrations of signalling factors to achieve the previously observed response in OE-E6/E7 cells, but also that the solubilised ammonium bicarbonate that the protein samples would be suspended in for proteomic analysis did not interfere with the observed $[Ca^{2+}]_i$ signalling.

The results of the proteomic analysis revealed a surprisingly small cohort of proteins present in the <3 kDa fraction of pooled sperm conditioned media, which has elicited the strongest level of $[Ca^{2+}]_i$ response in the OE-E6/E7 cells. Just 6 proteins were identified from the peptides present in this fraction, with the most abundant being semenogelin-1 and semenogelin-2. The 3-50 kDa fraction contained a wider range of proteins, with 18 in total being identified. Again, semenogelin-1 and semenogelin-2 were the most abundant in this fraction, with the third most abundant being PSA- an enzyme responsible for the cleavage and break down of the semenogelin proteins in seminal fluid (Mattsson, Ravela et al. 2014). A range of other proteins were identified, however, only a relatively low number of peptides were present from each of them in this fraction. The >50 kDa fraction contained the largest number of

proteins out of the three fractions tested, with over 400 proteins identified, with semenogelin-1, semenogelin-2 and PSA amongst the most abundant proteins in this fraction. Many other large proteins were present, including prolactin-inducible protein, mucin 6, epididymis secretory sperm binding protein and lactoferrin, however, due to their absence in the other fractions they were not deemed to be candidates for the male ejaculate signalling factors. The only proteins that were present in all three fractions of pooled sperm conditioned media were semenogelin-1 and semenogelin-2, therefore these two proteins were subject to further investigation as the potential source of the observed $[Ca^{2+}]_i$ signalling in the OE-E6/E7 cells.

Semenogelin-1 and semenogelin-2 are excreted by the seminal vesicles (Lilja and Lundwall 1992) and they are the most abundant proteins in human seminal plasma, representing approximately 30% of the protein concentration present in seminal plasma (Malm, Hellman et al. 1996). Together with fibronectin, these proteins form a gelatinous meshwork in freshly ejaculated semen, that entraps spermatozoa and inhibits their mobility (Robert, Gibbs et al. 1997). A fragment of the C-terminal of semenogelin-2 (amino acids 164 to 283 in the sequence) has been demonstrated to have an inhibitory effect on the motility of human spermatozoa (Mitra, Richardson et al. 2010). The N-terminal fragment of the same protein has also been shown to be the site of seminal plasma motility inhibitor (SPMI), which inhibits sperm motility in a dose-dependent and reversible manner (Robert and Gagnon 1996). Other notable biological functions of the semenogelin proteins include the increasing of sperm hyaluronidase activity (Mandal and Bhattacharyya 1995), contributing to the hyperpolarization and permeability of the sperm membrane (Yoshida, Krasznai et al. 2009), as well as antibacterial activity within the seminal plasma (Edström, Malm et al. 2008).

The retention of semenogelin 1 and semenogelin 2 peptides in each fraction of sperm conditioned media could be explained by the identified presence of the prostatic fluid enzymes which carry out the endogenous proteolysis of these proteins (Jonsson, Linse et al. 2005). Kallikrein-related peptidase 3, also known as PSA, is a protein that is secreted by the prostate gland (Lilja and Abrahamsson 1988). It is a trypsin-like protease that is produced in the prostatic epithelial cells, along with prostatic acid phosphatase and prostate secretory protein (Anamthathmakula and Winuthayanon 2020). The liquefaction of human semen is carried out by these proteases, by breaking down the gel matrix of semenogelin-1 and semenogelin-2, through the progressive and site-specific cleavage of the proteins into smaller peptides after their deposition into the FRT (Mattsson, Ravela et al. 2014). This process causes the semen to liquefy which leads to the facilitation of sperm cell motility (Lilja 1988). Upon the triggering of male ejaculation, seminal vesicle secretions (containing semenogelin-1 and semenogelin-1) are mixed with prostatic fluid secretions (enriched with PSA, prostatic acid phosphatase and prostate secretory protein, as well as inhibitory Zn^{2+} ions) and epididymal fluid containing spermatozoa. This mixture forms a matrix like gel of crosslinked semenogelin proteins which entrap the spermatozoa. The semenogelins have a higher affinity to Zn^{2+} than the prostatic fluid proteases, which leads to their disinhibition and the activation of their proteolytic activity in a Zn^{2+} dependent manner (Anamthathmakula and Winuthayanon 2020). This proteolytic activity causes the breakdown of semenogelin-1 and semenogelin-2, which liquefies the semen and allows the spermatozoa to gain progressive motility in the FRT (Anamthathmakula and Winuthayanon 2020).

The peptides formed by the breakdown of semenogelin-1 and semenogelin-2 have been shown to contribute to the progressive motility of spermatozoa and the prostatic fluid derived proteases are known to play important roles in the cleavage of precursor proteins into kinins, growth factors and other biologically active peptides (Lilja 1985, Lilja, Abrahamsson et al. 1989). It has been hypothesized that many of the other peptides formed by the proteolytic cleavage of semenogelin-1 and semenogelin-2 could have currently undiscovered biological functions, which makes these proteins ideal candidates for further investigation as potential male ejaculate derived signalling factors than interact with the cells of the FRT (Lilja, Abrahamsson et al. 1989). This series of experiments has demonstrated that many of the peptides formed by the breakdown of the semenogelins can potentially be carried into the upper FRT, since they were present in sperm conditioned media, showing that they were able to be carried through a cervical mucus substitute by motile spermatozoa (Ivic 2002). The reversible binding of semenogelin-1 and semenogelin-2 peptides to the surface of spermatozoa could be mediated by the Eppin protein, which forms a complex bound with semenogelins the surface of ejaculated spermatozoa (Wang, Widgren et al. 2005).

A comparison of the individual peptides derived from semenogelin-1 and semenogelin-2 that were present in each fraction was carried out. The <3 kDa fraction contained a much lower number of individual peptides than the other two fractions, which both contained similar amounts of peptides from each protein. Many of the peptides identified from semenogelin-1 were also present in semenogelin-2 due to the similarities in the amino acid sequence of between the two proteins (Lundwall, Bjartell et al. 2002). Due to their efficacy in eliciting $[Ca^{2+}]_i$ responses in the OE-E6/E7 cells to varying extents, it was hypothesised that each of the three

fractions contained signalling factors from the male ejaculate. Therefore, a search was carried out to identify which semenogelin-1 and semenogelin-2 peptides were consistently found within each of the fractions of pooled sperm conditioned media that were sent for proteomic analysis. This search greatly narrowed down the range of peptides that warranted further investigation, with just 3 semenogelin-1 peptides present in each fraction and 6 peptides derived from semenogelin-2. Only one of these 9 peptides was present in the sequence of both proteins (RLWVHGLSKE), so this was the logical initial candidate peptide for further experimentation.

The precipitated proteins from each of the fractions of sperm conditioned media underwent digestion by the enzyme trypsin prior to the proteomic analysis (Simpson 2006). For this reason, models were made of the predicted trypsin cleavage sites on semenogelin-1 and semenogelin-2, to see if the predicted sites of cleavage on the proteins was aligned with the observed peptides identified by the proteomic analysis (Siepen, Keevil et al. 2007). Each of the peptides identified in the <3 kDa fraction was in alignment with sites on the protein that would be cleaved by trypsin. This suggests that the peptides formed by the proteolytic cleavage of the semenogelins by prostatic fluid proteases could have been further broken down by the trypsin digestion as a preparation step for the proteomic analysis. This would mean that the peptides identified in the proteomic analysis could belong to larger peptides and this represents one of the limitations of this type of proteomic analysis (Siepen, Keevil et al. 2007). In attempting to identify, synthesize and assess the efficacy of the candidate male ejaculate derived signalling factors, we may be missing key parts of the amino acid sequence of the peptides that have been cleaved away by trypsin digestion. This is a commonly occurring problem in proteomics as over-digestion by trypsin can lead to a decline in amino acid coverage and the loss of tryptic peptides,

with an increased number of small peptides that are not detectable (Hildonen, Halvorsen et al. 2014).

The predicted 3D protein structures of semenogelin-1 and semenogelin-2 are the first documented predictions of the tertiary structure of these proteins. The protein folding predictions were achieved using NovaFold, which is part of the DNASTAR Protean 3D interface software. This software uses the I-TASSER algorithm (Zhang 2008) which utilises a combination of “threading” and “ab initio folding” to predict the structure of proteins. “Threading” matches amino acid sequences are input to template sequence available in the protein data bank, whilst “ab initio” folding determines the structure of a protein based on biophysical properties of an input amino acid sequence (Roy, Kucukural et al. 2010). The primary sequences of semenogelin-1 and semenogelin-2 are very similar, however, based on the predicted 3D structures of the proteins shown in figures 4.10 and 4.11 the differences in their tertiary structure are surprisingly apparent. Semenogelin-2 appears to have a much higher amount of alpha helix structures than semenogelin-1, even in sections of the sequence where the amino acids are aligned. This could be due to differences in the overall primary sequence of the two proteins, or it could be a representation of the limitations of current protein structure prediction software (Zhang 2008).

In conclusion, this series of experiments has confirmed the hypothesis that soluble but stable protein factors, which are loosely associated with sperm cells and can be carried into the upper regions of the FRT elicit Ca^{2+} signalling in the epithelial cells of the oviduct. The proteomic analysis of the fractionated sperm conditioned media has provided a list of candidate proteins. By highlighting semenogelin-1 and semenogelin-2 as reoccurring proteins that were identified in each of the three fractions of media, it was possible to identify the range of peptides formed by the

breakdown of these proteins by prostatic fluid derived proteases (Mattsson, Ravela et al. 2014). A shortlist of 9 candidate peptides within semenogelin-1 and semenogelin-2 was produced. The scientific basis for these peptides having the potential to be biologically active has been established (Lilja, Abrahamsson et al. 1989) and they will be ideal primary targets for synthesis and further experimentation with the Ca^{2+} imaging setup utilised so far in this study due to their relative abundance within semen (Lilja, Abrahamsson et al. 1989, Jonsson, Lundwall et al. 2006) as well as their strong presence within the sperm conditioned media as indicated by the proteomic analysis herein, however, the other proteins identified in this study should also be considered as potential key signalling moieties or cofactors.

The next step in this investigation was the synthesis of candidate semenogelin peptides to assess their efficacy in eliciting Ca^{2+} signalling in OE-E6/E7 cells. In addition, experiments were carried out with a range of alterations to the experimental design and the use of inhibitors to elucidate the mechanism of action behind the observed Ca^{2+} signalling. TLR4 signalling has previously been identified as a major mediator of the female tract response to seminal fluid in murine models (Schjenken, Glynn et al. 2015), therefore, the involvement of this Ca^{2+} signalling pathway in the human derived OE-E6/E7 cells was investigated. Attempts were also made to establish whether the Ca^{2+} oscillations observed within the OE-E6/E7 cells are derived from an extracellular source or if they rely upon the release of Ca^{2+} from intracellular stores (Bouschet and Henley 2005).

Chapter 5

Semenogelin peptide synthesis and investigation into Oviductal Epithelial Cell $[Ca^{2+}]_i$ signalling mechanism of action

5.1- Introduction

5.1.1- Semenogelin peptide experiments

Peptides derived from the proteolytic cleavage of semenogelin-1 and semenogelin-2 by endogenous PSA have been identified as candidate factors that may be responsible for the intracellular Ca^{2+} signalling events that have been observed in OE-E6/E7 cells in response to the perfusion of sperm conditioned media across their surface. The synthesis and purification of these peptides would allow for them to be assessed for their efficacy in eliciting Ca^{2+} signalling in OE-E6/E7 cells in the absence of contaminating factors. The next series of experiments set out to determine their identity as the male ejaculate derived factors capable of interacting with the epithelial cells of the human FRT. In addition to carrying out experiments with these specific semenogelin peptides, the intention of this series of experiments was to further elucidate the mechanism of action of the observed signalling by utilising a range of media, inhibitors, and techniques.

The development of solid-phase peptide synthesis (SPPS) has allowed for the synthesis of peptides to become a more prominent approach in recent scientific research (Coin, Beyermann et al. 2007). SPPS is a method of synthesising peptides in a way which retains chemical properties that have been proven in solution with the addition of a covalent attachment that links the chain of amino acids within the peptide to an insoluble polymeric support referred to as a resin (Fields 2001). The peptide can then be extended or replicated by addition cycles before the process is completed with the introduction of excess soluble reagents, which can then be removed by filtration and washed away without causing any detrimental manipulation to the peptide. Once the elongation of the peptide chain is complete, it can be

removed from the insoluble polymeric support, producing a purified peptide (Fields 2001).

The use of synthesised peptides in experiments aiming to discover ligands responsible for biological mechanisms of action and cellular signalling has been widely demonstrated (Labrou 2003, Gruber, Muttenthaler et al. 2010, Vishwanath, Banerjee et al. 2017, Quartararo, Gates et al. 2020). A common method is the selection of several candidate peptides that are determined to be potential ligands for the signalling being investigated which are then synthesised and used as stimuli in experiments. The negative control stimulus is often a “scrambled” control peptide (Bang, Park et al. 2020), which is a peptide that consists of the same amino acids as the experimental peptides but the sequence is scrambled into a random order to prove that the sequence specificity is essential. If amino acid composition was the sole determinant of biological activity, then the scrambled peptides should also elicit signalling (Hilpert, Elliott et al. 2006). This approach was used with the semenogelin peptides, with the synthesis of two candidate peptides as well as a scrambled negative control peptide for use in $[Ca^{2+}]_i$ imaging experiments with OE-E6/E7 cells.

It should not be neglected that certain signalling mechanisms may also involve or require posttranslational modifications, such as the tertiary glycosylation of the protein (Furukawa, Ohkawa et al. 2012). Glycosylation affects the three dimensional configuration of proteins, significantly altering their protein-protein interactions and thus plays a key role in the regulation of their function as signalling agents (Lee, Qi et al. 2015). This posttranslational modification has been demonstrated to have a role in the regulation of intracellular signalling proteins, such as the adenylate cyclase mediated conversion of cAMP to ATP (Beazely and Watts 2006). Such modifications are something that SPPS cannot deliver in the synthesised peptides,

which is a potential weakness of this experimental approach (Shen, Huang et al. 2011).

5.1.2- Elucidation of the mechanisms of action in the signalling pathway

Aside from investigating the specific factor responsible for the observed signalling, this series of experiments aims to elucidate the mechanism of action responsible for the Ca^{2+} oscillations within the FRT cells in response to the male ejaculate. The intention of a mechanism of action study is to attempt to understand the way in which a specific compound interacts with its target, seeking to determine the natural substrates and physiological concentrations that can modulate this activity (Strelow et al. 2012). There are a wide range of experimental approaches that can be utilised to elucidate a biological mechanism of action, perhaps the most common of which is the use of inhibitors (Li and Kang 2020).

A toll-like receptor 4 (TLR4) inhibitor was selected for experimentation with the OE-E6/E7 cells to investigate whether the inhibition of this receptor was able to prevent the observed $[Ca^{2+}]_i$ oscillations in response to sperm conditioned media. TLR4 acts as a mediator for transient receptor potential canonical (TRPC) channels which induce Ca^{2+} entry into cells (Tauseef, Knezevic et al. 2012) and has been identified as a major mediator of the female tract response to seminal fluid in a murine model (Schjenken, Glynn et al. 2015). Although the key differences between murine and human sites of ejaculation and potential for male ejaculate derived signalling in the female tract have been previously discussed (Suarez and Pacey 2005), a murine model in which affymetrix microarray was used to provide a comparison of gene expression between mice 8 hours after they had been mated with either intact males or males which had their seminal vesicles ablated showed differentiation in the expressed genes in the FRT cells and demonstrated that TLR4 signalling was a

predicted upstream regulator of the changes elicited by the murine seminal fluid (Schjenken, Glynn et al. 2015). The identification of TLR4 signalling as a vital component of the FRT response to seminal fluid in mice makes the inhibition of this pathway in a human model an ideal method of investigating the mechanism of action for the previously observed signalling, in lieu of similar human-based studies on male ejaculate signalling in the FRT cells.

Intracellular Ca^{2+}concentrations control a wide range of cellular processes such as gene transcription, cell death and many other cellular processes in involved in fertilisation (Puri 2020). Increases in intracellular Ca^{2+} can either occur via the influx of Ca^{2+} from an extracellular source across the plasma membrane or via release from intracellular Ca^{2+} stores, which in the case of epithelial cells is the endoplasmic reticulum (Clapham 2007). The release of Ca^{2+} from the endoplasmic reticulum can be initiated by a range of secondary messengers or pathways, such as cyclic ADP ribose (cADPr) (Lee 1997), inositol 1,4,5-triphosphate (IP_3) (Schlossmann, Ammendola et al. 2000) or even calcium-induced calcium release (Roderick, Berridge et al. 2003). One method of determining whether cellular Ca^{2+} signalling is derived from the influx of extracellular Ca^{2+} or due to the release of Ca^{2+} from intracellular stores is the use of Ca^{2+} free media during the introduction of stimuli that usually initiate the signalling (Brown and Iadarola 2015). By perfusing OE-E6/E7 cells with Ca^{2+} free sEBSS and then sperm conditioned media also produced using Ca^{2+} free sEBSS, it was possible to determine the source of the Ca^{2+} in the observed OE-E6/E7 cell Ca^{2+} oscillations elicited by the male ejaculate derived signalling factors. The absence of signalling in the presence of Ca^{2+} free media would suggest an extracellular source, whilst an intracellular peak in Ca^{2+} upon the addition of Ca^{2+}

free sperm conditioned media would suggest that the Ca^{2+} was released from intracellular stores.

Thapsigargin is a lactone derived from the root of the Thapsia garganica plant which has been shown to elicit transient elevations of intracellular Ca^{2+} and the depletion of intracellular Ca^{2+} stores in a wide range of cell types (Jackson, Patterson et al. 1988). This cellular response to thapsigargin is due to it acting as a highly specific, potent inhibitor of the ATPases present on intracellular Ca^{2+} stores, effectively preventing the reuptake of Ca^{2+} into the endoplasmic reticulum which leads to a depletion of intracellular Ca^{2+} stores and the prevention of any further signalling which relies upon those stores (Rogers, Inesi et al. 1995). This makes thapsigargin an ideal inhibitor to utilise in the experimental design outlined in this study, as the depletion of intracellular Ca^{2+} stores in the OE-E6/E7 cells, followed by the introduction of sperm conditioned media to the cells would clarify whether the observed $[Ca^{2+}]_i$ oscillations in the cells were derived from an extracellular source or from a signalling pathway initiating the release of Ca^{2+} from intracellular stores (Sabała, Amler et al. 1997).

Aside from the maintenance of signalling after acetone precipitation (Crowell, Wall et al. 2013), it has not been decisively determined whether these signalling events occurring in the cells of the FRT are being elicited by a protein, a small peptide, or some other form of signalling agent such as a metabolite. One method of clarifying this is to use a dialysis system to remove small molecules from the sperm conditioned media and then reassess the efficacy of the solution in eliciting $[Ca^{2+}]_i$ signalling in the OE-E6/E7 cells. Conventional methods of dialysis allow for the separation of small molecules, such as peptides and metabolites, from large molecules in a solution by diffusion through a selectively permeable membrane

(Andrew, Titus et al. 2002). An effective and relatively inexpensive method of carrying out the dialysis of small peptides from a solution is the use of dialysis cassettes, which are commercially available with a selection of molecular weight-cut off (MWCO) sizes to only allow for the permeation of molecules of specific sizes (Saokham, A et al. 2016). Utilising this method of dialysis with sperm conditioned media could elucidate the type and approximate size of the signalling molecule responsible for the observed signalling.

The intention of this series of experiments is initially to synthesise and assess the efficacy of the peptides derived from semenogelin-1 and semenogelin-2 that have previously been discussed and their ability to elicit the observed Ca^{2+} signalling events in the OE-E6/E7 cells. In addition, a range of inhibitors and experimental techniques discussed here will be employed to determine the involvement of the TLR4 signalling pathway in the elicitation of these signals in a human model (Schjenken, Glynn et al. 2015) and to further elucidate the mechanism of action for this signalling, seeking to identify the source of the Ca^{2+} responsible for the intracellular oscillations in the OE-E6/E7 cells in response to factors from the male ejaculate.

5.2- Materials & Methods

5.2.1- Materials

0.2 µM PES syringe filters, (Corning). 100mm tissue-culture treated culture dishes, (Corning). 12mm round coverslips, (Warner instruments). 15 mL centrifuge tubes, (Falcon). 15 mL plastic disposable syringes, (ThermoFisher Scientific). 2 mm inner diameter translucent silicone tubing (Fisher Scientific). 22x32mm coverslips, (Appleton Woods). 25cm^2 tissue culture flasks, (Falcon). 5 mL Round Bottom High Clarity PP Test Tubes, (Falcon). 75cm^2 tissue culture flasks, (Falcon). Adenosine-5'-triphosphate (ATP), (Sigma). Calcium Green-1 AM, (Invitrogen). Dulbecco's modified Eagle's medium (DMEM), no phenol red, (Gibco™). DMEM/F12, no phenol red, (Gibco™). Earle's balanced salt solution, no calcium, no phenol red, (ThermoFisher Scientific). Iscove's modified Dublecco's medium (IMDM), no phenol red, (Gibco™). DMEM/F12, no phenol red, (Gibco™). Foetal bovine serum, (Sigma-Aldrich). Methylcellulose, viscosity: 4000cP, (Sigma-Aldrich). PBS tablets, (ThermoFisher Scientific). Penicillin-Streptomycin (10,000 U/mL), (Gibco™). Pluronic F-127 10% in DMSO, (Sigma-Aldrich). PureSperm 40, (Nidacon). PureSperm 80 (Nidacon). Series 20 perfusion chambers, (Warner Instruments). Slide-A-Lyzer™ Dialysis Cassettes, 2K MWCO, 3 mL, (ThermoFisher Scientific). Supplemented Modified Earle's balanced salt solution (sEBSS), (Lab Industries) (described in Appendix I). Thapsigargin ≥98% (HPLC), solid film, (Merck). TLR4-IN-C34, ≥98% (HPLC), (Merck). Trypsin-EDTA solution 10x, (Sigma-Aldrich).

5.2.2- Synthesis of semenogelin peptides

Two peptides were selected for synthesis based on their presence in each of the three fractions of sperm conditioned media that were utilised as stimuli in $[Ca^{2+}]_i$ imaging experiments on OE-E6/E7 cells as outlined in section 2.2.8. The first peptide selected was also present in both semenogelin-1 and semenogelin-2, meaning that it was the most common denominator peptide out of the 9 candidates identified. The first peptide selected for synthesis was “RLWVHGLSKE” whilst the second was “REQDLLSHEQKG”, which is a semenogelin-1 specific peptide that was identified in each of the three fractions of sperm conditioned media. The sequence of these two peptides was extended to include the full amino acid sequence of their parent peptides that would be produced endogenously based on the cleavage sites of PSA, meaning that the sequence of peptides sent for synthesis were “SNTEERLWVHGLSKEQTSVSGAQKGRKQGGSQSSYVLQTEEL VANKQQRETKNSHQNKGHYQ” and “REQDLLSHEQKGRHQHGSHGGLDIVIIEQEDDSDRHLAQHLN NDRNPLFT”, forming “peptide 1” and “peptide 2” respectively. In addition to these peptides, the synthesis of a third scrambled peptide using the same amino acids present in peptide 2 intended was carried out. Peptide 3 was intended for use as a negative control for sequence specificity and its sequence was “LGQEDRDLLTDVIFLSRRIEQKHDLQNSEPNHDEGRANIHLQQ HHGSDGH”.

The synthesis of the two semenogelin peptides and the negative control scrambled peptide was carried out by Pepscan, a company based in the Netherlands which specialises in custom peptide synthesis. The sequence of the peptides were delivered to Pepscan and they were then synthesised using SPPS. The use of ultra-high performance liquid chromatography (UPLC) equipment in combination with

stringent analytical conditions allowed them to synthesise the peptides which were then delivered as a lyophilized white powder, with a certificate of analysis containing all the relevant analytical data including the ES-MS mass spectrometric details and reversed-phase UPLC-profiles.

5.2.3- Ca^{2+} imaging experiments with semenogelin peptides

The three synthesized semenogelin peptides were used as stimuli in Ca^{2+} imaging perfusion timelapse experiments with OE-E6/E7 cells as described in section 2.2.8 after being solubilised in sEBSS at 100 µM concentration. Following an initial 3 minute period of sEBSS perfusion to assess baseline levels of $[Ca^{2+}]_i$ fluorescence, the three solubilised semenogelin peptides were each gently perfused over the surface of the OE-E6/E7 cells for 2 minutes each. Three replicates of this experiment were carried out, each with the three peptides perfused across the OE-E6/E7 cells in different orders. An additional Ca^{2+} imaging perfusion timelapse was carried out in which the OE-E6/E7 cells were perfused with peptides one, two and three in consecutive order, before 3-minute sEBSS wash period, followed by 3 minutes of sperm conditioned media perfusion. All of these experiments ended with a 3-minute period of 100 µM ATP solution in sEBSS as a positive control stimulus.

5.2.4- Ca^{2+} imaging experiments with TLR4 inhibitor

To investigate the involvement of the TLR4 signalling pathway in the observed $[Ca^{2+}]_i$ signalling in OE-E6/E7 cells, the TLR4 inhibitor TLR4-IN-C34 was utilised. Briefly, TLR4-IN-C34 was solubilised in a small volume of DMSO, before being diluted to 100 µM concentration in sEBSS. This TLR4-IN-C34 solution was added to the perfusion chamber with OE-E6/E7 and incubated for 30 minutes, prior to the addition of Calcium Green-1 AM solution to the chamber as described in section 2.2.7. Ca^{2+} imaging perfusion timelapse experiments were then carried out (section 2.2.8) to

assess the effect of TLR4 inhibition on the capability of sperm conditioned media to elicit $[Ca^{2+}]_i$ signalling in OE-E6/E7 cells.

5.2.5- Ca^{2+} imaging experiments with Ca^{2+} free sEBSS

The effect of removing Ca^{2+} from the perfusion media on the $[Ca^{2+}]_i$ signalling in OE-E6/E7 cells was assessed using calcium free sEBSS. A standard Ca^{2+} imaging perfusion timelapse experiment was then carried out, according to the protocol laid out in section 2.2.8, but the initial 3-minute perfusion period was carried out using calcium free sEBSS, the sperm conditioned media was produced with calcium free sEBSS, calcium free sEBSS was perfused during the proceeding wash period and the 100 µM solution was suspended in calcium free sEBSS.

5.2.6- Ca^{2+} imaging experiments with <2 kDa dialysed sperm conditioned media

Dialysis of the sperm conditioned media was performed using a Slide-A-Lyzer™ Dialysis Cassettes, 2K MWCO, 3 mL, to remove peptides that were smaller than 2 kDa from the media and then assess the capacity of the dialysed media to elicit $[Ca^{2+}]_i$ signalling in OE-E6/E7 cells. The dialysis was performed by inserting a syringe into the port on the dialysis cassette and injecting a 3 mL sample of the sperm conditioned media, before withdrawing the excess air inside the cassette. The cassette was then suspended in a beaker filled with sEBSS and left at room temperature for 2 hours before being placed into a 4°C fridge and left overnight to dialyse. The next day an empty syringe was inserted into the port on the cassette and air was injected into it until full before the dialysed media was aspirated. This <2 kDa dialysed sperm conditioned media was then used in Ca^{2+} imaging timelapse experiments with OE-E6/E7 cells according to the protocol laid out in section 2.2.8.

5.2.7- Ca^{2+} imaging experiments with thapsigargin

Thapsigargin was used to block the sarco/endoplasmic reticulum Ca^{2+} ATPase (SERCA) on the OE-E6/E7 cells to assess the effect of blocking reuptake of Ca^{2+} back into the intracellular stores after it has been released. Thapsigargin was suspended in sEBSS at a working concentration of 2 μM. A Ca^{2+} imaging perfusion timelapse experiment with OE-E6/E7 cells was then carried according to the protocol laid out in section 2.2.8, but after the initial 3-minute period of sEBSS perfusion, the 2 μM thapsigargin solution was introduced to the perfusion chamber and continuously perfused across the surface of the OE-E6/E7 cells for a prolonged period of 20 minutes, before sperm conditioned media containing 2 μM thapsigargin was perfused across the cells for 2 minutes, a wash period then commenced with sEBSS perfusion for 10 minutes until the $[Ca^{2+}]_i$ reached a steady baseline again, before 5 minutes of positive control 100 μM ATP solution perfusion.

5.3- Results

5.3.1- Ca^{2+} imaging experiments with semenogelin peptides

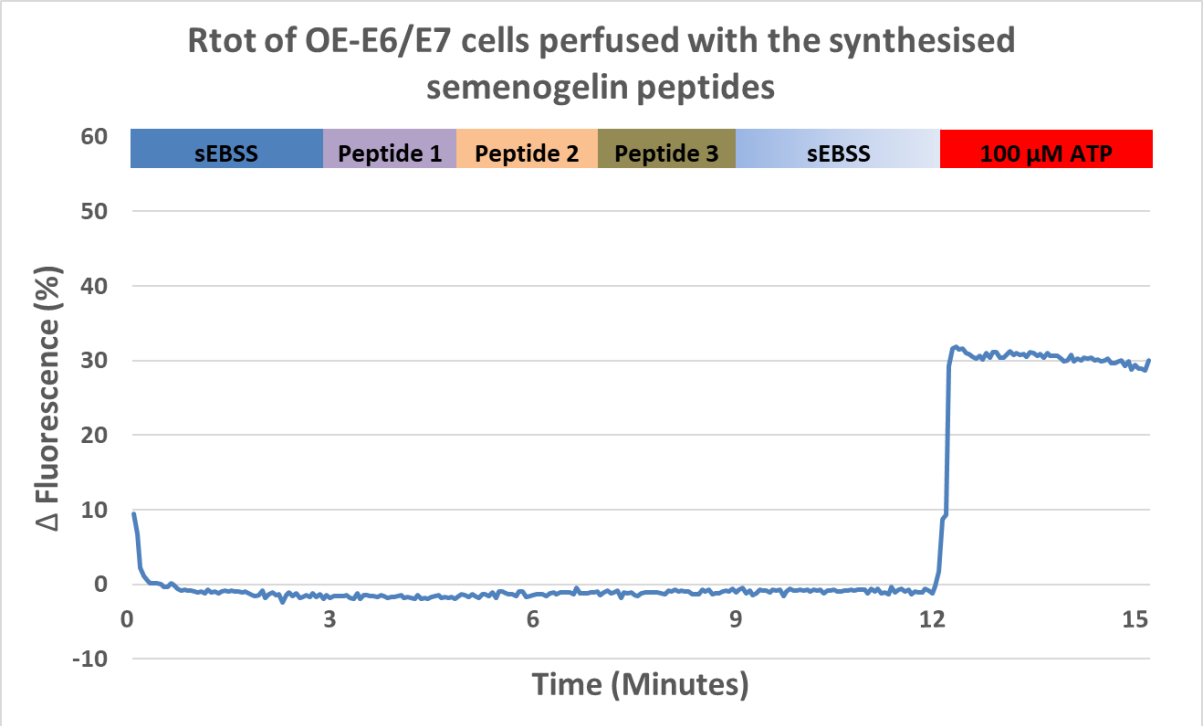


Figure 5.1- Rtot average fluorescence timelapse plot from 2 experiments in which a total of 244 OE-E6/E7 cells were perfused with the three synthesized semenogelin peptides. The cells were initially perfused with sEBSS for 3 minutes, followed by 2 minutes of solubilised peptide 1 perfusion, then peptide 2 and 3, each for 2 minutes. This period was followed by a 3-minute sEBSS perfusion wash and finally a 3-minute ATP solution perfusion.

The three synthesised semenogelin peptides were assessed for their efficacy in eliciting Ca^{2+} signalling in the OE-E6/E7 cells. The peptides were perfused across the surface of the cells in two separate experiments in which the fluorescence levels in a total of 244 cells were measured. Figure 5.1 is the Rtot plot showing the average fluorescence within each of the 244 from both experiments during these experiments. It is clear from these average fluorescence timelapse plots that none of the three semenogelin peptides were capable of eliciting the previously observed $[Ca^{2+}]_i$ signalling in OE-E6/E7 cells. The average fluorescence intensity consistently

remains at baseline levels throughout the stimulus perfusion periods and sEBSS wash, with a sustained elevation in $[Ca^{2+}]_i$ observed when the ATP positive control stimulus is added to the perfusion chamber.

Between the control period of sEBSS perfusion and the introduction of peptide 1 to the perfusion chamber 85% of the cells across both experiments were identified as showing no change in fluorescence, whilst 9.8% of the cells showed a decrease and 5.1% of the cells increased. Between the perfusion of peptide 1 and peptide 2, 85% of cells again showed no change in $[Ca^{2+}]_i$ whilst 2.4% decreased and 12.6% increased. Between peptide 2 and peptide 3 perfusion 85.8% of the cells showed no change in fluorescence again, 6.3% decreased and 7.9% increased. As the sEBSS wash period of perfusion began, 88.2% of OE-E6/E7 cells showed no change in fluorescence whilst 2.8% decreased and 9% increased. The perfusion of ATP solution across the surface of the cells elicited a rise in $[Ca^{2+}]_i$ within 95.7% of the OE-E6/E7 cells. A subset of the cells from one of these experiments exhibited a constant, gradual rise in $[Ca^{2+}]_i$ throughout the entire perfusion experiment which represents the majority of the cells identified as showing a rise in fluorescence. A full table of response rates from these experiments is shown in appendix VII.i.

This experiment was repeated in duplicate with alternating orders of peptide perfusion, with two experiments carried out in the perfusion order of peptide 3-2-1 and another two experiments carried out in the order of peptide 2-1-3. Similar results were observed and the data from these experiments are included in appendix VII.io and VII.iii.

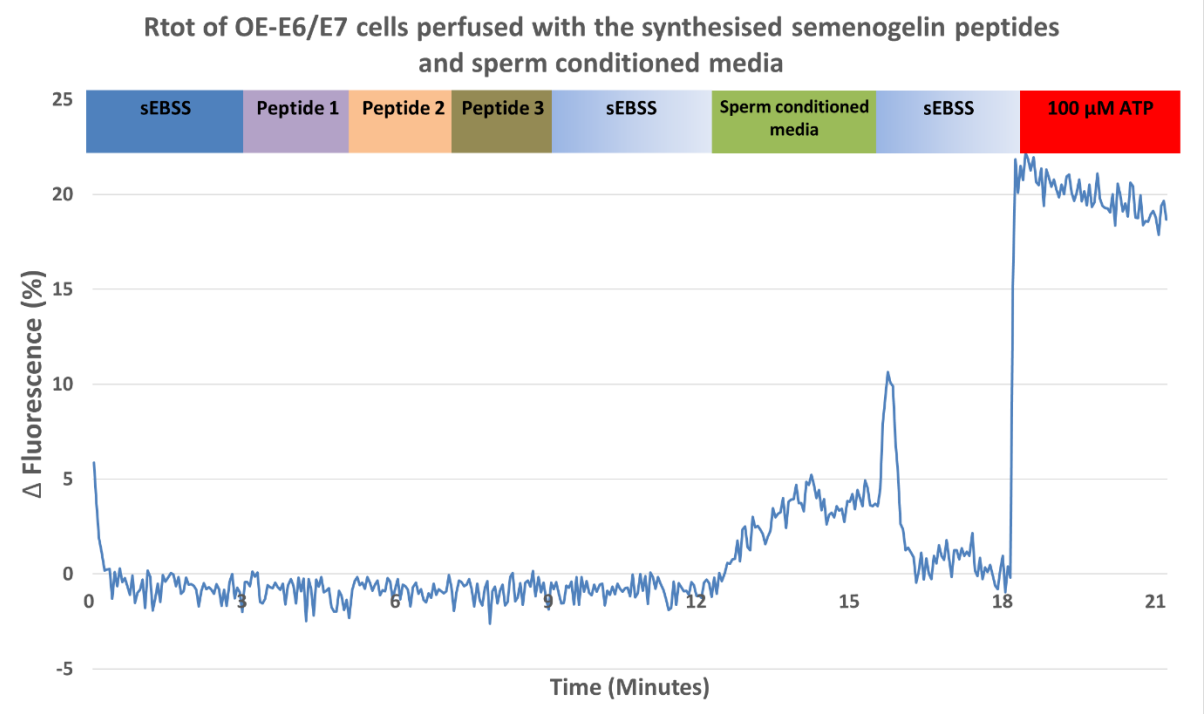


Figure 5.2- Rtot average fluorescence timelapse plot from an experiment in which 103 OE-E6/E7 cells were perfused with the three synthesized semenogelin peptides and sperm conditioned media for comparison of response. The cells were initially perfused with sEBSS for 3 minutes, followed by 2 minutes of solubilised peptide 1 perfusion, then peptide 2 and 3, each for 2 minutes. This period was followed by a 3-minute sEBSS perfusion wash, then 3 minutes of sperm conditioned media before another 3-minute sEBSS wash period and finally a 3-minute ATP solution perfusion.

To compare the OE-E6/E7 cell $[Ca^{2+}]_i$ response to the three synthesised semenogelin peptides with sperm conditioned media, an experiment was carried out in which all three solubilised peptides were perfused across the surface of the cells, followed by sperm conditioned media to allow for direct comparison of the response. Figure 5.4 shows the Rtot plot from this experiment. It is clear from this data that none of the three semenogelin peptides were able to elicit the previously observed $[Ca^{2+}]_i$ responses in the OE-E6/E7 cells when directly compared to the clear

response observed with the perfusion of sperm conditioned media. ATP, as usual, elicited a strong and sustained peak in $[Ca^{2+}]_i$.

The introduction of peptide one to the perfusion chamber elicited a rise in $[Ca^{2+}]_i$ within 1.9% of the cells in this experiment, whilst peptide 2 caused a rise in 2.9% of the cells and peptide 3 elicited a further increase in none of the OE-E6/E7 cells. In contrast, an increase in fluorescence was identified in 57.3% of the cells when they were perfused with sperm conditioned media and the ATP solution elicited a rise in 100% of the cells in this experiment. Full details of the OE-E6/E7 cells responses to these stimuli are included in appendix VII.iv.

5.3.2- Ca^{2+} imaging experiment with TLR4-IN-C34

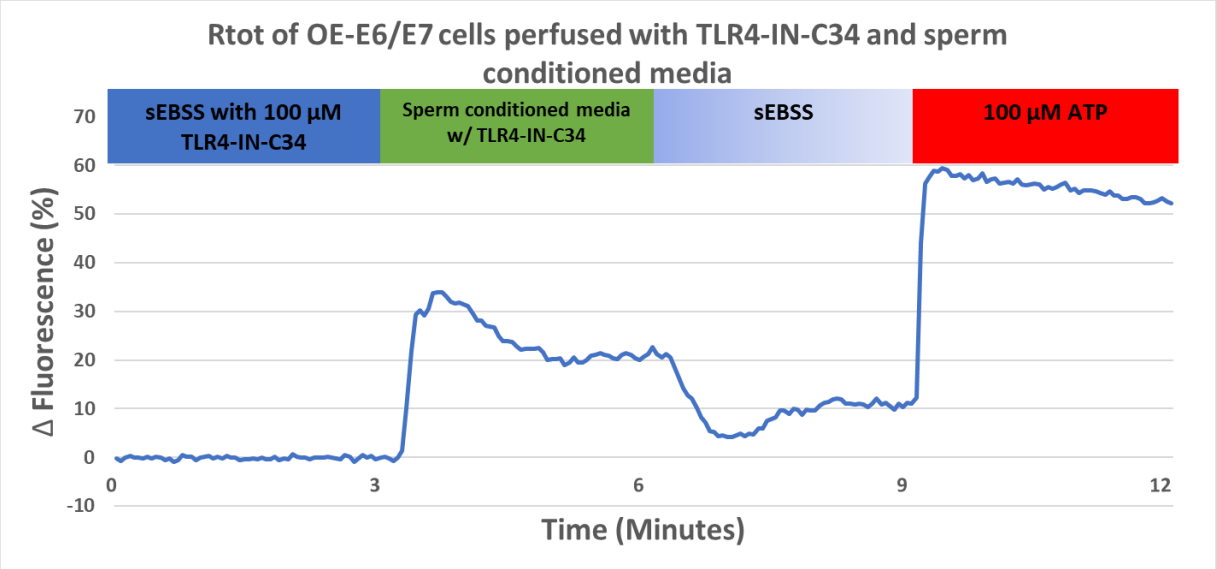


Figure 5.3- Rtot average fluorescence timelapse plot from an experiment in which 97 OE-E6/E7 cells which had been co-incubated with TLR4-IN-C34 were perfused with sperm conditioned media. The cells were initially perfused with sEBSS with 100 µM of TLR4-IN-C34 for 3 minutes, followed by 3 minutes of sperm conditioned media containing 100 µM of TLR4-IN-C34 perfusion. This period was followed by a 3-minute sEBSS perfusion wash and finally a 3-minute ATP solution perfusion.

To investigate the involvement of the TLR4 signalling pathway in the induction of the observed Ca^{2+} signalling, the OE-E6/E7 cells imaged in this experiment had been incubated with TLR4-IN-C34 for 30 minutes prior to being stained with Calcium green-1 AM. The initial 3 minutes of the experiments involved the perfusion of sEBSS with 100 µM of the TLR4-IN-C34 to ensure that inhibition of the TLR4 receptors was maintained. Upon the introduction of sperm conditioned media with 100 µM TLR4-IN-C34 to the perfusion chamber, a clear rise in $[Ca^{2+}]_i$ was observed in the OE-E6/E7 cells, which was sustained until the proceeding sEBSS wash period began. The $[Ca^{2+}]_i$ levels were reduced by this wash but did not quite reach the observed baseline levels of fluorescence before the ATP positive control elicited a strong, sustained peak in $[Ca^{2+}]_i$.

Despite the presence of TLR4-IN-C34, the introduction of sperm conditioned media into the perfusion chamber elicited an increase in $[Ca^{2+}]_i$ within 97.9% of the OE-E6/E7 cells, whilst 2.1% showed no increase and none of them exhibited a decrease in fluorescence. The perfusion of the ATP solution across their surface led to 100% of the cells in this experiment being identified as showing an increase in fluorescence. Full details of the OE-E6/E7 cells responses during this experiment are included in appendix VII.v.

5.3.3- Ca^{2+} imaging experiments with Ca^{2+} free media

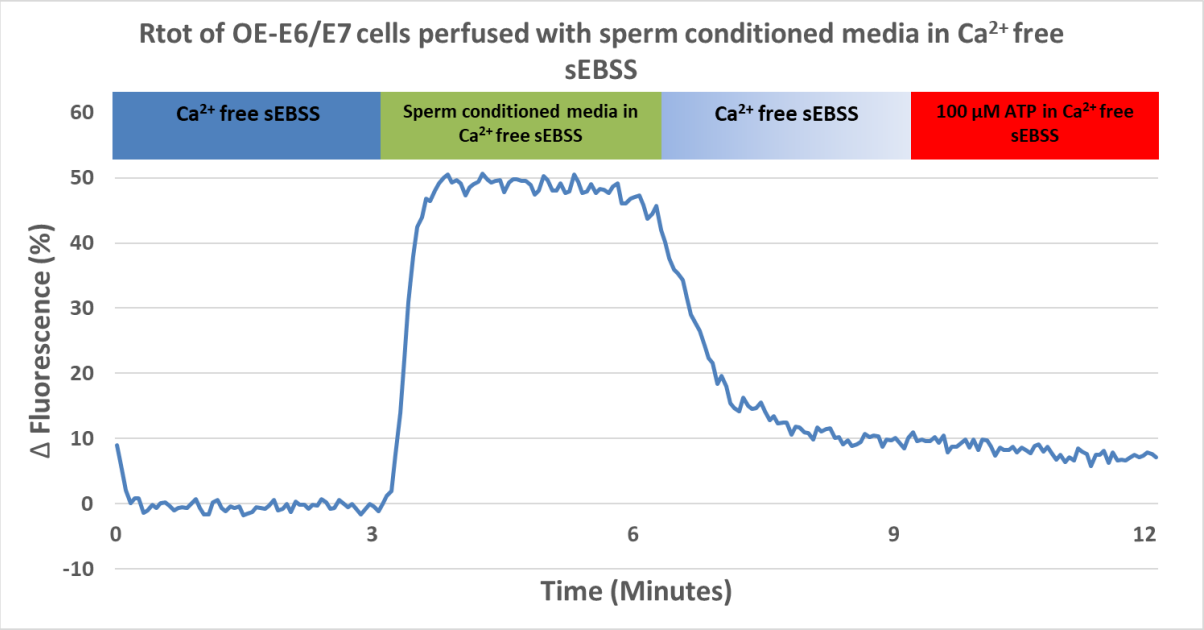


Figure 5.4- Rtot average fluorescence timelapse plot from an experiment in which 176 OE-E6/E7 cells were exposed to Ca^{2+} free sEBSS and sperm conditioned media. The cells were initially perfused with Ca^{2+} free sEBSS 3 minutes, followed by 3 minutes of sperm conditioned media Ca^{2+} free sEBSS perfusion. This period was followed by a 3-minute Ca^{2+} free sEBSS perfusion wash and finally a 3-minute ATP solution in Ca^{2+} free sEBSS perfusion.

The necessity of extracellular Ca^{2+} in the maintenance of the previously observed Ca^{2+} signalling in the OE-E6/E7 cells was investigated in this experiment using Ca^{2+} free media. The initial 3 minutes of Ca^{2+} free sEBSS perfusion led to a steady baseline level of $[Ca^{2+}]_i$ in the OE-E6/E7 cells. When the perfusion of sperm conditioned media in Ca^{2+} free sEBSS began, a strong and sustained rise in $[Ca^{2+}]_i$ was observed, which was maintained until the beginning of the Ca^{2+} free sEBSS wash period. At this point, the $[Ca^{2+}]_i$ in the OE-E6/E7 cells began to reduce almost to baseline levels before settling. The introduction of the ATP positive control under these conditions did not elicit any form of $[Ca^{2+}]_i$ peak in the OE-E6/E7 cells and the reduced levels of $[Ca^{2+}]_i$ were maintained.

The perfusion of sperm conditioned media in Ca^{2+} free sEBSS across the surface of the OE-E6/E7 cells elicited an increase in fluorescence within 100% of the cells measured in this experiment. The initiation of the subsequent Ca^{2+} free sEBSS wash period caused a

decrease in fluorescence within 100% of the cells and then the introduction of the ATP solution to the perfusion chamber caused an increase in just 5.7% of the OE-E6/E7 cells, whilst 63.1% were identified as showing no change in fluorescence and 31.2% showed a decrease. Full details of the OE-E6/E7 cells responses during this experiment are included in appendix VII.vi.

5.3.4- Ca^{2+} imaging experiment with Thapsigargin

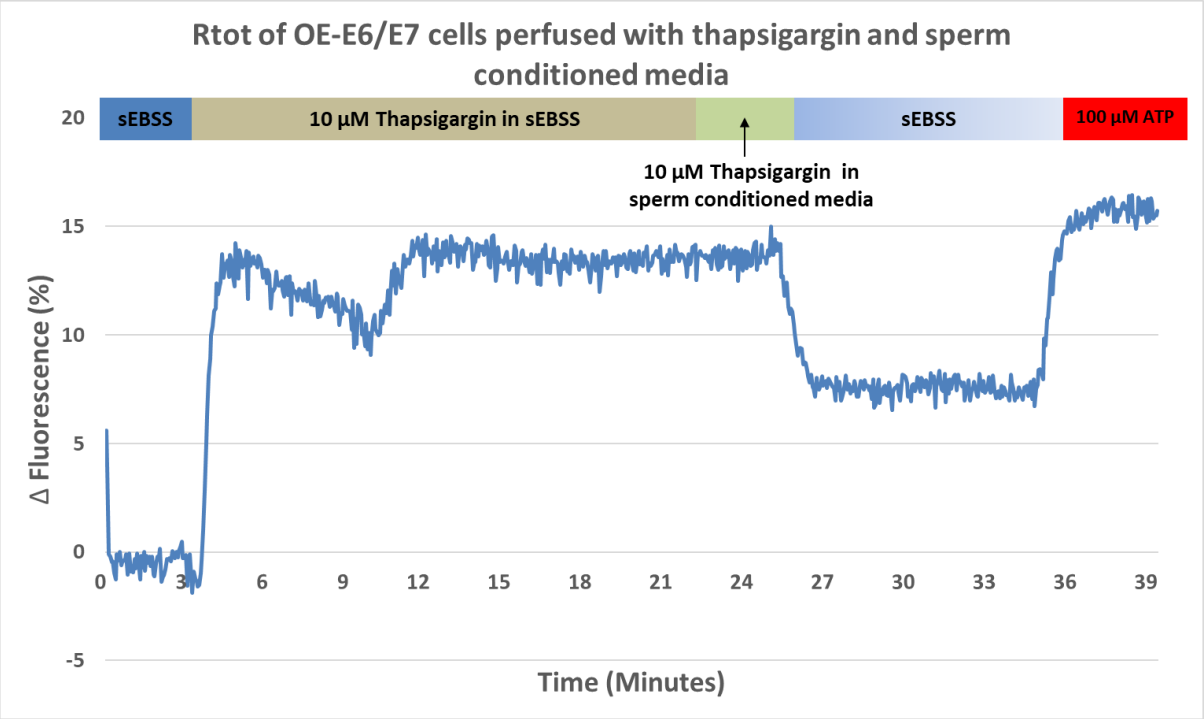


Figure 5.5- Rtot average fluorescence timelapse plot from an experiment in which OE-E6/E7 cells were treated with 10 µM thapsigargin before assessing the effect of sperm conditioned media. The cells were initially perfused with sEBSS for 3 minutes before an extended 20-minute period of perfusion with 10 µM thapsigargin solution in sEBSS. Sperm conditioned media containing 10 µM thapsigargin was then introduced to the perfusion chamber for 2 minutes, before being washed away by sEBSS for 10 minutes. Finally, the 100 µM ATP solution was perfused across the surface of the OE-E6/E7 cells for 4 minutes.

To test whether the release of Ca^{2+} from intracellular stores within the OE-E6/E7 cells is necessary for the initiation of the observed $[Ca^{2+}]_i$ signalling, the cells were treated with 10 µM thapsigargin before the perfusion of sperm conditioned media, also containing 10 µM thapsigargin, across their surface. The addition of 10 µM thapsigargin in sEBSS after the initial baseline sEBSS perfusion period led to a sharp rise in $[Ca^{2+}]_i$ which declined slightly before rising once again and reaching a plateau. As this $[Ca^{2+}]_i$ plateau was maintained by the thapsigargin solution, sperm conditioned media with 10 µM thapsigargin was introduced to the perfusion chamber. At this point, the levels of $[Ca^{2+}]_i$ in the OE-E6/E7 cells appeared to remain constant

despite the addition of the sperm conditioned media to the perfusion chamber. This elevated plateau of $[Ca^{2+}]_i$ was then washed away by sEBSS perfusion, stabilising at a higher level than was observed in the initial sEBSS perfusion period, before the introduction of ATP solution elicited a further sustained peak in $[Ca^{2+}]_i$.

The level of fluorescence within 134 OE-E6/E7 cells was recorded throughout this experiment. Upon the addition of the 10 μM thapsigargin in sEBSS to the perfusion chamber, a rise in $[Ca^{2+}]_i$ was identified in 86.6% of the cells, whilst 2.2% showed a decrease and 11.2% showed no change in fluorescence. After the $[Ca^{2+}]_i$ appeared to reach a plateau with the extended perfusion period of 10 μM thapsigargin in sEBSS, the addition of sperm conditioned media, also containing 10 μM thapsigargin, caused only 3.7% of the OE-E6/E7 cell to exhibit a further increase in fluorescence, whilst 96.3% showed no change and none of the cells were identified as decreasing. The initiation of the sEBSS wash period caused 89.6% of the cells to decrease in fluorescence and the final period of ATP solution perfusion elicited an increase in fluorescence within 73.9% of the OE-E6/E7 cells. Full details of the OE-E6/E7 cells responses during this experiment are included in appendix VII.vii.

5.3.5- Ca^{2+} imaging experiment with dialysed sperm conditioned media

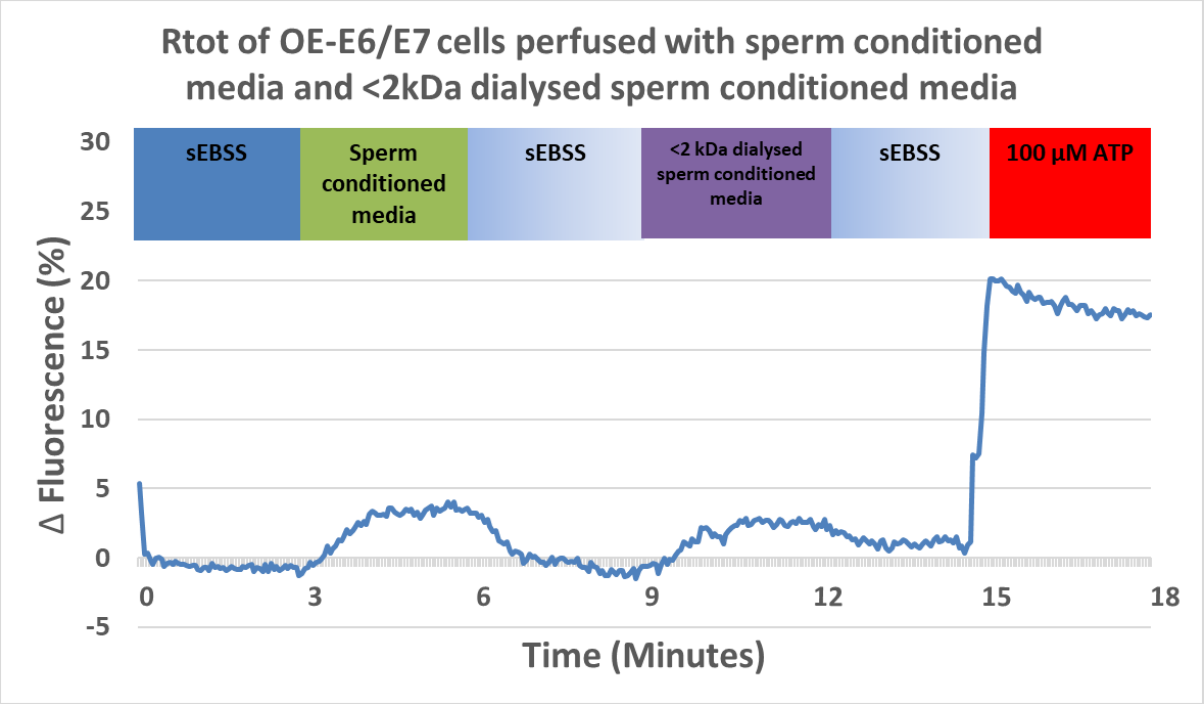


Figure 5.6- Rtot average fluorescence timelapse plot from experiments in which <2 kDa dialysed sperm conditioned media was compared to sperm conditioned media perfusion (total of 309 OE-E6/E7 cells across 3 experiments). The cells were initially perfused with sEBSS for 3 minutes before 3 minutes of sperm conditioned media perfusion. This was followed by a 3-minute sEBSS wash period and then a 3-minute period of <2kDa dialysed sperm conditioned media perfusion. An additional 3-minute sEBSS wash period then began before a final 3 minutes of ATP solution perfusion.

To assess the impact of removing small peptides below 2kDa from the sperm conditioned media on the observed $[Ca^{2+}]_i$ signalling in the OE-E6/E7 cells, dialysis was carried out on the sperm conditioned media before it was used as a stimulus in a Ca^{2+} imaging perfusion experiment. In this experiment the signalling elicited by sperm conditioned media could be directly compared to the signalling initiated by <2kDa dialysed sperm conditioned media on the same monolayer of OE-E6/E7 cells. Figure 5.8A shows the three individual Rtot plots from experiments in which OE-E6/E7 cells were perfused with both <2 kDa dialysed sperm conditioned media and sperm conditioned media for comparison. Figure 5.8 shows the overall Rtot plot for

these 3 experiments. Once the sperm conditioned media was introduced to the perfusion chamber after the initial 3 minutes sEBSS perfusion, a clear rise in $[Ca^{2+}]_i$ was observed in the OE-E6/E7 cells. This response was washed away by the subsequent sEBSS perfusion before a very similar rise in $[Ca^{2+}]_i$ was observed when <2 kDa dialysed sperm conditioned media was added to the chamber. This response was partially washed away by the following sEBSS perfusion period, with the ATP positive control once again eliciting a very strong and sustained peak in $[Ca^{2+}]_i$.

Throughout these three experiments, the perfusion of sperm conditioned media across the surface of the 309 OE-E6/E7 cells elicited an increase in $[Ca^{2+}]_i$. within 98.4% of the cells, whilst 1.6% were identified as showing no change in fluorescence and none of the cells exhibited a decrease. In comparison, the perfusion of <2 kDa dialysed sperm conditioned media across their surface elicited an increase in fluorescence within 61.4% of the OE-E6/E7 cells, whilst 37.3% showed no change and fluorescence was decrease in 1.3% of the cells. The ATP solution elicited an increase in $[Ca^{2+}]_i$ in 100% of the OE-E6/E7 cells. Full details of the OE-E6/E7 cells responses during this experiment are included in appendix VII.viii.

5.4- Discussion

5.4.1- Experiments with synthesised Semenogelin peptides

It was clear that none of the synthesised semenogelin peptides were capable of eliciting the $[Ca^{2+}]_i$ oscillations that had been observed in previous experiments with sperm conditioned media perfusion. This suggests that these specific peptides are not the male ejaculate derived signalling factors that this series of experiments was established to identify, however, the lack of observed signalling could also be due to the process of peptide synthesis and their lack of post-translational modifications (Müller 2018). A common negative aspect of the use of synthesised peptides as a substitute for purified endogenously produced peptides in biological mechanism of action studies are the differences in glycosylation and other post-translational modifications of proteins that may occur *in vivo* (Ramazi and Zahiri 2021), which may not be present in synthetically produced peptides of the same sequence. These modifications can have a significant impact on the physiochemical properties of peptides and alter the way in which they interact with receptors and biological membranes (Moradi, Hussein et al. 2016). For this reason, the experiments carried out with peptides 1, 2 and 3 may not provide conclusive evidence that the endogenous peptides of the same amino acid sequence, formed by the proteolytic cleavage of their parent proteins are incapable of eliciting $[Ca^{2+}]_i$ signalling in OE-E6/E7 cells.

In order to further investigate these peptides and the others identified in the proteomic analysis, which were not synthesised due to funding limits, it may be necessary to isolate and purify peptides derived from human semenogelin-1 and semenogelin-2, perhaps by deploying affinity chromatography (Cuatrecasas 1970),

before using them as stimuli in further Ca^{2+} imaging experiments to ensure that their physiologically acquired post-translational modifications are intact (Udeshi, Compton et al. 2008). Equally, as pointed out in the previous chapter, there are a number of other candidate proteins we have identified. The semenogelins are the most abundant proteins in the ejaculate (Lilja, Abrahamsson et al. 1989), but a less abundant protein could be the cause of this observed signalling.

5.4.2- Experiments to elucidate the signalling mechanism of action

A number of key aspects of the mechanism of action that causes the $[Ca^{2+}]_i$ signalling in OE-E6/E7 cells to arise in response to the presence of factors from the male ejaculate were elucidated. The treatment of OE-E6/E7 cells with TLR4-IN-C34 to inhibit the TRPC channels route of Ca^{2+} entry into the cells from an extracellular source (Tauseef, Knezevic et al. 2012) failed to prevent the $[Ca^{2+}]_i$ oscillations from occurring upon the introduction of sperm conditioned media into the perfusion chamber. This result suggests that the TLR4 mediated pathway of cellular Ca^{2+} signalling is not responsible for the communication between the male ejaculate signalling factors and the cells of the FRT in humans, despite evidence in murine models suggesting that this pathway is a significant upstream regulator of changes in gene expression which occur in FRT cells in response to seminal fluid (Schjenken, Glynn et al. 2015).

The use of Ca^{2+} free sEBSS in Ca^{2+} imaging experiments with OE-E6/E7 cells and sperm conditioned media led to some interesting results, in which the lack of extracellular Ca^{2+} from the sEBSS surrounding the OE-E6/E7 cells led to a sharp rise in $[Ca^{2+}]_i$ upon the introduction of sperm conditioned media made with Ca^{2+} free sEBSS to the perfusion chamber, which could then be washed away by further Ca^{2+} free sEBSS perfusion. The following period of positive control 100 μM ATP solution

in Ca^{2+} free sEBSS interestingly failed to elicit the usual sustained peak of $[Ca^{2+}]_i$ in the cells. This suggests that the perfusion of sperm conditioned media across the OE-E6/E7 cells stimulates the release of Ca^{2+} from the intracellular stores (Brown and Iadarola 2015). The subsequent wash with Ca^{2+} free sEBSS would elicit the expulsion of Ca^{2+} from the cells as there would be a large concentration gradient between the cytoplasm and the extracellular media (Joseph, Coll et al. 1985). Due to the lack of Ca^{2+} in the extracellular media, the intracellular Ca^{2+} stores would be unable to replenish significantly during this wash period, which would cause the observed lack of $[Ca^{2+}]_i$ response to the perfusion of 100 μM ATP solution in Ca^{2+} free sEBSS. ATP is known to stimulate the release of Ca^{2+} from intracellular stores via the phospholipase C beta/IP3 pathway (Salter and Hicks 1995), so the lack of response demonstrated with Ca^{2+} free media suggests that the intracellular stores have been depleted by the signalling elicited by sperm conditioned media in Ca^{2+} free sEBSS.

The treatment of the OE-E6/E7 cells with thapsigargin provided further evidence that the observed $[Ca^{2+}]_i$ signalling events are derived from the release of Ca^{2+} from intracellular stores. After perfusing the thapsigargin solution across the surface of the cells for an extended period to allow the intracellular Ca^{2+} levels to plateau and the stores to become depleted (Shoback, Chen et al. 1995), the introduction of sperm conditioned media containing 10 μM of thapsigargin did not elicit a further rise in intracellular Ca^{2+} in the cells. This suggests that the depletion of the intracellular Ca^{2+} stores was sufficient to prevent the usual Ca^{2+} oscillations elicited by the signalling factors present in the male ejaculate (Sabała, Amler et al. 1997). If the source of the Ca^{2+} that causes the observed oscillations in the OE-E6/E7 cells originated from an extracellular source, then a further rise in fluorescence would have been observed

upon the addition of sperm conditioned media to the perfusion chamber, as additional Ca^{2+} would have entered the cell from the extracellular media (Kline and Kline 1992). In addition to the results from the experiments with Ca^{2+} free sEBSS, this observation provides further evidence that the signalling factor from the male ejaculate that interacts with the cells of the FRT initiates a signalling cascade that stimulates the release of Ca^{2+} from the intracellular stores.

The use of Slide-A-Lyzer™ dialysis membrane cassettes to remove peptides and metabolites less than 2 kDa from the sperm conditioned media solution did not completely eliminate the $[Ca^{2+}]_i$ signalling in the OE-E6/E7 cells. There was, however, a reduction in the number of cells exhibiting an increase in $[Ca^{2+}]_i$, with 61.4% of the cells responding to the dialysed media with increased fluorescence compared to 98.4% of cells responding to standard sperm conditioned media. This result suggests that this method of dialysis was not sufficient to remove the signalling factors from the media, however, the concentration of the signalling factors was reduced sufficiently to cause a reduction in response rates. This data is not definitive, but it does suggest that the molecule eliciting the $[Ca^{2+}]_i$ signalling in the OE-E6/E7 cells is a small ligand, less than 2 kDa in size, which may be either a peptide belonging to a larger protein or a small metabolite. In order to confirm this hypothesis, a more effective method of small peptide removal must be carried out, such as high-resolution size exclusion chromatography (Stein, Heinen-Kreuzig et al. 2016).

In conclusion, this series of experiments has definitively demonstrated that protein-based/linked signalling factors present within the human male ejaculate are capable of eliciting $[Ca^{2+}]_i$ signalling events in the epithelial cells lining the upper FRT. The signalling factors responsible have not been specifically identified, however, the

data from this study has demonstrated that they are present in the seminal fluid and that they can be carried by spermatozoa through the cervical mucus into the upper regions of the FRT. The signalling factors do not appear to be present endogenously within the spermatozoa acrosomal sheath or on the plasma membrane, suggesting that they loosely associate with the sperm cell surface (Manjunath, Bergeron et al. 2007). These signalling factors are then able to interact with the oviductal epithelial cells as the spermatozoa make their way to the site of fertilisation in the ampulla region (Suarez and Ho 2003), initiating a signalling cascade that results in the release of Ca^{2+} from the endoplasmic reticulum intracellular stores. This intracellular Ca^{2+} release has been demonstrated to not be mediated by the TRPC channel pathway and relies upon ATPases on the surface of the endoplasmic reticulum to elicit oscillations in $[Ca^{2+}]_i$ (Tauseef, Knezevic et al. 2012). The signalling factors are proteins or small biologically active peptides that are derived from the proteolytic cleavage of proteins, due to the fact signalling still occurred after acetone precipitation of the sperm conditioned media (Simpson and Beynon 2010), as well as dialysis through a >2 kDa membrane (Andrew, Titus et al. 2002).

Candidate peptides derived from the proteolytic cleavage of the semenogelins were successfully synthesised, however, they were unable to elicit the previously observed signalling in the OE-E6/E7 cells. A range of experimental methods were employed to elucidate the mechanism of action for the observed Ca^{2+} signalling and it was revealed that the Ca^{2+} oscillations originate from the intracellular stores via pathways that are independent of the TLR4 mediated signalling pathway, as seen in murine models of similar signalling (Schjenken, Glynn et al. 2015). The signalling pathway identified within this study may have a significant impact on rates of embryo implantation, unexplained spontaneous miscarriage and other later maternal and

foetal phenotypes in humans (Saravelos and Li 2012), therefore it warrants further investigation to elucidate the biological mechanisms and specific factors that are involved.

Chapter 6

General Discussion

6.1- Semen factors induce signalling in human female reproductive tract cells

Single cell Ca^{2+} imaging has been utilised to observe and analyse cellular signalling elicited in the cells of the FRT in response to factors derived from the male ejaculate. The use of calcium-green 1AM staining allowed for stable recording of relative levels of intracellular Ca^{2+} within cultured cells over long periods of time during timelapse experiments, which allowed for the perfusion of multiple types of stimuli containing media over the surface of cells to assess their efficacy in eliciting signalling. Initial experiments were focused on identifying a candidate FRT cell line which exhibited a clear $[Ca^{2+}]_i$ response to the perfusion of semen sample preparations across their surface, to be utilised in a deeper subsequent investigation into the identity of the factors involved. The initial assumption that Ca^{2+} signalling within FRT cells could be elicited by factors within the male ejaculate was based on previous observations within our group (Connolly 2011), in addition to a single study carried out on equine oviductal epithelial cells which were demonstrated to exhibit $[Ca^{2+}]_i$ signalling in response to co-culture with equine semen. (Ellington, Varner et al. 1993).

Three secondary cell line cultures from the FRT were developed: an endometrial epithelial cell line (HEC-1B) (Kurarmoto, Hamano et al. 2002, Korch, Spillman et al. 2012), an oviductal epithelial cell line (OE-E6/E7) (Lee, Lee et al. 2001) and an ovarian granulosa cell line (COV434) (Zhang, Vollmer et al. 2000). An additional human foreskin fibroblast cell line (HFF) was cultured with the intention of forming a negative control cell line for future experiments. The relative levels of $[Ca^{2+}]_i$ within each of these cell lines was observed during the perfusion of three different semen sample preparations across their surface: filtered seminal plasma, sperm cells prepared by the swimup method and sperm cells prepared by density gradient centrifugation. The purpose of these initial experiments was not only to find an ideal

candidate FRT cell line for further experiments with male ejaculate induced signalling, but also to begin to establish the source of any signalling factors present in the male ejaculate.

Each of the three FRT cell lines were responsive in terms of $[Ca^{2+}]_i$ signalling to the perfusion of seminal plasma across their surface. This may be accounted for by the wide range of inflammatory factors and other signalling molecules (Song, Li et al. 2016, Han, Ma et al. 2017) that are known to be present in seminal plasma, which have documented effects on the regulation of $[Ca^{2+}]_i$ in cells (Ramadan, Steiner et al. 2011). The fact that the human cervix and cervical mucus act as an effective barrier to selectively allow motile spermatozoa into the upper FRT whilst keeping seminal plasma in the distal vagina and ectocervix (Chumduri and Turco 2021) meant that seminal plasma itself could be discounted from further investigation as the source of the signalling factor responsible for the observed signalling. This is because each of the cell lines assessed originated from regions of the FRT that were beyond the cervical barrier and motile spermatozoa are separated from seminal plasma and resuspended in endometrial and oviductal fluids once they are transported through the cervical canal (Hafez 1979).

The density gradient prepped sperm cells were able to elicit strong $[Ca^{2+}]_i$ signalling in the OE-E6/E7 cells, with significantly lower rates of signalling elicited in the COV434 and HEC-1B cells. These results were particularly interesting because the density gradient centrifugation method of isolating motile sperm cells from the semen sample should not contain raw seminal plasma (Santiago-Moreno, Esteso et al. 2017), suggesting that different signalling factors that were still able to elicit $[Ca^{2+}]_i$ signals in the oviductal epithelial cell line were present in this preparation. The intensity and significantly higher rates of signalling observed within the OE-E6/E7

established them as an ideal candidate cell line for further experiments to elucidate the identity of the signalling factors and the mechanism of action by which they cause $[Ca^{2+}]_i$ signalling.

This initial series of experiments represents a novel approach to investigating sperm cell signalling in the cells of the FRT. Whilst other researchers have carried out studies into the genomics (Fazeli, Affara et al. 2004) and alterations to the proteomic output (Georgiou, Sostaric et al. 2005) of mammalian FRT cells in response to male gamete exposure, this study is the first to use Ca^{2+} imaging as a means of identifying signalling mechanisms in a range of human FRT cells in response to different components of the male ejaculate. Unfortunately, the HFF cells assessed in this series of experiments was deemed unsuitable for use as a negative control cell line for this study, as the well documented mechanosensitivity of fibroblast cells (Kim, Han et al. 2009) led to the elicitation of $[Ca^{2+}]_i$ signalling in response to the shear caused by the gentle perfusion of any type of media across their surface. Whilst this excluded the use of HFF cells for the purpose of this study, this observation may prove useful in later studies where mechanosensitivity is a subject of investigation.

The key limitation of this initial investigation was the exclusive use of secondary cell lines, which may provide biological responses different from cells within the original host tissue (Kaur and Dufour 2012). Attempts were made to maintain the secondary cell cultures at a low number of passages, however, these cells may still have genetic changes or mutations acquired during repeated passaging and culture maintenance (Kim, Rhee et al. 2017). Whilst the use of secondary cell lines provides a reproducible source of a pure population of cells, it would have been advantageous to repeat these experiments with primary cells (Honegger 2001). The initial intention for this study was to acquire primary human tissues from hysterectomy patients, from

which oviductal and endometrial epithelial cell populations would have been isolated and cultured for use in parallel Ca^{2+} imaging experiments. This would have provided a more representative cell population to investigate the interactions between the male ejaculate and FRT cells, however, due to the COVID-19 pandemic it was challenging to access the hospital to acquire the necessary samples.

6.2- The semen derived signalling molecules are carried by sperm cells

Once the OE-E6/E7 cell line had been identified as the candidate FRT cell line for investigation, the next step was to isolate and identify the source of the signalling factors within the male ejaculate. There were a range of possibilities due to the complexity of the components of the male ejaculate and the various organs from which the mixture is derived (Wang, Yang et al. 2020). The factor could be present on the sperm cell surface membrane proteome (Brewis and Gadella 2010), within the acrosomal sheath to be revealed or released during capacitation (Breitbart and Spungin 1997) or a factor that loosely associated with the surface of sperm cells from the seminal plasma (Szczykutowicz, Kałuża et al. 2019). To narrow down the range of proteins that could be candidate signalling factors, a novel intricate series of semen sample preparation pathways were developed to isolate specific groups of proteins within the male ejaculate.

Table 6.1- A summary of the semen sample preparations described in section 3.2.2 and their intended proteomic content.

Semen sample preparation	Intended cellular and proteomic content of stimulus
Clean DGC Sperm Cells	Intact, capacitated sperm cells without seminal plasma components
"Contaminated" DGC Sperm Cells	Intact, capacitated sperm cells with seminal plasma contamination
Non-Conditioned Media	Negative control, no sperm cells and no seminal plasma components
Time Zero Post-Swimup Sperm Cells	Intact sperm cells swam through viscous media, not capacitated
Swimup Capacitated Sperm Cells	Intact, capacitated sperm cells swam through viscous media
Sperm Conditioned Media	Proteomic content of swimup capacitated sperm cells, with cells removed

A novel modified version of the swimup preparation technique was developed using methylcellulose media as a fertile cervical mucus substitute (Ivic 2002) to allow for the passage of motile spermatozoa into the media above. This condition, referred to as swimup sperm cells, led to significant levels of $[Ca^{2+}]_i$ signalling in the OE-E6/E7 cells, confirming that the factors responsible were either present on the sperm cell surface (Brewis and Gadella 2010) or postacrosomal sheath (Wu, Sutovsky et al. 2007), released during the process of capacitation from within the acrosome (Breitbart and Spungin 1997) or a factor present in the seminal plasma which loosely associated with motile spermatozoa as they pass through the cervical mucus (Szczykutowicz, Kałuża et al. 2019). A non-conditioned media preparation succeeded as a negative control stimulus, as it did not elicit $[Ca^{2+}]_i$ signalling in substantial number of OE-E6/E7 cells. showing that the sEBSS media itself was incapable of eliciting signalling and that the modified swimup preparation technique did not cause contamination with seminal plasma components, as could have been the case with a standard swimup preparation (Björndahl, Mohammadieh et al. 2005).

The time-zero post swimup sperm cell preparation was intended to contain the same potential signalling components as the swimup sperm cells except for any factors that were released or exposed during the process of capacitation and the AR (Breitbart and Spungin 1997, Wu, Sutovsky et al. 2007). This stimulus caused significantly lower levels of signalling in the OE-E6/E7 cells compared to the swimup sperm cells stimulus, which could either mean that the longer period of incubation for the swimup sperm cells led to a higher concentration of the same signalling factors being released into the media or that the process of capacitation and the AR stimulate the release of additional signalling factors (Yoshida, Ito et al. 2010). The factors causing signalling are thereby implied to not be very-loosely carried by sperm

as a ‘contaminant’ from seminal plasma, but be something that has actively bound to sperm and is then released.

The sperm conditioned media stimulus was prepared in the same manner as the swimup sperm cells, however, this conditioned was centrifuged and filtered to remove all of the sperm cells from the media. The purpose of this condition was to assess the efficacy of the factors released into the media by the sperm cells after they had navigated their way through the viscous methylcellulose solution, whilst discounting any signalling elicited by the factors present on the sperm cell surface via direct contact with the FRT cells (Brewis and Gadella 2010). The OE-E6/E7 cells responded strongly to this stimulus, confirming that direct sperm cell contact was not necessary for the $[Ca^{2+}]_i$ signalling to be elicited and that the factors responsible could be shed or released from the motile spermatozoa which navigate into the upper FRT.

In addition to these conditions, two methods of density gradient centrifugation preparation of semen samples were used as stimuli. The clean DGC sperm cells condition used the standard method of density gradient centrifugation (Malvezzi, Sharma et al. 2014) to separate motile spermatozoa from the seminal plasma, with each of the subsequent wash steps taking place in a new falcon tube. The “contaminated” DGC sperm cells stimulus was prepared in the same manner, but each of the wash steps was carried out in the same tube as the original centrifugation. The difference between the two was that the “contaminated” DGC sperm cells condition would likely contain traces of the seminal plasma from the sides of the tube. The comparison between the signalling rates in the OE-E6/E7 cells with these two stimuli was interesting, as the “contaminated” DGC sperm cells elicited significantly more signalling than the clean DGC sperm cells, which

performed similarly to the non-conditioned media negative control, suggesting that the low concentration of seminal plasma components was sufficient in eliciting signalling. This observation aligns with the hypothesis that factors derived from the seminal plasma are responsible for the mediation of signalling with human FRT cells, as seen in a range of mammalian species (Robertson 2007, Rodríguez-Martínez, Kvist et al. 2011, Bromfield 2014, Sharkey, Schjenken et al. 2015, Schjenken and Robertson 2020). In combination with the earlier data, it would imply that the molecules responsible for the signalling are surface molecules that are stripped from sperm cells by the process of density gradient centrifugation. As such they are unlikely to be transmembrane tethered or of acrosomal origin as allowing the cells to undergo capacitation did not regain this signalling ability.

Overall, the network of semen sample preparation pathways that was developed for this study was successful in assisting with the identification of the source of the signalling factor within the male ejaculate. The evidence collected within this series of experiments suggests that the signalling factor is a component of the seminal plasma which loosely associates with the surface of the sperm cells (Szczykutowicz, Kałuża et al. 2019) at the site of semen deposition or during transit through the male tract. This factor is then carried by motile spermatozoa as they navigate through the viscous cervical mucus into the upper regions of the FRT (Rodríguez-Martínez, Kvist et al. 2011) where it can be shed or released into the oviductal fluid to elicit signalling in the cells of the oviductal epithelial lining. A key implication is that different routine sperm preparations methods such as density gradient centrifugation and swimup are likely to provide radically different levels of this signalling ability, for example if sperm were prepared for intrauterine insemination (IUI) (Boomsma, Cohlen et al. 2019). This requires further study when considering how different techniques may be

optimal, such as the emerging use of microfluidic preparation of sperm (Denissenko, Kantsler et al. 2012), which would be expected to have a higher level of this signal than density gradient preparations.

This series of experiments not only revealed the source of the signalling factor within the male ejaculate, but also provided an ideal media preparation for further proteomic analysis to identify the candidate factors. The sperm conditioned media stimulus caused the highest rate and relative strength of $[Ca^{2+}]_i$ response in the OE-E6/E7 cells, despite the lack of intact sperm cells within the media. The absence of the expansive sperm cell proteome (Gilany, Lakpour et al. 2011) was advantageous as the sperm conditioned media would contain a narrower range of proteins which would shorten the list of candidate factors discovered in subsequent proteomic analysis. The novel concept of isolating different proteomic groups from the male ejaculate with the use of conventional and modified methods of semen sample preparation to investigate their interactions with FRT cells had never previously been carried out. By combining this approach with the previously established Ca^{2+} imaging of FRT cells in conjunction with the timelapse imaging within a perfusion chamber, an effective assay for the identification of male ejaculate factor signalling has been established. The next step was the proteomic analysis of sperm conditioned media to acquire a list of candidate factors for further investigation.

The use of an immortalised oviductal epithelial cell lines was again the primary limitation of this series of experiments (Kaur and Dufour 2012). In addition to the planned experiments with primary human cell cultures acquired from patients undergoing hysterectomy, parallel experiments were planned to be carried out using primary tissues acquired from canine and porcine models. The intention was to investigate whether the reported alterations to the oviductal secretory proteome by

interactions with the male gametes (Georgiou, Sostaric et al. 2005) were regulated by Ca^{2+} signalling, to provide translatory evidence for similar mechanisms occurring in humans. Initial attempts were made to isolate and culture canine primary oviductal epithelial cells (described in appendix VIII), however, this line of investigation was suspended due to the outbreak of the COVID-19 pandemic.

6.3- Proteomic analysis of sperm conditioned media

The sperm conditioned media was fractionated using ultracentrifugal filters prior to proteomic analysis being carried out, this was done to further separate the media into fractions containing distinct components separated by their molecular weight. Although each of the three factions were able to elicit a $[Ca^{2+}]_i$ response in the OE-E6/E7 cells, there were clear differences in the relative strength of the rise in $[Ca^{2+}]_i$ rise that was evoked, with the <3 kDa fraction eliciting a very similar change in $[Ca^{2+}]_i$ to the pooled sperm conditioned media, whilst the >50 kDa fraction elicited a much weaker response and the 3-50 kDa fraction an even weaker rise in $[Ca^{2+}]_i$. This result could mean one of several things, either that the separation of the media by ultracentrifugal filters was sufficient to lower the concentration of the signalling factors in the >50 kDa and 3-50 kDa fractions such that a lower strength $[Ca^{2+}]_i$ response was observed in the OE-E6/E7 cells, or that there were different signalling factors present in each of the fractions that were eliciting strengths of signalling via different mechanisms of action. Due to the similarities in the $[Ca^{2+}]_i$ kinetics observed with the perfusion of each fraction, as well as the knowledge that the ultracentrifugal filters do not have a 100% retention rate (Vergauwen, Dhondt et al. 2017), it was assumed that the same signalling factors were responsible for the signalling elicited by each fraction.

The acetone precipitation of the fractionated sperm conditioned media was an effective method of purifying the proteins and peptides within the media (Simpson and Beynon 2010) so that they could be resuspended at a suitable concentration for proteomic analysis. This precipitation method also yielded interesting results when the resuspended <3 kDa fraction protein pellet was assessed for signalling efficacy in a Ca^{2+} imaging experiment with the OE-E6/E7 cells, demonstrating that the signalling factor was still present after the precipitation process. This confirms that the factor in question is some sort of protein or peptide that can be precipitated out of solution by treatment with acetone (Crowell, Wall et al. 2013).

The proteomic analysis of the precipitated fractions of sperm conditioned media yielded a surprisingly low number of results for the <3 kDa and 3-50 kDa fractions, whilst the >400 proteins identified in the >50 kDa fraction was more in line with expected results based on previously published analyses of semen and sperm cell proteomics (Brewis and Gadella 2010, Jodar, Soler-Ventura et al. 2017, Cao, Cui et al. 2018, Castillo, Bogle et al. 2019, Agarwal, Panner Selvam et al. 2020). This showed that the separation of the fractions by ultracentrifugal filtration was effective in separating the protein content of the media to such an extent that most large proteins were either completely removed from the smaller fractions or at least removed sufficiently for them to be unidentifiable by the mass spectrometry-based analysis (Easterling, Yerabolu et al. 2020). The proteomic data produced in this study represents the first ever examination of media that has been conditioned by motile spermatozoa, revealing the types of proteins that are shed by sperm cells into their surroundings. These findings were particularly interesting as the sperm cells which formed the sperm conditioned media had already passed through a modified version of swimup preparation intended to simulate the passage of motile cells

through the fertile cervical mucus (Ivic 2002), providing similar proteomic content as would be present in the sperm conditioned fluids of the upper FRT.

The efficacy of the <3 kDa fraction of sperm conditioned media in eliciting $[Ca^{2+}]_i$ signalling kinetics very similar to those observed with the pre-fractionated sperm conditioned media, coupled with the relatively low number of proteins identified within the fraction made it an ideal framework to begin the identification of the male ejaculate derived signalling factor. The proteomic data between each fraction was compared and it was clear that semenogelin-1 and semenogelin-2 were the common denominator proteins between each fraction. Deeper analysis and comparison of the peptides derived from these two proteins within each fraction were also compared and a list of candidate peptides was produced. Theoretically, the peptides produced by the proteolytic cleavage of semenogelin-1 and semenogelin-2 by PSA (Mattsson, Ravela et al. 2014) could have $[Ca^{2+}]_i$ signalling efficacy, as they are known to loosely bind to spermatozoa via the EPPIN receptor (Wang, Widgren et al. 2005) and it has already been discussed that there are various semenogelin peptides with currently unknown functions (Lilja, Abrahamsson et al. 1989). For these reasons, a selection of commonly occurring semenogelin peptides within our data, as well as a scrambled peptide negative control were synthesised to be used as stimuli in our Ca^{2+} imaging setup.

The fractionation of the sperm conditioned media by ultracentrifugal filters provided a simple method to separate proteins within the media into distinct fractions based on their molecular weight (Johnsen, Brandtzaeg et al. 2016) and allowed for the proteins to easily be resolubilised and used as stimuli in Ca^{2+} imaging experiments. Due to the preservation of signalling efficacy in all three of the fractions produced it may have been more beneficial to use an alternative method of separating the

proteins such as gel filtration chromatography or absorption chromatography (Friesen 1987, Coskun 2016, Ó'Fágáin, Cummins et al. 2017), which would have been a more effective method of separating the proteins into distinct weight groups with a higher yield, however, it would have been more challenging to resolubilise the proteins to use as stimuli whilst ensuring that their tertiary structure was intact (Ó'Fágáin, Cummins et al. 2017, Ventouri, Malheiro et al. 2020).

6.4- Signalling relies on the release of Ca^{2+} from intracellular stores

Unfortunately none of the synthesised semenogelin peptides were able to elicit the previously observed $[Ca^{2+}]_i$ signalling in the OE-E6/E7 cells. This does not necessarily mean that these peptides are not responsible for signalling with the cells of the FRT *in vivo*, as a key limitation of synthesised peptides is the lack of any posttranslational modifications that may occur endogenously (Ramazi and Zahiri 2021). In addition, there were a wide range of other peptides and proteins identified within the sperm conditioned media that warrant further investigation. Semenogelin-1 and semenogelin-2 were particularly difficult to predict their precise structure and the presence of any modification such as glycosylation due to the lack of availability of a crystalised 3d structure of the proteins. The predicted 3D structure of both proteins produced using DNASTAR LASERGENE Bioinformatics Software (Version 17.3.1) was the first of its kind, however, the predicted structure may not be completely representative of the *in vivo* human semenogelin-1 and semenogelin-2 structures.

Other peptides and proteins identified could be synthesised or purchased commercially for use in further Ca^{2+} imaging experiments to attempt to identify the specific signalling factor. It would also be logical to attempt to purify semenogelin-1 and semenogelin-2 by a method such as affinity chromatography purification (Urh, Simpson et al. 2009), the purified proteins could then be suspended in solution and

used as a stimulus in Ca^{2+} imaging experiments. The purified proteins could also undergo proteolytic lysis *in vitro* by the addition of PSA (Mattsson, Ravela et al. 2014), before suspending the resulting peptides in solution and using them as a stimulus on the OE-E6/E7 cells. This type of experiment would allow for the assessment of physiologically occurring semenogelin peptides as the male ejaculate derived signalling factor, along with their post-translational modifications that may have been missing from the synthesised peptides (Ramazi and Zahiri 2021).

The use of the toll-like receptor 4 inhibitor, TLR-IN-C34, did not prevent the usually observed $[Ca^{2+}]_i$ oscillations in the OE-E6/E7 cells in response to the perfusion of sperm conditioned media. This discounted the involvement of the TRPC6-dependent calcium signalling pathway (Tauseef, Knezevic et al. 2012) in the induction of these signals, which has previously been demonstrated to regulate similar signalling mechanisms in murine models (Schjenken, Glynn et al. 2015). This suggests that another signalling cascade such as the IP3 receptor-mediated calcium signalling pathway (Kania, Roest et al. 2017) must mediate the observed response to sperm conditioned media.

The experiment with Ca^{2+} free media showed that the Ca^{2+} oscillations observed in the OE-E6/E7 cells originated from intracellular stores, rather than the influx and efflux of Ca^{2+} from the extracellular media (Brown and Iadarola 2015). This evidence further suggests that a pathway such as IP_3 receptor-mediated calcium signalling (Kania, Roest et al. 2017) is responsible for the interactions between male ejaculate factors and the FRT cells. The depletion of the intracellular Ca^{2+} stores with thapsigargin (Scharff and Foder 1996) treatment further confirmed this theory, as signalling in response to sperm conditioned media was absent in the OE-E6/E7 cells after the stores had been depleted.

The final Ca^{2+} imaging experiment in this study which utilised sperm conditioned media that had undergone dialysis of all proteins and peptides smaller than 2 kDa in size demonstrated that similar rates and strength of signalling was present in comparison to non-dialysed sperm conditioned media. suggesting that the signalling factor did not originate from a protein smaller than 2 kDa in size, however, this does not necessarily mean that the factor is not a small peptide belonging to a much larger parent protein.

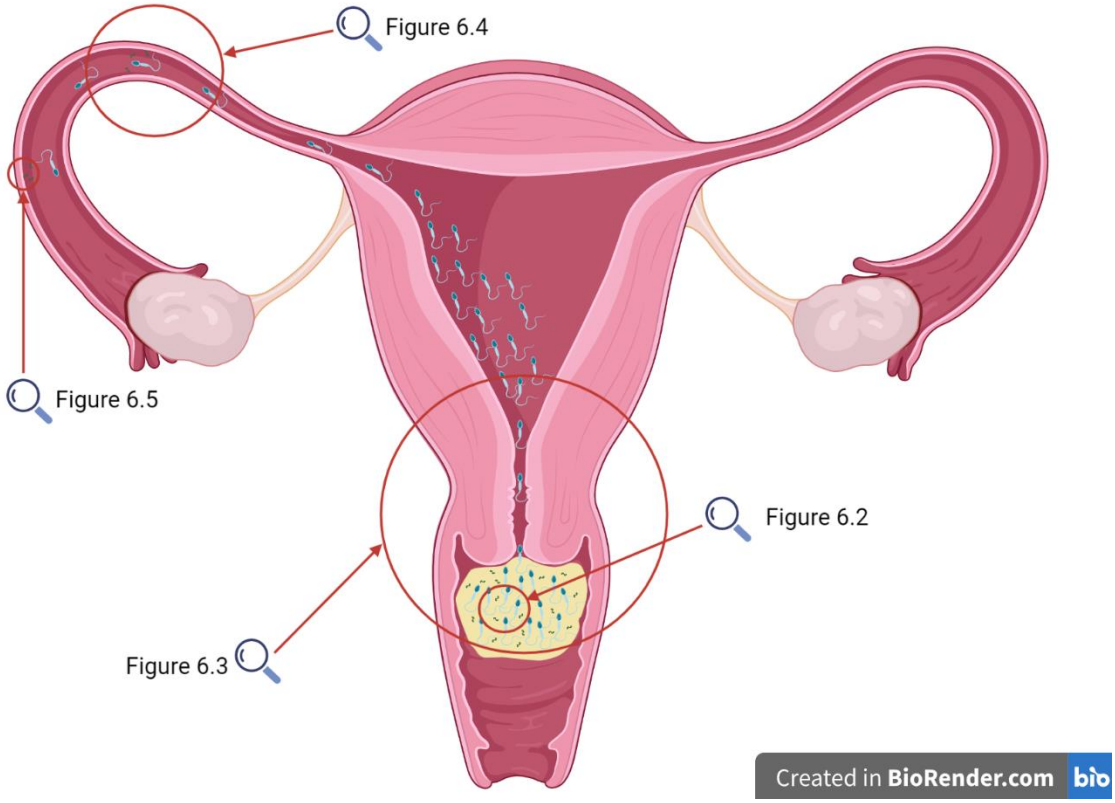


Figure 6.1- An overview of the proposed signalling mechanism through which protein/peptide factors present in the male ejaculate elicit Ca^{2+} signalling in the oviductal epithelial cells. Created with BioRender.com.

Figure 6.1 shows the anatomy of the female tract, with semen deposited at the external cervical os (Suarez and Pacey 2006). Signalling factors from the seminal fluid loosely associate with motile spermatozoa and are carried through the cervical mucus into the upper FRT (Tecle, Reynoso et al. 2019), where they interact with oviductal epithelial cells to elicit Ca^{2+} release from intracellular stores via a signalling pathway that is independent of TLR4. Key sections of the transit of the signalling factors and their contact with the oviductal epithelial cells have been highlighted in this diagram and will be shown in more detail in the proceeding figures.



Figure 6.2- The loose association of the protein/peptide signalling factors with the surface of spermatozoa from the seminal plasma. Created with BioRender.com.

The evidence derived from the results of the experiments in which OE-E6/E7 cells were introduced to a range of semen sample preparations (described in chapter 3) suggested that sperm cells are coated with a signalling factor that is present in the seminal plasma. This factor loosely associated with the surface of motile spermatozoa and is carried into the upper FRT where it can dissociate from the sperm cells and interact with the oviductal epithelial cells.

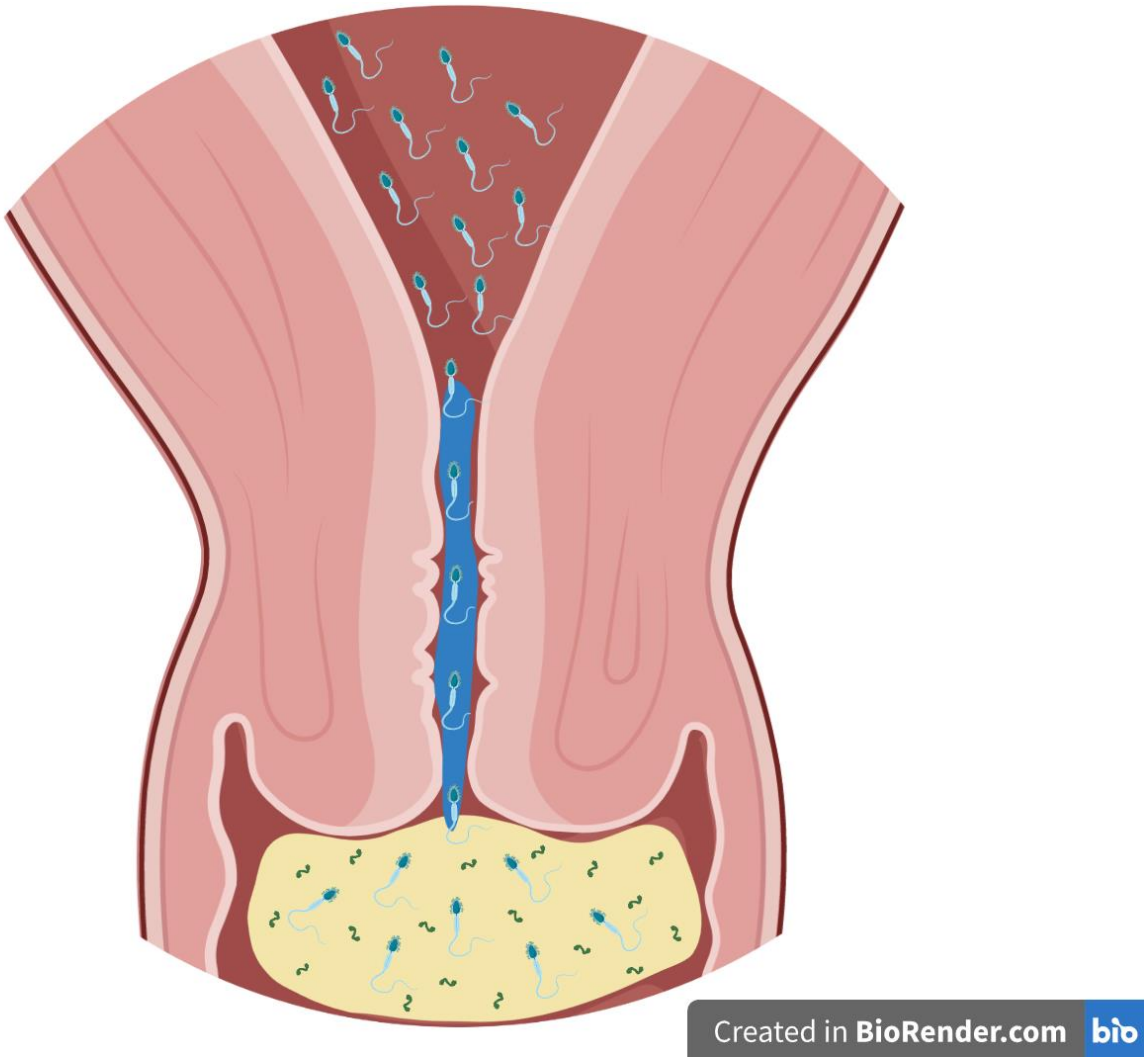


Figure 6.3- The transit of the signalling factors, loosely associated with motile sperm cells, carried through the cervical mucus and into the upper regions of the female reproductive tract. Created with BioRender.com.

The use of viscous media in the preparation of the swimup capacitated sperm cells condition was intended to simulate the passage of motile sperm cells from the seminal plasma through the cervical mucus (Ivic 2002). It was demonstrated that this stimulus could still elicit signalling in the OE-E6/E7 cells, suggesting that the factor is able to be carried into the upper FRT by motile sperm cells, as shown in figure 6.3.

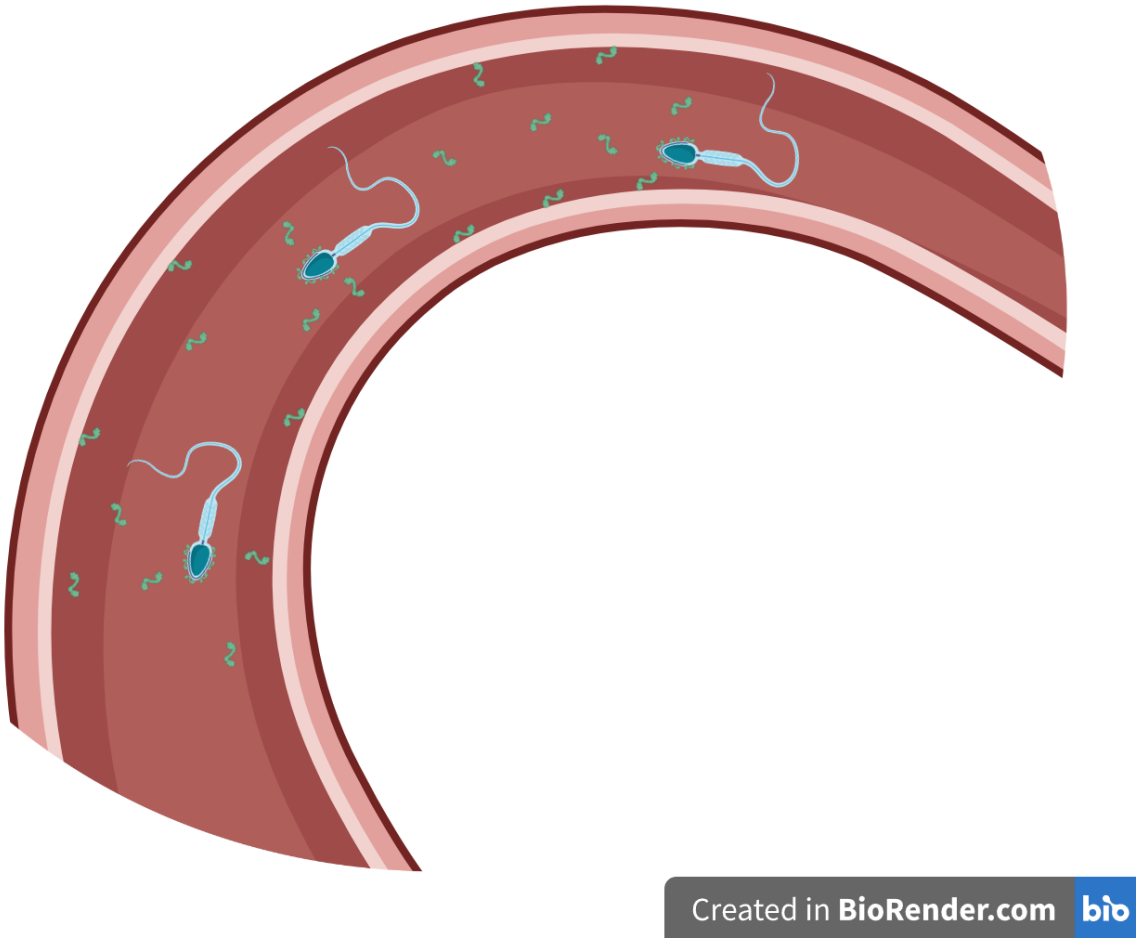


Figure 6.4- The release of the male ejaculate signalling factors into the fluid within the lumen of the oviduct. Created with BioRender.com.

The use of sperm conditioned media, which had been filtered and centrifuged to remove all the sperm cells from the swimup capacitated sperm cells condition showed that direct contact between intact sperm cells and the OE-E6/E7 cells was not necessary for the elicitation of Ca^{2+} signalling. The retention of signalling capacity by the sperm conditioned media suggested that the signalling factors responsible could be shed into the media by sperm cells that had passed through viscous media from seminal plasma. Figure 6.4 shows the proposed mechanism by which the signalling factors are shed into the oviductal fluid within the lumen on the fallopian tubes where they can interact with the epithelial cells.

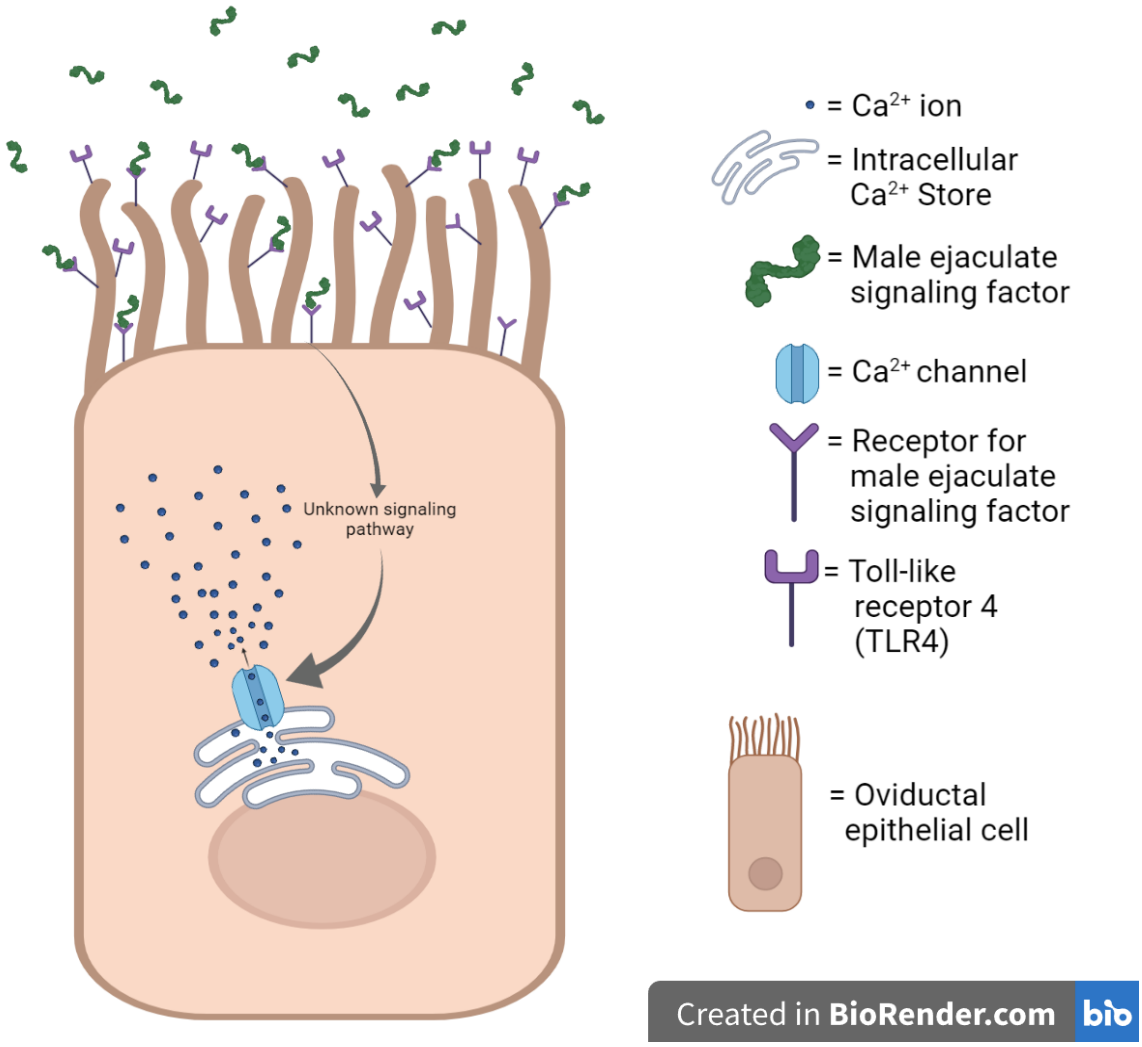


Figure 6.5- The proposed signalling mechanism by which the protein/peptide factors from the male ejaculate elicit Ca^{2+} signalling in the oviductal epithelial cells. Created with BioRender.com.

The results of the experiments carried out to further elucidate the molecular mechanisms by which the Ca^{2+} signalling is elicited within the OE-E6/E7 cells (discussed in chapter 5) demonstrated that the male ejaculate signalling factors interact with oviductal epithelial cells through a receptor that is not TLR4, as is the case in murine models (Schjenken, Glynn et al. 2015). An unknown signalling pathway, potentially the IP_3 signal transduction pathway (Taylor and Thorn 2001), is then activated and a second messenger elicits the release of Ca^{2+} from the intracellular stores within the OE-E6/E7 cells.

6.5- Conclusions and considerations for future research

Overall, this novel study has established the clear presence of signals passed from sperm cells navigating through the FRT directly to the cells in the epithelial lining of the oviduct. The factor responsible for the observed signalling appears to be a protein or peptide present in the seminal plasma that reversibly, loosely associates with the surface of motile sperm cells (Tecle, Reynoso et al. 2019) and is shed into the fluid within the oviduct as sperm cells make their way to the site of fertilisation. The signalling factor can elicit the release of Ca^{2+} from intracellular stores within the oviductal epithelial cells via a pathway that is independent of TLR4 receptor regulation. The specific identity of the signalling factor responsible has not been identified, however, a list of candidate proteins and peptides has been produced and can be referred to in future experiments.

Based on these findings, the current hypothesis is that small protein factors derived from the seminal plasma loosely associate with motile sperm cells and interact with the cells of the upper FRT, eliciting Ca^{2+} signalling which is upstream of alterations to gene expression and proteomic output. This signalling could lead to the optimisation of the periconception environment to prepare to for the arrival of an early developing embryo prior to implantation, as has been observed in animal models (Ellington, Ignotz et al. 1993, Thomas, Ignotz et al. 1995, Georgiou, Sostaric et al. 2005, Kapelnikov, Zelinger et al. 2008, Bromfield, Schjenken et al. 2014, Ghersevich, Massa et al. 2015). It is clear that this signalling is not essential for healthy early embryo development and implantation to occur, as patients undergoing ART treatment without sexual intercourse are still capable of carrying out healthy pregnancy to full term (Baldwin 2012). Instead, the signalling described herein could optimise the FRT environment by stimulating the release of embryotrophic and

implantation factors (Robertson 2005, Bromfield, Schjenken et al. 2014) to improve success rates and early healthy development of the embryo, as potentially evidenced by the increased rate of clinical pregnancy in couples receiving IVF treatment who still have regular sexual intercourse prior to embryo transfer (Hou, Yuan et al. 2023).

If it can be demonstrated that the downstream effects of this signalling include the optimisation of the periconception environment then it could have implications on the diagnosis of currently unexplained cases of subfertility (Nandi and Homburg 2016), as well as forming the basis for potential treatments to be used in assisted reproductive technology clinics. There could be currently unexplained cases of male factor infertility where the gene for the expression of the signalling factor are absent or non-functional, or female factor infertility cases where they lack the receptors or other key components of the signalling pathway to detect the presence of the male ejaculate factor (Hjort and Hansen 1971, Quaas and Dokras 2008). If the specific signalling factors could be identified then their purification and use as an add-on treatment for patients undergoing fertility treatment could lead to improved pregnancy outcomes, as there are currently a range of similar emerging add-on treatments being developed (Perrotta and Hamper 2021).

The findings discussed herein also have implications on commonly used protocols for intrauterine insemination. In many cases, sperm samples for this treatment are prepared by density gradient centrifugation due to the higher total number of motile spermatozoa that are recovered with this method (Henkel and Schill 2003). Evidence from this study suggests that the male ejaculate derived signalling factor can be removed by the process of density gradient centrifugation, suggesting that the modified swimup through viscous media method of semen sample preparation used

herein (Ivic 2002) may lead to improvements in the periconception environment and endometrial receptivity. A recent meta-analysis compared the effectiveness of different semen preparation techniques in subfertile couple undergoing IUI, but there was insufficient evidence available to identify any differences in the clinical pregnancy or miscarriage rates between sperm prepared via DGC or conventional swimup (Boomsma, Cohlen et al. 2019), highlighting the need for further research on this topic.

In terms of future research, further characterisation of the mechanism of action of the release of Ca^{2+} from the intracellular stores of the OE-E6/E7 cells could be carried out by inhibiting other commonly occurring pathways of Ca^{2+} signalling such as the IP_3 pathway, the activation of which can lead to an oscillatory response in cellular $[Ca^{2+}]_i$ (Taylor and Thorn 2001) much like the type observed in this study. $[Ca^{2+}]_i$ release via the IP_3 signalling pathway can be prevented by various means, such as the inhibition of phospholipase C by U73122 or by directly inhibiting IP_3 with heparin, which is a readily available and potent antagonist of the receptor (Broad, Braun et al. 2001). It would also be beneficial to completely rule out the involvement of semen derived ATP in the elicitation of the observed signalling. The preservation of signalling after sperm conditioned media underwent acetone precipitation suggests that ATP is not responsible, as ATP is not a protein and would therefore not be expected to be precipitated by acetone (Simpson and Beynon 2010). To confirm this the sperm conditioned media could be stripped of ATP by ultra-performance liquid chromatography and then used as a stimulus in Ca^{2+} imaging experiments (Law, Hafen et al. 2022).

The development of primary endometrial and oviductal epithelial cell cultures from tissue samples acquired from patients undergoing hysterectomy would be an ideal

model system to further investigate the presence of these signalling mechanisms (Kazuhiro, Maruyama et al. 1991, Classen-Linke, Kusche et al. 1996). The use of 2D cell culture systems forming monolayers on cover slips is ideal for Ca^{2+} imaging experiments, but 3-D cell culture systems could be developed to more closely mimic the *in vivo* physiology of oviductal epithelial cells by including their stromal cell layer to produce an ‘organ on a chip' (Ferraz, Henning et al. 2017). The incorporation of fibroblasts directly beneath oviductal epithelial cells within in vitro cultures has also been demonstrated to more faithfully represent the in vivo environment and impacts the composition of in vitro derived oviductal fluid (Simintiras, Fröhlich et al. 2016). This could lead to interesting lines of experimentation such as the co-culture with semen sample preparations to assess the impact of signalling on the proteomics and gene expression within the cells.

The downstream effects of the observed signalling could be investigated by using two-dimensional gel electrophoresis and liquid chromatography-tandem mass spectrometry (Zhan, Huang et al. 2018) to compare cell culture media conditioned by primary oviductal epithelial cells before and after the addition of sperm conditioned media. The proteomic data generated could then be searched to identify the upregulation of any known proteins with functions in endometrial receptivity and early embryo development (Yang, Yang et al. 2018). This type of experiment would confirm the presence of similar interactions between male ejaculate and FRT cells that have been observed in a porcine model (Georgiou, Sostaric et al. 2005).

Another interesting approach would be to carry out comparative gene expression analysis between primary oviductal epithelial cells exposed to sperm conditioned media. This could be achieved by isolating RNA and using microarray hybridisation, using similar methods to those deployed in the murine model study which identified

sperm-induced modifications to the oviductal gene expression profile after insemination (Fazeli, Affara et al. 2004). This would allow for the identification of any alterations in gene expression which arise as a result of the $[Ca^{2+}]_i$ oscillations in the cells, which are known to be upstream regulators of changes in gene expression (Puri 2020). This type of experiment would show which gene expression alterations occur downstream of the $[Ca^{2+}]_i$ oscillations in the OE-E6/E7 cells in response to signals from the male ejaculate and the proteins which they encode.

Appendices

Appendix I

Supplemented Earle's balanced salt solution (sEBSS)

The sEBSS media used throughout this study was custom made by Biological Industries, a cell culture media developer and manufacturer based in Israel. The media was produced by modifying supplemented Earle's balanced salt solution w/o phenol red with the addition of:

Sodium Dihyd. Phosphate 0.122 g/l (1.0 mM)

Potassium Chloride 0.4 g/l (5.4 mM)

Magnesium Sulphate.7H2O 0.2g/l (0.81 mM)

Dextrose Anhydrous 1.0 g/l (5.6 mM)

Sodium Pyruvate 0.3g/l (2.7 mM)

DL-Lactic Acid, Sodium 4.68 g/l (41.8 mM)

Calcium Chloride.2H2O 0.73 g/l (5.0 mM)

Sodium Bicarbonate 2.2 g/l (26.2 mM)

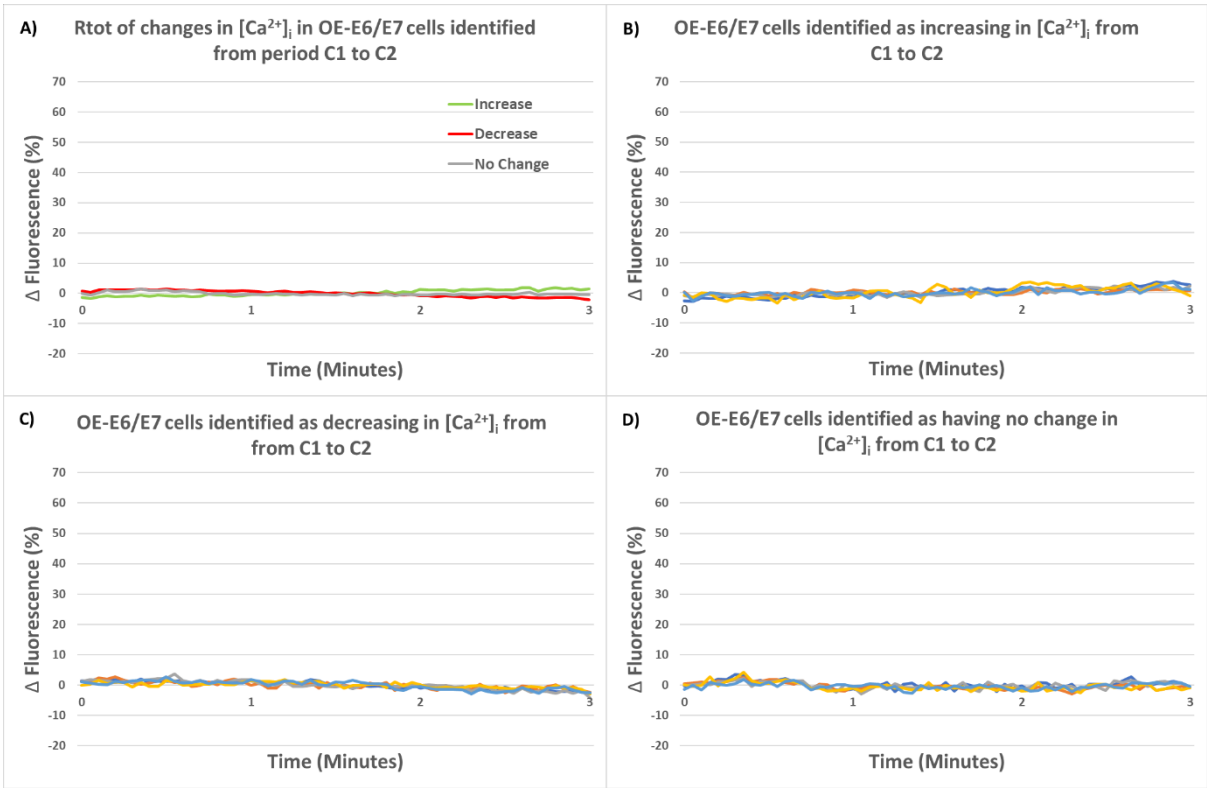
Sodium Chloride 5.0 g/l (85.6 mM)

HEPES 2.38 g/l (10.0 mM)

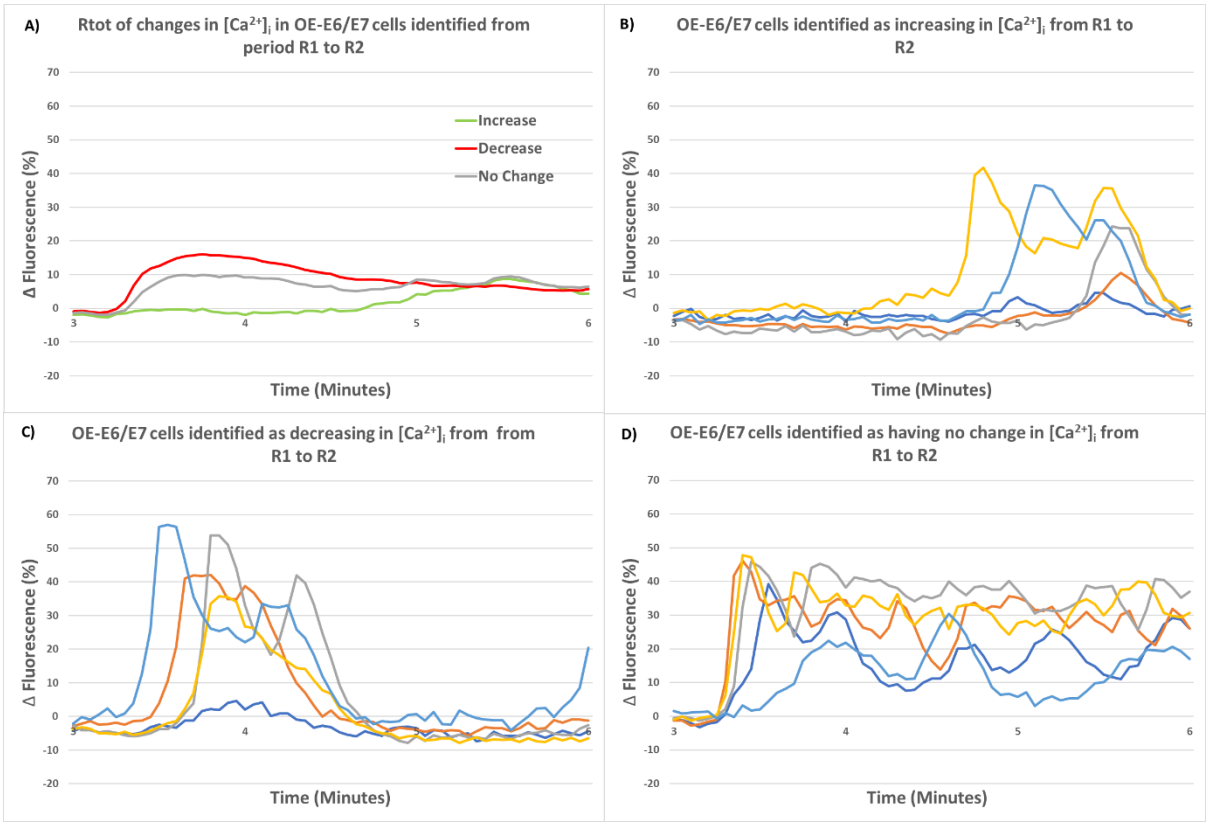
Before sEBSS was used in experiments, sodium chloride was added until osmolarity was 285-295 mOsm and the pH was adjusted to 7.4 with 1M HCl and 1M NaOH after being further supplemented with 0.3% fatty acid free bovine serum albumin.

Appendix II

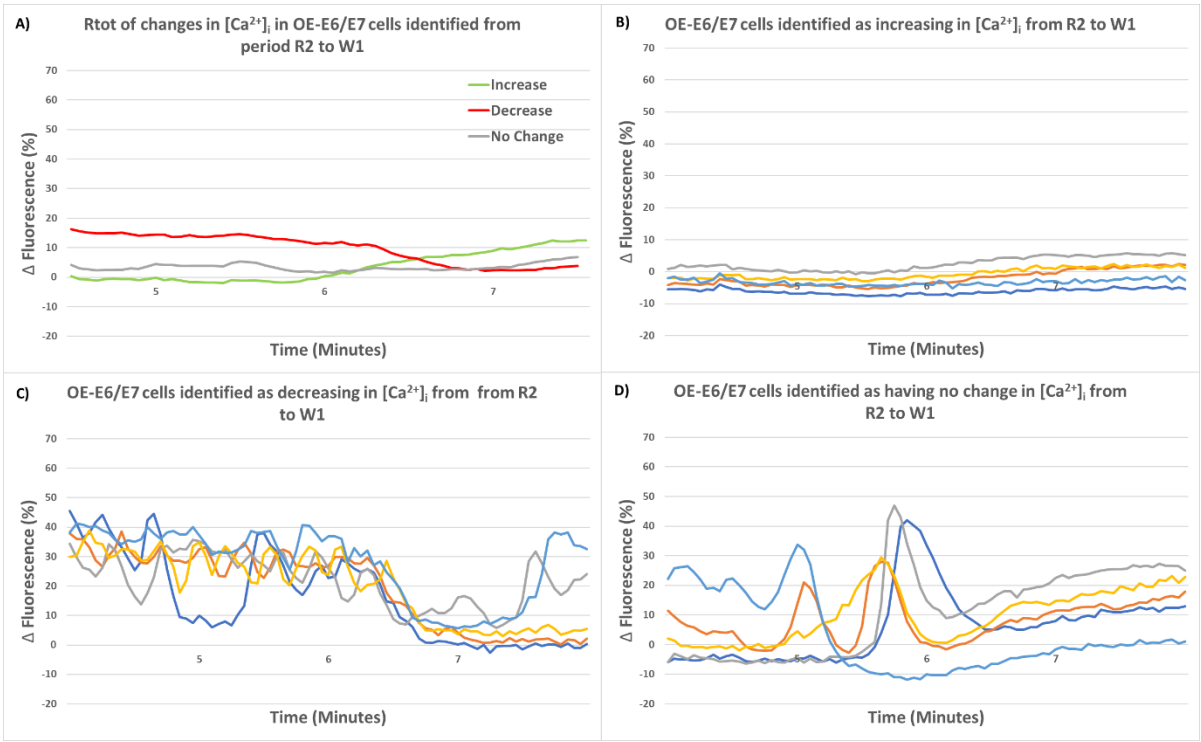
Validation of of Ca^{2+} imaging timelapse experimental protocol



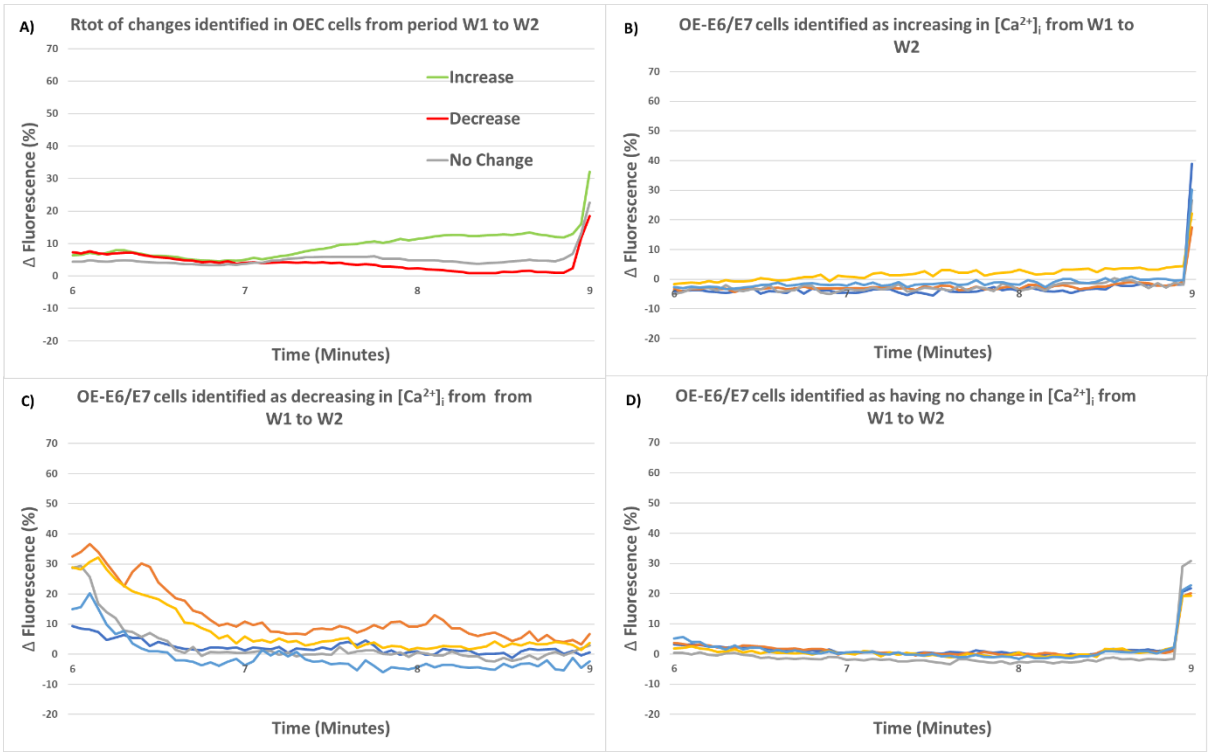
Appendix II.i- Perfusion timelapse plots showing a comparison between periods C1 and C2 from 4 experiments in which a total of 666 OE-E6/E7 cells were perfused with swimup sperm cells as a stimulus. A) Rtot plots separating cells which were identified as increasing, decreasing or having no change in fluorescence between C1 and C2. B) five random individual cells identified as showing an increase in $[Ca^{2+}]_i$ between C1 and C2. C) five random individual cells identified as showing a decrease in $[Ca^{2+}]_i$ between C1 and C2. D) five random individual cells identified as showing no change in $[Ca^{2+}]_i$ between C1 and C2.



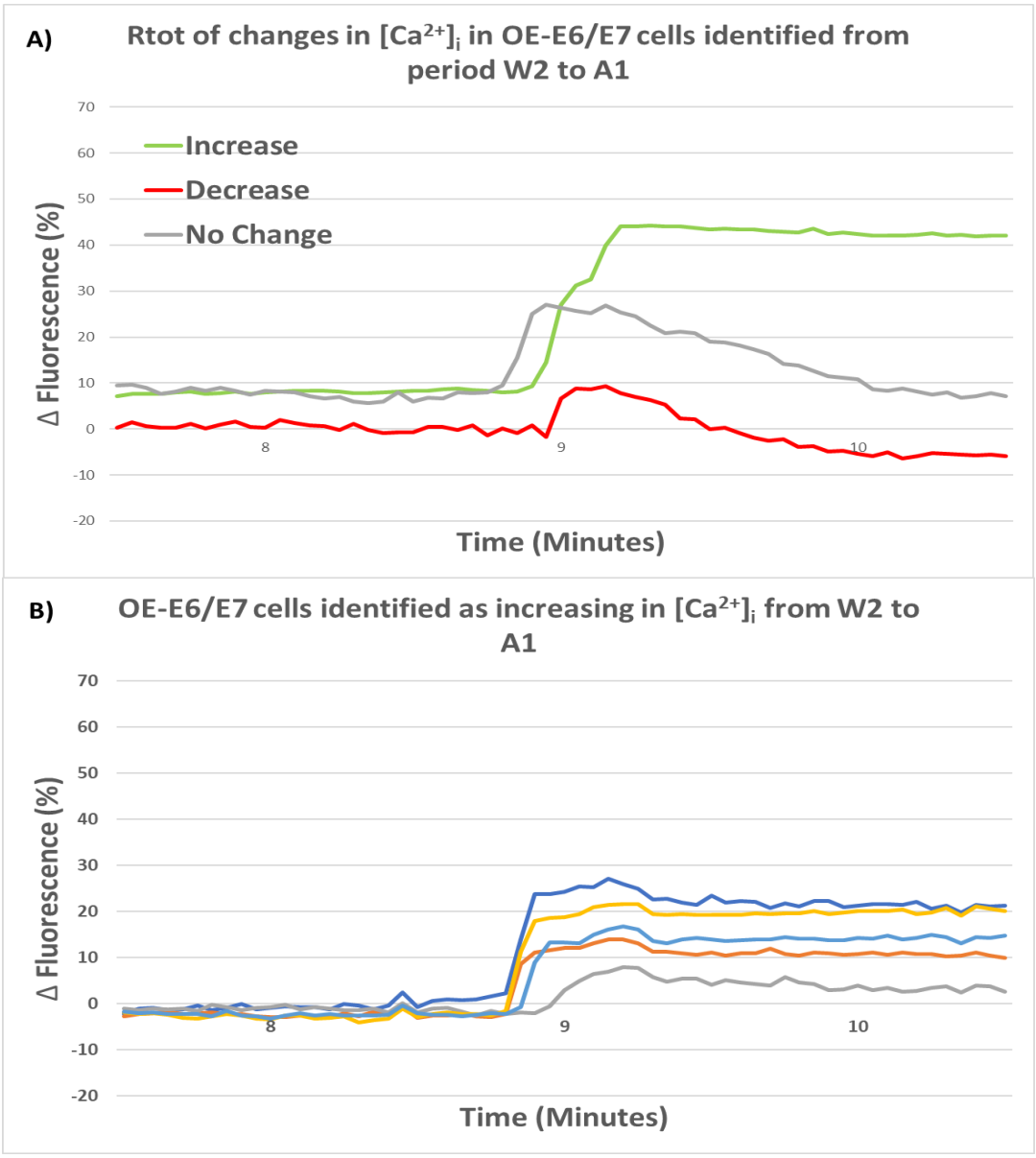
Appendix II.ii- Perfusion timelapse plots showing a comparison between periods R1 and R2 from 4 experiments in which a total of 666 OE-E6/E7 cells were perfused with swimup sperm cells as a stimulus. A) Rtot plots separating cells which were identified as increasing, decreasing or having no change in fluorescence between R1 and R2. B) five random individual cells identified as showing an increase in $[Ca^{2+}]_i$ between R1 and R2. C) five random individual cells identified as showing a decrease in $[Ca^{2+}]_i$ between R1 and R2. D) five random individual cells identified as showing no change in $[Ca^{2+}]_i$ between R1 and R2.



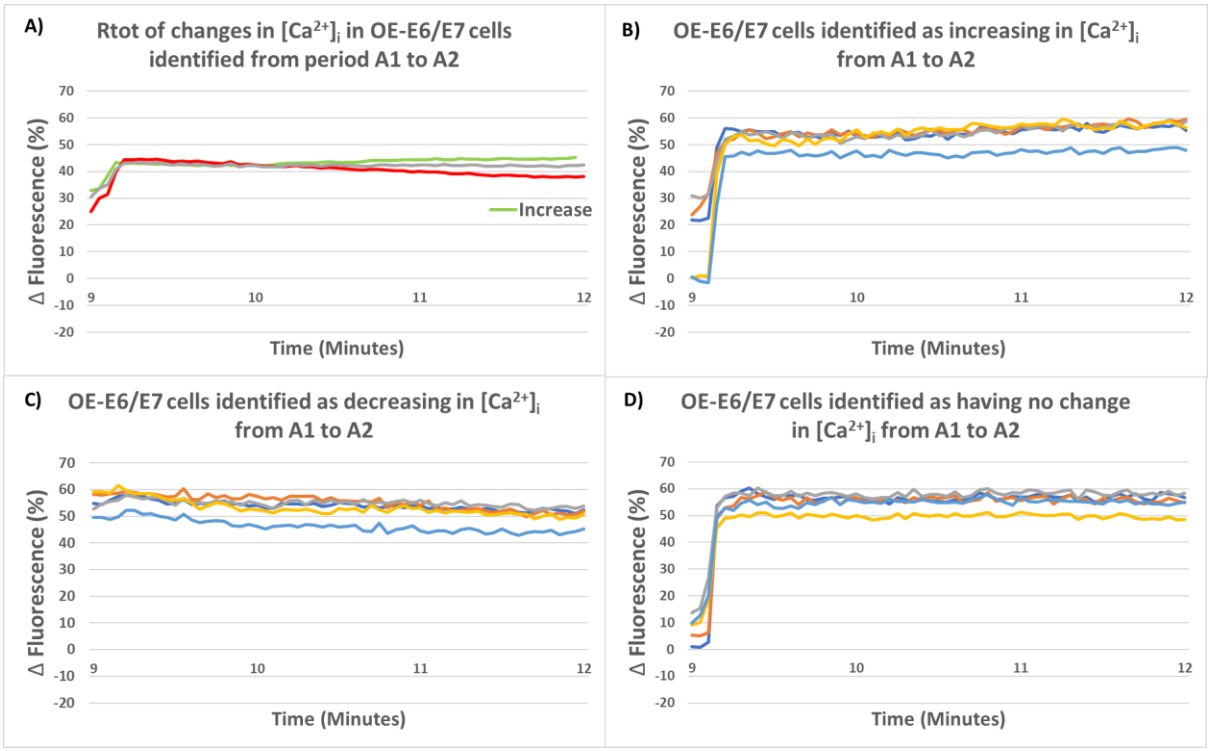
Appendix II.iii- Perfusion timelapse plots showing a comparison between periods R2 and W1 from 4 experiments in which a total of 666 OE-E6/E7 cells were perfused with swimup sperm cells as a stimulus. A) Rtot plots separating cells which were identified as increasing, decreasing or having no change in fluorescence between R2 and W1. B) five random individual cells identified as showing an increase in $[Ca^{2+}]_i$ between R2 and W1. C) five random individual cells identified as showing a decrease in $[Ca^{2+}]_i$ between R2 and W1. D) five random individual cells identified as showing no change in $[Ca^{2+}]_i$ between R2 and W1.



Appendix II.iv- Perfusion timelapse plots showing a comparison between periods W1 and W2 from 4 experiments in which a total of 666 OE-E6/E7 cells were perfused with swimup sperm cells as a stimulus. A) Rtot plots separating cells which were identified as increasing, decreasing or having no change in fluorescence between W1 and W2. B) five random individual cells identified as showing an increase in $[Ca^{2+}]_i$ between W1 and W2. C) five random individual cells identified as showing a decrease in $[Ca^{2+}]_i$ between W1 and W2. D) five random individual cells identified as showing no change in $[Ca^{2+}]_i$ between W1 and W2.



Appendix II.v- Perfusion timelapse plots showing a comparison between periods W2 and A1 from 4 experiments in which a total of 666 OE-E6/E7 cells were perfused with swimup sperm cells as a stimulus. A) Rtot plots separating cells which were identified as increasing, decreasing or having no change in fluorescence between W2 and A1. B) five random individual cells identified as showing an increase in $[Ca^{2+}]_i$ between W2 and A21. Plots for cells identified as decreasing or having no change for these periods were not included as the corresponding Rtot plots in (A) represent the only cells in these experiments which exhibited a decrease or no change.



Appendix II.iv- Perfusion timelapse plots showing a comparison between periods A1 and A2 from 4 experiments in which a total of 666 OE-E6/E7 cells were perfused with swimup sperm cells as a stimulus. A) Rtot plots separating cells which were identified as increasing, decreasing or having no change in fluorescence between A1 and A2. B) five random individual cells identified as showing an increase in $[Ca^{2+}]_i$ between A1 and A2. C) five random individual cells identified as showing a decrease in $[Ca^{2+}]_i$ between A1 and A2. D) five random individual cells identified as showing no change in $[Ca^{2+}]_i$ between A1 and A2.

Appendix III

Cell response summaries during initial Ca^{2+} imaging experiments

Summary of HEC-1-B cells perfused with DGC Sperm Cells		
Comparison Period	Median Proportion of cell $[Ca^{2+}]_i$ responses (%)	Standard error of the median (%)
C1 to C2- Decrease	69.55	16.58
C1 to C2- No change	25.78	9.58
C1 to C2- Increase	4.67	8.02
C2 to R1- Decrease	93.97	3.60
C2 to R1- No Change	5.07	3.09
C2 to R1- Increase	0.80	0.64
R1 to R2- Decrease	54.12	10.12
R1 to R2- No Change	36.42	6.86
R1 to R2- Increase	9.46	3.68
R2 to W1- Decrease	6.64	19.64
R2 to W1- No Change	24.31	8.45
R2 to W1- Increase	66.59	24.55
W1 to W2- Decrease	15.41	11.80
W1 to W2- No Change	42.47	14.61
W1 to W2- Increase	27.34	21.45
W2 to A1- Decrease	0.00	0.30
W2 to A1- No Change	0.24	1.75
W2 to A1- Increase	99.76	2.05
A1 to A2- Decrease	96.98	0.88
A1 to A2- No change	3.02	0.79
A1 to A2- Increase	0.00	0.15

Appendix III.i- A summary table of the types of response observed during Ca^{2+} imaging experiments in which HEC-1-B cells were perfused with DGC sperm cells. The table displays the median average proportion of cells identified as increasing, decreasing or showing no change in fluorescence between each of the experimental periods outlined in section 2.2.9, as well as the standard error of the median.

Summary of HEC-1-B cells perfused with Swimup Sperm Cells		
Comparison Period	Median Proportion of cell $[Ca^{2+}]_i$ responses (%)	Standard error of the median (%)
C1 to C2- Decrease	42.86	15.25
C1 to C2- No change	45.41	12.32
C1 to C2- Increase	7.02	3.66
C2 to R1- Decrease	61.16	22.08
C2 to R1- No Change	26.86	13.03
C2 to R1- Increase	12.37	9.41
R1 to R2- Decrease	38.02	6.64
R1 to R2- No Change	38.71	6.64
R1 to R2- Increase	23.98	7.74
R2 to W1- Decrease	11.16	5.99
R2 to W1- No Change	42.98	11.61
R2 to W1- Increase	45.87	16.97
W1 to W2- Decrease	27.04	13.48
W1 to W2- No Change	40.08	8.55
W1 to W2- Increase	18.37	18.74
W2 to A1- Decrease	0.00	0.45
W2 to A1- No Change	0.00	0.67
W2 to A1- Increase	100.00	1.12
A1 to A2- Decrease	93.88	32.68
A1 to A2- No change	6.12	12.32
A1 to A2- Increase	1.24	20.41

Appendix III.ii- A summary table of the types of response observed during Ca^{2+} imaging experiments in which HEC-1-B cells were perfused with Swimup sperm cells. The table displays the median average proportion of cells identified as increasing, decreasing or showing no change in fluorescence between each of the experimental periods outlined in section 2.2.9, as well as the standard error of the median.

Summary of HEC-1-B cells perfused with Seminal Plasma		
Comparison Period	Median Proportion of cell $[Ca^{2+}]_i$ responses (%)	Standard error of the median (%)
C1 to C2- Decrease	75.30	14.39
C1 to C2- No change	21.41	9.62
C1 to C2- Increase	3.29	5.09
C2 to R1- Decrease	0.20	0.29
C2 to R1- No Change	1.61	2.37
C2 to R1- Increase	97.90	2.52
R1 to R2- Decrease	95.27	1.85
R1 to R2- No Change	3.28	1.36
R1 to R2- Increase	1.30	0.52
R2 to W1- Decrease	99.80	0.29
R2 to W1- No Change	0.20	0.29
R2 to W1- Increase	0.00	0.00
W1 to W2- Decrease	91.15	6.87
W1 to W2- No Change	6.57	5.85
W1 to W2- Increase	2.28	1.29
W2 to A1- Decrease	0.00	0.00
W2 to A1- No Change	0.00	0.00
W2 to A1- Increase	100.00	0.00
A1 to A2- Decrease	100.00	0.83
A1 to A2- No change	0.00	0.72
A1 to A2- Increase	0.00	0.10

Appendix III.iii- A summary table of the types of response observed during Ca^{2+} imaging experiments in which HEC-1-B cells were perfused with Seminal Plasma. The table displays the median average proportion of cells identified as increasing, decreasing or showing no change in fluorescence between each of the experimental periods outlined in section 2.2.9, as well as the standard error of the median.

Summary of OE-E6/E7 cells perfused with DGC Sperm Cells		
Comparison Period	Median Proportion of cell $[Ca^{2+}]_i$ responses (%)	Standard error of the median (%)
C1 to C2- Decrease	52.88	12.91
C1 to C2- No change	29.81	12.43
C1 to C2- Increase	5.97	3.26
C2 to R1- Decrease	18.27	17.78
C2 to R1- No Change	13.46	4.06
C2 to R1- Increase	68.27	21.18
R1 to R2- Decrease	58.65	16.47
R1 to R2- No Change	31.18	5.21
R1 to R2- Increase	4.81	12.48
R2 to W1- Decrease	75.00	17.82
R2 to W1- No Change	17.74	12.40
R2 to W1- Increase	7.26	5.69
W1 to W2- Decrease	43.48	16.87
W1 to W2- No Change	40.86	13.38
W1 to W2- Increase	11.94	10.90
W2 to A1- Decrease	0.00	0.00
W2 to A1- No Change	0.00	0.00
W2 to A1- Increase	100.00	0.00
A1 to A2- Decrease	94.78	4.62
A1 to A2- No change	2.24	3.04
A1 to A2- Increase	2.88	1.67

Appendix III.iv- A summary table of the types of response observed during Ca^{2+} imaging experiments in which OE-E6/E7 cells were perfused with DGC sperm cells. The table displays the median average proportion of cells identified as increasing, decreasing or showing no change in fluorescence between each of the experimental periods outlined in section 2.2.9, as well as the standard error of the median.

Summary of OE-E6/E7 cells perfused with Swimup Sperm Cells		
Comparison Period	Median Proportion of cell $[Ca^{2+}]_i$ responses (%)	Standard error of the median (%)
C1 to C2- Decrease	68.18	21.76
C1 to C2- No change	27.27	17.45
C1 to C2- Increase	4.55	8.22
C2 to R1- Decrease	26.23	12.87
C2 to R1- No Change	13.11	7.06
C2 to R1- Increase	60.66	19.89
R1 to R2- Decrease	75.00	10.19
R1 to R2- No Change	23.17	7.33
R1 to R2- Increase	3.03	3.36
R2 to W1- Decrease	11.11	26.64
R2 to W1- No Change	10.37	14.06
R2 to W1- Increase	26.80	22.52
W1 to W2- Decrease	7.19	7.01
W1 to W2- No Change	40.52	9.14
W1 to W2- Increase	52.29	12.52
W2 to A1- Decrease	0.00	0.16
W2 to A1- No Change	0.00	0.74
W2 to A1- Increase	100.00	0.71
A1 to A2- Decrease	61.76	5.33
A1 to A2- No change	23.53	2.57
A1 to A2- Increase	14.71	3.02

Appendix III.v- A summary table of the types of response observed during Ca^{2+} imaging experiments in which OE-E6/E7 cells were perfused with Swimup sperm cells. The table displays the median average proportion of cells identified as increasing, decreasing or showing no change in fluorescence between each of the experimental periods outlined in section 2.2.9, as well as the standard error of the median.

Summary of OE-E6/E7 cells perfused with Seminal Plasma		
Comparison Period	Median Proportion of cell $[Ca^{2+}]_i$ responses (%)	Standard error of the median (%)
C1 to C2- Decrease	75.35	4.10
C1 to C2- No change	18.91	4.28
C1 to C2- Increase	3.88	1.22
C2 to R1- Decrease	0.00	1.62
C2 to R1- No Change	1.03	1.35
C2 to R1- Increase	97.73	2.23
R1 to R2- Decrease	59.31	13.72
R1 to R2- No Change	25.09	7.36
R1 to R2- Increase	15.60	6.42
R2 to W1- Decrease	89.09	4.53
R2 to W1- No Change	8.10	3.79
R2 to W1- Increase	2.85	1.33
W1 to W2- Decrease	55.35	19.07
W1 to W2- No Change	22.85	9.10
W1 to W2- Increase	20.07	10.46
W2 to A1- Decrease	0.00	0.00
W2 to A1- No Change	0.00	0.00
W2 to A1- Increase	100.00	0.00
A1 to A2- Decrease	53.70	21.63
A1 to A2- No change	21.41	7.03
A1 to A2- Increase	16.59	25.14

Appendix III.vi- A summary table of the types of response observed during Ca^{2+} imaging experiments in which OE-E6/E7 cells were perfused with seminal plasma. The table displays the median average proportion of cells identified as increasing, decreasing or showing no change in fluorescence between each of the experimental periods outlined in section 2.2.9, as well as the standard error of the median.

Summary of COV434 cells perfused with DGC sperm cells		
Comparison Period	Median Proportion of cell $[Ca^{2+}]_i$ responses (	Standard error of the median
C1 to C2- Decrease	33.18	16.93
C1 to C2- No change	39.25	15.63
C1 to C2- Increase	12.21	6.49
C2 to R1- Decrease	78.55	16.18
C2 to R1- No Change	15.07	13.71
C2 to R1- Increase	6.38	2.76
R1 to R2- Decrease	68.32	27.17
R1 to R2- No Change	29.77	7.88
R1 to R2- Increase	7.25	20.05
R2 to W1- Decrease	61.16	26.27
R2 to W1- No Change	31.31	2.99
R2 to W1- Increase	9.86	23.49
W1 to W2- Decrease	24.06	12.39
W1 to W2- No Change	44.86	6.78
W1 to W2- Increase	26.67	18.58
W2 to A1- Decrease	0.00	1.76
W2 to A1- No Change	0.00	2.73
W2 to A1- Increase	100.00	4.49
A1 to A2- Decrease	99.24	2.20
A1 to A2- No change	0.38	1.88
A1 to A2- Increase	0.38	0.34

Appendix III.vii- A summary table of the types of response observed during Ca^{2+} imaging experiments in which COV434 cells were perfused with DGC sperm cells. The table displays the median average proportion of cells identified as increasing, decreasing or showing no change in fluorescence between each of the experimental periods outlined in section 2.2.9, as well as the standard error of the median.

Summary of COV434 cells perfused with Swimup Sperm Cells		
Comparison Period	Median Proportion of cell $[Ca^{2+}]_i$ responses (	Standard error of the median
C1 to C2- Decrease	45.27	2.28
C1 to C2- No change	36.83	6.70
C1 to C2- Increase	16.74	5.72
C2 to R1- Decrease	40.72	18.35
C2 to R1- No Change	26.05	7.08
C2 to R1- Increase	25.91	14.48
R1 to R2- Decrease	58.10	10.39
R1 to R2- No Change	25.48	5.27
R1 to R2- Increase	16.45	5.47
R2 to W1- Decrease	42.33	13.93
R2 to W1- No Change	33.76	7.72
R2 to W1- Increase	23.91	6.30
W1 to W2- Decrease	33.80	4.16
W1 to W2- No Change	41.77	7.37
W1 to W2- Increase	28.14	8.45
W2 to A1- Decrease	0.00	0.00
W2 to A1- No Change	0.00	0.24
W2 to A1- Increase	100.00	0.24
A1 to A2- Decrease	95.58	2.35
A1 to A2- No change	4.17	2.25
A1 to A2- Increase	0.19	0.16

Appendix III.viii- A summary table of the types of response observed during Ca^{2+} imaging experiments in which COV434 cells were perfused with Swimup sperm cells. The table displays the median average proportion of cells identified as increasing, decreasing or showing no change in fluorescence between each of the experimental periods outlined in section 2.2.9, as well as the standard error of the median.

Summary of COV434 cells perfused with Seminal Plasma		
Comparison Period	Median Proportion of cell $[Ca^{2+}]_i$ responses (1	Standard error of the median
C1 to C2- Decrease	60.72	9.36
C1 to C2- No change	23.06	7.50
C1 to C2- Increase	13.04	3.47
C2 to R1- Decrease	22.38	7.38
C2 to R1- No Change	24.37	8.35
C2 to R1- Increase	53.26	15.66
R1 to R2- Decrease	37.57	19.69
R1 to R2- No Change	26.58	8.76
R1 to R2- Increase	34.43	11.04
R2 to W1- Decrease	66.94	13.57
R2 to W1- No Change	17.98	5.79
R2 to W1- Increase	14.88	7.79
W1 to W2- Decrease	39.14	10.13
W1 to W2- No Change	31.53	4.74
W1 to W2- Increase	29.33	5.73
W2 to A1- Decrease	0.00	0.10
W2 to A1- No Change	0.44	0.39
W2 to A1- Increase	99.56	0.47
A1 to A2- Decrease	98.98	0.67
A1 to A2- No change	0.84	0.57
A1 to A2- Increase	0.15	0.12

Appendix III.ix- A summary table of the types of response observed during Ca^{2+} imaging experiments in which COV434 cells were perfused with seminal plasma. The table displays the median average proportion of cells identified as increasing, decreasing or showing no change in fluorescence between each of the experimental periods outlined in section 2.2.9, as well as the standard error of the median.

Mann-Whitney U Test with Dunn's test results	
Cell line and stimulus compared	P
COV434 DGC sperm to COV434 swimup sperm	0.086
COV434 DGC sperm to COV434 seminal plasma	0.021
COV434 DGC sperm to OE-E6/E7 DGC sperm	0.027
COV434 DGC sperm to OE-E6/E7 seminal plasma	0.043
COV434 DGC sperm to OE-E6/E7 swimup sperm	0.014
COV434 seminal plasma to OE-E6/E7 DGC sperm	1
COV434 seminal plasma to OE-E6/E7 seminal plasma	0.386
COV434 seminal plasma to OE-E6/E7 swimup sperm	0.806
COV434 swimup sperm to COV434 seminal plasma	0.086
COV434 swimup sperm to OE-E6/E7 DGC sperm	0.175
COV434 swimup sperm to OE-E6/E7 seminal plasma	0.027
COV434 swimup sperm to OE-E6/E7 swimup sperm	0.117
HEC-1B DGC sperm to COV434 DGC sperm	0.083
HEC-1B DGC sperm to COV434 seminal plasma	0.021
HEC-1B DGC sperm to COV434 swimup sperm	0.027
HEC-1B DGC sperm to OE-E6/E7 DGC sperm	0.014
HEC-1B DGC sperm to OE-E6/E7 seminal plasma	0.043
HEC-1B DGC sperm to OE-E6/E7 swimup sperm	0.014
HEC-1B DGC sperm to HEC-1B seminal plasma	0.043
HEC-1B DGC sperm to HEC-1B swimup sperm	0.034
HEC-1B seminal plasma to COV434 DGC sperm	0.043
HEC-1B seminal plasma to COV434 seminal plasma	0.386
HEC-1B seminal plasma to COV434 swimup sperm	0.043
HEC-1B seminal plasma to OE-E6/E7 DGC sperm	0.149
HEC-1B seminal plasma to OE-E6/E7 seminal plasma	1
HEC-1B seminal plasma to OE-E6/E7 swimup sperm	0.149
HEC-1B swimup sperm to COV434 DGC sperm	0.157
HEC-1B swimup sperm to COV434 seminal plasma	0.034
HEC-1B swimup sperm to COV434 swimup sperm	0.881
HEC-1B swimup sperm to HEC-1B seminal plasma	0.034
HEC-1B swimup sperm to OE-E6/E7 DGC sperm	0.001
HEC-1B swimup sperm to OE-E6/E7 seminal plasma	0.034
HEC-1B swimup sperm to OE-E6/E7 swimup sperm	4.3E-06
OE-E6/E7 DGC sperm to OE-E6/E7 seminal plasma	0.086
OE-E6/E7 DGC sperm to OE-E6/E7 swimup sperm	0.754
OE-E6/E7 swimup sperm to OE-E6/E7 seminal plasma	0.22

Appendix III.x- A table of the P values acquired from carrying out comparisons between the response rates of the three FRT cell lines with the swimup sperm cells, DGC sperm cells and seminal plasma stimuli. Comparisons were carried out using Mann-Whitney U Tests with Dunn's test to correct for multiple comparison.

Mann-Whitney U Test with Dunn's test results	
Cell line and stimulus compared	P
COV434 DGC sperm to COV434 swimup sperm	0.624
COV434 DGC sperm to COV434 seminal plasma	0.564
COV434 DGC sperm to OE-E6/E7 DGC sperm	0.141
COV434 DGC sperm to OE-E6/E7 seminal plasma	0.043
COV434 DGC sperm to OE-E6/E7 swimup sperm	0.05
COV434 seminal plasma to OE-E6/E7 DGC sperm	0.142
COV434 seminal plasma to OE-E6/E7 seminal plasma	0.021
COV434 seminal plasma to OE-E6/E7 swimup sperm	0.086
COV434 swimup sperm to COV434 seminal plasma	1
COV434 swimup sperm to OE-E6/E7 DGC sperm	0.076
COV434 swimup sperm to OE-E6/E7 seminal plasma	0.014
COV434 swimup sperm to OE-E6/E7 swimup sperm	0.076
HEC-1B DGC sperm to COV434 DGC sperm	0.773
HEC-1B DGC sperm to COV434 seminal plasma	0.248
HEC-1B DGC sperm to COV434 swimup sperm	0.221
HEC-1B DGC sperm to OE-E6/E7 DGC sperm	0.142
HEC-1B DGC sperm to OE-E6/E7 seminal plasma	0.021
HEC-1B DGC sperm to OE-E6/E7 swimup sperm	0.027
HEC-1B DGC sperm to HEC-1B seminal plasma	0.021
HEC-1B DGC sperm to HEC-1B swimup sperm	0.724
HEC-1B seminal plasma to COV434 DGC sperm	0.043
HEC-1B seminal plasma to COV434 seminal plasma	0.021
HEC-1B seminal plasma to COV434 swimup sperm	0.014
HEC-1B seminal plasma to OE-E6/E7 DGC sperm	0.142
HEC-1B seminal plasma to OE-E6/E7 seminal plasma	0.773
HEC-1B seminal plasma to OE-E6/E7 swimup sperm	0.624
HEC-1B swimup sperm to COV434 DGC sperm	0.724
HEC-1B swimup sperm to COV434 seminal plasma	0.289
HEC-1B swimup sperm to COV434 swimup sperm	0.297
HEC-1B swimup sperm to HEC-1B seminal plasma	0.034
HEC-1B swimup sperm to OE-E6/E7 DGC sperm	0.18
HEC-1B swimup sperm to OE-E6/E7 seminal plasma	0.034
HEC-1B swimup sperm to OE-E6/E7 swimup sperm	0.101
OE-E6/E7 DGC sperm to OE-E6/E7 seminal plasma	0.462
OE-E6/E7 DGC sperm to OE-E6/E7 swimup sperm	0.754
OE-E6/E7 swimup sperm to OE-E6/E7 seminal plasma	0.806

Appendix III.xi- A table of the P values acquired from carrying out comparisons between the peak strength of the three FRT cell lines with the swimup sperm cells, DGC sperm cells and seminal plasma stimuli. Comparisons were carried out using Mann-Whitney U Tests with Dunn's test to correct for multiple comparison.

Appendix IV

OE-E6/E7 Cell response summaries during Ca^{2+} imaging experiments

Summary of OE-E6/E7 cells perfused with Non-Conditioned Media		
Comparison Period	Median Proportion of cell $[Ca^{2+}]_i$ responses (%)	Standard error of the median
C1 to C2- Decrease	62.40	8.85
C1 to C2- No change	25.00	6.55
C1 to C2- Increase	7.76	2.80
C2 to R1- Decrease	96.17	15.92
C2 to R1- No Change	2.29	2.59
C2 to R1- Increase	1.64	13.77
R1 to R2- Decrease	35.43	8.26
R1 to R2- No Change	54.86	4.03
R1 to R2- Increase	9.71	8.48
R2 to W1- Decrease	3.20	14.94
R2 to W1- No Change	14.44	4.11
R2 to W1- Increase	77.22	15.27
W1 to W2- Decrease	1.19	3.95
W1 to W2- No Change	50.00	9.35
W1 to W2- Increase	40.00	10.94
W2 to A1- Decrease	0.00	0.17
W2 to A1- No Change	0.00	0.25
W2 to A1- Increase	100.00	0.41
A1 to A2- Decrease	59.44	10.30
A1 to A2- No change	24.00	3.27
A1 to A2- Increase	9.14	8.47

Appendix IV.i- A summary table of the types of response observed during Ca^{2+} imaging experiments in which OE-E6/E7 cells were perfused with non-conditioned media. The table displays the median average proportion of cells identified as increasing, decreasing or showing no change in fluorescence between each of the experimental periods outlined in section 2.2.9, as well as the standard error of the median.

Summary of OE-E6/E7 cells perfused with Time Zero Post-Swimup Sperm Cells		
Comparison Period	Median Proportion of cell $[Ca^{2+}]_i$ responses (%)	Standard error of the median
C1 to C2- Decrease	73.74	15.17
C1 to C2- No change	19.30	12.81
C1 to C2- Increase	5.20	7.46
C2 to R1- Decrease	27.32	10.99
C2 to R1- No Change	23.37	7.84
C2 to R1- Increase	36.23	12.65
R1 to R2- Decrease	43.68	5.96
R1 to R2- No Change	38.36	3.68
R1 to R2- Increase	12.79	4.16
R2 to W1- Decrease	50.39	12.61
R2 to W1- No Change	27.43	9.68
R2 to W1- Increase	12.37	7.77
W1 to W2- Decrease	41.16	10.51
W1 to W2- No Change	32.29	6.35
W1 to W2- Increase	19.61	10.47
W2 to A1- Decrease	0.00	0.29
W2 to A1- No Change	0.00	2.24
W2 to A1- Increase	100.00	2.51
A1 to A2- Decrease	50.00	11.44
A1 to A2- No change	23.21	5.73
A1 to A2- Increase	14.04	13.62

Appendix IV.ii- A summary table of the types of response observed during Ca^{2+} imaging experiments in which OE-E6/E7 cells were perfused with time zero post-swimup sperm cells. The table displays the median average proportion of cells identified as increasing, decreasing or showing no change in fluorescence between each of the experimental periods outlined in section 2.2.9, as well as the standard error of the median.

Summary of OE-E6/E7 cells perfused with Swimup Capacitated Sperm Cells		
Comparison Period	Median Proportion of cell $[Ca^{2+}]_i$ responses (%)	Standard error of the median
C1 to C2- Decrease	55.37	11.67
C1 to C2- No change	40.50	10.75
C1 to C2- Increase	4.67	1.49
C2 to R1- Decrease	3.49	8.69
C2 to R1- No Change	12.79	4.30
C2 to R1- Increase	78.89	11.57
R1 to R2- Decrease	45.33	13.94
R1 to R2- No Change	25.35	9.63
R1 to R2- Increase	9.33	9.64
R2 to W1- Decrease	57.33	13.79
R2 to W1- No Change	29.20	6.48
R2 to W1- Increase	6.67	9.18
W1 to W2- Decrease	11.68	6.13
W1 to W2- No Change	51.76	7.21
W1 to W2- Increase	29.65	7.28
W2 to A1- Decrease	0.00	0.12
W2 to A1- No Change	0.00	0.25
W2 to A1- Increase	100.00	0.31
A1 to A2- Decrease	56.00	5.47
A1 to A2- No change	30.71	5.25
A1 to A2- Increase	6.98	1.74

Appendix IV.iii- A summary table of the types of response observed during Ca^{2+} imaging experiments in which OE-E6/E7 cells were perfused with swimup capacitated sperm cells. The table displays the median average proportion of cells identified as increasing, decreasing or showing no change in fluorescence between each of the experimental periods outlined in section 2.2.9, as well as the standard error of the median.

Summary of OE-E6/E7 cells perfused with Sperm Conditioned Media		
Comparison Period	Median Proportion of cell $[Ca^{2+}]_i$ responses (%)	Standard error of the median
C1 to C2- Decrease	44.99	10.39
C1 to C2- No change	33.13	7.58
C1 to C2- Increase	7.06	6.03
C2 to R1- Decrease	2.13	1.93
C2 to R1- No Change	3.51	3.29
C2 to R1- Increase	92.28	4.79
R1 to R2- Decrease	70.12	7.71
R1 to R2- No Change	21.83	5.24
R1 to R2- Increase	2.34	4.69
R2 to W1- Decrease	72.21	12.46
R2 to W1- No Change	21.11	6.91
R2 to W1- Increase	8.12	6.31
W1 to W2- Decrease	23.49	7.89
W1 to W2- No Change	45.26	8.74
W1 to W2- Increase	19.14	6.79
W2 to A1- Decrease	0.00	0.16
W2 to A1- No Change	0.00	0.14
W2 to A1- Increase	100.00	0.22
A1 to A2- Decrease	57.23	8.35
A1 to A2- No change	24.17	4.77
A1 to A2- Increase	9.21	7.78

Appendix IV.iv- A summary table of the types of response observed during Ca^{2+} imaging experiments in which OE-E6/E7 cells were perfused with sperm conditioned media. The table displays the median average proportion of cells identified as increasing, decreasing or showing no change in fluorescence between each of the experimental periods outlined in section 2.2.9, as well as the standard error of the median.

Summary of OE-E6/E7 cells perfused with Clean DGC sperm cells		
Comparison Period	Median Proportion of cell $[Ca^{2+}]_i$ responses (%)	Standard error of the median
C1 to C2- Decrease	53.41	7.43
C1 to C2- No change	42.56	6.02
C1 to C2- Increase	5.98	3.10
C2 to R1- Decrease	96.36	3.82
C2 to R1- No Change	3.30	3.63
C2 to R1- Increase	0.67	0.27
R1 to R2- Decrease	24.45	8.02
R1 to R2- No Change	62.37	6.53
R1 to R2- Increase	6.55	6.83
R2 to W1- Decrease	8.03	3.52
R2 to W1- No Change	56.49	8.05
R2 to W1- Increase	25.58	9.52
W1 to W2- Decrease	12.06	5.16
W1 to W2- No Change	68.33	4.83
W1 to W2- Increase	11.62	4.16
W2 to A1- Decrease	0.00	0.00
W2 to A1- No Change	0.00	0.38
W2 to A1- Increase	100.00	0.38
A1 to A2- Decrease	67.54	10.17
A1 to A2- No change	26.74	6.26
A1 to A2- Increase	3.90	6.10

Appendix IV.v- A summary table of the types of response observed during Ca^{2+} imaging experiments in which OE-E6/E7 cells were perfused with clean DGC sperm cells. The table displays the median average proportion of cells identified as increasing, decreasing or showing no change in fluorescence between each of the experimental periods outlined in section 2.2.9, as well as the standard error of the median.

Summary of OE-E6/E7 cells perfused with "Contaminated" DGC Sperm Cells		
Comparison Period	Median Proportion of cell $[Ca^{2+}]_i$ responses (%)	Standard error of the median
C1 to C2- Decrease	43.83	10.93
C1 to C2- No change	36.00	10.25
C1 to C2- Increase	6.55	5.04
C2 to R1- Decrease	42.71	15.33
C2 to R1- No Change	15.87	3.27
C2 to R1- Increase	37.96	17.19
R1 to R2- Decrease	31.44	13.04
R1 to R2- No Change	38.92	6.99
R1 to R2- Increase	26.48	7.94
R2 to W1- Decrease	63.89	11.18
R2 to W1- No Change	26.86	7.54
R2 to W1- Increase	9.59	4.04
W1 to W2- Decrease	43.30	12.29
W1 to W2- No Change	39.42	8.87
W1 to W2- Increase	17.45	9.22
W2 to A1- Decrease	0.00	6.56
W2 to A1- No Change	0.00	9.16
W2 to A1- Increase	100.00	14.72
A1 to A2- Decrease	84.63	21.31
A1 to A2- No change	2.44	1.97
A1 to A2- Increase	5.12	21.72

Appendix IV.vi- A summary table of the types of response observed during Ca^{2+} imaging experiments in which OE-E6/E7 cells were perfused with “contaminated” DGC sperm cells. The table displays the median average proportion of cells identified as increasing, decreasing or showing no change in fluorescence between each of the experimental periods outlined in section 2.2.9, as well as the standard error of the median.

Mann-Whitney U Test with Dunn's test results	
Stimuli compared	P value
Clean DGC sperm cells to Sperm conditioned media	0.0002
Clean DGC sperm cells to "Contaminated" DGC sperm cells	0.0004
Clean DGC sperm cells to Non-conditioned media	0.205
Clean DGC sperm cells to Swimup capacitated sperm cells	0.0002
Clean DGC sperm cells to Time zero post-swimup sperm cells	0.0002
"Contaminated" DGC sperm cells to Non-conditioned media	0.028
"Contaminated" DGC sperm cells to Sperm conditioned media	0.016
"Contaminated" DGC sperm cells to Swimup capacitated sperm cells	0.102
"Contaminated" DGC sperm cells to Time zero post-swimup sperm cells	0.859
Sperm conditioned media to Non-conditioned media	0.001
Swimup capacitated sperm cells to Non-conditioned media	0.004
Swimup capacitated sperm cells to Sperm conditioned media	0.221
Swimup capacitated sperm cells to Time zero post-swimup sperm cells	0.05
Time zero post-swimup sperm cells to Non-conditioned media	0.019
Time zero post-swimup sperm cells to Sperm conditioned media	0.003

Appendix IV.vii- A table of the P values acquired from carrying out comparisons between the response rates of the OE-E6/E7 cells with the clean DGC sperm cells, “contaminated” DGC sperm cells, swimup capacitated sperm cells, time zero post-swimup sperm cells, sperm conditioned media and non-conditioned media stimuli. Comparisons were carried out using Mann-Whitney U Tests with Dunn’s test to correct for multiple comparison.

Mann-Whitney U Test with Dunn's test results	
Stimuli compared	P value
Clean DGC sperm cells to Sperm conditioned media	4.37E-0.5
Clean DGC sperm cells to "Contaminated" DGC sperm cells	0.076
Clean DGC sperm cells to Non-conditioned media	0.77
Clean DGC sperm cells to Swimup capacitated sperm cells	4.37E-0.5
Clean DGC sperm cells to Time zero post-swimup sperm cells	0.01
"Contaminated" DGC sperm cells to Non-conditioned media	0.105
"Contaminated" DGC sperm cells to Sperm conditioned media	0.11
"Contaminated" DGC sperm cells to Swimup capacitated sperm cells	0.083
"Contaminated" DGC sperm cells to Time zero post-swimup sperm cells	0.722
Sperm conditioned media to Non-conditioned media	0.001
Swimup capacitated sperm cells to Non-conditioned media	0.001
Swimup capacitated sperm cells to Sperm conditioned media	0.87
Swimup capacitated sperm cells to Time zero post-swimup sperm cells	0.05
Time zero post-swimup sperm cells to Non-conditioned media	0.118
Time zero post-swimup sperm cells to Sperm conditioned media	0.041

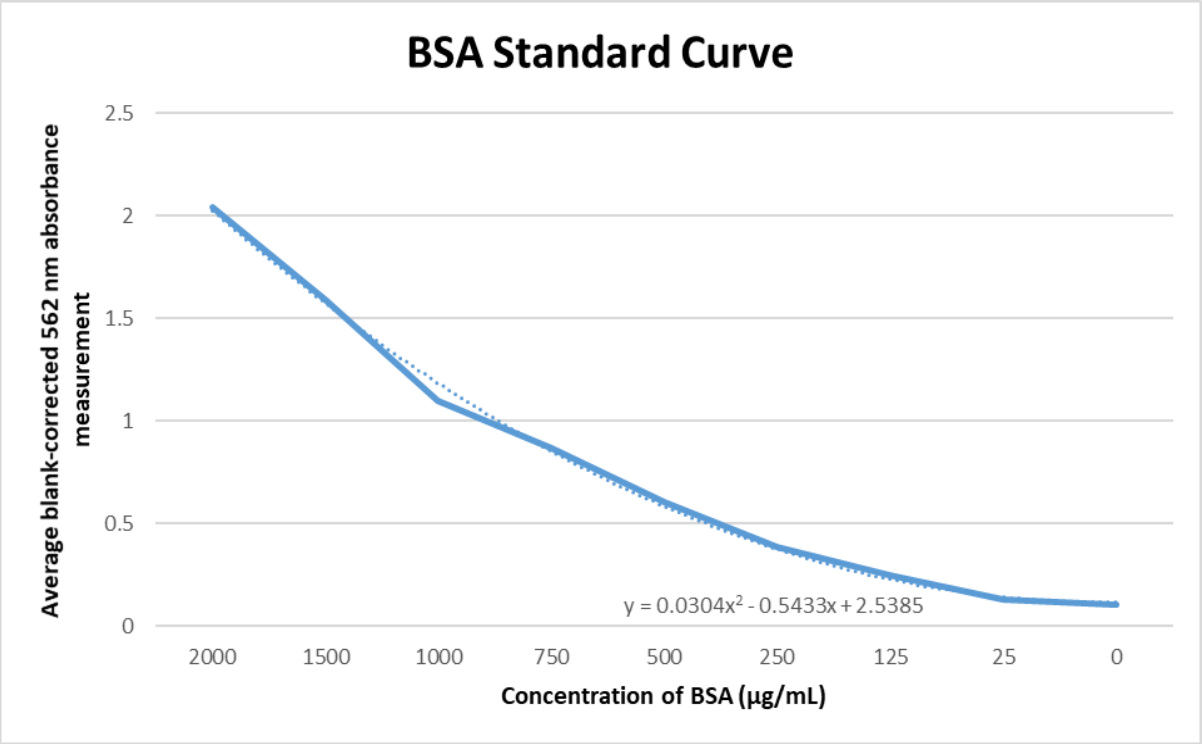
Appendix IV.viii- A table of the P values acquired from carrying out comparisons between the strength of response of the OE-E6/E7 cells with the clean DGC sperm cells, “contaminated” DGC sperm cells, swimup capacitated sperm cells, time zero post-swimup sperm cells, sperm conditioned media and non-conditioned media stimuli. Comparisons were carried out using Mann-Whitney U Tests with Dunn’s test to correct for multiple comparison.

Appendix V

BCA protein quantification assay results

The Pierce™ BCA Protein Assay was carried out, according to the manufacturers protocol, to quantify the protein concentration within each of the precipitated protein pellets suspended in 100 µL ammonium bicarbonate solution to allow for the dilution of the samples to 5-10 µg/mL so that they could undergo proteomic analysis.

A standard curve was produced by measuring the absorbance of solutions containing known concentrations of bovine serum albumin (BSA) at 562 nm:



Appendix V.i- The BSA standard curve from the BCA protein assay

The equation of this standard curve was used to calculate the concentration of the <3 kDa, 3-50 kDa and >50 kDa sperm conditioned media fractions which had average blank-corrected 562 nm absorbance measurements of 0.113, 0.599 and 1.782, respectively.

Appendix VI

>50 kDa fraction of sperm conditioned media proteomic analysis data

The proteomic analysis of the >50 kDa fraction of sperm conditioned media revealed the presence of over 400 proteins. The table of results from this proteomic analysis, showing the name of the proteins identified as well as the number of peptides, unique peptides, amino acids and their molecular weight are as follows:

Description	# Peptides	# Unique Peptides	# AAs	MW [kDa]
Kallikrein 3, (Prostate specific antigen), isoform CRA_m	13	12	261	28.7
Fibronectin 1, isoform CRA_n	59	59	2355	259
Prolactin-inducible protein	11	11	146	16.6
Lactoferrin	41	1	711	78.3
Semenogelin-2	27	1	582	65.4
Mucin-6	40	1	2439	256.9
Semenogelin-1	28	10	462	52.1
Prostatic acid phosphatase	21	21	386	44.5
Aminopeptidase (Fragment)	40	40	977	110.5
Epididymis secretory sperm binding protein Li 71p	39	5	698	77
cDNA FLJ53691, highly similar to Serotransferrin	39	5	678	74.8
SEMG1 protein (Fragment)	20	2	326	36.9
Testicular tissue protein Li 227	22	22	298	34.2
Protein-glutamine gamma-glutamyltransferase 4	30	30	684	77.1
Testicular tissue protein Li 61	23	23	540	60.6
Prosaposin	22	22	524	58.1
Clusterin	18	18	501	57.8
Dipeptidyl peptidase 4	26	26	766	88.2
Angiotensin-converting enzyme	24	24	1306	149.6
IgGFc-binding protein	24	24	5405	571.6
Membrane metallo-endopeptidase	21	21	750	85.5
Alpha-1-antitrypsin	19	2	418	46.7
Epididymis secretory sperm binding protein	17	17	476	53.1
Lectin galactoside-binding soluble 3 binding protein isoform 1 (Fragment)	15	15	585	65.3
Epididymis secretory sperm binding protein	18	1	418	46.7
Uncharacterized protein DKFZp686C11235	11	1	473	52.1
Sulfhydryl oxidase 1	17	17	747	82.5
Beta-hexosaminidase subunit beta	16	15	556	63.1
Polymeric immunoglobulin receptor	16	16	764	83.2

Amine oxidase	15	15	751	85.3
Plastin-2	15	15	627	70.2
Plasma serine protease inhibitor	10	10	406	45.6
Hemopexin	13	13	462	51.6
Kallikrein-2	8	7	261	28.7
Nucleobindin-2	12	12	420	50.2
Cystatin-S	8	8	141	16.2
CD177 antigen	8	2	437	46.4
cDNA FLJ55673, highly similar to Complement factor B	14	14	1266	140.9
Triosephosphate isomerase	11	11	286	30.8
cDNA FLJ90373 fis, clone NT2RP2004606, highly similar to Metalloproteinase inhibitor 1	9	9	207	23.2
NPC intracellular cholesterol transporter 2 (Fragment)	8	8	221	23.7
Uncharacterized protein DKFZp686I04196 (Fragment)	10	3	417	46
Alpha-1-acid glycoprotein	8	6	201	23.5
Cathepsin B	10	10	339	37.8
Cysteine-rich secretory protein 1	9	9	249	28.5
Golgi apparatus protein 1	12	12	1179	134.5
Fructose-bisphosphate aldolase	10	10	364	39.4
N-acylsphingosine amidohydrolase (Acid ceramidase) 1, isoform CRA_c	11	6	546	60.6
Carboxypeptidase M	8	8	443	50.5
L-lactate dehydrogenase	12	11	332	36.3
cDNA, FLJ93778, highly similar to Homo sapiens CD38 antigen (p45) (CD38), mRNA	9	9	300	34.3
Ribonuclease T2	8	8	307	35.6
cDNA FLJ75006, highly similar to Homo sapiens CD177 molecule, mRNA	7	1	437	46.3
IGK@ protein	6	5	236	25.8
Peptidyl-prolyl cis-trans isomerase B	10	10	216	23.7
Immunoglobulin heavy constant gamma 4 (Fragment)	9	2	396	43.8
L-lactate dehydrogenase B chain	10	8	334	36.6
Cation-independent mannose-6-phosphate receptor	11	11	2491	274.2
Cysteine-rich secretory protein LCCL domain-containing 2	9	9	497	55.9
Isocitrate dehydrogenase [NADP]	10	10	414	46.6
cDNA FLJ54658, highly similar to Limbic system-associated membrane protein	9	9	358	39.7
Uncharacterized protein DKFZp686E01144	9	9	967	105.3
Epididymis secretory sperm binding protein Li 95n	10	10	357	38.3
Kallikrein-11	7	7	282	31
Follistatin-related protein 1 OS=Homo sapiens OX=9606 GN=FSTL1 PE=1 SV=1	7	7	308	35
Phosphatidylethanolamine-binding protein 4 OS=Homo sapiens OX=9606 GN=PEBP4 PE=1 SV=3	6	6	227	25.7

Elongation factor 1-alpha (Fragment) OS=Homo sapiens OX=9606 PE=2 SV=1	9	9	462	50.1
cDNA FLJ56402, highly similar to Tripeptidyl-peptidase 1 OS=Homo sapiens OX=9606 PE=2 SV=1	9	9	572	62.2
cDNA, FLJ92074, highly similar to Homo sapiens progestagen-associated endometrial protein (placentalprotein 14, pregnancy-associated endometrial alpha-2-globulin,alpha uterine protein) (PAEP), mRNA OS=Homo sapiens OX=9606 PE=2 SV=1	6	6	162	18.9
Cysteine-rich secretory protein 3 OS=Homo sapiens OX=9606 GN=CRISP3 PE=1 SV=1	6	2	276	31
Calsyntenin-1 OS=Homo sapiens OX=9606 GN=CLSTN1 PE=1 SV=1	10	10	981	109.7
YWHAE/FAM22A fusion protein (Fragment) OS=Homo sapiens OX=9606 GN=YWHAE/FAM22A fusion PE=2 SV=1	8	6	384	41.2
Creatine kinase brain isoform 2 (Fragment) OS=Homo sapiens OX=9606 GN=CKB PE=2 SV=1	8	8	405	44.9
Acrosin OS=Homo sapiens OX=9606 GN=ACR PE=1 SV=4	8	8	421	45.8
Sialate O-acetylesterase OS=Homo sapiens OX=9606 GN=SIAE PE=1 SV=1	7	7	523	58.3
Laminin, beta 2 (Laminin S), isoform CRA_a OS=Homo sapiens OX=9606 GN=LAMB2 PE=4 SV=1	8	8	1798	195.9
Progranulin OS=Homo sapiens OX=9606 GN=GRN PE=1 SV=2	8	8	593	63.5
Alpha-1-acid glycoprotein 2 OS=Homo sapiens OX=9606 GN=ORM2 PE=1 SV=2	6	4	201	23.6
cDNA FLJ59147, highly similar to Cysteine-rich secretory protein 3 OS=Homo sapiens OX=9606 PE=2 SV=1	5	1	155	17.3
Transmembrane protease serine 2 OS=Homo sapiens OX=9606 GN=TMPRSS2 PE=1 SV=3	5	5	492	53.8
Attractin OS=Homo sapiens OX=9606 GN=ATRN PE=1 SV=2	9	9	1429	158.4
Glucose-6-phosphate isomerase OS=Homo sapiens OX=9606 GN=GPI PE=1 SV=1	8	8	597	67.2
Lactoylglutathione lyase OS=Homo sapiens OX=9606 GN=GLO1 PE=1 SV=4	7	7	184	20.8
Dopamine receptor interacting protein 4 OS=Homo sapiens OX=9606 GN=DRIP4 PE=2 SV=1	8	8	868	96
cDNA FLJ77770, highly similar to Homo sapiens nucleobindin 1 (NUCB1), mRNA OS=Homo sapiens OX=9606 PE=2 SV=1	8	8	461	53.9
Maltase-glucoamylase, intestinal OS=Homo sapiens OX=9606 GN=MGAM PE=1 SV=2	8	8	2753	311.8
Epididymis luminal protein 4 OS=Homo sapiens OX=9606 GN=YWHAZ PE=2 SV=1	7	5	245	27.7
Malate dehydrogenase, cytoplasmic OS=Homo sapiens OX=9606 GN=MDH1 PE=1 SV=4	7	7	334	36.4
Lipoprotein lipase OS=Homo sapiens OX=9606 PE=2 SV=1	7	7	475	53.2
Epididymis secretory protein Li 34 OS=Homo sapiens OX=9606 GN=HEL-S-34 PE=2 SV=1	6	6	187	21

IgG H chain OS=Homo sapiens OX=9606 PE=2 SV=1	5	1	300	32.2
Epididymis secretory sperm binding protein OS=Homo sapiens OX=9606 GN=RAB3D PE=2 SV=1	6	3	219	24.3
Prostaglandin-H2 D-isomerase OS=Homo sapiens OX=9606 GN=PTGDS PE=1 SV=1	4	4	190	21
Epididymis secretory sperm binding protein Li 89n OS=Homo sapiens OX=9606 GN=HEL-S-89n PE=2 SV=1	6	5	654	72.3
Beta-mannosidase OS=Homo sapiens OX=9606 GN=MANBA PE=1 SV=1	7	7	886	101.1
Cathelicidin antimicrobial peptide OS=Homo sapiens OX=9606 GN=CAMP PE=1 SV=1	6	6	173	19.6
Superoxide dismutase [Cu-Zn] OS=Homo sapiens OX=9606 PE=2 SV=1	5	5	240	25.9
Ras-related protein Rab-3B OS=Homo sapiens OX=9606 GN=RAB3B PE=1 SV=2	6	3	219	24.7
Haptoglobin OS=Homo sapiens OX=9606 GN=HP PE=1 SV=1	6	6	406	45.2
Glutathione S-transferase (Fragment) OS=Homo sapiens OX=9606 PE=2 SV=1	5	5	231	27.2
Agrin OS=Homo sapiens OX=9606 GN=AGRN PE=1 SV=6	6	6	2068	217.2
N-acylsphingosine amidohydrolase 1 (Fragment) OS=Homo sapiens OX=9606 GN=ASAH1 PE=4 SV=1	6	1	219	24.7
Aldo-keto reductase family 1 member B1 OS=Homo sapiens OX=9606 GN=AKR1B1 PE=1 SV=3	6	6	316	35.8
Vitamin D-binding protein OS=Homo sapiens OX=9606 GN=GC PE=1 SV=1	5	5	476	53
Annexin A1 OS=Homo sapiens OX=9606 GN=ANXA1 PE=1 SV=2	6	6	346	38.7
Epididymis secretory sperm binding protein OS=Homo sapiens OX=9606 PE=2 SV=1	5	5	223	26.1
N(G),N(G)-dimethylarginine dimethylaminohydrolase 1 OS=Homo sapiens OX=9606 GN=DDAH1 PE=1 SV=3	5	5	285	31.1
Biotinidase OS=Homo sapiens OX=9606 GN=BTD PE=1 SV=2	5	5	543	61.1
Phospholipase A1 member A OS=Homo sapiens OX=9606 GN=PLA1A PE=2 SV=2	5	5	456	49.7
RAB27A, member RAS oncogene family OS=Homo sapiens OX=9606 GN=RAB27A PE=2 SV=1	4	3	221	24.9
Laminin subunit gamma-1 OS=Homo sapiens OX=9606 GN=LAMC1 PE=1 SV=3	6	6	1609	177.5
HCG2010666, isoform CRA_a OS=Homo sapiens OX=9606 GN=hCG_2010666 PE=4 SV=1	6	6	569	61.4
Epididymis luminal protein 33 OS=Homo sapiens OX=9606 GN=HEL-S-72p PE=2 SV=1	5	2	646	70.9
Epididymis luminal secretory protein 52 OS=Homo sapiens OX=9606 GN=EL52 PE=2 SV=1	6	3	732	84.6
IGL@ protein OS=Homo sapiens OX=9606 GN=IGL@ PE=1 SV=1	4	1	236	24.8

Calcium activated nucleotidase 1, isoform CRA_b OS=Homo sapiens OX=9606 GN=CANT1 PE=4 SV=1	6	6	401	44.8
Nucleotide exchange factor SIL1 OS=Homo sapiens OX=9606 GN=SIL1 PE=1 SV=1	6	6	468	52.7
Pancreatic secretory granule membrane major glycoprotein GP2 OS=Homo sapiens OX=9606 GN=GP2 PE=2 SV=3	5	5	537	59.4
Peroxiredoxin-6 OS=Homo sapiens OX=9606 GN=PRDX6 PE=1 SV=3	6	6	224	25
Alpha-N-acetylglucosaminidase OS=Homo sapiens OX=9606 GN=NAGLU PE=1 SV=2	5	5	743	82.2
IGL@ protein OS=Homo sapiens OX=9606 GN=IGL@ PE=2 SV=1	4	1	236	24.7
Uncharacterized protein DKFZp686K18196 (Fragment) OS=Homo sapiens OX=9606 GN=DKFZp686K18196 PE=2 SV=1	6	3	519	56.4
Cathepsin Z OS=Homo sapiens OX=9606 PE=2 SV=1	5	5	303	33.8
Uncharacterized protein OS=Homo sapiens OX=9606 PE=2 SV=1	4	1	235	24.7
Kunitz-type protease inhibitor 1 OS=Homo sapiens OX=9606 GN=SPINT1 PE=1 SV=2	6	6	529	58.4
Acid sphingomyelinase-like phosphodiesterase 3a OS=Homo sapiens OX=9606 GN=SMPDL3A PE=1 SV=2	5	5	453	51.2
Fibromodulin OS=Homo sapiens OX=9606 GN=FMOD PE=1 SV=2	3	3	376	43.2
Brain acid soluble protein 1 OS=Homo sapiens OX=9606 GN=BASP1 PE=1 SV=2	4	4	227	22.7
Beta-microseminoprotein OS=Homo sapiens OX=9606 GN=MSMB PE=1 SV=1	2	2	114	12.9
Tetraspanin OS=Homo sapiens OX=9606 GN=CD9 PE=1 SV=2	4	4	251	28.1
Epididymis secretory protein Li 2 OS=Homo sapiens OX=9606 GN=HEL-S-2 PE=2 SV=1	5	5	146	15.8
Heat shock 70kDa protein 1A variant (Fragment) OS=Homo sapiens OX=9606 PE=2 SV=1	5	4	709	77.4
Epididymis secretory sperm binding protein OS=Homo sapiens OX=9606 PE=2 SV=1	4	1	639	69.9
Nephroblastoma overexpressed gene, isoform CRA_a OS=Homo sapiens OX=9606 GN=NOV PE=4 SV=1	5	5	357	39.1
CD59 glycoprotein OS=Homo sapiens OX=9606 GN=CD59 PE=1 SV=1	3	3	128	14.2
Ganglioside GM2 activator OS=Homo sapiens OX=9606 GN=GM2A PE=1 SV=4	4	4	193	20.8
Cytosolic non-specific dipeptidase OS=Homo sapiens OX=9606 GN=CNDP2 PE=1 SV=2	5	5	475	52.8
Peroxiredoxin-2 OS=Homo sapiens OX=9606 GN=PRDX2 PE=1 SV=5	5	4	198	21.9
cDNA, FLJ95483, highly similar to Homo sapiens chitobiase, di-N-acetyl- (CTBS), mRNA OS=Homo sapiens OX=9606 PE=2 SV=1	5	5	385	43.8
Glyceraldehyde-3-phosphate dehydrogenase OS=Homo sapiens OX=9606 GN=GAPDH PE=1 SV=3	5	5	335	36

Heat shock protein 90kDa alpha (Cytosolic), class B member 1, isoform CRA_a OS=Homo sapiens OX=9606 GN=HSP90AB1 PE=3 SV=1	5	2	724	83.2
Rab GDP dissociation inhibitor OS=Homo sapiens OX=9606 PE=2 SV=1	5	5	449	51.1
Lysosome-associated membrane glycoprotein 2 OS=Homo sapiens OX=9606 GN=LAMP2 PE=1 SV=2	5	5	410	44.9
Laminin subunit alpha-5 OS=Homo sapiens OX=9606 GN=LAMA5 PE=1 SV=8	5	5	3695	399.5
Interleukin-6 receptor subunit beta OS=Homo sapiens OX=9606 GN=IL6ST PE=1 SV=2	4	4	918	103.5
Alpha-enolase OS=Homo sapiens OX=9606 GN=ENO1 PE=1 SV=1	4	4	434	47.3
Diazepam binding inhibitor, splice form 1D(2) OS=Homo sapiens OX=9606 GN=DBI PE=2 SV=1	4	4	144	16.1
L-lactate dehydrogenase A chain OS=Homo sapiens OX=9606 GN=LDHA PE=1 SV=2	4	2	332	36.7
Cysteine-rich secretory protein LCCL domain-containing 1 OS=Homo sapiens OX=9606 GN=CRISPLD1 PE=2 SV=1	3	3	500	56.9
Matrix metallopeptidase 2 (Gelatinase A, 72kDa gelatinase, 72kDa type IV collagenase), isoform CRA_a OS=Homo sapiens OX=9606 GN=MMP2 PE=3 SV=1	4	4	660	73.8
Glutamate carboxypeptidase 2 OS=Homo sapiens OX=9606 GN=FOLH1 PE=1 SV=1	4	4	750	84.3
Immunoglobulin alpha-2 heavy chain OS=Homo sapiens OX=9606 PE=1 SV=2	4	1	455	48.9
Lysosomal-associated membrane protein 1, isoform CRA_a OS=Homo sapiens OX=9606 GN=LAMP1 PE=3 SV=1	4	4	417	44.9
Testicular tissue protein Li 48 OS=Homo sapiens OX=9606 PE=2 SV=1	3	3	710	79.2
Cartilage acidic protein 1 OS=Homo sapiens OX=9606 GN=CRTAC1 PE=1 SV=2	4	4	661	71.4
cDNA FLJ76704, highly similar to Homo sapiens leukemia inhibitory factor receptor (LIFR), mRNA OS=Homo sapiens OX=9606 PE=2 SV=1	4	4	1097	123.8
Phosphatidic acid phosphatase type 2A, isoform CRA_b OS=Homo sapiens OX=9606 GN=PPAP2A PE=4 SV=1	3	3	285	32.1
WAP four-disulfide core domain protein 2 OS=Homo sapiens OX=9606 GN=WFDC2 PE=1 SV=2	3	3	124	13
Apolipoprotein H (Beta-2-glycoprotein I), isoform CRA_a OS=Homo sapiens OX=9606 GN=APOH PE=2 SV=1	4	4	345	38.3
Tissue alpha-L-fucosidase OS=Homo sapiens OX=9606 GN=FUCA1 PE=1 SV=4	4	4	466	53.7
Apolipoprotein D (Fragment) OS=Homo sapiens OX=9606 GN=APOD PE=1 SV=1	4	4	215	24.1
Nucleoside diphosphate kinase A OS=Homo sapiens OX=9606 GN=NME1 PE=1 SV=1	3	3	152	17.1
Methanethiol oxidase OS=Homo sapiens OX=9606 GN=SELENBP1 PE=1 SV=2	3	3	472	52.4
Monocyte differentiation antigen CD14 OS=Homo sapiens OX=9606 PE=2 SV=1	4	4	375	40

cDNA FLJ78452, highly similar to Homo sapiens legumain (LGMN), transcript variant 2, mRNA OS=Homo sapiens OX=9606 PE=2 SV=1	3	3	433	49.4
Phosphoglycerate mutase (Fragment) OS=Homo sapiens OX=9606 PE=2 SV=1	3	3	254	28.8
BPI fold-containing family B member 2 OS=Homo sapiens OX=9606 GN=BPIFB2 PE=1 SV=2	4	4	458	49.1
Phosphoglycerate kinase OS=Homo sapiens OX=9606 GN=HEL-S-68p PE=2 SV=1	4	4	417	44.6
Alpha-2-macroglobulin OS=Homo sapiens OX=9606 GN=A2M PE=1 SV=3	3	3	1474	163.2
Sphingomyelin phosphodiesterase 1, acid lysosomal isoform 1 variant (Fragment) OS=Homo sapiens OX=9606 PE=2 SV=1	3	3	664	73
Prostasin OS=Homo sapiens OX=9606 GN=PRSS8 PE=1 SV=1	2	2	343	36.4
CP protein OS=Homo sapiens OX=9606 GN=CP PE=2 SV=1	3	3	1065	122.1
Protein CutA OS=Homo sapiens OX=9606 GN=CUTA PE=1 SV=2	3	3	179	19.1
Carboxypeptidase Q OS=Homo sapiens OX=9606 GN=CPQ PE=1 SV=1	3	3	472	51.9
Annexin A3 OS=Homo sapiens OX=9606 GN=ANXA3 PE=1 SV=3	3	3	323	36.4
RAB2, member RAS oncogene family, isoform CRA_a OS=Homo sapiens OX=9606 GN=RAB2 PE=4 SV=1	3	3	212	23.5
Metalloproteinase inhibitor 2 OS=Homo sapiens OX=9606 GN=TIMP2 PE=1 SV=2	3	3	220	24.4
Tetraspanin OS=Homo sapiens OX=9606 GN=CD81 PE=1 SV=1	3	3	274	29.8
Carbonic anhydrase 4 OS=Homo sapiens OX=9606 GN=CA4 PE=1 SV=2	3	3	312	35
Toll-like receptor OS=Homo sapiens OX=9606 PE=2 SV=1	1	1	786	90.1
Endocrine and exocrine protein OS=Homo sapiens OX=9606 GN=EECP PE=2 SV=1	3	3	208	22.7
Protein FAM3B OS=Homo sapiens OX=9606 GN=FAM3B PE=1 SV=2	3	3	258	28.3
Glutathione S-transferase theta-1 OS=Homo sapiens OX=9606 GN=GSTT1 PE=1 SV=4	3	3	240	27.3
Antileukoproteinase OS=Homo sapiens OX=9606 GN=SLPI PE=1 SV=2	3	3	132	14.3
Seizure 6-like protein 2 OS=Homo sapiens OX=9606 GN=SEZ6L2 PE=1 SV=1	3	3	923	99.1
Collectin-12 OS=Homo sapiens OX=9606 GN=COLEC12 PE=1 SV=3	3	3	742	81.5
cDNA FLJ14168 fis, clone NT2RP2001440, highly similar to 14-3-3 protein gamma OS=Homo sapiens OX=9606 PE=2 SV=1	3	1	247	28.2
Beta-hexosaminidase OS=Homo sapiens OX=9606 PE=2 SV=1	2	1	540	62
Selenoprotein P OS=Homo sapiens OX=9606 GN=SELENOP PE=1 SV=3	3	3	381	43.2
RAB1B protein OS=Homo sapiens OX=9606 GN=RAB1B PE=2 SV=1	3	3	201	22.2
Testis tissue sperm-binding protein Li 94mP OS=Homo sapiens OX=9606 PE=2 SV=1	3	3	956	106.8

Uncharacterized protein OS=Homo sapiens OX=9606 PE=4 SV=1	3	3	631	71.3
Deoxyribonuclease II, lysosomal, isoform CRA_a OS=Homo sapiens OX=9606 GN=DNASE2 PE=4 SV=1	3	3	360	39.6
Dynein light chain 2, cytoplasmic OS=Homo sapiens OX=9606 GN=DYNLL2 PE=1 SV=1	2	2	89	10.3
WD repeat-containing protein 53 (Fragment) OS=Homo sapiens OX=9606 GN=WDR53 PE=1 SV=1	1	1	160	17.2
Tubulin beta-4B chain OS=Homo sapiens OX=9606 GN=TUBB4B PE=1 SV=1	3	3	445	49.8
14-3-3 protein beta/alpha OS=Homo sapiens OX=9606 GN=YWHAB PE=2 SV=1	3	1	246	28.1
Syndecan binding protein (Syntenin), isoform CRA_a OS=Homo sapiens OX=9606 GN=SDCBP PE=1 SV=1	3	3	318	34.8
Tubulin alpha chain OS=Homo sapiens OX=9606 PE=2 SV=1	3	3	451	50.1
cDNA FLJ56912, highly similar to Fibulin-2 OS=Homo sapiens OX=9606 PE=2 SV=1	3	3	1210	129.3
Gastricsin OS=Homo sapiens OX=9606 GN=PGC PE=1 SV=1	2	2	388	42.4
Dipeptidase OS=Homo sapiens OX=9606 GN=DPEP3 PE=2 SV=1	3	3	512	56.3
Prostate stem cell antigen OS=Homo sapiens OX=9606 GN=PSCA PE=1 SV=2	3	3	114	12
Golgi membrane protein 1 OS=Homo sapiens OX=9606 GN=GOLM1 PE=1 SV=1	3	3	401	45.3
Glucosidase, alpha acid (Pompe disease, glycogen storage disease type II), isoform CRA_a OS=Homo sapiens OX=9606 GN=GAA PE=3 SV=1	3	3	952	105.3
Protein tyrosine phosphatase, receptor type, sigma isoform 3 variant (Fragment) OS=Homo sapiens OX=9606 PE=2 SV=1	3	3	1560	174.5
Tetraspanin-1 OS=Homo sapiens OX=9606 GN=TSPAN1 PE=1 SV=2	2	2	241	26.3
Mucin 5AC, oligomeric mucus/gel-forming OS=Homo sapiens OX=9606 GN=MUC5AC PE=4 SV=1	3	3	6207	648.4
cDNA, FLJ92973, highly similar to Homo sapiens villin 2 (ezrin) (VIL2), mRNA OS=Homo sapiens OX=9606 PE=2 SV=1	3	3	586	69.4
Leucine-rich alpha-2-glycoprotein OS=Homo sapiens OX=9606 GN=LRG1 PE=1 SV=2	2	2	347	38.2
Adhesion G-protein coupled receptor G2 OS=Homo sapiens OX=9606 GN=ADGRG2 PE=1 SV=2	3	3	1017	111.5
14-3-3 protein theta OS=Homo sapiens OX=9606 GN=YWHAQ PE=1 SV=1	3	1	245	27.7
cDNA FLJ59607, moderately similar to D-dopachrome decarboxylase OS=Homo sapiens OX=9606 PE=2 SV=1	2	2	234	25.3
Epididymis secretory sperm binding protein Li 67p OS=Homo sapiens OX=9606 GN=HEL-S-67p PE=2 SV=1	2	2	189	19.9
Putative phospholipase B-like 2 OS=Homo sapiens OX=9606 GN=PLBD2 PE=1 SV=2	2	2	589	65.4

Insulin-like growth factor-binding protein 2 OS=Homo sapiens OX=9606 GN=IGFBP2 PE=1 SV=2	2	2	325	34.8
Dihydropyridine receptor alpha 2 subunit OS=Homo sapiens OX=9606 GN=CACNA2D1 PE=4 SV=1	2	2	1110	125.2
Translin OS=Homo sapiens OX=9606 GN=TSN PE=1 SV=1	2	2	228	26.2
Alpha-1B-glycoprotein OS=Homo sapiens OX=9606 GN=A1BG PE=1 SV=4	2	2	495	54.2
Dipeptidyl peptidase 2 OS=Homo sapiens OX=9606 GN=DPP7 PE=1 SV=3	2	2	492	54.3
HCG1647920 OS=Homo sapiens OX=9606 GN=RAM2 PE=4 SV=1	2	2	147	17.6
Myosin-reactive immunoglobulin light chain variable region (Fragment) OS=Homo sapiens OX=9606 PE=2 SV=1	2	1	109	11.6
UDP-GlcNAc:betaGal beta-1,3-N-acetylglucosaminyltransferase 6, isoform CRA_a OS=Homo sapiens OX=9606 GN=B3GNT6 PE=4 SV=1	2	2	415	47.1
cDNA FLJ55486, highly similar to Semaphorin-3C OS=Homo sapiens OX=9606 PE=2 SV=1	2	2	769	87.1
Discoidin domain receptor family, member 1, isoform CRA_b OS=Homo sapiens OX=9606 GN=DDR1 PE=4 SV=1	2	2	919	101.7
D-3-phosphoglycerate dehydrogenase OS=Homo sapiens OX=9606 GN=PHGDH PE=1 SV=4	2	2	533	56.6
Cell adhesion molecule 4 OS=Homo sapiens OX=9606 GN=CADM4 PE=1 SV=1	2	2	388	42.8
Beta-galactosidase OS=Homo sapiens OX=9606 PE=2 SV=1	2	2	725	81.8
Delta-aminolevulinic acid dehydratase OS=Homo sapiens OX=9606 PE=2 SV=1	2	2	359	39
Amyloid-like protein 2 OS=Homo sapiens OX=9606 GN=APLP2 PE=1 SV=2	2	2	763	86.9
cDNA FLJ78122 OS=Homo sapiens OX=9606 PE=2 SV=1	2	2	346	36
Glutathione reductase OS=Homo sapiens OX=9606 GN=HEL-75 PE=2 SV=1	2	2	522	56.2
Olfactory receptor OS=Homo sapiens OX=9606 GN=OR13C3 PE=3 SV=1	1	1	347	38.7
Spondin-2 OS=Homo sapiens OX=9606 GN=SPON2 PE=1 SV=3	2	2	331	35.8
Vitronectin OS=Homo sapiens OX=9606 GN=VTN PE=4 SV=1	2	2	478	54.3
cDNA FLJ76207, highly similar to Homo sapiens delta-notch-like EGF repeat-containing transmembrane (DNER), mRNA OS=Homo sapiens OX=9606 PE=2 SV=1	2	2	737	78.5
S-(hydroxymethyl)glutathione dehydrogenase OS=Homo sapiens OX=9606 PE=2 SV=1	2	2	374	39.7
cDNA FLJ77654, highly similar to Homo sapiens guanine nucleotide binding protein (G protein), beta polypeptide 4 (GNB4), mRNA OS=Homo sapiens OX=9606 PE=2 SV=1	2	2	340	37.6
Ceroid-lipofuscinosis neuronal protein 5 OS=Homo sapiens OX=9606 GN=CLN5 PE=1 SV=1	2	2	407	46.3

Single-chain Fv (Fragment) OS=Homo sapiens OX=9606 GN=scFv PE=2 SV=1	1	1	244	26.1
Ras-related C3 botulinum toxin substrate 1 (Rho family, small GTP binding protein Rac1) OS=Homo sapiens OX=9606 GN=RAC1 PE=2 SV=1	2	2	211	23.5
Nucleoside diphosphate kinase 3 OS=Homo sapiens OX=9606 GN=NME3 PE=1 SV=2	2	2	169	19
Vascular endothelial growth factor A OS=Homo sapiens OX=9606 GN=VEGFA PE=1 SV=1	2	2	412	45.4
Beta-galactoside alpha-2,6-sialyltransferase 1 OS=Homo sapiens OX=9606 GN=ST6GAL1 PE=1 SV=1	2	2	406	46.6
Epididymis secretory sperm binding protein OS=Homo sapiens OX=9606 GN=RAM1 PE=2 SV=1	2	2	147	17.6
cDNA, FLJ96792, highly similar to Homo sapiens calmodulin 2 (phosphorylase kinase, delta) (CALM2), mRNA OS=Homo sapiens OX=9606 PE=2 SV=1	2	2	149	16.8
Chromosome 9 open reading frame 19, isoform CRA_a (Fragment) OS=Homo sapiens OX=9606 GN=C9orf19 PE=4 SV=1	2	2	351	37.8
Arylsulfatase A, isoform CRA_a OS=Homo sapiens OX=9606 GN=ARSA PE=4 SV=1	2	2	509	53.8
Protein S100 OS=Homo sapiens OX=9606 GN=HEL-S-43 PE=2 SV=1	2	2	105	11.7
Transthyretin OS=Homo sapiens OX=9606 GN=TTR PE=1 SV=1	2	2	185	20.1
Cadherin-1 OS=Homo sapiens OX=9606 GN=CDH1 PE=1 SV=1	2	2	903	100
Complement decay-accelerating factor OS=Homo sapiens OX=9606 GN=CD55 PE=1 SV=2	2	2	550	58.9
Glutathione synthetase OS=Homo sapiens OX=9606 GN=HEL-S-64p PE=2 SV=1	2	2	474	52.4
Pyruvate kinase OS=Homo sapiens OX=9606 GN=PKM2 PE=3 SV=1	2	2	531	58
Asparaginase like 1, isoform CRA_a OS=Homo sapiens OX=9606 GN=ASRGL1 PE=2 SV=1	2	2	308	32
Plasma alpha-L-fucosidase OS=Homo sapiens OX=9606 GN=FUCA2 PE=1 SV=2	2	2	467	54
Carbonyl reductase [NADPH] 3 OS=Homo sapiens OX=9606 GN=CBR3 PE=1 SV=3	2	2	277	30.8
Peroxiredoxin-4 OS=Homo sapiens OX=9606 GN=PRDX4 PE=1 SV=1	2	1	271	30.5
Profilin-1 OS=Homo sapiens OX=9606 GN=PFN1 PE=1 SV=2	2	2	140	15
Prostate and testis expressed protein 4 OS=Homo sapiens OX=9606 GN=PATE4 PE=2 SV=2	2	2	98	11.4
EGF containing fibulin-like extracellular matrix protein 1 isoform 1 (Fragment) OS=Homo sapiens OX=9606 GN=EFEMP1 PE=2 SV=1	2	2	493	54.6
Ras-related protein Rab-27B OS=Homo sapiens OX=9606 GN=RAB27B PE=1 SV=4	2	1	218	24.6
HEBP2 protein (Fragment) OS=Homo sapiens OX=9606 GN=HEBP2 PE=2 SV=1	2	2	214	24
CD44 antigen OS=Homo sapiens OX=9606 GN=CD44 PE=1 SV=3	1	1	742	81.5

Ribonuclease A C1 OS=Homo sapiens OX=9606 GN=RAC1 PE=3 SV=1	2	2	156	17.6
Hypoxia up-regulated protein 1 OS=Homo sapiens OX=9606 GN=HYOU1 PE=1 SV=1	2	2	1000	111.3
Protein disulfide-isomerase OS=Homo sapiens OX=9606 GN=HEL-S-269 PE=2 SV=1	2	2	505	56.7
Inositol-1-monophosphatase OS=Homo sapiens OX=9606 PE=2 SV=1	2	2	336	36.7
Complement C3 OS=Homo sapiens OX=9606 GN=C3 PE=1 SV=2	2	2	1663	187
Actinin alpha 4 isoform 1 (Fragment) OS=Homo sapiens OX=9606 GN=ACTN4 PE=2 SV=1	2	2	911	104.8
Anti-(ED-B) scFV (Fragment) OS=Homo sapiens OX=9606 PE=2 SV=1	2	1	238	25.1
cDNA FLJ61136, highly similar to Ras-related protein Rab-11A OS=Homo sapiens OX=9606 PE=2 SV=1	2	2	261	28.8
Beta-1,4-galactosyltransferase 1 OS=Homo sapiens OX=9606 GN=B4GALT1 PE=1 SV=5	2	2	398	43.9
Epididymis secretory sperm binding protein (Fragment) OS=Homo sapiens OX=9606 GN=MIF PE=2 SV=1	1	1	115	12.5
Binder of sperm protein homolog 1 OS=Homo sapiens OX=9606 GN=BSPH1 PE=2 SV=1	1	1	132	15.7
Poly(rC)-binding protein 3 OS=Homo sapiens OX=9606 GN=PCBP3 PE=2 SV=2	1	1	371	39.4
Fructose-1,6-bisphosphatase isozyme 2 OS=Homo sapiens OX=9606 GN=FBP2 PE=1 SV=2	1	1	339	36.7
Testicular tissue protein Li 2 OS=Homo sapiens OX=9606 PE=2 SV=1	1	1	770	86.9
Alpha-N-acetylgalactosaminidase OS=Homo sapiens OX=9606 GN=NAGA PE=1 SV=2	1	1	411	46.5
cDNA FLJ53231, highly similar to 4-trimethylaminobutyraldehyde dehydrogenase OS=Homo sapiens OX=9606 PE=2 SV=1	1	1	508	55.2
Nuclear transport factor 2, isoform CRA_a OS=Homo sapiens OX=9606 GN=NUTF2 PE=4 SV=1	1	1	127	14.5
cDNA, FLJ93199, highly similar to Homo sapiens acrosin binding protein (ACRBP), mRNA OS=Homo sapiens OX=9606 PE=2 SV=1	1	1	543	61.3
Phospholipase A2, membrane associated OS=Homo sapiens OX=9606 GN=PLA2G2A PE=1 SV=2	1	1	144	16.1
Responsive to centrifugal force and shear stress gene 1 OS=Homo sapiens OX=9606 GN=RECS1 PE=2 SV=1	1	1	311	34.6
NEU1 OS=Homo sapiens OX=9606 PE=4 SV=1	1	1	415	45.5
Disintegrin and metalloproteinase domain-containing protein 10 OS=Homo sapiens OX=9606 GN=ADAM10 PE=1 SV=1	1	1	748	84.1
Immunoglobulin J chain OS=Homo sapiens OX=9606 GN=JCHAIN PE=1 SV=4	1	1	159	18.1
Prostate and testis expressed protein 1 OS=Homo sapiens OX=9606 GN=PATE1 PE=1 SV=1	1	1	126	14.3
Cysteine-rich secretory protein 2 OS=Homo sapiens OX=9606 GN=CRISP2 PE=1 SV=1	1	1	243	27.2

Nephronectin (Fragment) OS=Homo sapiens OX=9606 GN=NPNT PE=1 SV=1	1	1	609	66.9
Neutrophil defensin 1 OS=Homo sapiens OX=9606 GN=DEFA1 PE=1 SV=1	1	1	94	10.2
Secretoglobin family 1A member 1 isoform 1 (Fragment) OS=Homo sapiens OX=9606 GN=SCGB1A1 PE=2 SV=1	1	1	91	10
Titin OS=Homo sapiens OX=9606 GN=TTN PE=1 SV=1	1	1	35991	3992.2
Neutrophil gelatinase-associated lipocalin OS=Homo sapiens OX=9606 GN=LCN2 PE=1 SV=1	1	1	200	22.8
Alpha-2-antiplasmin OS=Homo sapiens OX=9606 GN=SERPINF2 PE=1 SV=3	1	1	491	54.5
UTP--glucose-1-phosphate uridylyltransferase OS=Homo sapiens OX=9606 PE=2 SV=1	1	1	517	57.8
von Willebrand factor A domain-containing protein 1 OS=Homo sapiens OX=9606 GN=VWA1 PE=1 SV=1	1	1	445	46.8
CD63 antigen OS=Homo sapiens OX=9606 GN=CD63 PE=1 SV=2	1	1	238	25.6
Mucin-15 OS=Homo sapiens OX=9606 GN=MUC15 PE=1 SV=1	1	1	361	39.3
Reticulon-4 receptor-like 1 OS=Homo sapiens OX=9606 GN=RTN4RL1 PE=1 SV=1	1	1	441	49
Cellular repressor of E1A-stimulated genes 1, isoform CRA_a OS=Homo sapiens OX=9606 GN=CREG1 PE=1 SV=1	1	1	255	28
Chromosome 7 open reading frame 24 OS=Homo sapiens OX=9606 GN=C7orf24 PE=4 SV=1	1	1	188	21
Protocadherin gamma-C3 OS=Homo sapiens OX=9606 GN=PCDHGC3 PE=1 SV=1	1	1	934	101
PCAF_N domain-containing protein (Fragment) OS=Homo sapiens OX=9606 PE=4 SV=1	1	1	282	31.4
Aspartate aminotransferase, cytoplasmic OS=Homo sapiens OX=9606 GN=GOT1 PE=1 SV=3	1	1	413	46.2
Poliovirus receptor OS=Homo sapiens OX=9606 GN=PVR PE=1 SV=1	1	1	417	45.3
Testis expressed sequence 101, isoform CRA_a OS=Homo sapiens OX=9606 GN=TEX101 PE=4 SV=1	1	1	267	28.5
Dexamethasone-induced Ras-related protein 1 OS=Homo sapiens OX=9606 GN=RASD1 PE=1 SV=1	1	1	281	31.6
Beta-defensin 125 OS=Homo sapiens OX=9606 GN=DEFB125 PE=2 SV=2	1	1	156	17.5
Proteasome subunit alpha type-3 OS=Homo sapiens OX=9606 GN=PSMA3 PE=1 SV=2	1	1	255	28.4
Proteasome subunit alpha-type 8 OS=Homo sapiens OX=9606 GN=PSMA8 PE=2 SV=3	1	1	256	28.5
Epididymis secretory sperm binding protein OS=Homo sapiens OX=9606 GN=LMAN2 PE=2 SV=1	1	1	356	40.2
Pterin-4-alpha-carbinolamine dehydratase OS=Homo sapiens OX=9606 GN=PCBD1 PE=1 SV=2	1	1	104	12
Phosphoglucomutase-1 OS=Homo sapiens OX=9606 GN=PGM1 PE=1 SV=1	1	1	584	63.9

Putative uncharacterized protein DNAJC9-AS1 OS=Homo sapiens OX=9606 GN=DNAJC9-AS1 PE=2 SV=2	1	1	148	15.6
Complement C4-A OS=Homo sapiens OX=9606 GN=C4A PE=1 SV=1	1	1	1744	192.8
Epididymis luminal protein 35 OS=Homo sapiens OX=9606 GN=HEL-S-125m PE=2 SV=1	1	1	803	92.4
Neuropilin-1 OS=Homo sapiens OX=9606 GN=NRP1 PE=1 SV=3	1	1	923	103.1
Proteasome subunit alpha type OS=Homo sapiens OX=9606 PE=2 SV=1	1	1	241	26.4
Protein S isoform 2 (Fragment) OS=Homo sapiens OX=9606 GN=PROS1 PE=1 SV=1	1	1	708	78.8
Epididymis secretory sperm binding protein Li 129m OS=Homo sapiens OX=9606 GN=HEL-S-129m PE=2 SV=1	1	1	249	28.7
Arrestin domain-containing protein 1 OS=Homo sapiens OX=9606 GN=ARRDC1 PE=1 SV=1	1	1	433	46
Transcription regulator protein BACH2 OS=Homo sapiens OX=9606 GN=BACH2 PE=1 SV=1	1	1	841	92.5
Myosin light polypeptide 6 OS=Homo sapiens OX=9606 GN=MYL6 PE=1 SV=1	1	1	238	26.7
Glycoprotein hormones alpha chain OS=Homo sapiens OX=9606 GN=CGA PE=1 SV=1	1	1	147	16.3
Purine nucleoside phosphorylase OS=Homo sapiens OX=9606 PE=2 SV=1	1	1	293	32.5
Protein shisa-9 OS=Homo sapiens OX=9606 GN=SHISA9 PE=2 SV=3	1	1	424	46.9
Platelet-derived growth factor alpha polypeptide OS=Homo sapiens OX=9606 GN=PDGFA PE=2 SV=1	1	1	234	26.2
Glutaminyl-peptide cyclotransferase OS=Homo sapiens OX=9606 GN=QPCT PE=1 SV=1	1	1	361	40.9
Testis-expressed protein 30 OS=Homo sapiens OX=9606 GN=TEX30 PE=1 SV=1	1	1	186	21.2
Calumenin, isoform CRA_a OS=Homo sapiens OX=9606 GN=CALU PE=4 SV=1	1	1	315	37.1
Pro-cathepsin H OS=Homo sapiens OX=9606 GN=CTSH PE=1 SV=4	1	1	335	37.4
Protein dopey-2 OS=Homo sapiens OX=9606 GN=DOP1B PE=1 SV=5	1	1	2298	258.1
Chloride intracellular channel protein 1 OS=Homo sapiens OX=9606 GN=CLIC1 PE=1 SV=4	1	1	241	26.9
Plexin domain-containing protein 2 OS=Homo sapiens OX=9606 GN=PLXDC2 PE=1 SV=1	1	1	529	59.5
cDNA FLJ76746, highly similar to Homo sapiens brevican (BCAN), transcript variant 1, mRNA OS=Homo sapiens OX=9606 PE=2 SV=1	1	1	911	99.1
Cofilin-1 OS=Homo sapiens OX=9606 GN=CFL1 PE=1 SV=1	1	1	204	22.7
Galectin-4 (Fragment) OS=Homo sapiens OX=9606 GN=LGALS4 PE=4 SV=1	1	1	38	4
Cathepsin L1 OS=Homo sapiens OX=9606 GN=CTSL1 PE=2 SV=1	1	1	333	37.5
DUF1907 domain-containing protein OS=Homo sapiens OX=9606 PE=4 SV=1	1	1	838	93.4
Adenosylhomocysteinase OS=Homo sapiens OX=9606 GN=AHCY PE=1 SV=4	1	1	432	47.7

Kallikrein 1, renal/pancreas/salivary, isoform CRA_a OS=Homo sapiens OX=9606 GN=KLNA1 PE=3 SV=1	1	1	262	28.9
cDNA FLJ51495, highly similar to ADP-ribosylation factor 5 OS=Homo sapiens OX=9606 PE=2 SV=1	1	1	229	25.4
Testican-1 OS=Homo sapiens OX=9606 GN=SPOCK1 PE=1 SV=1	1	1	439	49.1
HGFL gene, isoform CRA_a OS=Homo sapiens OX=9606 GN=MGC17330 PE=4 SV=1	1	1	263	28.2
Growth/differentiation factor 15 OS=Homo sapiens OX=9606 GN=GDF15 PE=1 SV=3	1	1	308	34.1
Eukaryotic initiation factor 4A-I OS=Homo sapiens OX=9606 GN=EIF4A1 PE=4 SV=1	1	1	50	5.9
Puromycin-sensitive aminopeptidase OS=Homo sapiens OX=9606 GN=NPEPPS PE=1 SV=2	1	1	919	103.2
Uncharacterized protein DKFZp686I05169 OS=Homo sapiens OX=9606 GN=DKFZp686I05169 PE=2 SV=1	1	1	1268	145.6
Putative ubiquitin-conjugating enzyme E2 N-like OS=Homo sapiens OX=9606 GN=UBE2NL PE=1 SV=1	1	1	153	17.4
Elongation factor 2 OS=Homo sapiens OX=9606 GN=EEF2 PE=1 SV=4	1	1	858	95.3
Collagen alpha-1(XVIII) chain OS=Homo sapiens OX=9606 GN=COL18A1 PE=1 SV=5	1	1	1754	178.1
WD repeat-containing protein 1 isoform 1 variant (Fragment) OS=Homo sapiens OX=9606 PE=2 SV=1	1	1	624	68.1
Proteasome subunit alpha type OS=Homo sapiens OX=9606 GN=PSMA6 PE=1 SV=1	1	1	252	28.1
Mannosyl (Alpha-1,3-)-glycoprotein beta-1,2-N-acetylglucosaminyltransferase variant (Fragment) OS=Homo sapiens OX=9606 PE=2 SV=1	1	1	473	53.5
Fatty acid synthase OS=Homo sapiens OX=9606 GN=FASN PE=1 SV=3	1	1	2511	273.3
Olfactomedin 4, isoform CRA_a OS=Homo sapiens OX=9606 GN=OLFM4 PE=4 SV=1	1	1	510	57.2
Epididymis secretory sperm binding protein OS=Homo sapiens OX=9606 GN=HINT1 PE=2 SV=1	1	1	126	13.8
Dehydrogenase/reductase SDR family member 13 OS=Homo sapiens OX=9606 GN=DHRS13 PE=2 SV=1	1	1	377	40.8
Protein Niban 1 OS=Homo sapiens OX=9606 GN=NIBAN1 PE=1 SV=1	1	1	928	103.1
60S ribosomal protein L9 (Fragment) OS=Homo sapiens OX=9606 GN=RPL9 PE=1 SV=1	1	1	166	18.9
Phosphoglucomutase-2 OS=Homo sapiens OX=9606 GN=PGM2 PE=1 SV=4	1	1	612	68.2
Putative annexin A2-like protein OS=Homo sapiens OX=9606 GN=ANXA2P2 PE=5 SV=2	1	1	339	38.6
Carboxypeptidase Z, isoform CRA_b OS=Homo sapiens OX=9606 GN=CPZ PE=2 SV=1	1	1	652	73.6
Sorting nexin-14 (Fragment) OS=Homo sapiens OX=9606 GN=SNX14 PE=1 SV=1	1	1	212	24.6
cAMP-dependent protein kinase type II-beta regulatory subunit OS=Homo sapiens OX=9606 GN=PRKAR2B PE=1 SV=3	1	1	418	46.3

Peptidyl-glycine alpha-amidating monooxygenase OS=Homo sapiens OX=9606 GN=PAM PE=1 SV=2	1	1	973	108.3
Spermine synthase OS=Homo sapiens OX=9606 GN=SMS PE=1 SV=2	1	1	366	41.2
CD109 antigen OS=Homo sapiens OX=9606 GN=CD109 PE=1 SV=2	1	1	1445	161.6
Epididymis secretory sperm binding protein OS=Homo sapiens OX=9606 PE=2 SV=1	1	1	205	23.8
Heat shock protein beta-1 OS=Homo sapiens OX=9606 GN=HSPB1 PE=1 SV=2	1	1	205	22.8
Proteasome subunit alpha type OS=Homo sapiens OX=9606 PE=2 SV=1	1	1	261	29.4
Retinoid-inducible serine carboxypeptidase OS=Homo sapiens OX=9606 GN=SCPEP1 PE=1 SV=1	1	1	452	50.8
PPM-type phosphatase domain-containing protein (Fragment) OS=Homo sapiens OX=9606 PE=4 SV=8	1	1	271	30.3
Angiotensinogen variant (Fragment) OS=Homo sapiens OX=9606 PE=2 SV=1	1	1	491	53.7
Protein tyrosine phosphatase, non-receptor type substrate 1, isoform CRA_a OS=Homo sapiens OX=9606 GN=PTPNS1 PE=4 SV=1	1	1	504	54.9
FLJ00120 protein (Fragment) OS=Homo sapiens OX=9606 GN=FLJ00120 PE=2 SV=1	1	1	1171	134.9
COL21A1 protein OS=Homo sapiens OX=9606 GN=COL21A1 PE=2 SV=1	1	1	957	99.3
Histone H4 OS=Homo sapiens OX=9606 GN=HIST1H4H PE=2 SV=1	1	1	103	11.4
Tetraspanin (Fragment) OS=Homo sapiens OX=9606 PE=2 SV=1	1	1	285	31.7
Sperm acrosome membrane-associated protein 1 OS=Homo sapiens OX=9606 GN=SPACA1 PE=1 SV=1	1	1	294	32.1
Malate dehydrogenase OS=Homo sapiens OX=9606 GN=MDH2 PE=2 SV=1	1	1	338	35.5
Tubulin alpha-1A chain OS=Homo sapiens OX=9606 GN=TUBA1A PE=1 SV=1	1	1	231	24.8
cDNA FLJ51188, highly similar to N-acetylglucosamine-6-sulfatase (EC3.1.6.14) OS=Homo sapiens OX=9606 PE=2 SV=1	1	1	584	65.8

Appendix VI.i- The table of results from the proteomic analysis of the >50 kDa sperm conditioned media fraction.

Appendix VII

OE-E6/E7 cell responses to semenogelin peptide perfusion

OE-E6/E7 cell responses to semenogelin peptides 1, 2 and 3		
Experimental Period Compared	Number of cells	Percentage of Cells
Control period to Peptide 1 decrease	25	9.8
Control period to Peptide 1 no change	216	85.0
Control period to Peptide 1 increase	13	5.1
Peptide 1 to Peptide 2 decrease	6	2.4
Peptide 1 to Peptide 2 no change	216	85.0
Peptide 1 to Peptide 2 increase	32	12.6
Peptide 2 to Peptide 3 decrease	16	6.3
Peptide 2 to Peptide 3 no change	218	85.8
Peptide 2 to Peptide 3 increase	20	7.9
Peptide 3 to Wash decrease	7	2.8
Peptide 3 to Wash no change	224	88.2
Peptide 3 to Wash increase	23	9.1
Wash to ATP decrease	3	1.2
Wash to ATP no change	8	3.1
Wash to ATP increase	243	95.7

Appendix VII.i- A summary table of the types of response observed during the Ca^{2+} imaging experiments in which OE-E6/E7 cells were perfused with synthesised semenogelin peptides 1, 2 and 3, respectively. The table displays the number of cells identified as increasing, decreasing or showing no change in fluorescence between each of the experimental periods of perfusion, as well as the overall percentage of cells identified as showing each type of response throughout the two experiments.

OE-E6/E7 cell responses to semenogelin peptides 2, 1 and 3		
Experimental Period Compared	Number of cells	Percentage of Cells
Control period to Peptide 2 decrease	9	2.9
Control period to Peptide 2 no change	289	93.5
Control period to Peptide 2 increase	11	3.6
Peptide 2 to Peptide 1 decrease	8	2.6
Peptide 2 to Peptide 1 no change	282	91.3
Peptide 2 to Peptide 1 increase	19	6.1
Peptide 1 to Peptide 3 decrease	10	3.2
Peptide 1 to Peptide 3 no change	276	89.3
Peptide 1 to Peptide 3 increase	23	7.4
Peptide 3 to Wash decrease	11	3.6
Peptide 3 to Wash no change	289	93.5
Peptide 3 to Wash increase	9	2.9
Wash to ATP decrease	0	0.0
Wash to ATP no change	0	0.0
Wash to ATP increase	309	100.0

Appendix VII.ii- A summary table of the types of response observed during the Ca^{2+} imaging experiments in which OE-E6/E7 cells were perfused with synthesised semenogelin peptides 2, 1 and 3, respectively. The table displays the number of cells identified as increasing, decreasing or showing no change in fluorescence between each of the experimental periods of perfusion, as well as the overall percentage of cells identified as showing each type of response throughout the two experiments.

OE-E6/E7 cell responses to semenogelin peptides 3, 2 and 1		
Experimental Period Compared	Number of cells	Percentage of Cells
Control period to Peptide 3 decrease	12	4.8
Control period to Peptide 3 no change	226	90.8
Control period to Peptide 3 increase	11	4.4
Peptide 3 to Peptide 2 decrease	31	12.4
Peptide 3 to Peptide 2 no change	205	82.3
Peptide 3 to Peptide 2 increase	13	5.2
Peptide 2 to Peptide 1 decrease	13	5.2
Peptide 2 to Peptide 1 no change	231	92.8
Peptide 2 to Peptide 1 increase	5	2.0
Peptide 1 to Wash decrease	15	6.0
Peptide 1 to Wash no change	225	90.4
Peptide 1 to Wash increase	9	3.6
Wash to ATP decrease	0	0.0
Wash to ATP no change	3	1.2
Wash to ATP increase	246	98.8

Appendix VII.iii- A summary table of the types of response observed during the Ca^{2+} imaging experiments in which OE-E6/E7 cells were perfused with synthesised semenogelin peptides 3, 2 and 1, respectively. The table displays the number of cells identified as increasing, decreasing or showing no change in fluorescence between each of the experimental periods of perfusion, as well as the overall percentage of cells identified as showing each type of response throughout the two experiments.

OE-E6/E7 cell responses to semenogelin peptides 1, 2, 3 and sperm conditioned media		
Experimental Period Compared	Number of cells	Percentage of Cells
Control period to Peptide 1 decrease	0	0.0
Control period to Peptide 1 no change	101	98.1
Control period to Peptide 1 increase	2	1.9
Peptide 1 to Peptide 2 decrease	0	0.0
Peptide 1 to Peptide 2 no change	100	97.1
Peptide 1 to Peptide 2 increase	3	2.9
Peptide 2 to Peptide 3 decrease	2	1.9
Peptide 2 to Peptide 3 no change	101	98.1
Peptide 2 to Peptide 3 increase	0	0.0
Peptide 3 to Wash decrease	2	1.9
Peptide 3 to Wash no change	101	98.1
Peptide 3 to Wash increase	0	0.0
Wash to Sperm Conditioned Media decrease	0	0.0
Wash to Sperm Conditioned Media no change	33	32.0
Wash to Sperm Conditioned Media increase	70	68.0
Sperm Conditioned Media to Wash 2 decrease	8	7.8
Sperm Conditioned Media to Wash 2 no chang	59	57.3
Sperm Conditioned Media to Wash 2 increase	36	35.0
Wash 2 to ATP decrease	0	0.0
Wash 2 to ATP no change	0	0.0
Wash 2 to ATP increase	103	100.0

Appendix VII.iv- A summary table of the types of response observed during the Ca^{2+} imaging experiment in which OE-E6/E7 cells were perfused with synthesised semenogelin peptides 1, 2 and 3, respectively. The OE-E6/E7 cells were then washed during a 3-minute period of sEBSS perfusion before a 3 minute period of sperm conditioned media perfusion. This was followed by another 3-minute sEBSS wash and finally 3 minutes of ATP solution perfusion. The table displays the number of cells identified as increasing, decreasing or showing no change in fluorescence between each of the experimental periods of perfusion, as well as the overall percentage of cells identified as showing each type of response throughout the experiment.

OE-E6/E7 cell response to sperm conditioned media with TLR-IN-C34

OE-E6/E7 cell responses to sperm conditioned media with TLR-IN-C34		
Experimental Period Compared	Number of cells	Percentage of Cells
C1 to C2- Decrease	23	23.7
C1 to C2- No change	52	53.6
C1 to C2- Increase	22	22.7
C2 to R1- Decrease	0	0.0
C2 to R1- No Change	2	2.1
C2 to R1- Increase	95	97.9
R1 to R2- Decrease	67	69.1
R1 to R2- No Change	26	26.8
R1 to R2- Increase	4	4.1
R2 to W1- Decrease	89	91.8
R2 to W1- No Change	7	7.2
R2 to W1- Increase	1	1.0
W1 to W2- Decrease	10	10.3
W1 to W2- No Change	20	20.6
W1 to W2- Increase	67	69.1
W2 to A1- Decrease	0	0.0
W2 to A1- No Change	0	0.0
W2 to A1- Increase	97	100.0
A1 to A2- Decrease	60	61.9
A1 to A2- No change	21	21.6
A1 to A2- Increase	16	16.5

Appendix VII.v- A summary table of the types of response observed during the Ca^{2+} imaging experiment in which OE-E6/E7 cells were perfused with sperm conditioned media in the presence of TLR4-IN-C34. The table displays the number of cells identified as increasing, decreasing or showing no change in fluorescence between each of the experimental periods of perfusion, as well as the overall percentage of cells identified as showing each type of response throughout the experiment.

OE-E6/E7 cell response to sperm conditioned media in Ca^{2+} free sEBSS

OE-E6/E7 cell response to sperm conditioned media in Ca^{2+} free sEBSS		
Experimental Period Compared	Number of cells	Percentage of Cells
c1 c2 decrease	0	0.0
c1 c2 no change	170	96.6
c1 c2 increase	6	3.4
c2 r1 decrease	0	0.0
c2 r1 no change	0	0.0
c2 r1 increase	176	100.0
r1 r2 decrease	65	36.9
r1 r2 no change	85	48.3
r1 r2 increase	26	14.8
r2 w1 decrease	176	100.0
r2 w1 no change	0	0.0
r2 w1 increase	0	0.0
w1 w2 decrease	134	76.1
w1 w2 no change	42	23.9
w1 w2 increase	0	0.0
w2 a1 decrease	55	31.3
w2 a1 no change	111	63.1
w2 a1 increase	10	5.7
a1 a2 decrease	97	55.1
a1 a2 no change	78	44.3
a1 a2 increase	1	0.6

Appendix VII.vi- A summary table of the types of response observed during the Ca^{2+} imaging experiment in which OE-E6/E7 cells were perfused with sperm conditioned media in Ca^{2+} free sEBSS. The table displays the number of cells identified as increasing, decreasing or showing no change in fluorescence between each of the experimental periods of perfusion, as well as the overall percentage of cells identified as showing each type of response throughout the experiment.

OE-E6/E7 cell response to thapsigargin and sperm conditioned media

OE-E6/E7 cell responses to thapsigargin and sperm conditioned media		
Experimental Period Compared	Number of cells	Percentage of Cells
Control to Thapsigargin- decrease	3	2.2
Control to Thapsigargin- no change	15	11.2
Control to Thapsigargin- increase	116	86.6
Thapsigargin to sperm conditioned media w/ thapsigargin- decrease	0	0.0
Thapsigargin to sperm conditioned media w/ thapsigargin- no change	129	96.3
Thapsigargin to sperm conditioned media w/ thapsigargin- increase	5	3.7
Sperm conditioned media w/ thapsigargin to sEBSS wash- decrease	120	89.6
Sperm conditioned media w/ thapsigargin to sEBSS wash- no change	14	10.4
Sperm conditioned media w/ thapsigargin to sEBSS wash- increase	0	0.0
sEBSS wash to ATP- decrease	8	6.0
sEBSS wash to ATP- no change	27	20.1
sEBSS wash to ATP- increase	99	73.9

Appendix VII.vii- A summary table of the types of response observed during the Ca^{2+} imaging experiment in which OE-E6/E7 cells were perfused with thapsigargin and sperm conditioned media. The table displays the number of cells identified as increasing, decreasing or showing no change in fluorescence between each of the experimental periods of perfusion, as well as the overall percentage of cells identified as showing each type of response throughout the experiment.

OE-E6/E7 cell response to sperm conditioned media and <2kDa dialysed sperm conditioned media

OE-E6/E7 cell responses to sperm conditioned media and <2kDa dialysed sperm conditioned media		
Experimental Period Compared	**Number of cells**	**Percentage of Cells**
Control sEBSS perfusion to sperm conditioned media- decrease	0	0.0
Control sEBSS perfusion to sperm conditioned media- no change	5	1.6
Control sEBSS perfusion to sperm conditioned media- increase	303	98.4
Sperm conditioned media to sEBSS wash 1- decrease	295	95.8
Sperm conditioned media to sEBSS wash 1- no change	12	3.9
Sperm conditioned media to sEBSS wash 1- increase	1	0.3
sEBSS wash 1 to <2kDa dialysed sperm conditioned media- decrease	4	1.3
sEBSS wash 1 to <2kDa dialysed sperm conditioned media- no change	115	37.3
sEBSS wash 1 to <2kDa dialysed sperm conditioned media- increase	189	61.4
<2kDa dialysed sperm conditioned media to sEBSS wash 2- decrease	112	36.4
<2kDa dialysed sperm conditioned media to sEBSS wash 2- no change	169	54.9
<2kDa dialysed sperm conditioned media to sEBSS wash 2- increase	27	8.8
sEBSS wash 2 to ATP solution- decrease	0	0.0
sEBSS wash 2 to ATP solution- no change	0	0.0
sEBSS wash 2 to ATP solution- increase	308	100.0

Appendix VII.viii- A summary table of the types of response observed during the Ca^{2+} imaging experiments in which OE-E6/E7 cells were perfused with sperm conditioned media and <2kDa dialysed sperm conditioned media. The table displays the number of cells identified as increasing, decreasing or showing no change in fluorescence between each of the experimental periods of perfusion, as well as the overall percentage of cells identified as showing each type of response throughout these experiments.

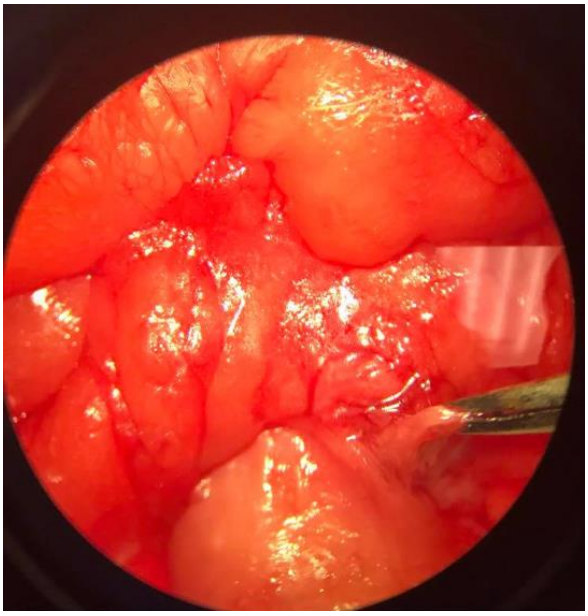
Appendix VIII

Attempts to develop canine oviductal epithelial cell cultures

In collaboration with my co-supervisors Professor Richard Lea and Professor Gary England at the University of Nottingham, attempts were made to develop a canine model of oviductal epithelial cell cultures to use in the series of experiments described in this thesis. These experiments were intended to run in parallel with the human secondary cell line cultures utilised herein to establish the presence of male ejaculate factor signalling in the cells of the canine reproductive tract to examine the conservation of the mechanism across mammalian species. Excised canine reproductive tract tissue was kindly provided by the veterinary surgeons at Pride Veterinary Centre, Derby from female dogs undergoing routine spaying procedures and attempts were made to isolate oviductal epithelial cells for culture.



Appendix VIII.i- A photo of the excised canine reproductive tract tissue from a routine spaying procedure.



Appendix VIII.ii- A magnified image of the adipose tissue surrounding the very small canine oviduct (gripped by the forceps).



Appendix VIII.iii- A closer image of the canine oviduct, extended between the forceps and surgical scissors in this image, demonstrating the relatively small size of the oviduct in comparison to the much larger canine uterine horn.

The attempted isolation of the canine oviductal epithelial cells was carried out by removing the oviduct from the reproductive tract tissue and washing thoroughly with PBS. The lumen of the oviduct was filled with 1.5% tryspin in PBS before both ends were tied tightly with twine and then left in a 37^{o}C incubator for 20 minutes. The twine was then removed and the trypsin in PBS/cell suspension was squeezed from the lumen of the oviduct before being centrifuged and resuspended in DMEM (no phenol red) supplemented with 10% foetal bovine serum (FBS) and 0.3% Penicillin-Streptomycin (10,000 U/mL) (PenStrep) to be cultured in 25cm^2 tissue culture flasks. Additional cell cultures were produced by using a scalpel to open the oviduct and scraping epithelial cells from the inner surface of the lumen.

Unfortunately, attempts to culture oviductal epithelial cells from a canine model were unsuccessful due to the size of the canine oviducts and the amount of adipose tissue surrounding them, making it very difficult to specifically isolate the epithelial cells. The methods used failed to produce canine oviductal epithelial cell line cultures, as most of the cells in the culture flasks appeared to be adipose cells and the few epithelial cells present failed to develop into substantial monolayers.

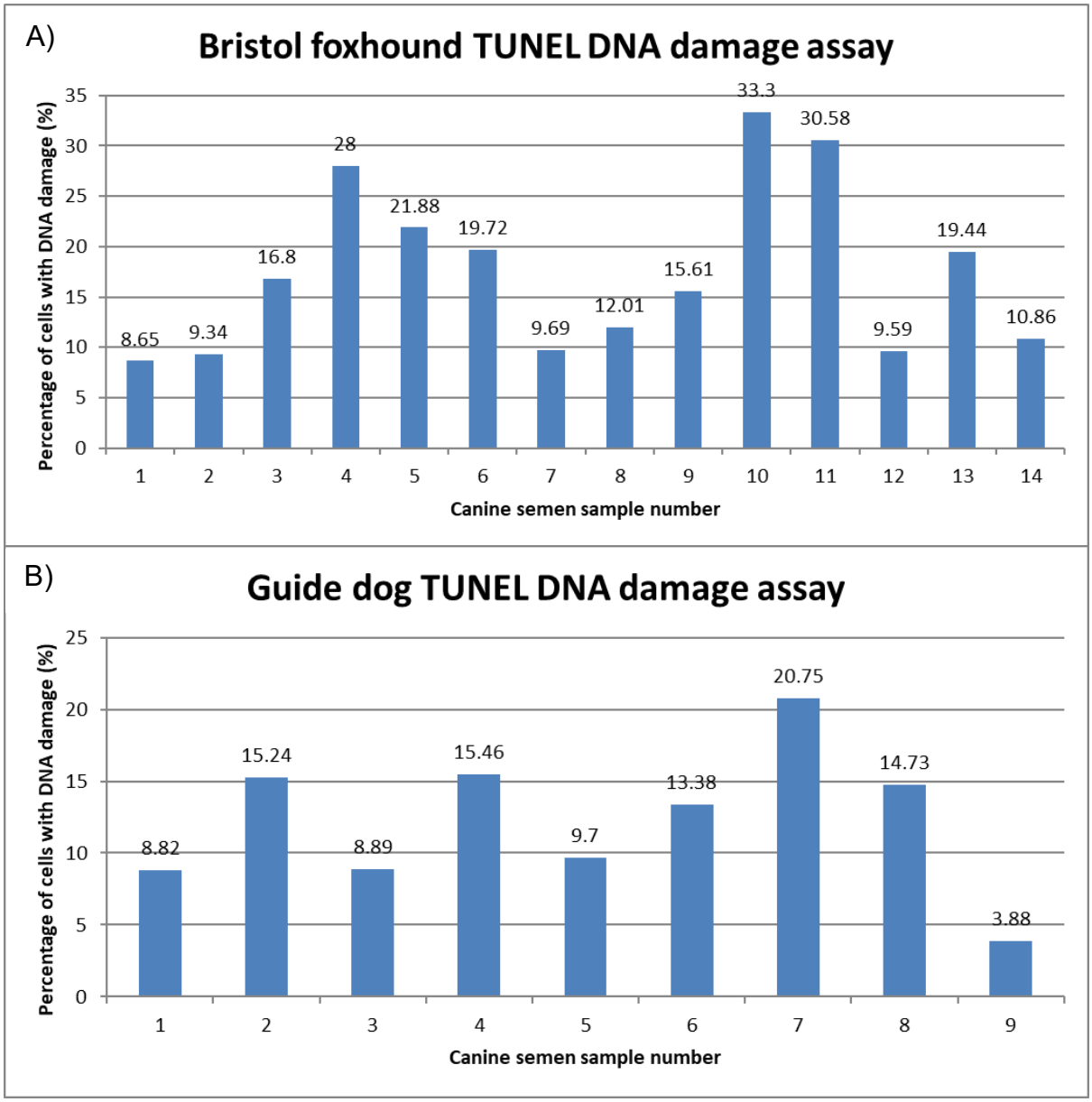
The effect of diet of canine semen sample quality and DNA damage

Aside from the attempted culture of canine oviductal epithelial cells, work was carried out in collaboration with my co-supervisor Dr Richard Lea and Professor David Gardner at the University of Nottingham School of Veterinary Medicine and Science to assist them with experiments comparing the semen quality of canines fed a raw meat diet in comparison to canines fed a processed dog food diet. This was part of a translational study in which human sperm samples from western males with a diet of heavily processed foods were being compared to sperm samples from males in Amazonian tribes with a much less processed, “clean” diet. As part of this currently

unpublished study, I carried out computer assisted semen analysis (CASA) and hypoosmotic swelling tests on canine semen samples from dogs at the National Breeding Centre for guide dogs in leamington spa, as well as beagles from a Labcorp Drug Development (formerly Covance) and fox hound beagles from a farm in Bristol. The data from these studies is not yet published.

In addition to the CASA analysis and hypoosmotic swelling tests, DNA damage assays were carried out on the canine semen samples to assess the effect of their diets on the levels of DNA damage within their sperm cells. Mammalian sperm cells are susceptible to DNA damage and most ejaculates contain a subpopulation of cells exhibiting DNA fragmentation. Elevated levels of DNA damage have been associated with subfertility and there a range of assays have been developed to measure the proportions of cells within an ejaculate that have significantly damaged DNA (Robinson, Gallos et al. 2012). The terminal deoxynucleotidyl transferase dUTP nick end labelling (TUNEL) assay is a method of assessing DNA damage in spermatozoa that relies upon the protein terminal transferase to access DNA strand breaks and catalyse the insertion of labelled bases, which can then be visualised and quantified (Mitchell, De Iuliis et al. 2011). Due to the compact nature of sperm cell chromatin (Brewer, Corzett et al. 2003) and the presence of intermolecular protamine disulphide bonds (Balhorn, Corzett et al. 1992), treatment of the sperm cells with dithiothreitol (DTT) is necessary to relax the chromatin and allow the terminal transferases to access the DNA strand breaks in the nucleus (Codrington, Hales et al. 2007).

TUNEL analysis was carried out on the semen samples acquired from the foxhounds from the farm in bristol and the guide dogs to compare the effect of their differing diets on the levels of DNA damage present in their ejaculate.



Appendix VIII.iv- Bar charts displaying the results from TUNEL DNA damage assays on canine semen samples.

Appendix IV.ivA shows the TUNEL DNA damage assay results from the 14 semen samples gathered from the foxhounds in Bristol which were predominantly fed a raw meat diet, whilst appendix IV.ivB shows the same results from 9 semen samples acquired from guide dogs fed a processed dog food diet. A two-tailed T test between the two groups of data revealed that there was no significant difference in the amount of DNA damage present in the sperm cells between dogs fed a processed diet and dogs fed a raw meat diet (P= 0.107).

References

Aalberts, M., T. A. Stout and W. Stoorvogel (2014). "Prostasomes: extracellular vesicles from the prostate." Reproduction **147**(1): R1-14.

Aarabi, M., H. Balakier, S. Bashar, S. I. Moskovtsev, P. Sutovsky, C. L. Librach and R. Oko (2014). "Sperm-derived WW domain-binding protein, PAWP, elicits calcium oscillations and oocyte activation in humans and mice." The FASEB Journal **28**(10): 4434-4440.

Abdallah, K. S., S. Hunt, S. A. Abdullah, B. W. J. Mol and M. A. Youssef (2020). "How and Why to Define Unexplained Infertility?" Semin Reprod Med **38**(1): 55-60.

Abe, H. (1996). "The mammalian oviductal epithelium: regional variations in cytological and functional aspects of the oviductal secretory cells." Histol Histopathol **11**(3): 743-768.

Agarwal, A., A. Mulgund, A. Hamada and M. R. Chyatte (2015). "A unique view on male infertility around the globe." Reprod Biol Endocrinol **13**: 37.

Agarwal, A., M. K. Panner Selvam and S. Baskaran (2020). "Proteomic Analyses of Human Sperm Cells: Understanding the Role of Proteins and Molecular Pathways Affecting Male Reproductive Health." International Journal of Molecular Sciences **21**(5): 1621.

Agarwal, A., M. K. Panner Selvam and S. Baskaran (2020). "Proteomic Analyses of Human Sperm Cells: Understanding the Role of Proteins and Molecular Pathways Affecting Male Reproductive Health." Int J Mol Sci **21**(5).

Ajdary, M., Z. Zandieh, F. S. Amjadi, F. Keyhanfar, M. Mehdizadeh and R. Aflatoonian (2020). "Interaction of sperm with endometrium can regulate genes involved in endometrial receptivity pathway in mice: An experimental study." Int J Reprod Biomed **18**(10): 815-824.

Alasmari, W., S. Costello, J. Correia, S. K. Oxenham, J. Morris, L. Fernandes, J. Ramalho-Santos, J. Kirkman-Brown, F. Michelangeli, S. Publicover and C. L. Barratt (2013). "Ca2+ signals generated by CatSper and Ca2+ stores regulate different behaviors in human sperm." J Biol Chem **288**(9): 6248-6258.

Alasmari, W., S. Costello, J. Correia, S. K. Oxenham, J. Morris, L. Fernandes, J. Ramalho-Santos, J. Kirkman-Brown, F. Michelangeli, S. Publicover and C. R. Barratt (2013). "Ca2+ Signals Generated by CatSper and Ca2+ Stores Regulate Different Behaviors in Human Sperm*." Journal of Biological Chemistry **288**(9): 6248-6258.

Alwaal, A., B. N. Breyer and T. F. Lue (2015). "Normal male sexual function: emphasis on orgasm and ejaculation." Fertil Steril **104**(5): 1051-1060.

Amann, R. P. (2008). "The cycle of the seminiferous epithelium in humans: a need to revisit?" J Androl **29**(5): 469-487.

Amaral, A., J. Castillo, J. M. Estanyol, J. L. Ballescà, J. Ramalho-Santos and R. Oliva (2013). "Human sperm tail proteome suggests new endogenous metabolic pathways." Mol Cell Proteomics **12**(2): 330-342.

Ambudkar, I. S. (2012). "Polarization of calcium signaling and fluid secretion in salivary gland cells." Curr Med Chem **19**(34): 5774-5781.

Anamthathmakula, P. and W. Winuthayanon (2020). "Mechanism of semen liquefaction and its potential for a novel non-hormonal contraception†." Biology of Reproduction **103**(2): 411-426.

Anderson, D. J., J. Marathe and J. Pudney (2014). "The structure of the human vaginal stratum corneum and its role in immune defense." Am J Reprod Immunol **71**(6): 618-623.

Andrade, Y. N., J. Fernandes, E. Vázquez, J. M. Fernández-Fernández, M. Arniges, T. M. Sánchez, M. Villalón and M. A. Valverde (2005). "TRPV4 channel is involved in the coupling of fluid viscosity changes to epithelial ciliary activity." J Cell Biol **168**(6): 869-874.
Andrew, S. M., J. A. Titus and L. Zumstein (2002). "Dialysis and concentration of protein solutions." Curr Protoc Toxicol **Appendix 3**: A.3h.1-5.
Antunes, G., A. C. Roque and F. M. Simoes de Souza (2016). "Modelling intracellular competition for calcium: kinetic and thermodynamic control of different molecular modes of signal decoding." Scientific Reports **6**(1): 23730.
Aquila, S. and F. De Amicis (2014). "Steroid receptors and their ligands: effects on male gamete functions." Exp Cell Res **328**(2): 303-313.
Arnoult, C., Y. Zeng and H. M. Florman (1996). "ZP3-dependent activation of sperm cation channels regulates acrosomal secretion during mammalian fertilization." J Cell Biol **134**(3): 637-645.
Aslam, B., M. Basit, M. A. Nisar, M. Khurshid and M. H. Rasool (2017). "Proteomics: Technologies and Their Applications." Journal of Chromatographic Science **55**(2): 182-196.
Attia, M. A. (1998). "Cyclic changes in genital organs and vaginal cytology in cynomolgus monkeys (Macaca fascicularis)." Dtsch Tierarztl Wochenschr **105**(11): 399-404.
Austin, C. R. (1951). "Observations on the penetration of the sperm in the mammalian egg." Aust J Sci Res B **4**(4): 581-596.
Austin, C. R. (1952). "The 'capacitation'of the mammalian sperm." Nature **170**(4321): 326-326.
Avidor-Reiss, T., M. Mazur, E. L. Fishman and P. Sindhwani (2019). "The Role of Sperm Centrioles in Human Reproduction – The Known and the Unknown." Frontiers in Cell and Developmental Biology **7**.
Avilés, M., P. Coy and D. Rizos (2015). "The oviduct: A key organ for the success of early reproductive events." Animal Frontiers **5**(1): 25-31.
Avilés, M., A. Gutiérrez-Adán and P. Coy (2010). "Oviductal secretions: will they be key factors for the future ARTs?" Molecular Human Reproduction **16**(12): 896-906.
Aydin, H., A. Sultana, S. Li, A. Thavalingam and J. E. Lee (2016). "Molecular architecture of the human sperm IZUMO1 and egg JUNO fertilization complex." Nature **534**(7608): 562-565.
Babcock, D. F. (2003). "Development. Smelling the roses?" Science **299**(5615): 1993-1994.
Bagur, R. and G. Hajnóczky (2017). "Intracellular Ca(2+) Sensing: Its Role in Calcium Homeostasis and Signaling." Molecular cell **66**(6): 780-788.
Bahat, A., I. Tur-Kaspa, A. Gakamsky, L. C. Giojalas, H. Breitbart and M. Eisenbach (2003). "Thermotaxis of mammalian sperm cells: a potential navigation mechanism in the female genital tract." Nat Med **9**(2): 149-150.
Baker, M. A. (2016). "Proteomics of post-translational modifications of mammalian spermatozoa." Cell Tissue Res **363**(1): 279-287.
Baker, M. A., B. Nixon, N. Naumovski and R. J. Aitken (2012). "Proteomic insights into the maturation and capacitation of mammalian spermatozoa." Syst Biol Reprod Med **58**(4): 211-217.
Baldwin, T. (2012). "Reproduction without sex: social and ethical implications." EMBO Rep **13**(12): 1049-1053.
Balhorn, R., M. Corzett and J. A. Mazrimas (1992). "Formation of intraprotamine disulfides in vitro." Arch Biochem Biophys **296**(2): 384-393.

Bang, J., H. Park, J. Yoo, D. Lee, W. I. Choi, J. H. Lee, Y.-R. Lee, C. Kim, H. Koo and S. Kim (2020). "Selection and identification of a novel bone-targeting peptide for biomedical imaging of bone." Scientific Reports **10**(1): 10576.
Barratt, C. L., R. J. Aitken, L. Björndahl, D. T. Carrell, P. de Boer, U. Kvist, S. E. Lewis, S. D. Perreault, M. J. Perry and L. Ramos (2010). "Sperm DNA: organization, protection and vulnerability: from basic science to clinical applications—a position report." Human reproduction **25**(4): 824-838.
Bartok, A., D. Weaver, T. Golenár, Z. Nichtova, M. Katona, S. Bánsághi, K. J. Alzayady, V. K. Thomas, H. Ando, K. Mikoshiba, S. K. Joseph, D. I. Yule, G. Csordás and G. Hajnóczky (2019). "IP3 receptor isoforms differently regulate ER-mitochondrial contacts and local calcium transfer." Nature Communications **10**(1).
Beazely, M. A. and V. J. Watts (2006). "Regulatory properties of adenylate cyclases type 5 and 6: A progress report." Eur J Pharmacol **535**(1-3): 1-12.
Beckmann, C. R. (1995). Obstetrics and gynecology, Williams & Wilkins.
Bedford, J. M. (1965). "EFFECT OF ENVIRONMENT ON PHAGOCYTOSIS OF RABBIT SPERMATOZOA." Reproduction **9**(2): 249-256.
Ben-Johny, M. and D. T. Yue (2014). "Calmodulin regulation (calmodulation) of voltage-gated calcium channels." J Gen Physiol **143**(6): 679-692.
Berridge, M. J. (1993). "Inositol trisphosphate and calcium signalling." Nature **361**(6410): 315-325.
Berridge, M. J. (1995). "Calcium signalling and cell proliferation." Bioessays **17**(6): 491-500.
Berridge, M. J. (1997). "Elementary and global aspects of calcium signalling." J Physiol **499 (Pt 2)**(Pt 2): 291-306.
Berridge, M. J., M. D. Bootman and H. L. Roderick (2003). "Calcium signalling: dynamics, homeostasis and remodelling." Nature Reviews Molecular Cell Biology **4**(7): 517-529.
Berridge, M. J., P. Lipp and M. D. Bootman (2000). "The versatility and universality of calcium signalling." Nature Reviews Molecular Cell Biology **1**(1): 11-21.
Besenfelder, U., V. Havlicek and G. Brem (2012). "Role of the Oviduct in Early Embryo Development." Reproduction in Domestic Animals **47**: 156-163.
Bigelow, J. L., D. B. Dunson, J. B. Stanford, R. Ecochard, C. Gnoth and B. Colombo (2004). "Mucus observations in the fertile window: a better predictor of conception than timing of intercourse." Hum Reprod **19**(4): 889-892.
Bill, C. A. and C. M. Vines (2020). "Phospholipase C." Adv Exp Med Biol **1131**: 215-242.
Björndahl, L., M. Mohammadieh, M. Pourian, I. Söderlund and U. Kvist (2005). "Contamination by Seminal Plasma Factors During Sperm Selection." Journal of Andrology **26**(2): 170-173.
Björndahl, L., D. Mortimer, C. L. Barratt, J. A. Castilla, R. Menkveld, U. Kvist, J. G. Alvarez and T. B. Haugen (2010). A practical guide to basic laboratory andrology, Cambridge University Press.
Blackmore, P. F., J. Neulen, F. Lattanzio and S. J. Beebe (1991). "Cell surface-binding sites for progesterone mediate calcium uptake in human sperm." J Biol Chem **266**(28): 18655-18659.
Blaustein, M. P. and W. J. Lederer (1999). "Sodium/calcium exchange: its physiological implications." Physiol Rev **79**(3): 763-854.
Boerke, A., P. S. Tsai, N. Garcia-Gil, I. A. Brewis and B. M. Gadella (2008). "Capacitation-dependent reorganization of microdomains in the apical sperm head

plasma membrane: functional relationship with zona binding and the zona-induced acrosome reaction." Theriogenology **70**(8): 1188-1196.
Boivin, J., L. Bunting, J. A. Collins and K. G. Nygren (2007). "International estimates of infertility prevalence and treatment-seeking: potential need and demand for infertility medical care." Human reproduction **22**(6): 1506-1512.
Boomsma, C. M., B. J. Cohlen and C. Farquhar (2019). "Semen preparation techniques for intrauterine insemination." Cochrane Database Syst Rev **10**(10): Cd004507.
Bootman, M., E. Niggli, M. Berridge and P. Lipp (1997). "Imaging the hierarchical Ca2+ signalling system in HeLa cells." J Physiol **499 (Pt 2)**(Pt 2): 307-314.
Boskey, E. R., R. A. Cone, K. J. Whaley and T. R. Moench (2001). "Origins of vaginal acidity: high D/L lactate ratio is consistent with bacteria being the primary source." Hum Reprod **16**(9): 1809-1813.
Boulware, M. J. and J. S. Marchant (2008). "Timing in cellular Ca2+ signaling." Curr Biol **18**(17): R769-r776.
Bouschet, T. and J. M. Henley (2005). "Calcium as an extracellular signalling molecule: perspectives on the Calcium Sensing Receptor in the brain." C R Biol **328**(8): 691-700.
Breitbart, H. and B. Spungin (1997). "The biochemistry of the acrosome reaction." Mol Hum Reprod **3**(3): 195-202.
Brewer, L., M. Corzett, E. Y. Lau and R. Balhorn (2003). "Dynamics of protamine 1 binding to single DNA molecules." J Biol Chem **278**(43): 42403-42408.
Brewis, I. A. and B. M. Gadella (2010). "Sperm surface proteomics: from protein lists to biological function." Molecular Human Reproduction **16**(2): 68-79.
Brini, M. and E. Carafoli (2011). "The plasma membrane Ca²+ ATPase and the plasma membrane sodium calcium exchanger cooperate in the regulation of cell calcium." Cold Spring Harb Perspect Biol **3**(2).
Broad, L. M., F. J. Braun, J. P. Lievremont, G. S. Bird, T. Kurosaki and J. W. Putney, Jr. (2001). "Role of the phospholipase C-inositol 1,4,5-trisphosphate pathway in calcium release-activated calcium current and capacitative calcium entry." J Biol Chem **276**(19): 15945-15952.
Bromfield, J. J. (2014). "Seminal fluid and reproduction: much more than previously thought." Journal of Assisted Reproduction and Genetics **31**(6): 627-636.
Bromfield, J. J. (2014). "Seminal fluid and reproduction: much more than previously thought." J Assist Reprod Genet **31**(6): 627-636.
Bromfield, J. J., J. E. Schjenken, P. Y. Chin, A. S. Care, M. J. Jasper and S. A. Robertson (2014). "Maternal tract factors contribute to paternal seminal fluid impact on metabolic phenotype in offspring." Proc Natl Acad Sci U S A **111**(6): 2200-2205.
Brosens, I., W. B. Robertson and H. G. Dixon (1967). "The physiological response of the vessels of the placental bed to normal pregnancy." J Pathol Bacteriol **93**(2): 569-579.
Brown, D. C. and M. J. Iadarola (2015). Chapter 6 - TRPV1 Agonist Cytotoxicity for Chronic Pain Relief: From Mechanistic Understanding to Clinical Application. TRP Channels as Therapeutic Targets. A. Szallasi. Boston, Academic Press**:** 99-118.
Brown, W. E. (1956). "Human Semen." Fertility and Sterility **7**(4): 368-386.
Bruce, J. I., S. V. Straub and D. I. Yule (2003). "Crosstalk between cAMP and Ca2+ signaling in non-excitable cells." Cell Calcium **34**(6): 431-444.
Budd, S. L. and D. G. Nicholls (1996). "A reevaluation of the role of mitochondria in neuronal Ca2+ homeostasis." J Neurochem **66**(1): 403-411.

Buhi, W., I. Alvarez and A. Kouba (2000). "Secreted proteins of the oviduct." Cells Tissues Organs **166**(2): 165-179.
Bulletti, C., D. de Ziegler, V. Polli, L. Diotallevi, E. Del Ferro and C. Flamigni (2000). "Uterine contractility during the menstrual cycle." Hum Reprod **15 Suppl 1**: 81-89.
Buonanno, A. and R. D. Fields (1999). "Gene regulation by patterned electrical activity during neural and skeletal muscle development." Curr Opin Neurobiol **9**(1): 110-120.
Bygdeman, M., E. Bendvold, C. Gottlieb, K. Svanborg and P. Eneroth (1985). Prostaglandins in Human Seminal Fluid and Its Relation to Fertility. Prostaglandins, Leukotrienes, and Lipoxins: Biochemistry, Mechanism of Action, and Clinical Applications. J. M. Bailey. Boston, MA, Springer US**:** 423-431.
Cao, X., Y. Cui, X. Zhang, J. Lou, J. Zhou, H. Bei and R. Wei (2018). "Proteomic profile of human spermatozoa in healthy and asthenozoospermic individuals." Reprod Biol Endocrinol **16**(1): 16.
Carafoli, E., L. Santella, D. Branca and M. Brini (2001). "Generation, control, and processing of cellular calcium signals." Crit Rev Biochem Mol Biol **36**(2): 107-260.
Carlson, A. E., R. E. Westenbroek, T. Quill, D. Ren, D. E. Clapham, B. Hille, D. L. Garbers and D. F. Babcock (2003). "CatSper1 required for evoked Ca2+ entry and control of flagellar function in sperm." Proceedings of the National Academy of Sciences **100**(25): 14864-14868.
Carrasco, S. and I. Mérida (2007). "Diacylglycerol, when simplicity becomes complex." Trends Biochem Sci **32**(1): 27-36.
Casas, E. and T. Vavouri (2014). "Sperm epigenomics: challenges and opportunities." Front Genet **5**: 330.
Castillo, J., O. A. Bogle, M. Jodar, F. Torabi, D. Delgado-Dueñas, J. M. Estanyol, J. L. Ballescà, D. Miller and R. Oliva (2019). "Proteomic Changes in Human Sperm During Sequential in vitro Capacitation and Acrosome Reaction." Frontiers in Cell and Developmental Biology **7**(295).
Catterall, W. A. (2011). "Voltage-gated calcium channels." Cold Spring Harb Perspect Biol **3**(8): a003947.
Chang, M. C. (1951). "Fertilizing capacity of spermatozoa deposited into the fallopian tubes." Nature **168**(4277): 697-698.
Chang, S. J., C. R. Tzeng, Y. H. Lee and C. J. Tai (2008). "Extracellular ATP activates the PLC/PKC/ERK signaling pathway through the P2Y2 purinergic receptor leading to the induction of early growth response 1 expression and the inhibition of viability in human endometrial stromal cells." Cell Signal **20**(7): 1248-1255.
Chemes, H. E., S. Brugo, F. Zanchetti, C. Carrere and J. C. Lavieri (1987). "Dysplasia of the fibrous sheath: an ultrastructural defect of human spermatozoa associated with sperm immotility and primary sterility." Fertil Steril **48**(4): 664-669.
Cheng, H., W. J. Lederer and M. B. Cannell (1993). "Calcium sparks: elementary events underlying excitation-contraction coupling in heart muscle." Science **262**(5134): 740-744.
Chiu, P. C., M. K. Chung, H. Y. Tsang, R. Koistinen, H. Koistinen, M. Seppala, K. F. Lee and W. S. Yeung (2005). "Glycodelin-S in human seminal plasma reduces cholesterol efflux and inhibits capacitation of spermatozoa." J Biol Chem **280**(27): 25580-25589.
Cho, C., D. O. Bunch, J. E. Faure, E. H. Goulding, E. M. Eddy, P. Primakoff and D. G. Myles (1998). "Fertilization defects in sperm from mice lacking fertilin beta." Science **281**(5384): 1857-1859.

Chrétien, F. C. (2003). "Involvement of the glycoproteic meshwork of cervical mucus in the mechanism of sperm orientation." Acta Obstet Gynecol Scand **82**(5): 449-461.
Chu, T. M., M. A. Nocera, K. C. Flanders and E. Kawinski (1996). "Localization of seminal plasma transforming growth factor-beta1 on human spermatozoa: an immunocytochemical study." Fertil Steril **66**(2): 327-330.
Chumduri, C. and M. Y. Turco (2021). "Organoids of the female reproductive tract." J Mol Med (Berl) **99**(4): 531-553.
Chung, J.-J., S.-H. Shim, R. A. Everley, S. P. Gygi, X. Zhuang and D. E. Clapham (2014). "Structurally distinct Ca2+ signaling domains of sperm flagella orchestrate tyrosine phosphorylation and motility." Cell **157**(4): 808-822.
Clapham, D. E. (1995). "Calcium signaling." Cell **80**(2): 259-268.
Clapham, D. E. (2007). "Calcium Signaling." Cell **131**(6): 1047-1058.
Clapper, D. L., T. F. Walseth, P. J. Dargie and H. C. Lee (1987). "Pyridine nucleotide metabolites stimulate calcium release from sea urchin egg microsomes desensitized to inositol trisphosphate." J Biol Chem **262**(20): 9561-9568.
Clarke, F. M., C. Orozco, A. V. Perkins, I. Cock, K. F. Tonissen, A. J. Robins and J. R. Wells (1991). "Identification of molecules involved in the 'early pregnancy factor' phenomenon." J Reprod Fertil **93**(2): 525-539.
Classen-Linke, I., M. Kusche, R. Knauthe and H. M. Beier (1996). "Establishment of a human endometrial cell culture system and characterization of its polarized hormone responsive epithelial cells." Cell and Tissue Research **287**(1): 171-185.
Clerc, F., K. R. Reiding, B. C. Jansen, G. S. Kammeijer, A. Bondt and M. Wuhrer (2016). "Human plasma protein N-glycosylation." Glycoconj J **33**(3): 309-343.
Codrington, A. M., B. F. Hales and B. Robaire (2007). "Exposure of male rats to cyclophosphamide alters the chromatin structure and basic proteome in spermatozoa." Hum Reprod **22**(5): 1431-1442.
Coin, I., M. Beyermann and M. Bienert (2007). "Solid-phase peptide synthesis: from standard procedures to the synthesis of difficult sequences." Nature Protocols **2**(12): 3247-3256.
Comhaire, F., L. Vermeulen, K. Ghedira, J. Mas, S. Irvine and G. Callipolitis (1983). "Adenosine triphosphate in human semen: a quantitative estimate of fertilizing potential." Fertil Steril **40**(4): 500-504.
Compton, T. (1993). "An immortalized human fibroblast cell line is permissive for human cytomegalovirus infection." J Virol **67**(6): 3644-3648.
Connolly, T. J. (2011). CALCIUM SIGNALLING DURING HUMAN SPERM INTERACTION WITH CELLS OF THE FEMALE REPRODUCTIVE TRACT. DOCTOR OF PHILOSOPHY, The University of Birmingham.
Conrad, K. P., M. B. Rabaglino and E. D. Post Uiterweer (2017). "Emerging role for dysregulated decidualization in the genesis of preeclampsia." Placenta **60**: 119-129.
Corner, G. W. and W. M. Allen (1929). "Physiology of the corpus luteum: II. Production of a special uterine reaction (progestational proliferation) by extracts of the corpus luteum." American Journal of Physiology-Legacy Content **88**(2): 326-339.
Coskun, O. (2016). "Separation techniques: Chromatography." North Clin Istanb **3**(2): 156-160.
Costello, S., F. Michelangeli, K. Nash, L. Lefievre, J. Morris, G. Machado-Oliveira, C. Barratt, J. Kirkman-Brown and S. Publicover (2009). "Ca2+-stores in sperm: their identities and functions." Reproduction (Cambridge, England) **138**(3): 425.
Cox, C. I. and H. J. Leese (1995). "Effect of purinergic stimulation on intracellular calcium concentration and transepithelial potential difference in cultured bovine oviduct cells." Biol Reprod **52**(6): 1244-1249.

Coy, P., F. A. García-Vázquez, P. E. Visconti and M. Avilés (2012). "Roles of the oviduct in mammalian fertilization." Reproduction **144**(6): 649-660.
Crane, L. H. and L. Martin (1991). "Postcopulatory myometrial activity in the rat as seen by video-laparoscopy." Reprod Fertil Dev **3**(6): 685-698.
Crawford, G., A. Ray, A. Gudi, A. Shah and R. Homburg (2015). "The role of seminal plasma for improved outcomes during in vitro fertilization treatment: review of the literature and meta-analysis." Hum Reprod Update **21**(2): 275-284.
Critchley, H. O. D., J. A. Maybin, G. M. Armstrong and A. R. W. Williams (2020). "Physiology of the Endometrium and Regulation of Menstruation." Physiol Rev **100**(3): 1149-1179.
Cross, N. L. (2004). "Reorganization of lipid rafts during capacitation of human sperm." Biol Reprod **71**(4): 1367-1373.
Crowell, A. M. J., M. J. Wall and A. A. Doucette (2013). "Maximizing recovery of water-soluble proteins through acetone precipitation." Analytica Chimica Acta **796**: 48-54.
Csordás, G., A. P. Thomas and G. Hajnóczky (1999). "Quasi-synaptic calcium signal transmission between endoplasmic reticulum and mitochondria." The EMBO journal **18**(1): 96-108.
Cuatrecasas, P. (1970). "Protein Purification by Affinity Chromatography: DERIVATIZATIONS OF AGAROSE AND POLYACRYLAMIDE BEADS." Journal of Biological Chemistry **245**(12): 3059-3065.
Cunha, G. R., A. Sinclair, W. A. Ricke, S. J. Robboy, M. Cao and L. S. Baskin (2019). "Reproductive tract biology: Of mice and men." Differentiation **110**: 49-63.
D'Cruz, O. J., B. L. Wang and G. G. Haas, Jr. (1992). "Phagocytosis of immunoglobulin G and C3-bound human sperm by human polymorphonuclear leukocytes is not associated with the release of oxidative radicals." Biol Reprod **46**(4): 721-732.
De Jonge, C. (2005). "Biological basis for human capacitation." Hum Reprod Update **11**(3): 205-214.
De Koninck, P. and H. Schulman (1998). "Sensitivity of CaM kinase II to the frequency of Ca2+ oscillations." Science **279**(5348): 227-230.
de Lamirande, E. and C. Gagnon (1995). "Capacitation-associated production of superoxide anion by human spermatozoa." Free Radic Biol Med **18**(3): 487-495.
De, M., R. Choudhuri and G. W. Wood (1991). "Determination of the number and distribution of macrophages, lymphocytes, and granulocytes in the mouse uterus from mating through implantation." J Leukoc Biol **50**(3): 252-262.
Ded, L., N. Sebkova, M. Cerna, F. Elzeinova, P. Dostalova, J. Peknicova and K. Dvorakova-Hortova (2013). "In vivo exposure to 17β-estradiol triggers premature sperm capacitation in cauda epididymis." Reproduction **145**(3): 255-263.
Deng, H., S. Mondal, S. Sur and C. D. Woodworth (2019). "Establishment and optimization of epithelial cell cultures from human ectocervix, transformation zone, and endocervix optimization of epithelial cell cultures." J Cell Physiol **234**(6): 7683-7694.
Denissenko, P., V. Kantsler, D. J. Smith and J. Kirkman-Brown (2012). "Human spermatozoa migration in microchannels reveals boundary-following navigation." Proc Natl Acad Sci U S A **109**(21): 8007-8010.
Di Benedetto, G., C. J. Magnus, P. T. Gray and A. Mehta (1991). "Calcium regulation of ciliary beat frequency in human respiratory epithelium in vitro." J Physiol **439**: 103-113.

Dickens, C. J., M. T. Comer, J. Southgate and H. J. Leese (1996). "Human Fallopian tubal epithelial cells in vitro: establishment of polarity and potential role of intracellular calcium and extracellular ATP in fluid secretion." Hum Reprod **11**(1): 212-217.
Dickens, C. J., C. I. Cox and H. J. Leese (1996). "Intracellular calcium in cultured rabbit oviduct epithelial cells." Reprod Fertil Dev **8**(2): 243-247.
Dolmetsch, R. E., R. S. Lewis, C. C. Goodnow and J. I. Healy (1997). "Differential activation of transcription factors induced by Ca2+ response amplitude and duration." Nature **386**(6627): 855-858.
Dolmetsch, R. E., K. Xu and R. S. Lewis (1998). "Calcium oscillations increase the efficiency and specificity of gene expression." Nature **392**(6679): 933-936.
Dostál, J., L. Veselský, M. Marounek, B. Zelezná and V. Jonáková (1997). "Inhibition of bacterial and boar epididymal sperm immunogenicity by boar seminal immunosuppressive component in mice." J Reprod Fertil **111**(1): 135-141.
Drabovich, A. P., P. Saraon, K. Jarvi and E. P. Diamandis (2014). "Seminal plasma as a diagnostic fluid for male reproductive system disorders." Nat Rev Urol **11**(5): 278-288.
Duchen, M. R. (1999). "Contributions of mitochondria to animal physiology: from homeostatic sensor to calcium signalling and cell death." J Physiol **516 (Pt 1)**(Pt 1): 1-17.
Dunn, M. J. (2014). Gel electrophoresis of proteins, Elsevier.
Easterling, L. F., R. Yerabolu, R. Kumar, K. Z. Alzarieni and H. I. Kenttämaa (2020). "Factors Affecting the Limit of Detection for HPLC/Tandem Mass Spectrometry Experiments Based on Gas-Phase Ion–Molecule Reactions." Analytical Chemistry **92**(11): 7471-7477.
Edström, A. M., J. Malm, B. Frohm, J. A. Martellini, A. Giwercman, M. Mörgelin, A. M. Cole and O. E. Sørensen (2008). "The major bactericidal activity of human seminal plasma is zinc-dependent and derived from fragmentation of the semenogelins." J Immunol **181**(5): 3413-3421.
Edwards, J. J., S. L. Tollaksen and N. G. Anderson (1981). "Proteins of human semen. I. Two-dimensional mapping of human seminal fluid." Clin Chem **27**(8): 1335-1340.
Ellington, J. E., G. G. Ignotz, B. A. Ball, V. N. Meyers-Wallen and W. B. Currie (1993). "De novo protein synthesis by bovine uterine tube (oviduct) epithelial cells changes during co-culture with bull spermatozoa." Biol Reprod **48**(4): 851-856.
Ellington, J. E., G. G. Ignotz, B. A. Ball, V. N. Meyers-Wallen and W. B. Currie (1993). "De Novo Protein Synthesis by Bovine Uterine Tube (Oviduct) Epithelial Cells Changes during Co-Culture with Bull Spermatozoa1." Biology of Reproduction **48**(4): 851-856.
Ellington, J. E., D. D. Varner, R. C. Burghardt, V. N. Meyers-Wallen, R. Barhoumi, S. P. Brinsko and B. A. Ball (1993). "Cell-to-cell communication of equine uterine tube (oviduct) cells as determined by anchored cell analysis in culture." Animal Reproduction Science **30**(4): 313-324.
Eppig, J. J. (1991). "Intercommunication between mammalian oocytes and companion somatic cells." Bioessays **13**(11): 569-574.
Evans, J. H. and M. J. Sanderson (1999). "Intracellular calcium oscillations regulate ciliary beat frequency of airway epithelial cells." Cell Calcium **26**(3): 103-110.
Fabro, G., R. A. Rovasio, S. Civalero, A. Frenkel, S. R. Caplan, M. Eisenbach and L. C. Giojalas (2002). "Chemotaxis of capacitated rabbit spermatozoa to follicular fluid revealed by a novel directionality-based assay." Biol Reprod **67**(5): 1565-1571.

Fadel, H. E., D. Berns, L. J. Zaneveld, G. D. Wilbanks and E. E. Brueschke (1976). "The human uterotubal junction: a scanning electron microscope study during different phases of the menstrual cycle." Fertil Steril **27**(10): 1176-1186.
Fan, M., J. Zhang, C.-W. Tsai, B. J. Orlando, M. Rodriguez, Y. Xu, M. Liao, M.-F. Tsai and L. Feng (2020). "Structure and mechanism of the mitochondrial Ca2+ uniporter holocomplex." Nature **582**(7810): 129-133.
Fawcett, D. W. (1970). "A comparative view of sperm ultrastructure." Biology of reproduction **2**(suppl_2): 90-127.
Fawcett, D. W. (1975). "The mammalian spermatozoon." Developmental biology **44**(2): 394-436.
Fazeli, A., N. A. Affara, M. Hubank and W. V. Holt (2004). "Sperm-Induced Modification of the Oviductal Gene Expression Profile After Natural Insemination in Mice1." Biology of Reproduction **71**(1): 60-65.
Feist, P. and A. B. Hummon (2015). "Proteomic challenges: sample preparation techniques for microgram-quantity protein analysis from biological samples." Int J Mol Sci **16**(2): 3537-3563.
Ferenczy, A. (1977). "Surface ultrastructural response of the human uterine lining epithelium to hormonal environment. A scanning electron microscopic study." Acta Cytol **21**(4): 566-572.
Fernandes, J., I. M. Lorenzo, Y. N. Andrade, A. Garcia-Elias, S. A. Serra, J. M. Fernández-Fernández and M. A. Valverde (2008). "IP3 sensitizes TRPV4 channel to the mechano- and osmotransducing messenger 5'-6'-epoxyeicosatrienoic acid." J Cell Biol **181**(1): 143-155.
Ferraz, M. A. M. M., H. H. W. Henning, T. A. E. Stout, P. L. A. M. Vos and B. M. Gadella (2017). "Designing 3-Dimensional In Vitro Oviduct Culture Systems to Study Mammalian Fertilization and Embryo Production." Annals of Biomedical Engineering **45**(7): 1731-1744.
Fields, G. B. (2001). "Introduction to Peptide Synthesis." Current Protocols in Protein Science **26**(1).
Fishman, E., K. Jo, Q. Nguyen, D. Kong, R. Royfman, A. Cekic, S. Khanal, A. Miller, C. Simerly and G. Schatten (2018). A novel atypical sperm centriole is functional during human fertilization. Nat Commun 9 (1): 2210.
Fluhmann, C. F. (1957). "The nature and development of the so-called glands of the cervix uteri." American journal of obstetrics and gynecology **74**(4): 753-768.
Foley, C. W. and W. L. Williams (1967). "Effect of Bicarbonate and Oviduct Fluid on Respiration of Spermatozoa." Proceedings of the Society for Experimental Biology and Medicine **126**(3): 634-637.
Friesen, A. D. (1987). "Chromatographic methods of fractionation." Dev Biol Stand **67**: 3-13.
Fukuda, M. and K. Fukuda (1994). "Uterine endometrial cavity movement and cervical mucus." Hum Reprod **9**(6): 1013-1016.
Furukawa, K., Y. Ohkawa, Y. Yamauchi, K. Hamamura, Y. Ohmi and K. Furukawa (2012). "Fine tuning of cell signals by glycosylation." The Journal of Biochemistry **151**(6): 573-578.
Gaffney, E. A., H. Gadêlha, D. J. Smith, J. R. Blake and J. C. Kirkman-Brown (2011). "Mammalian Sperm Motility: Observation and Theory." Annual Review of Fluid Mechanics **43**(1): 501-528.
Gardner, D. K., M. Lane, I. Calderon and J. Leeton (1996). "Environment of the preimplantation human embryo in vivo: metabolite analysis of oviduct and uterine fluids and metabolism of cumulus cells." Fertility and sterility **65**(2): 349-353.

Gasdaska, J. R., M. Berggren and G. Powis (1995). "Cell growth stimulation by the redox protein thioredoxin occurs by a novel helper mechanism." Cell Growth Differ **6**(12): 1643-1650.
Georgiou, A. S., A. P. Snijders, E. Sostaric, R. Aflatoonian, J. L. Vazquez, J. M. Vazquez, J. Roca, E. A. Martinez, P. C. Wright and A. Fazeli (2007). "Modulation of the oviductal environment by gametes." J Proteome Res **6**(12): 4656-4666.
Georgiou, A. S., E. Sostaric, C. H. Wong, A. P. Snijders, P. C. Wright, H. D. Moore and A. Fazeli (2005). "Gametes alter the oviductal secretory proteome." Mol Cell Proteomics **4**(11): 1785-1796.
Georgiou, A. S., E. Sostaric, C. H. Wong, A. P. L. Snijders, P. C. Wright, H. D. Moore and A. Fazeli (2005). "Gametes Alter the Oviductal Secretory Proteome." Molecular & Cellular Proteomics **4**(11): 1785-1796.
Ghasemian Nafchi, H., Y. Azizi and I. Halvaei (2022). "The role of growth factors in human sperm parameters: A review of in vitro studies." Int J Reprod Biomed **20**(10): 807-818.
Ghavideldarestani, M., S. L. Atkin, H. J. Leese and R. G. Sturmey (2016). "Expression and function of transient receptor potential channels in the female bovine reproductive tract." Theriogenology **86**(2): 551-561.
Ghersevich, S., E. Massa and C. Zumoffen (2015). "Oviductal secretion and gamete interaction." Reproduction **149**(1): R1-r14.
Gilany, K., N. Lakpour, M. Vafakhah and M. R. Sadeghi (2011). "The Profile of Human Sperm Proteome; A Mini-review." J Reprod Infertil **12**(3): 193-199.
Giuliano, F. and P. Clément (2005). "Physiology of ejaculation: emphasis on serotonergic control." Eur Urol **48**(3): 408-417.
Grasa, P., K. Coward, C. Young and J. Parrington (2008). "The pattern of localization of the putative oocyte activation factor, phospholipase Czeta, in uncapacitated, capacitated, and ionophore-treated human spermatozoa." Hum Reprod **23**(11): 2513-2522.
Griveau, J. F., P. Renard and D. Le Lannou (1994). "An in vitro promoting role for hydrogen peroxide in human sperm capacitation." Int J Androl **17**(6): 300-307.
Gruber, C. W., M. Muttenthaler and M. Freissmuth (2010). "Ligand-based peptide design and combinatorial peptide libraries to target G protein-coupled receptors." Curr Pharm Des **16**(28): 3071-3088.
Guerin, L. R., J. R. Prins and S. A. Robertson (2009). "Regulatory T-cells and immune tolerance in pregnancy: a new target for infertility treatment?" Hum Reprod Update **15**(5): 517-535.
Guido, C., I. Perrotta, S. Panza, E. Middea, P. Avena, M. Santoro, S. Marsico, P. Imbrogno, S. Andò and S. Aquila (2011). "Human sperm physiology: estrogen receptor alpha (ERα) and estrogen receptor beta (ERβ) influence sperm metabolism and may be involved in the pathophysiology of varicocele-associated male infertility." J Cell Physiol **226**(12): 3403-3412.
Guo, H., Z. Chang, Z. Zhang, Y. Zhao, X. Jiang, H. Yu, Y. Zhang, R. Zhao and B. He (2019). "Extracellular ATPs produced in seminal plasma exosomes regulate boar sperm motility and mitochondrial metabolism." Theriogenology **139**: 113-120.
Guzhova, I., K. Kislyakova, O. Moskaliova, I. Fridlanskaya, M. Tytell, M. Cheetham and B. Margulis (2001). "In vitro studies show that Hsp70 can be released by glia and that exogenous Hsp70 can enhance neuronal stress tolerance." Brain Res **914**(1-2): 66-73.
Hafez, E. S. (1979). "In vivo and in vitro sperm penetration in cervical mucus." Acta Eur Fertil **10**(2): 41-49.

Hagaman, J. R., J. S. Moyer, E. S. Bachman, M. Sibony, P. L. Magyar, J. E. Welch, O. Smithies, J. H. Krege and D. A. O'Brien (1998). "Angiotensin-converting enzyme and male fertility." Proc Natl Acad Sci U S A **95**(5): 2552-2557.
Hagiwara, H., N. Ohwada, T. Aoki, T. Suzuki and K. Takata (2008). "The primary cilia of secretory cells in the human oviduct mucosa." Med Mol Morphol **41**(4): 193-198.
Han, R. Y., J. Ma, J. Y. Ma, X. C. Wang, X. T. An, Z. D. Zhang and S. S. Wang (2017). "[Correlation of semen parameters with inflammatory factors in the seminal plasma of obese males]." Zhonghua Nan Ke Xue **23**(10): 894-898.
Harper, C., C. Barratt, S. Publicover and J. Kirkman-Brown (2007). "Kinetics of the Progesterone-Induced Acrosome Reaction and Its Relation to Intracellular Calcium Responses in Individual Human Spermatozoa." Biology of reproduction **75**: 933-939.
Harper, C., J. Kirkman-Brown, C. Barratt and S. Publicover (2003). "Encoding of progesterone stimulus intensity by intracellular [Ca] ([Ca]i) in human spermatozoa." The Biochemical journal **372**: 407-417.
Hart, R. and R. J. Norman (2013). "The longer-term health outcomes for children born as a result of IVF treatment: Part I--General health outcomes." Hum Reprod Update **19**(3): 232-243.
Health, N. I. f. and C. Excellence (2017). Fertility problems: assessment and treatment, National Institute for Health and Care Excellence (NICE).
Heller, C. G. and Y. Clermont (1963). "Spermatogenesis in man: an estimate of its duration." Science **140**(3563): 184-186.
Hempstock, J., T. Cindrova-Davies, E. Jauniaux and G. J. Burton (2004). "Endometrial glands as a source of nutrients, growth factors and cytokines during the first trimester of human pregnancy: a morphological and immunohistochemical study." Reprod Biol Endocrinol **2**: 58.
Henkel, R. R. and W. B. Schill (2003). "Sperm preparation for ART." Reprod Biol Endocrinol **1**: 108.
Henzel, W. J., T. M. Billeci, J. T. Stults, S. C. Wong, C. Grimley and C. Watanabe (1993). "Identifying proteins from two-dimensional gels by molecular mass searching of peptide fragments in protein sequence databases." Proceedings of the National Academy of Sciences **90**(11): 5011-5015.
Herrero, M. B., E. de Lamirande and C. Gagnon (1999). "Nitric oxide regulates human sperm capacitation and protein-tyrosine phosphorylation in vitro." Biol Reprod **61**(3): 575-581.
Hess, K. C., B. H. Jones, B. Marquez, Y. Chen, T. S. Ord, M. Kamenetsky, C. Miyamoto, J. H. Zippin, G. S. Kopf, S. S. Suarez, L. R. Levin, C. J. Williams, J. Buck and S. B. Moss (2005). "The "soluble" adenylyl cyclase in sperm mediates multiple signaling events required for fertilization." Dev Cell **9**(2): 249-259.
Hickey, K. D. and M. M. Buhr (2011). "Lipid bilayer composition affects transmembrane protein orientation and function." J Lipids **2011**: 208457.
Hildonen, S., T. G. Halvorsen and L. Reubsaet (2014). "Why less is more when generating tryptic peptides in bottom-up proteomics." Proteomics **14**(17-18): 2031-2041.
Hilpert, K., M. R. Elliott, R. Volkmer-Engert, P. Henklein, O. Donini, Q. Zhou, D. F. H. Winkler and R. E. W. Hancock (2006). "Sequence Requirements and an Optimization Strategy for Short Antimicrobial Peptides." Chemistry & Biology **13**(10): 1101-1107.

Hinton, B. T., M. A. Palladino, D. Rudolph, Z. J. Lan and J. C. Labus (1996). "The role of the epididymis in the protection of spermatozoa." Curr Top Dev Biol **33**: 61-102.
Hjort, T. and K. B. Hansen (1971). "Immunofluorescent studies on human spermatozoa. I. The detection of different spermatozoal antibodies and their occurrence in normal and infertile women." Clin Exp Immunol **8**(1): 9-23.
Ho, H. C., K. A. Granish and S. S. Suarez (2002). "Hyperactivated motility of bull sperm is triggered at the axoneme by Ca2+ and not cAMP." Dev Biol **250**(1): 208-217.
Ho, H. C. and S. S. Suarez (2001). "Hyperactivation of mammalian spermatozoa: function and regulation." Reproduction **122**(4): 519-526.
Holesh, J. E., A. N. Bass and M. Lord (2022). Physiology, Ovulation. StatPearls. Treasure Island (FL), StatPearls Publishing

Copyright © 2022, StatPearls Publishing LLC.

Honegger, P. (2001). "Overview of cell and tissue culture techniques." Curr Protoc Pharmacol **Chapter 12**: Unit12.11.
Hopkins, B. R., I. Sepil and S. Wigby (2017). "Seminal fluid." Current Biology **27**(11): R404-R405.
Hou, J. W., L. H. Yuan, X. L. Cao, J. Y. Song and Z. G. Sun (2023). "Impact of sexual intercourse on frozen-thawed embryo transfer outcomes: a randomized controlled trial." Contracept Reprod Med **8**(1): 19.
Huang, L., Y. Liu, P. Zhang, R. Kang, Y. Liu, X. Li, L. Bo and Z. Dong (2013). "In vitro dose-dependent inhibition of the intracellular spontaneous calcium oscillations in developing hippocampal neurons by ketamine." PLoS One **8**(3): e59804.
Hunter, R. H. and H. Rodriguez-Martinez (2004). "Capacitation of mammalian spermatozoa in vivo, with a specific focus on events in the Fallopian tubes." Mol Reprod Dev **67**(2): 243-250.
Ibrahim, L. A., J. A. Rizo, P. L. P. Fontes, G. C. Lamb and J. J. Bromfield (2019). "Seminal plasma modulates expression of endometrial inflammatory meditators in the bovine†." Biol Reprod **100**(3): 660-671.
Ikawa, M., N. Inoue, A. M. Benham and M. Okabe (2010). "Fertilization: a sperm's journey to and interaction with the oocyte." J Clin Invest **120**(4): 984-994.
Ikawa, M., I. Wada, K. Kominami, D. Watanabe, K. Toshimori, Y. Nishimune and M. Okabe (1997). "The putative chaperone calmegin is required for sperm fertility." Nature **387**(6633): 607-611.
Ivic, A. (2002). "Critical evaluation of methylcellulose as an alternative medium in sperm migration tests." Human Reproduction **17**(1): 143-149.
Jackson, T. R., S. I. Patterson, O. Thastrup and M. R. Hanley (1988). "A novel tumour promoter, thapsigargin, transiently increases cytoplasmic free Ca2+ without generation of inositol phosphates in NG115-401L neuronal cells." Biochem J **253**(1): 81-86.
James, E. R., D. T. Carrell, K. I. Aston, T. G. Jenkins, M. Yeste and A. Salas-Huetos (2020). "The Role of the Epididymis and the Contribution of Epididymosomes to Mammalian Reproduction." Int J Mol Sci **21**(15).
Jansen, R. P. (1980). "Cyclic changes in the human fallopian tube isthmus and their functional importance." Am J Obstet Gynecol **136**(3): 292-308.
Jiang, S., S. C. Chow, P. Nicotera and S. Orrenius (1994). "Intracellular Ca2+ signals activate apoptosis in thymocytes: studies using the Ca(2+)-ATPase inhibitor thapsigargin." Exp Cell Res **212**(1): 84-92.

Jin, S. K. and W. X. Yang (2017). "Factors and pathways involved in capacitation: how are they regulated?" Oncotarget **8**(2): 3600-3627.
Jodar, M., A. Soler-Ventura and R. Oliva (2017). "Semen proteomics and male infertility." Journal of Proteomics **162**: 125-134.
Johnsen, E., O. K. Brandtzaeg, T. Vehus, H. Roberg-Larsen, V. Bogoeva, O. Ademi, J. Hildahl, E. Lundanes and S. R. Wilson (2016). "A critical evaluation of Amicon Ultra centrifugal filters for separating proteins, drugs and nanoparticles in biosamples." J Pharm Biomed Anal **120**: 106-111.
Johnston, D. S., J. Wooters, G. S. Kopf, Y. Qiu and K. P. Roberts (2005). "Analysis of the human sperm proteome." Ann N Y Acad Sci **1061**: 190-202.
Jones, R. E. and K. H. Lopez (2013). Human reproductive biology, Academic Press.
Jonsson, M., S. Linse, B. Frohm, A. Lundwall and J. Malm (2005). "Semenogelins I and II bind zinc and regulate the activity of prostate-specific antigen." Biochem J **387**(Pt 2): 447-453.
Jonsson, M., Å. Lundwall and J. Malm (2006). "The semenogelins: proteins with functions beyond reproduction?" Cellular and Molecular Life Sciences CMLS **63**(24): 2886-2888.
Joseph, S. K., K. E. Coll, A. P. Thomas, R. Rubin and J. R. Williamson (1985). "The role of extracellular Ca2+ in the response of the hepatocyte to Ca2+-dependent hormones." J Biol Chem **260**(23): 12508-12515.
Kania, E., G. Roest, T. Vervliet, J. B. Parys and G. Bultynck (2017). "IP3 Receptor-Mediated Calcium Signaling and Its Role in Autophagy in Cancer." Frontiers in Oncology **7**.
Kapelnikov, A., E. Zelinger, Y. Gottlieb, K. Rhrissorrakrai, K. C. Gunsalus and Y. Heifetz (2008). "Mating induces an immune response and developmental switch in the Drosophila oviduct." Proc Natl Acad Sci U S A **105**(37): 13912-13917.
Katz, D. F., R. N. Mills and T. R. Pritchett (1978). "The movement of human spermatozoa in cervical mucus." J Reprod Fertil **53**(2): 259-265.
Katz, D. F., P. Morales, S. J. Samuels and J. W. Overstreet (1990). "Mechanisms of filtration of morphologically abnormal human sperm by cervical mucus." Fertil Steril **54**(3): 513-516.
Kaur, G. and J. M. Dufour (2012). "Cell lines: Valuable tools or useless artifacts." Spermatogenesis **2**(1): 1-5.
Kazuhiro, T., I. Maruyama, Y. Sinichi, O. Toshimichi and N. Yukihiro (1991). "Isolation and Monolayer Culture of Human Fallopian Tube Epithelial Cells." In Vitro Cellular & Developmental Biology **27A**(9): 720-724.
Khawar, M. B., H. Gao and W. Li (2019). "Mechanism of Acrosome Biogenesis in Mammals." Frontiers in Cell and Developmental Biology **7**.
Kho, E. M., L. M. McCowan, R. A. North, C. T. Roberts, E. Chan, M. A. Black, R. S. Taylor and G. A. Dekker (2009). "Duration of sexual relationship and its effect on preeclampsia and small for gestational age perinatal outcome." J Reprod Immunol **82**(1): 66-73.
Kim, D. H., K. Han, K. Gupta, K. W. Kwon, K. Y. Suh and A. Levchenko (2009). "Mechanosensitivity of fibroblast cell shape and movement to anisotropic substratum topography gradients." Biomaterials **30**(29): 5433-5444.
Kim, E., M. Yamashita, M. Kimura, A. Honda, S. Kashiwabara and T. Baba (2008). "Sperm penetration through cumulus mass and zona pellucida." Int J Dev Biol **52**(5-6): 677-682.
Kim, M., J. K. Rhee, H. Choi, A. Kwon, J. Kim, G. D. Lee, D. W. Jekarl, S. Lee, Y. Kim and T. M. Kim (2017). "Passage-dependent accumulation of somatic mutations

in mesenchymal stromal cells during in vitro culture revealed by whole genome sequencing." Sci Rep **7**(1): 14508.
Kim, M. C., W. S. Chung, D. J. Yun and M. J. Cho (2009). "Calcium and calmodulin-mediated regulation of gene expression in plants." Mol Plant **2**(1): 13-21.
Kirichok, Y., G. Krapivinsky and D. E. Clapham (2004). "The mitochondrial calcium uniporter is a highly selective ion channel." Nature **427**(6972): 360-364.
Kirichok, Y., B. Navarro and D. E. Clapham (2006). "Whole-cell patch-clamp measurements of spermatozoa reveal an alkaline-activated Ca2+ channel." Nature **439**(7077): 737-740.
Kirkman-Brown, J., C. Barratt and S. Publicover (2003). "Nifedipine reveals the existence of two discrete components of the progesterone-induced [Ca2+]i transient in human spermatozoa." Developmental biology **259**: 71-82.
Kirkman-Brown, J., C. Barratt and S. Publicover (2004). "Slow calcium oscillations in human spermatozoa." The Biochemical journal **378**: 827-832.
Kirkman-Brown, J., C. Bray, P. Stewart, C. Barratt and S. Publicover (2000). "Biphasic Elevation of [Ca2+]i in Individual Human Spermatozoa Exposed to Progesterone." Developmental biology **222**: 326-335.
Kirkman-Brown, J., L. Lefièvre, C. Bray, P. Stewart, C. Barratt and S. Publicover (2002). "Inhibitors of receptor tyrosine kinases do not suppress progesterone-induced [Ca2+]i signalling in human spermatozoa." Molecular human reproduction **8**: 326-332.
Kirkman-Brown, J., E. Punt, C. Barratt and S. Publicover (2002). "Zona Pellucida and Progesterone-Induced Ca2+ Signaling and Acrosome Reaction in Human Spermatozoa." Journal of andrology **23**: 306-315.
Kline, D. and J. T. Kline (1992). "Thapsigargin activates a calcium influx pathway in the unfertilized mouse egg and suppresses repetitive calcium transients in the fertilized egg." Journal of Biological Chemistry **267**(25): 17624-17630.
Kodithuwakku, S. P., A. Miyamoto and M. P. Wijayagunawardane (2007). "Spermatozoa stimulate prostaglandin synthesis and secretion in bovine oviductal epithelial cells." Reproduction **133**(6): 1087-1094.
Koistinen, H., R. Koistinen, M. Kämäräinen, J. Salo and M. Seppälä (1997). "Multiple forms of messenger ribonucleic acid encoding glycodelin in male genital tract." Lab Invest **76**(5): 683-690.
Kopf, A. H., J. M. Dörr, M. C. Koorengevel, F. Antoniciello, H. Jahn and J. A. Killian (2020). "Factors influencing the solubilization of membrane proteins from Escherichia coli membranes by styrene–maleic acid copolymers." Biochimica et Biophysica Acta (BBA) - Biomembranes **1862**(2): 183125.
Korch, C., M. A. Spillman, T. A. Jackson, B. M. Jacobsen, S. K. Murphy, B. A. Lessey, V. C. Jordan and A. P. Bradford (2012). "DNA profiling analysis of endometrial and ovarian cell lines reveals misidentification, redundancy and contamination." Gynecol Oncol **127**(1): 241-248.
Koyama, H., D. Shi and T. Fujimori (2019). "Biophysics in oviduct: Planar cell polarity, cilia, epithelial fold and tube morphogenesis, egg dynamics." Biophys Physicobiol **16**: 89-107.
Kupzig, S., S. A. Walker and P. J. Cullen (2005). "The frequencies of calcium oscillations are optimized for efficient calcium-mediated activation of Ras and the ERK/MAPK cascade." Proceedings of the National Academy of Sciences **102**(21): 7577-7582.

Kuramoto, H., S. Tamura and Y. Notake (1972). "Establishment of a cell line of human endometrial adenocarcinoma in vitro." Am J Obstet Gynecol **114**(8): 1012-1019.
Kurarmoto, H., M. Hamano and M. Imai (2002). "HEC-1 cells." Hum Cell **15**(2): 81-95.
Kurien, B. T. and R. H. Scofield (2006). "Western blotting." Methods **38**(4): 283-293.
Kvist, U., L. Björndahl and S. Kjellberg (1987). "Sperm nuclear zinc, chromatin stability, and male fertility." Scanning microscopy **1**(3): 38.
Labrou, N. E. (2003). "Design and selection of ligands for affinity chromatography." Journal of Chromatography B **790**(1): 67-78.
Lacroix, G., V. Gouyer, F. Gottrand and J. L. Desseyn (2020). "The Cervicovaginal Mucus Barrier." Int J Mol Sci **21**(21).
Lansley, A. B. and M. J. Sanderson (1999). "Regulation of airway ciliary activity by Ca2+: simultaneous measurement of beat frequency and intracellular Ca2+." Biophys J **77**(1): 629-638.
Law, A. S., P. S. Hafen and J. J. Brault (2022). "Liquid chromatography method for simultaneous quantification of ATP and its degradation products compatible with both UV-Vis and mass spectrometry." J Chromatogr B Analyt Technol Biomed Life Sci **1206**: 123351.
Lee, H. C. (1997). "Mechanisms of calcium signaling by cyclic ADP-ribose and NAADP." Physiol Rev **77**(4): 1133-1164.
Lee, H. S., Y. Qi and W. Im (2015). "Effects of N-glycosylation on protein conformation and dynamics: Protein Data Bank analysis and molecular dynamics simulation study." Scientific Reports **5**(1): 8926.
Lee, Y. L., K. F. Lee, J. S. Xu, Y. L. Wang, S. W. Tsao and W. S. Yeung (2001). "Establishment and characterization of an immortalized human oviductal cell line." Mol Reprod Dev **59**(4): 400-409.
Leese, H., J. Tay, J. Reischl and S. Downing (2001). "Formation of Fallopian tubal fluid: role of a neglected epithelium." Reproduction **121**(3): 339-346.
Lequin, R. M. (2005). "Enzyme immunoassay (EIA)/enzyme-linked immunosorbent assay (ELISA)." Clin Chem **51**(12): 2415-2418.
Leybaert, L. and M. J. Sanderson (2012). "Intercellular Ca(2+) waves: mechanisms and function." Physiol Rev **92**(3): 1359-1392.
Li, Q. and C. Kang (2020). "Mechanisms of Action for Small Molecules Revealed by Structural Biology in Drug Discovery." Int J Mol Sci **21**(15).
Li, W., J. Llopis, M. Whitney, G. Zlokarnik and R. Y. Tsien (1998). "Cell-permeant caged InsP3 ester shows that Ca2+ spike frequency can optimize gene expression." Nature **392**(6679): 936-941.
Lilja, H. (1985). "A kallikrein-like serine protease in prostatic fluid cleaves the predominant seminal vesicle protein." J Clin Invest **76**(5): 1899-1903.
Lilja, H. (1988). "Structure and function of prostatic- and seminal vesicle-secreted proteins involved in the gelation and liquefaction of human semen." Scand J Clin Lab Invest Suppl **191**: 13-20.
Lilja, H. and P. A. Abrahamsson (1988). "Three predominant proteins secreted by the human prostate gland." Prostate **12**(1): 29-38.
Lilja, H., P. A. Abrahamsson and A. Lundwall (1989). "Semenogelin, the predominant protein in human semen. Primary structure and identification of closely related proteins in the male accessory sex glands and on the spermatozoa." J Biol Chem **264**(3): 1894-1900.

Lilja, H., P. A. Abrahamsson and Å. Lundwall (1989). "Semenogelin, the Predominant Protein in Human Semen." Journal of Biological Chemistry **264**(3): 1894-1900.
Lilja, H. and A. Lundwall (1992). "Molecular cloning of epididymal and seminal vesicular transcripts encoding a semenogelin-related protein." Proc Natl Acad Sci U S A **89**(10): 4559-4563.
Linck, R. W., H. Chemes and D. F. Albertini (2016). "The axoneme: the propulsive engine of spermatozoa and cilia and associated ciliopathies leading to infertility." Journal of assisted reproduction and genetics **33**(2): 141-156.
Lishko, P. V. and Y. Kirichok (2010). "The role of Hv1 and CatSper channels in sperm activation." J Physiol **588**(Pt 23): 4667-4672.
Litvin, T. N., M. Kamenetsky, A. Zarifyan, J. Buck and L. R. Levin (2003). "Kinetic properties of "soluble" adenylyl cyclase. Synergism between calcium and bicarbonate." J Biol Chem **278**(18): 15922-15926.
Liu, D. Y. and H. W. Baker (1992). "Morphology of spermatozoa bound to the zona pellucida of human oocytes that failed to fertilize in vitro." J Reprod Fertil **94**(1): 71-84.
Liu, L. P., S. T. Chan, P. C. Ho and W. S. Yeung (1998). "Partial purification of embryotrophic factors from human oviductal cells." Hum Reprod **13**(6): 1613-1619.
Liu, X., W. Wang, P. Zhu, J. Wang, Y. Wang, X. Wang, J. Liu, N. Li, X. Wang, C. Lin and F. Liu (2018). "In-depth quantitative proteome analysis of seminal plasma from men with oligoasthenozoospermia and normozoospermia." Reprod Biomed Online **37**(4): 467-479.
López-Torres, A. S. and M. Chirinos (2017). "Modulation of Human Sperm Capacitation by Progesterone, Estradiol, and Luteinizing Hormone." Reprod Sci **24**(2): 193-201.
Loveland, K. L., B. Klein, D. Pueschl, S. Indumathy, M. Bergmann, B. E. Loveland, M. P. Hedger and H. C. Schuppe (2017). "Cytokines in Male Fertility and Reproductive Pathologies: Immunoregulation and Beyond." Front Endocrinol (Lausanne) **8**: 307.
Ludwig, H. and U. M. Spornitz (1991). "Microarchitecture of the human endometrium by scanning electron microscopy: menstrual desquamation and remodeling." Ann N Y Acad Sci **622**: 28-46.
Lundwall, Å., A. Bjartell, A. Y. Olsson and J. Malm (2002). "Semenogelin I and II, the predominant human seminal plasma proteins, are also expressed in non-genital tissues." Molecular Human Reproduction **8**(9): 805-810.
Lundwall, A., A. Giwercman, Y. Ruhayel, Y. Giwercman, H. Lilja, C. Halldén and J. Malm (2003). "A frequent allele codes for a truncated variant of semenogelin I, the major protein component of human semen coagulum." Mol Hum Reprod **9**(6): 345-350.
Luppi, S., M. Martinelli, E. Giacomini, E. Giolo, G. Zito, R. C. Garcia and G. Ricci (2015). "Comparative proteomic analysis of spermatozoa isolated by swim-up or density gradient centrifugation." Reproductive Biology and Endocrinology **13**(1).
Lyons, E. A., P. J. Taylor, X. H. Zheng, G. Ballard, C. S. Levi and J. V. Kredentser (1991). "Characterization of subendometrial myometrial contractions throughout the menstrual cycle in normal fertile women." Fertil Steril **55**(4): 771-774.
Lyons, R. A., E. Saridogan and O. Djahanbakhch (2006). "The reproductive significance of human Fallopian tube cilia." Human Reproduction Update **12**(4): 363-372.

Mack, P. D., A. Kapelnikov, Y. Heifetz and M. Bender (2006). "Mating-responsive genes in reproductive tissues of female Drosophila melanogaster." Proc Natl Acad Sci U S A **103**(27): 10358-10363.
Malm, J., J. Hellman, H. Magnusson, C. B. Laurell and H. Lilja (1996). "Isolation and characterization of the major gel proteins in human semen, semenogelin I and semenogelin II." Eur J Biochem **238**(1): 48-53.
Malvezzi, H., R. Sharma, A. Agarwal, A. M. Abuzenadah and M. Abu-Elmagd (2014). "Sperm quality after density gradient centrifugation with three commercially available media: a controlled trial." Reprod Biol Endocrinol **12**: 121.
Mandal, A. and A. K. Bhattacharyya (1995). "Sperm hyaluronidase activation by purified predominant and major basic human seminal coagulum proteins." Hum Reprod **10**(7): 1745-1750.
Manjunath, P., A. Bergeron, J. Lefebvre and J. Fan (2007). "Seminal plasma proteins: functions and interaction with protective agents during semen preservation." Soc Reprod Fertil Suppl **65**: 217-228.
Martyn, F., F. M. McAuliffe and M. Wingfield (2014). "The role of the cervix in fertility: is it time for a reappraisal?" Hum Reprod **29**(10): 2092-2098.
Master, V. A. and P. J. Turek (2001). "Ejaculatory physiology and dysfunction." Urol Clin North Am **28**(2): 363-375, x.
Mattsson, J. M., S. Ravela, C. Hekim, M. Jonsson, J. Malm, A. Närvänen, U.-H. Stenman and H. Koistinen (2014). "Proteolytic Activity of Prostate-Specific Antigen (PSA) towards Protein Substrates and Effect of Peptides Stimulating PSA Activity." PLoS ONE **9**(9): e107819.
Mattsson, J. M., S. Ravela, C. Hekim, M. Jonsson, J. Malm, A. Närvänen, U. H. Stenman and H. Koistinen (2014). "Proteolytic activity of prostate-specific antigen (PSA) towards protein substrates and effect of peptides stimulating PSA activity." PLoS One **9**(9): e107819.
Maturana, A. D., A. J. Casal, N. Demaurex, M. B. Vallotton, A. M. Capponi and M. F. Rossier (1999). "Angiotensin II negatively modulates L-type calcium channels through a pertussis toxin-sensitive G protein in adrenal glomerulosa cells." J Biol Chem **274**(28): 19943-19948.
Matzuk, M. M. and D. J. Lamb (2008). "The biology of infertility: research advances and clinical challenges." Nat Med **14**(11): 1197-1213.
Mayorga, L. S., C. N. Tomes and S. A. Belmonte (2007). "Acrosomal exocytosis, a special type of regulated secretion." IUBMB Life **59**(4-5): 286-292.
McCarthy, S., C. Tauber and J. Gore (1986). "Female pelvic anatomy: MR assessment of variations during the menstrual cycle and with use of oral contraceptives." Radiology **160**(1): 119-123.
McCluggage, W. G., V. P. Sumathi and P. Maxwell (2001). "CD10 is a sensitive and diagnostically useful immunohistochemical marker of normal endometrial stroma and of endometrial stromal neoplasms." Histopathology **39**(3): 273-278.
Meizel, S. and K. O. Turner (1983). "Serotonin or its agonist 5-methoxytryptamine can stimulate hamster sperm acrosome reactions in a more direct manner than catecholamines." J Exp Zool **226**(1): 171-174.
Mellor, H. and P. J. Parker (1998). "The extended protein kinase C superfamily." Biochem J **332 (Pt 2)**(Pt 2): 281-292.
Menkveld, R., F. S. Stander, T. J. v. Kotze, T. F. Kruger and J. A. v. Zyl (1990). "The evaluation of morphological characteristics of human spermatozoa according to stricter criteria." Human Reproduction **5**(5): 586-592.

Miller, D. J. (2018). "Review: The epic journey of sperm through the female reproductive tract." Animal **12**(s1): s110-s120.
Mitchell, L. A., G. N. De Iuliis and R. J. Aitken (2011). "The TUNEL assay consistently underestimates DNA damage in human spermatozoa and is influenced by DNA compaction and cell vitality: development of an improved methodology." International Journal of Andrology **34**(1): 2-13.
Mitra, A., R. T. Richardson and M. G. O'Rand (2010). "Analysis of Recombinant Human Semenogelin as an Inhibitor of Human Sperm Motility1." Biology of Reproduction **82**(3): 489-496.
Mol, B. W., R. Tjon-Kon-Fat, E. Kamphuis and M. van Wely (2018). "Unexplained infertility: Is it over-diagnosed and over-treated?" Best Pract Res Clin Obstet Gynaecol **53**: 20-29.
Moldenhauer, L. M., K. R. Diener, D. M. Thring, M. P. Brown, J. D. Hayball and S. A. Robertson (2009). "Cross-presentation of male seminal fluid antigens elicits T cell activation to initiate the female immune response to pregnancy." J Immunol **182**(12): 8080-8093.
Moradi, S. V., W. M. Hussein, P. Varamini, P. Simerska and I. Toth (2016). "Glycosylation, an effective synthetic strategy to improve the bioavailability of therapeutic peptides." Chem Sci **7**(4): 2492-2500.
Morales, P., V. Palma, A. M. Salgado and M. Villalon (1996). "Sperm interaction with human oviductal cells in vitro." Hum Reprod **11**(7): 1504-1509.
Mortimer, D. (1994). Practical laboratory andrology, Oxford University Press on Demand.
Mortimer, D. (2018). "The functional anatomy of the human spermatozoon: relating ultrastructure and function." Molecular Human Reproduction **24**(12): 567-592.
Mortimer, D. and R. Menkveld (2001). "Sperm morphology assessment--historical perspectives and current opinions." J Androl **22**(2): 192-205.
Mortimer, S. T. and M. A. Swan (1995). "Variable kinematics of capacitating human spermatozoa." Hum Reprod **10**(12): 3178-3182.
Mortimer, S. T., M. A. Swan and D. Mortimer (1998). "Effect of seminal plasma on capacitation and hyperactivation in human spermatozoa." Hum Reprod **13**(8): 2139-2146.
Müller, M. M. (2018). "Post-Translational Modifications of Protein Backbones: Unique Functions, Mechanisms, and Challenges." Biochemistry **57**(2): 177-185.
Nachtigall, R. D. (2006). "International disparities in access to infertility services." Fertility and sterility **85**(4): 871-875.
Nakamura, H., M. Matsuda, K. Furuke, Y. Kitaoka, S. Iwata, K. Toda, T. Inamoto, Y. Yamaoka, K. Ozawa and J. Yodoi (1994). "Adult T cell leukemia-derived factor/human thioredoxin protects endothelial F-2 cell injury caused by activated neutrophils or hydrogen peroxide." Immunol Lett **42**(1-2): 75-80.
Nandi, A. and R. Homburg (2016). "Unexplained subfertility: diagnosis and management." The Obstetrician & Gynaecologist **18**(2): 107-115.
Neto, F. T., P. V. Bach, B. B. Najari, P. S. Li and M. Goldstein (2016). "Spermatogenesis in humans and its affecting factors." Semin Cell Dev Biol **59**: 10-26.
Ney, P. G. (1986). "The intravaginal absorption of male generated hormones and their possible effect on female behaviour." Med Hypotheses **20**(2): 221-231.
NHS. (2022, 18 February 2020). "Infertility." from https://www.nhs.uk/conditions/infertility/.

Nigg, E. A. and J. W. Raff (2009). "Centrioles, centrosomes, and cilia in health and disease." Cell **139**(4): 663-678.
Nixon, B., G. N. De Iuliis, M. D. Dun, W. Zhou, N. A. Trigg and A. L. Eamens (2019). "Profiling of epididymal small non-protein-coding RNAs." Andrology **7**(5): 669-680.
Nomikos, M., J. R. Sanders, J. Kashir, R. Sanusi, L. Buntwal, D. Love, P. Ashley, D. Sanders, P. Knaggs and A. Bunkheila (2015). "Functional disparity between human PAWP and PLCζ in the generation of Ca2+ oscillations for oocyte activation." Mhr: Basic science of reproductive medicine **21**(9): 702-710.
Nott, J. P., E. A. Bonney, J. D. Pickering and N. A. Simpson (2016). "The structure and function of the cervix during pregnancy." Translational Research in Anatomy **2**: 1-7.
Noyes, R. W., A. T. Hertig and J. Rock (1975). "Dating the endometrial biopsy." Am J Obstet Gynecol **122**(2): 262-263.
Ó'Fágáin, C., P. M. Cummins and B. F. O'Connor (2017). "Gel-Filtration Chromatography." Methods Mol Biol **1485**: 15-25.
O'Flaherty, C. (2019). "Orchestrating the antioxidant defenses in the epididymis." Andrology **7**(5): 662-668.
Ochoa-Bernal, M. A. and A. T. Fazleabas (2020). "Physiologic Events of Embryo Implantation and Decidualization in Human and Non-Human Primates." Int J Mol Sci **21**(6).
Okamura, N., Y. Tajima, H. Ishikawa, S. Yoshii, K. Koiso and Y. Sugita (1986). "Lowered levels of bicarbonate in seminal plasma cause the poor sperm motility in human infertile patients**Supported in part by Science Research grants 59770174 and 60770193 from the Ministry of Education of Japan." Fertility and Sterility **45**(2): 265-272.
Oko, R., R. Aul, A. Wu and P. Sutovsky (2001). "The sperm head cytoskeleton." Andrology in the 21st Century. Medimond Publishing Company, Englewood: 37-51.
Oliva, R., S. De Mateo and J. M. Estanyol (2009). "Sperm cell proteomics." PROTEOMICS **9**(4): 1004-1017.
Olson, S., L. Fauci and S. Suarez (2011). "Mathematical modeling of calcium signaling during sperm hyperactivation." MHR: Basic science of reproductive medicine **17**(8): 500-510.
Ombelet, W., I. Cooke, S. Dyer, G. Serour and P. Devroey (2008). "Infertility and the provision of infertility medical services in developing countries." Human reproduction update **14**(6): 605-621.
Ostermeier, G. C., C. Cardona, M. A. Moody, A. J. Simpson, R. Mendoza, E. Seaman and A. J. Travis (2018). "Timing of sperm capacitation varies reproducibly among men." Mol Reprod Dev **85**(5): 387-396.
Otwinowski, Z. and W. i. Minor (1997). Methods in Enzymology, Vol. 276, Macromolecular Crystallography, Part A, edited by CW Carter Jr & RM Sweet, New York: Academic Press.
Owen, D. H. and D. F. Katz (2005). "A review of the physical and chemical properties of human semen and the formulation of a semen simulant." J Androl **26**(4): 459-469.
Pacey, A. A., C. J. Hill, I. W. Scudamore, M. A. Warren, C. L. Barratt and I. D. Cooke (1995). "The interaction in vitro of human spermatozoa with epithelial cells from the human uterine (fallopian) tube." Hum Reprod **10**(2): 360-366.
Panner Selvam, M. K., A. Agarwal, P. N. Pushparaj, S. Baskaran and H. Bendou (2019). "Sperm Proteome Analysis and Identification of Fertility-Associated Biomarkers in Unexplained Male Infertility." Genes (Basel) **10**(7).

Parekh, A. B. (2011). "Decoding cytosolic Ca2+ oscillations." Trends in Biochemical Sciences **36**(2): 78-87.
Parekh, A. B. and J. W. Putney, Jr. (2005). "Store-operated calcium channels." Physiol Rev **85**(2): 757-810.
Parrington, J., F. A. Lai and K. Swann (2000). "The soluble mammalian sperm factor protein that triggers Ca2+ oscillations in eggs: evidence for expression of mRNA(s) coding for sperm factor protein(s) in spermatogenic cells." Biol Cell **92**(3-4): 267-275.
Patek, E., L. Nilsson and E. Johannisson (1972). "Scanning electron microscopic study of the human fallopian tube. Report I. The proliferative and secretory stages." Fertil Steril **23**(7): 549-565.
Patek, E., L. Nilsson and E. Johannisson (1972). "Scanning electron microscopic study of the human fallopian tube. Report II. Fetal life, reproductive life, and postmenopause." Fertil Steril **23**(10): 719-733.
Pauerstein, C. J. and C. A. Eddy (1979). "The role of the oviduct in reproduction; our knowledge and our ignorance." Reproduction **55**(1): 223-229.
Pérez-Cerezales, S., P. Ramos-Ibeas, O. S. Acuña, M. Avilés, P. Coy, D. Rizos and A. Gutiérrez-Adán (2018). "The oviduct: from sperm selection to the epigenetic landscape of the embryo." Biol Reprod **98**(3): 262-276.
Periasamy, M. and A. Kalyanasundaram (2007). "SERCA pump isoforms: their role in calcium transport and disease." Muscle Nerve **35**(4): 430-442.
Perrotta, M. and J. Hamper (2021). "The crafting of hope: Contextualising add-ons in the treatment trajectories of IVF patients." Soc Sci Med **287**: 114317.
Petersen, O. H. (1992). "Stimulus-secretion coupling: cytoplasmic calcium signals and the control of ion channels in exocrine acinar cells." J Physiol **448**: 1-51.
Petersen, O. H. and A. Verkhratsky (2016). "Calcium and ATP control multiple vital functions." Philos Trans R Soc Lond B Biol Sci **371**(1700).
Petrounkina, A. M., R. A. Harrison, R. Petzoldt, K. F. Weitze and E. Töpfer-Petersen (2000). "Cyclical changes in sperm volume during in vitro incubation under capacitating conditions: a novel boar semen characteristic." J Reprod Fertil **118**(2): 283-293.
Piomboni, P., R. Focarelli, A. Stendardi, A. Ferramosca and V. Zara (2012). "The role of mitochondria in energy production for human sperm motility." International journal of andrology **35**(2): 109-124.
Plant, T. M. and A. J. Zeleznik (2014). Knobil and Neill's physiology of reproduction, Chapter 22- The Epididymis, Academic Press.
Pozzan, T., R. Rizzuto, P. Volpe and J. Meldolesi (1994). "Molecular and cellular physiology of intracellular calcium stores." Physiol Rev **74**(3): 595-636.
Publicover, S., C. V. Harper and C. Barratt (2007). "[Ca 2+] i signalling in sperm—making the most of what you've got." Nature cell biology **9**(3): 235-242.
Pudney, J., A. J. Quayle and D. J. Anderson (2005). "Immunological microenvironments in the human vagina and cervix: mediators of cellular immunity are concentrated in the cervical transformation zone." Biol Reprod **73**(6): 1253-1263.
Puppo, V. and G. Puppo (2016). "Comprehensive review of the anatomy and physiology of male ejaculation: Premature ejaculation is not a disease." Clin Anat **29**(1): 111-119.
Puri, B. K. (2020). "Calcium Signaling and Gene Expression." Adv Exp Med Biol **1131**: 537-545.
Quaas, A. and A. Dokras (2008). "Diagnosis and treatment of unexplained infertility." Rev Obstet Gynecol **1**(2): 69-76.

Quartararo, A. J., Z. P. Gates, B. A. Somsen, N. Hartrampf, X. Ye, A. Shimada, Y. Kajihara, C. Ottmann and B. L. Pentelute (2020). "Ultra-large chemical libraries for the discovery of high-affinity peptide binders." Nature Communications **11**(1): 3183.
Quill, T. A., S. A. Sugden, K. L. Rossi, L. K. Doolittle, R. E. Hammer and D. L. Garbers (2003). "Hyperactivated sperm motility driven by CatSper2 is required for fertilization." Proc Natl Acad Sci U S A **100**(25): 14869-14874.
Rajeev, S. K. and K. V. R. Reddy (2004). "Sperm membrane protein profiles of fertile and infertile men: identification and characterization of fertility-associated sperm antigen." Human Reproduction **19**(2): 234-242.
Rajender, S., P. Rahul and A. A. Mahdi (2010). "Mitochondria, spermatogenesis and male infertility." Mitochondrion **10**(5): 419-428.
Ramadan, J. W., S. R. Steiner, C. M. O'Neill and C. S. Nunemaker (2011). "The central role of calcium in the effects of cytokines on beta-cell function: implications for type 1 and type 2 diabetes." Cell Calcium **50**(6): 481-490.
Ramathal, C. Y., I. C. Bagchi, R. N. Taylor and M. K. Bagchi (2010). "Endometrial decidualization: of mice and men." Semin Reprod Med **28**(1): 17-26.
Ramazi, S. and J. Zahiri (2021). "Posttranslational modifications in proteins: resources, tools and prediction methods." Database (Oxford) **2021**.
Reed, B. G. and B. R. Carr (2000). The Normal Menstrual Cycle and the Control of Ovulation. Endotext. K. R. Feingold, B. Anawalt, A. Boyce et al. South Dartmouth (MA), MDText.com, Inc.

Copyright © 2000-2022, MDText.com, Inc.
Ren, D. and J. Xia (2010). "Calcium signaling through CatSper channels in mammalian fertilization." Physiology (Bethesda) **25**(3): 165-175.
Reshi, Q. U. A., J. Viil, J. Ord, F. Lättekivi, K. Godakumara, M. M. Hasan, M. Nõmm, K. Jääger, A. Velthut-Meikas, Ü. Jaakma, A. Salumets and A. Fazeli (2020). "Spermatozoa induce transcriptomic alterations in bovine oviductal epithelial cells prior to initial contact." J Cell Commun Signal **14**(4): 439-451.
Robert, M. and C. Gagnon (1994). "Sperm motility inhibitor from human seminal plasma: presence of a precursor molecule in seminal vesicle fluid and its molecular processing after ejaculation." Int J Androl **17**(5): 232-240.
Robert, M. and C. Gagnon (1996). "Purification and characterization of the active precursor of a human sperm motility inhibitor secreted by the seminal vesicles: identity with semenogelin." Biol Reprod **55**(4): 813-821.
Robert, M., B. F. Gibbs, E. Jacobson and C. Gagnon (1997). "Characterization of prostate-specific antigen proteolytic activity on its major physiological substrate, the sperm motility inhibitor precursor/semenogelin I." Biochemistry **36**(13): 3811-3819.
Robertson, S. A. (2005). "Seminal plasma and male factor signalling in the female reproductive tract." Cell Tissue Res **322**(1): 43-52.
Robertson, S. A. (2007). "Seminal fluid signaling in the female reproductive tract: lessons from rodents and pigs." J Anim Sci **85**(13 Suppl): E36-44.
Robertson, S. A. and D. J. Sharkey (2016). "Seminal fluid and fertility in women." Fertil Steril **106**(3): 511-519.
Robinson, L., I. D. Gallos, S. J. Conner, M. Rajkhowa, D. Miller, S. Lewis, J. Kirkman-Brown and A. Coomarasamy (2012). "The effect of sperm DNA fragmentation on miscarriage rates: a systematic review and meta-analysis." Hum Reprod **27**(10): 2908-2917.

Robker, R. L., J. D. Hennebold and D. L. Russell (2018). "Coordination of Ovulation and Oocyte Maturation: A Good Egg at the Right Time." Endocrinology **159**(9): 3209-3218.
Roderick, H. L., M. J. Berridge and M. D. Bootman (2003). "Calcium-induced calcium release." Current Biology **13**(11): R425.
Rodríguez-Martínez, H., U. Kvist, J. Ernerudh, L. Sanz and J. J. Calvete (2011). "Seminal Plasma Proteins: What Role Do They Play?" American Journal of Reproductive Immunology **66**: 11-22.
Rodríguez-Martínez, H., U. Kvist, J. Ernerudh, L. Sanz and J. J. Calvete (2011). "Seminal plasma proteins: what role do they play?" Am J Reprod Immunol **66 Suppl 1**: 11-22.
Rogers, T. B., G. Inesi, R. Wade and W. J. Lederer (1995). "Use of thapsigargin to study Ca2+ homeostasis in cardiac cells." Bioscience Reports **15**(5): 341-349.
Ronquist, G. (2012). "Prostasomes are mediators of intercellular communication: from basic research to clinical implications." J Intern Med **271**(4): 400-413.
Roy, A., A. Kucukural and Y. Zhang (2010). "I-TASSER: a unified platform for automated protein structure and function prediction." Nature Protocols **5**(4): 725-738.
Russell, J. T. (2011). "Imaging calcium signals in vivo: a powerful tool in physiology and pharmacology." Br J Pharmacol **163**(8): 1605-1625.
Saaranen, M., U. Suistomaa, M. Kantola, S. Saarikoski and T. Vanha-Perttula (1987). "Lead, magnesium, selenium and zinc in human seminal fluid: comparison with semen parameters and fertility." Hum Reprod **2**(6): 475-479.
Sabała, P., E. Amler and J. Barańska (1997). "Intracellular Ca2+ signals induced by ATP and thapsigargin in glioma C6 cells. Calcium pools sensitive to inositol 1,4,5-trisphosphate and thapsigargin." Neurochem Int **31**(1): 55-64.
Saint-Dizier, M., J. Schoen, S. Chen, C. Banliat and P. Mermillod (2019). "Composing the Early Embryonic Microenvironment: Physiology and Regulation of Oviductal Secretions." Int J Mol Sci **21**(1).
Salicioni, A. M., M. D. Platt, E. V. Wertheimer, E. Arcelay, A. Allaire, J. Sosnik and P. E. Visconti (2007). "Signalling pathways involved in sperm capacitation." Soc Reprod Fertil Suppl **65**: 245-259.
Salter, M. W. and J. L. Hicks (1995). "ATP causes release of intracellular Ca2+ via the phospholipase C beta/IP3 pathway in astrocytes from the dorsal spinal cord." J Neurosci **15**(4): 2961-2971.
Salustri, A., M. Yanagishita, C. B. Underhill, T. C. Laurent and V. C. Hascall (1992). "Localization and synthesis of hyaluronic acid in the cumulus cells and mural granulosa cells of the preovulatory follicle." Dev Biol **151**(2): 541-551.
Samanta, L., R. Parida, T. R. Dias and A. Agarwal (2018). "The enigmatic seminal plasma: a proteomics insight from ejaculation to fertilization." Reproductive Biology and Endocrinology **16**(1): 41.
Sánchez-Cárdenas, C., F. Montoya, F. A. Navarrete, A. Hernández-Cruz, G. Corkidi, P. E. Visconti and A. Darszon (2018). "Intracellular Ca2+ threshold reversibly switches flagellar beat off and on†." Biology of Reproduction **99**(5): 1010-1021.
Sanders, D., J. Pelloux, C. Brownlee and J. F. Harper (2002). "Calcium at the crossroads of signaling." Plant Cell **14 Suppl**(Suppl): S401-417.
Santiago-Moreno, J., M. C. Esteso, C. Castaño, A. Toledano-Díaz, J. A. Delgadillo and A. López-Sebastián (2017). "Seminal plasma removal by density-gradient centrifugation is superior for goat sperm preservation compared with classical sperm washing." Animal Reproduction Science **181**: 141-150.

Saokham, P., S. C. A, A. Ryzhakov and T. Loftsson (2016). "The self-assemble of natural cyclodextrins in aqueous solutions: Application of miniature permeation studies for critical aggregation concentration (cac) determinations." Int J Pharm **505**(1-2): 187-193.
Saravelos, S. H. and T.-C. Li (2012). "Unexplained recurrent miscarriage: how can we explain it?" Human Reproduction **27**(7): 1882-1886.
Sathananthan, A., I. Kola, J. Osborne, A. Trounson, S. Ng, A. Bongso and S. Ratnam (1991). "Centrioles in the beginning of human development." Proceedings of the National Academy of Sciences **88**(11): 4806-4810.
Scharff, O. and B. Foder (1996). "Depletion of calcium stores by thapsigargin induces membrane depolarization by cation entry in human neutrophils." Cell Calcium **20**(1): 31-41.
Schatten, H. and Q. Y. Sun (2011). "New insights into the role of centrosomes in mammalian fertilization and implications for ART." Reproduction **142**(6): 793-801.
Schjenken, J. E., D. J. Glynn, D. J. Sharkey and S. A. Robertson (2015). "TLR4 Signaling Is a Major Mediator of the Female Tract Response to Seminal Fluid in Mice." Biol Reprod **93**(3): 68.
Schjenken, J. E., D. J. Glynn, D. J. Sharkey and S. A. Robertson (2015). "TLR4 Signaling Is a Major Mediator of the Female Tract Response to Seminal Fluid in Mice1." Biology of Reproduction **93**(3).
Schjenken, J. E. and S. A. Robertson (2014). "Seminal fluid and immune adaptation for pregnancy--comparative biology in mammalian species." Reprod Domest Anim **49 Suppl 3**: 27-36.
Schjenken, J. E. and S. A. Robertson (2020). "The Female Response to Seminal Fluid." Physiol Rev **100**(3): 1077-1117.
Schjenken, J. E., B. Zhang, H. Y. Chan, D. J. Sharkey, T. Fullston and S. A. Robertson (2016). "miRNA Regulation of Immune Tolerance in Early Pregnancy." Am J Reprod Immunol **75**(3): 272-280.
Schlossmann, J., A. Ammendola, K. Ashman, X. Zong, A. Huber, G. Neubauer, G. X. Wang, H. D. Allescher, M. Korth, M. Wilm, F. Hofmann and P. Ruth (2000). "Regulation of intracellular calcium by a signalling complex of IRAG, IP3 receptor and cGMP kinase Ibeta." Nature **404**(6774): 197-201.
Schmidhauser, M., S. E. Ulbrich and J. Schoen (2022). "Luminal and Glandular Epithelial Cells from the Porcine Endometrium maintain Cell Type-Specific Marker Gene Expression in Air–Liquid Interface Culture." Stem Cell Reviews and Reports **18**(8): 2928-2938.
Scott, I., A. Ramirez-Reveco and J. Parodi (2016). "The restraint of bovine sperm cell motility increases survival: role of extracellular calcium in the phenomena." J Vet Sci Technol **7**(359): 2.
Shalgi, R., T. T. Smith and R. Yanagimachi (1992). "A quantitative comparison of the passage of capacitated and uncapacitated hamster spermatozoa through the uterotubal junction." Biol Reprod **46**(3): 419-424.
Sharkey, D. J., J. E. Schjenken, D. G. Mottershead and S. A. Robertson (2015). "Seminal fluid factors regulate activin A and follistatin synthesis in female cervical epithelial cells." Mol Cell Endocrinol **417**: 178-190.
Sharlip, I. D., J. P. Jarow, A. M. Belker, L. I. Lipshultz, M. Sigman, A. J. Thomas, P. N. Schlegel, S. S. Howards, A. Nehra and M. D. Damewood (2002). "Best practice policies for male infertility." Fertility and sterility **77**(5): 873-882.

Shen, F., Y. C. Huang, S. Tang, Y. X. Chen and L. Liu (2011). "Chemical synthesis of integral membrane proteins: methods and applications." Israel Journal of Chemistry **51**(8-9): 940-952.
Shoback, D., T. H. Chen, S. Pratt and B. Lattyak (1995). "Thapsigargin stimulates intracellular calcium mobilization and inhibits parathyroid hormone release." J Bone Miner Res **10**(5): 743-750.
Shuttleworth, T. J. (1997). "Intracellular Ca2+ signalling in secretory cells." J Exp Biol **200**(Pt 2): 303-314.
Siepen, J. A., E. J. Keevil, D. Knight and S. J. Hubbard (2007). "Prediction of missed cleavage sites in tryptic peptides aids protein identification in proteomics." J Proteome Res **6**(1): 399-408.
Simintiras, C. A., T. Fröhlich, T. Sathyapalan, G. J. Arnold, S. E. Ulbrich, H. J. Leese and R. G. Sturmey (2016). "Modelling oviduct fluid formation in vitro." Reproduction.
Simpson, D. M. and R. J. Beynon (2010). "Acetone Precipitation of Proteins and the Modification of Peptides." Journal of Proteome Research **9**(1): 444-450.
Simpson, R. J. (2006). "Fragmentation of protein using trypsin." CSH Protoc **2006**(5).
Singer, A. and J. A. Jordan (2006). "The functional anatomy of the cervix, the cervical epithelium and the stroma." The Cervix: 13-37.
Slivkova, J., M. Popelkova, P. Massanyi, S. Toporcerova, R. Stawarz, G. Formicki, N. Lukac, A. Putała and M. Guzik (2009). "Concentration of trace elements in human semen and relation to spermatozoa quality." Journal of Environmental Science and Health, Part A **44**(4): 370-375.
Smedler, E. and P. Uhlén (2014). "Frequency decoding of calcium oscillations." Biochimica et Biophysica Acta (BBA) - General Subjects **1840**(3): 964-969.
Sobrero, A. J. and J. Macleod (1962). "The immediate postcoital test." Fertil Steril **13**: 184-189.
Song, M. Y. and J. X. Yuan (2010). "Introduction to TRP channels: structure, function, and regulation." Adv Exp Med Biol **661**: 99-108.
Song, Z.-H., Z.-Y. Li, D.-D. Li, W.-N. Fang, H.-Y. Liu, D.-D. Yang, C.-Y. Meng, Y. Yang and J.-P. Peng (2016). "Seminal plasma induces inflammation in the uterus through the γδ T/IL-17 pathway." Scientific Reports **6**(1): 25118.
Southan, C. (2004). "Has the yo-yo stopped? An assessment of human protein-coding gene number." Proteomics **4**(6): 1712-1726.
Spehr, M., G. Gisselmann, A. Poplawski, J. A. Riffell, C. H. Wetzel, R. K. Zimmer and H. Hatt (2003). "Identification of a testicular odorant receptor mediating human sperm chemotaxis." Science **299**(5615): 2054-2058.
Speroff, L. and M. A. Fritz (2005). "The ovary-embryology and development." Clinical gynecologic endocrinology and infertility. Lippincott Williams & Wilkins, Philadelphia: 97-111.
Stauss, C. R., T. J. Votta and S. S. Suarez (1995). "Sperm motility hyperactivation facilitates penetration of the hamster zona pellucida." Biol Reprod **53**(6): 1280-1285.
Stein, A., A. Heinen-Kreuzig, A. Kiesewetter and S. Schwarm (2016). "Size-exclusion chromatography for preparative purification of biomolecules." **29**: 30-52.
Stewart, L. and N. A. Turner (2021). "Channelling the Force to Reprogram the Matrix: Mechanosensitive Ion Channels in Cardiac Fibroblasts." Cells **10**(5): 990.
Strünker, T., N. Goodwin, C. Brenker, N. D. Kashikar, I. Weyand, R. Seifert and U. B. Kaupp (2011). "The CatSper channel mediates progesterone-induced Ca2+ influx in human sperm." Nature **471**(7338): 382-386.
Suarez, S. S. (2008). "Control of hyperactivation in sperm." Hum Reprod Update **14**(6): 647-657.

Suarez, S. S. (2016). "Mammalian sperm interactions with the female reproductive tract." Cell Tissue Res **363**(1): 185-194.
Suarez, S. S. and H. C. Ho (2003). "Hyperactivation of mammalian sperm." Cell Mol Biol (Noisy-le-grand) **49**(3): 351-356.
Suarez, S. S. and A. A. Pacey (2005). "Sperm transport in the female reproductive tract." Human Reproduction Update **12**(1): 23-37.
Suarez, S. S. and A. A. Pacey (2006). "Sperm transport in the female reproductive tract." Hum Reprod Update **12**(1): 23-37.
Sumigama, S., S. Mansell, M. Miller, P. V. Lishko, G. N. Cherr, S. A. Meyers and T. Tollner (2015). "Progesterone Accelerates the Completion of Sperm Capacitation and Activates CatSper Channel in Spermatozoa from the Rhesus Macaque." Biol Reprod **93**(6): 130.
Sun, Y. and P. Sethu (2018). "Low-stress Microfluidic Density-gradient Centrifugation for Blood Cell Sorting." Biomed Microdevices **20**(3): 77.
Swann, K. (2018). "The role of Ca(2+) in oocyte activation during In Vitro fertilization: Insights into potential therapies for rescuing failed fertilization." Biochim Biophys Acta Mol Cell Res **1865**(11 Pt B): 1830-1837.
Swann, K., S. Windsor, K. Campbell, K. Elgmati, M. Nomikos, M. Zernicka-Goetz, N. Amso, F. A. Lai, A. Thomas and C. Graham (2012). "Phospholipase C-ζ-induced Ca2+ oscillations cause coincident cytoplasmic movements in human oocytes that failed to fertilize after intracytoplasmic sperm injection." Fertil Steril **97**(3): 742-747.
Szalai, G., R. Krishnamurthy and G. Hajnóczky (1999). "Apoptosis driven by IP(3)-linked mitochondrial calcium signals." Embo j **18**(22): 6349-6361.
Szczykutowicz, J., A. Kałuża, M. Kaźmierowska-Niemczuk and M. Ferens-Sieczkowska (2019). "The Potential Role of Seminal Plasma in the Fertilization Outcomes." Biomed Res Int **2019**: 5397804.
Taiwo, B. G., R. L. Frettsome-Hook, A. E. Taylor, J. N. Correia, L. Lefievre, S. J. Publicover, S. J. Conner and J. C. Kirkman-Brown (2021). "Complex combined steroid mix of the female tract modulates human sperm." Reprod Biol **21**(4): 100561.
Tajima, Y., N. Okamura and Y. Sugita (1987). "The activating effects of bicarbonate on sperm motility and respiration at ejaculation." Biochim Biophys Acta **924**(3): 519-529.
Tateno, H., D. Krapf, T. Hino, C. Sánchez-Cárdenas, A. Darszon, R. Yanagimachi and P. E. Visconti (2013). "Ca²⁺ ionophore A23187 can make mouse spermatozoa capable of fertilizing in vitro without activation of cAMP-dependent phosphorylation pathways." Proceedings of the National Academy of Sciences **110**(46): 18543-18548.
Tauseef, M., N. Knezevic, K. R. Chava, M. Smith, S. Sukriti, N. Gianaris, A. G. Obukhov, S. M. Vogel, D. E. Schraufnagel, A. Dietrich, L. Birnbaumer, A. B. Malik and D. Mehta (2012). "TLR4 activation of TRPC6-dependent calcium signaling mediates endotoxin-induced lung vascular permeability and inflammation." J Exp Med **209**(11): 1953-1968.
Taylor, C. W. and P. Thorn (2001). "Calcium signalling: IP3 rises again… and again." Current Biology **11**(9): R352-R355.
Taylor, C. W. and S. C. Tovey (2010). "IP(3) receptors: toward understanding their activation." Cold Spring Harb Perspect Biol **2**(12): a004010.
Tecle, E., H. S. Reynoso, R. Wang and P. Gagneux (2019). "The female reproductive tract contains multiple innate sialic acid-binding immunoglobulin-like lectins (Siglecs) that facilitate sperm survival." J Biol Chem **294**(31): 11910-11919.

Teilmann, S. C., A. G. Byskov, P. A. Pedersen, D. N. Wheatley, G. J. Pazour and S. T. Christensen (2005). "Localization of transient receptor potential ion channels in primary and motile cilia of the female murine reproductive organs." Mol Reprod Dev **71**(4): 444-452.
Thimon, V., G. Frenette, F. Saez, M. Thabet and R. Sullivan (2008). "Protein composition of human epididymosomes collected during surgical vasectomy reversal: a proteomic and genomic approach." Hum Reprod **23**(8): 1698-1707.
Thomas, P. G., G. G. Ignotz, B. A. Ball, S. P. Brinsko and W. B. Currie (1995). "Effect of coculture with stallion spermatozoa on de novo protein synthesis and secretion by equine oviduct epithelial cells." Am J Vet Res **56**(12): 1657-1662.
Tompa, P., R. Töth-Boconádi and P. Friedrich (2001). "Frequency decoding of fast calcium oscillations by calpain." Cell Calcium **29**(3): 161-170.
Trebak, M. and J.-P. Kinet (2019). "Calcium signalling in T cells." Nature Reviews Immunology **19**(3): 154-169.
Trigg, N. A., A. L. Eamens and B. Nixon (2019). "The contribution of epididymosomes to the sperm small RNA profile." Reproduction **157**(6): R209-r223.
Udeshi, N. D., P. D. Compton, J. Shabanowitz, D. F. Hunt and K. L. Rose (2008). "Methods for analyzing peptides and proteins on a chromatographic timescale by electron-transfer dissociation mass spectrometry." Nat Protoc **3**(11): 1709-1717.
Urh, M., D. Simpson and K. Zhao (2009). "Affinity chromatography: general methods." Methods Enzymol **463**: 417-438.
Usoskin, D., M. Zilberter, S. Linnarsson, J. Hjerling Leffler, P. Uhlén, T. Harkany and P. Ernfors (2010). "En masse in vitro functional profiling of the axonal mechanosensitivity of sensory neurons." Proceedings of the National Academy of Sciences of the United States of America **107**: 16336-16341.
Utleg, A. G., E. C. Yi, T. Xie, P. Shannon, J. T. White, D. R. Goodlett, L. Hood and B. Lin (2003). "Proteomic analysis of human prostasomes." Prostate **56**(2): 150-161.
van den Berg-Bakker, C. A., A. Hagemeijer, E. M. Franken-Postma, V. T. Smit, P. J. Kuppen, H. H. van Ravenswaay Claasen, C. J. Cornelisse and P. I. Schrier (1993). "Establishment and characterization of 7 ovarian carcinoma cell lines and one granulosa tumor cell line: growth features and cytogenetics." Int J Cancer **53**(4): 613-620.
van Haasteren, G., S. Li, M. Muda, S. Susini and W. Schlegel (1999). "Calcium signalling and gene expression." J Recept Signal Transduct Res **19**(1-4): 481-492.
Vanoverberghe, K., P. Mariot, F. Vanden Abeele, P. Delcourt, J. B. Parys and N. Prevarskaya (2003). "Mechanisms of ATP-induced calcium signaling and growth arrest in human prostate cancer cells." Cell Calcium **34**(1): 75-85.
Ventouri, I. K., D. B. A. Malheiro, R. L. C. Voeten, S. Kok, M. Honing, G. W. Somsen and R. Haselberg (2020). "Probing Protein Denaturation during Size-Exclusion Chromatography Using Native Mass Spectrometry." Analytical Chemistry **92**(6): 4292-4300.
Vergauwen, G., B. Dhondt, J. Van Deun, E. De Smedt, G. Berx, E. Timmerman, K. Gevaert, I. Miinalainen, V. Cocquyt, G. Braems, R. Van den Broecke, H. Denys, O. De Wever and A. Hendrix (2017). "Confounding factors of ultrafiltration and protein analysis in extracellular vesicle research." Sci Rep **7**(1): 2704.
Visconti, P. E., J. L. Bailey, G. D. Moore, D. Pan, P. Olds-Clarke and G. S. Kopf (1995). "Capacitation of mouse spermatozoa. I. Correlation between the capacitation state and protein tyrosine phosphorylation." Development **121**(4): 1129-1137.
Vishwanath, S., S. Banerjee, A. K. Jamithireddy, N. Srinivasan, B. Gopal and J. Chatterjee (2017). "Design, Synthesis, and Experimental Validation of Peptide

Ligands Targeting Mycobacterium tuberculosis σ Factors." Biochemistry **56**(16): 2209-2218.
Voedisch, B. and H. Thie (2010). "Antibody Engineering."
Vollman, R. F. (1977). "The menstrual cycle." Major Probl Obstet Gynecol **7**: 1-193.
Volpes, A., F. Sammartano, S. Rizzari, S. Gullo, A. Marino and A. Allegra (2016). "The pellet swim-up is the best technique for sperm preparation during in vitro fertilization procedures." J Assist Reprod Genet **33**(6): 765-770.
Walsh, M. P. (1994). "Calmodulin and the regulation of smooth muscle contraction." Mol Cell Biochem **135**(1): 21-41.
Wang, F., W. Yang, S. Ouyang and S. Yuan (2020). "The Vehicle Determines the Destination: The Significance of Seminal Plasma Factors for Male Fertility." Int J Mol Sci **21**(22).
Wang, G., Y. Guo, T. Zhou, X. Shi, J. Yu, Y. Yang, Y. Wu, J. Wang, M. Liu, X. Chen, W. Tu, Y. Zeng, M. Jiang, S. Li, P. Zhang, Q. Zhou, B. Zheng, C. Yu, Z. Zhou, X. Guo and J. Sha (2013). "In-depth proteomic analysis of the human sperm reveals complex protein compositions." J Proteomics **79**: 114-122.
Wang, Z., E. E. Widgren, P. Sivashanmugam, M. G. O'Rand and R. T. Richardson (2005). "Association of Eppin with Semenogelin on Human Spermatozoa1." Biology of Reproduction **72**(5): 1064-1070.
West, R., A. Coomarasamy, L. Frew, R. Hutton, J. Kirkman-Brown, M. Lawlor, S. Lewis, R. Partanen, A. Payne-Dwyer, C. Román-Montañana, F. Torabi, S. Tsagdi and D. Miller (2022). "Sperm selection with hyaluronic acid improved live birth outcomes among older couples and was connected to sperm DNA quality, potentially affecting all treatment outcomes." Human Reproduction **37**(6): 1106-1125.
White, B. A., D. J. Creedon, K. E. Nelson and B. A. Wilson (2011). "The vaginal microbiome in health and disease." Trends Endocrinol Metab **22**(10): 389-393.
Williams, M., C. J. Hill, I. Scudamore, B. Dunphy, I. D. Cooke and C. L. Barratt (1993). "Sperm numbers and distribution within the human fallopian tube around ovulation." Hum Reprod **8**(12): 2019-2026.
Wiśniewski, J. R. (2018). "Filter-Aided Sample Preparation for Proteome Analysis." Methods Mol Biol **1841**: 3-10.
Wolkowicz, M. J., L. Digilio, K. Klotz, J. Shetty, C. J. Flickinger and J. C. Herr (2008). "Equatorial segment protein (ESP) is a human alloantigen involved in sperm-egg binding and fusion." J Androl **29**(3): 272-282.
Wu, A. T., P. Sutovsky, W. Xu, A. C. van der Spoel, F. M. Platt and R. Oko (2007). "The postacrosomal assembly of sperm head protein, PAWP, is independent of acrosome formation and dependent on microtubular manchette transport." Dev Biol **312**(2): 471-483.
Wyrobek, A., M. Meistrich, R. Furrer and W. Bruce (1976). "Physical characteristics of mouse sperm nuclei." Biophysical journal **16**(7): 811-825.
Yagi, H., S. Yanaka and K. Kato (2018). "Structure and Dynamics of Immunoglobulin G Glycoproteins." Adv Exp Med Biol **1104**: 219-235.
Yanagimachi, R. (2011). "Mammalian Sperm Acrosome Reaction: Where Does It Begin Before Fertilization?" Biology of Reproduction **85**(1): 4-5.
Yanagimachi, R. and M. C. Chang (1963). "SPERM ASCENT THROUGH THE OVIDUCT OF THE HAMSTER AND RABBIT IN RELATION TO THE TIME OF OVULATION." J Reprod Fertil **6**: 413-420.
Yang, M., Y. Yang, S. She and S. Li (2018). "Proteomic investigation of the effects of preimplantation factor on human embryo implantation." Mol Med Rep **17**(3): 3481-3488.

Yates III, J. R. (2011). "A century of mass spectrometry: from atoms to proteomes." nature methods **8**(8): 633-637.
Ye, X. (2020). "Uterine Luminal Epithelium as the Transient Gateway for Embryo Implantation." Trends Endocrinol Metab **31**(2): 165-180.
Yeung, W. S., K. F. Lee, R. Koistinen, H. Koistinen, M. Seppala, P. C. Ho and P. C. Chiu (2007). "Glycodelin: a molecule with multi-functions on spermatozoa." Soc Reprod Fertil Suppl **63**: 143-151.
Yoshida, K., C. Ito, K. Yamatoya, M. Maekawa, Y. Toyama, F. Suzuki-Toyota and K. Toshimori (2010). "A model of the acrosome reaction progression via the acrosomal membrane-anchored protein equatorin." REPRODUCTION **139**(3): 533-544.
Yoshida, K., Z. T. Krasznai, Z. Krasznai, M. Yoshiike, N. Kawano, M. Yoshida, M. Morisawa, Z. Tóth, Z. K. Bazsáné, T. Márián and T. Iwamoto (2009). "Functional implications of membrane modification with semenogelins for inhibition of sperm motility in humans." Cell Motil Cytoskeleton **66**(2): 99-108.
Zamboni, L. (1991). "Physiology and pathophysiology of the human spermatozoon: the role of electron microscopy." Journal of electron microscopy technique **17**(4): 412-436.
Zhan, X., Y. Huang and Y. Long (2018). "Two-dimensional Gel Electrophoresis Coupled with Mass Spectrometry Methods for an Analysis of Human Pituitary Adenoma Tissue Proteome." J Vis Exp(134).
Zhang, H., M. Vollmer, M. De Geyter, Y. Litzistorf, A. Ladewig, M. Dürrenberger, R. Guggenheim, P. Miny, W. Holzgreve and C. De Geyter (2000). "Characterization of an immortalized human granulosa cell line (COV434)." Mol Hum Reprod **6**(2): 146-153.
Zhang, M. I. and R. G. O'Neil (1999). "The diversity of calcium channels and their regulation in epithelial cells." Adv Pharmacol **46**: 43-83.
Zhang, Y. (2008). "I-TASSER server for protein 3D structure prediction." BMC Bioinformatics **9**(1): 40.
Zhang, Y. (2008). "Progress and challenges in protein structure prediction." Curr Opin Struct Biol **18**(3): 342-348.
Zhang, Y., B. R. Fonslow, B. Shan, M. C. Baek and J. R. Yates, 3rd (2013). "Protein analysis by shotgun/bottom-up proteomics." Chem Rev **113**(4): 2343-2394.
Zhou, C. X., X. F. Wang and H. C. Chan (2005). "Bicarbonate secretion by the female reproductive tract and its impact on sperm fertilizing capacity." Sheng Li Xue Bao **57**(2): 115-124.